



Uniwersytet Marii Curie-Skłodowskiej
w Lublinie

Wydział Matematyki, Fizyki i Informatyki

Instytut Matematyki

Nikodem Dymski

Conservation laws in the modelling
of collective phenomena

Promotor: **Prof. Massimiliano Daniele Rosini**

Kopromotor: **Prof. Paola Goatin**

Lublin 2019



$$\rho \left(\frac{\partial v}{\partial t} + v \cdot \nabla v \right) = -\nabla p + \nabla \cdot T + f$$

$$e^{i\pi} + 1 = 0$$

THÈSE DE DOCTORAT

Nikodem Dymski

Conservation laws in the modelling
of collective phenomena

Université Côte d'Azur

École Doctorale Sciences Fondamentales et Appliquées

Présentée en vue de l'obtention du
grade de docteur en mathématique
d'Université Côte d'Azur et
d'Université Maria Curie
Skłodowska

Dirigée par Paola Goatin

Co-encadrée par Massimiliano
Rosini

Soutenue le: 11.10.2019

Devant le jury, composé de :

Prof. Adam Bobrowski, LUT

Prof. Rinaldo Colombo, UNIBS

Prof. Andrea Corli, UNIFE

Prof. Paola Goatin, INRIA

Prof. Stéphane Junca, UNS

Prof. Tomasz Komorowski, IMPAN

Prof. Stanisław Prus, UMCS

Prof. Massimiliano Rosini, UMCS

Dla Agaty

Acknowledgments

Foremost, I would like to express my sincere gratitude to my advisors, Prof. Paola Goatin and Prof. Massimiliano Rosini, for the continuous support of my PhD study and research, for their motivation, enthusiasm and immense knowledge. I could not have imagined having better advisors for my PhD study.

I want to thank Prof. Rinaldo Colombo, Prof. Andrea Corli and Prof. Adam Bobrowski for accepting to be reviewers of my thesis. I thank also Prof. Stanisław Prus, Prof. Stéphane Junca and Prof. Tomasz Komorowski for accepting to be part of the jury.

I would like to offer my special thanks to the French Embassy in Poland for giving me the opportunity to study in France and for financial support. The time I spent in France is one of the most remarkable in my whole life. It would not be that great without the people I met there. I would like to thank all ACUMES team for making me feel like home. Big thanks to my Polish friends in Nice. I could always count on you and struggle with the life of PhD student together with you.

Nobody has been more important to me in the pursuit of this project than the members of my family. I am deeply indebted to my parents and my brother for their profound belief in my work and encouraging me to follow my ideas. Most importantly, I wish to thank my loving and supportive wife, Agata, for her constant motivation, practical suggestions and patience that cannot be underestimated.

This research was partially supported by the French Embassy in Poland under the BGF Cotutelle Grant.

Abstract

Over the last decades, traffic congestion, car accidents and pollution became daily issues. To understand and overcome road traffic problems, scientists from different research fields are creating advanced mathematical models. Mathematical models help to understand road traffic phenomena, develop optimal road network with efficient movement of traffic and minimal traffic congestion. This thesis is devoted to macroscopic traffic flow modelling, which describes traffic flow by variables averaged over multiple vehicles: density, velocity and flow. Macroscopic models naturally lead to conservation laws, which are hyperbolic partial differential equations. In recent years, this class of equations is more widely considered, but few theoretical results are available. This is caused by two main difficulties. The former is the non-linear hyperbolic nature of equations, which leads to consider weak solutions, instabilities and diffusivity of numerical schemes. The latter is the non-uniqueness of weak solutions and the need to introduce exotic functionals to select a unique physically reasonable solution.

In the first chapter, we introduce basic ideas of traffic modelling. First, we present the main classification of mathematical models with special attention to the level of details. Then we list the differences between the dynamics of traffic flow and that of flowing particles. Next, we show the minimal requirements to construct a physically reasonable macroscopic traffic flow model. We define three macroscopic variables to describe traffic flow, namely (average) density ρ , (average) speed v and (average) flow f . We derive the basic relation between them and formulate scalar conservation law. The chapter ends with a short presentation of the models under consideration, followed by the results obtained during my doctoral studies.

The second chapter is devoted to a detailed discussion of basic macroscopic traffic flow models. The first presented model is the model proposed by Lighthill, Witham [68] and Richards [81] (LWR). It describes the dynamics of traffic via a scalar conservation law under the hypothesis that $v = v(\rho)$. We define a rarefaction wave, a shock wave and a contact discontinuity for the LWR model, and define the Riemann solver $\mathcal{RS}_{\text{LWR}}$. In the end, we give a list of drawbacks of the LWR model.

The next considered model is the Aw, Rascle [7] and Zhang [85] model (ARZ). The ARZ model consists of two conservation laws, expressing the conservation of the number of vehicles and the conservation of the generalized momentum. We give the basic properties of the system, such as eigenvalues, eigenvectors and the corresponding Lagrangian markers. Next, we construct the Riemann solver $\mathcal{RS}_{\text{ARZ}}$ using elementary waves. Finally, we give definitions of weak and entropy solutions for the ARZ model corresponding to $\mathcal{RS}_{\text{ARZ}}$.

In the last part of this chapter, we describe models with phase transition (PT). The PT model treats differently traffic with low and high densities, on the basis of empirical studies. For this reason, we consider PT model described by the LWR model on the set Ω_f corresponding to the low densities and a 2×2 system of conservation laws on the set Ω_c corresponding to the high densities. We present two PT models, denoted by PT^a and PT^p , and introduced in [15, 53]. Then we recall from our paper [35] the generalization of these models for cases with a metastable phase ($\Omega_f \cap \Omega_c \neq \emptyset$) and without a metastable phase ($\Omega_f \cap \Omega_c = \emptyset$). Next, we introduce a notion of admissible solution for the Riemann problems and then Riemann solvers \mathcal{RS}_R and \mathcal{RS}_S accordingly. The chapter ends with propositions regarding consistency and \mathbf{L}_{loc}^1 -continuity for the Riemann solvers \mathcal{RS}_R and \mathcal{RS}_S .

In the third chapter, we describe the LWR model with a local point constraint on the flow. More precisely, we consider a situation in which the maximum flow of cars is limited at a fixed point along the road. Thanks to such considerations, we can model traffic flow through toll gates or construction sites. We define the Riemann solver $\mathcal{CRS}_{\text{LWR}}$ and list its main properties. Then we define the entropy solution of the Cauchy problem and recall the corresponding existence result.

The fourth chapter is devoted ARZ model with local point constraint on the flow and our results obtained in [42]. In our work we prove the existence of the weak solutions, corresponding to a non-conservative Riemann solver, in the class of functions with bounded variation. The goal is obtained by showing the convergence of a sequence of approximate solutions constructed via the Wave Front Tracking method. More precisely, we introduce grid, approximate Riemann solver $\mathcal{CRS}_{\text{ARZ}}^n$ by splitting a rarefaction wave and construct approximate Cauchy problems. Thanks to the decreasing in time functional Υ , we show that the total variation of the approximated solution is uniformly bounded. By Helly's theorem we obtain convergence of approximated solutions and then we show that the limit function is indeed a weak solution to the Cauchy problem for the ARZ model with local point constraint on the flow.

In the fifth chapter, we describe the models PT^a and PT^p with the local point constraint on the flow and present our results obtained in [10, 35]. More precisely, we introduce Riemann Solvers \mathcal{CRS}_R and \mathcal{CRS}_S , both with a metastable phase and without a metastable phase. Then we examine their consistency, \mathbf{L}_{loc}^1 -continuity and invariant domains. The remainder of the chapter is devoted to the existence result of a weak solution in the class of function with bounded variation for the PT^p model with a metastable phase. The goal is obtained by showing the convergence of

a sequence of approximate solutions constructed via Wave Front Tracking method. Similarly to the results from the previous chapter, we define grid and approximate Riemann solver $\mathcal{CRS}_R^{p,n}$. Then we introduce the decreasing in time function T and show that the approximate solution has bounded variation, the number of waves and interactions is finite in finite time. We apply Helly's theorem and then show that the limit function is an entropy solution of the Cauchy problem for the PT^a model with the metastable phase.

The sixth chapter is devoted to the results obtained in conference proceedings [34, 43]. We consider there two macroscopic models on road networks. The former is the LWR model with moving constraint on the flow. The concept of moving constraint on the flow allows us to model situations in which a truck (or other slower vehicle) reduces the flow at its position. From a mathematical point of view, the constraint is given by the ordinary differential equation depending on the trajectory of the truck. We give a detailed description of the model for a unidirectional road, introduce a Riemann solver \mathcal{BRS}_{LWR} and generalize it for the case of road networks. The latter considered model is the PT model introduced in the second chapter. We generalize it to the case of road networks by introducing an appropriate Riemann solver.

At last, for the sake of clarity and to ease of comprehension, we defer to the appendix technical proofs.

Streszczenie

Na przestrzeni ostatnich dziesięcioleci zatłoczone ulice, wypadki samochodowe oraz związane z ruchem samochodowym zanieczyszczenie powietrza stały się codziennością. Naukowcy z różnych dziedzin nauki tworzą zaawansowane modele matematyczne, pomagające zrozumieć zjawiska ruchu drogowego, rozwijać efektywnie sieć dróg oraz zmniejszać korki uliczne. Ta rozprawa doktorska poświęcona jest makroskopowemu modelowaniu ruchu drogowego, które formułuje zależności między uśrednionymi charakterystykami przepływu ruchu takimi jak gęstość, przepływ oraz prędkość. Modele makroskopowe w sposób naturalny prowadzą do stosowania praw zachowania, które są szczególnymi równaniami różniczkowymi cząstkowymi. W ostatnich latach ta klasa równań jest coraz chętniej rozpatrywana, ale wciąż dostępnych jest niewiele wyników teoretycznych. Spowodowane jest to dwoma poważnymi trudnościami. Pierwszym z nich jest nieliniowa, hiperboliczna natura równań, mogąca prowadzić do rozważania słabych rozwiązań, niestabilności lub dyfuzyjności schematów numerycznych. Drugim natomiast jest brak jednoznaczności słabych rozwiązań oraz potrzeba rozważania egzotycznych funkcjonałów w celu wybrania jednoznacznego, fizycznie uzasadnionego rozwiązania.

W rozdziale pierwszym prezentujemy wstęp do modelowania ruchu drogowego. Na początku podajemy główny podział modeli matematycznych, przy zwróceniu uwagi na poziom szczegółowości. Podajemy różnice pomiędzy strukturą płynów a strukturą ruchu drogowego, oraz wymieniamy podstawowe założenia potrzebne do skonstruowania poprawnego makroskopowego modelu ruchu drogowego. Definiujemy trzy charakterystyki przepływu ruchu, to jest (średnią) gęstość, (średnią) prędkość i (średni) przepływ, wyprowadzamy podstawową zależność pomiędzy nimi a następnie formujemy prawo zachowania. Rozdział zakończony jest krótkim przedstawieniem stosowanych modeli oraz wyników uzyskanych podczas trwania studiów doktoranckich.

Drugi rozdział poświęcony został szczegółowemu omówieniu podstawowych modeli makroskopowych dla ruchu drogowego. Jako pierwszy prezentujemy model zaproponowany przez Lighthilla, Withama [68] oraz Richardsa [81](LWR). Opisuje on dynamikę ruchu drogowego poprzez skalarne prawo zachowania wraz z warunkiem $v = v(\rho)$. Następnie wprowadzamy pojęcia fali rozrzedzającej, fali uderzeniowej oraz nieciągłości kontaktowej dla modelu LWR oraz definiujemy rozwiązanie zagadnienia Riemanna \mathcal{RS}_{LWR} . Na koniec podajemy listę wad modelu LWR.

Kolejny opisywany model został zaproponowany przez Aw, Rascla [7] oraz niezależnie Zhanga [85](ARZ). Jest on opisany poprzez układ dwóch praw zachowa-

nia. Pierwsze z nich jest prawem zachowania liczby pojazdów, natomiast drugie jest uogólnionym prawem zachowania pędu. Na początku rozdziału podajemy podstawowe własności układu, takie jak wartości i wektory własne oraz odpowiadające im znaczniki Lagrange’a. Następnie definiujemy rozwiązanie zagadnienia Riemanna $\mathcal{RS}_{\text{ARZ}}$ przy pomocy podstawowych fal. Na koniec podajemy definicje słabego rozwiązania oraz rozwiązania entropijnego dla modelu ARZ.

W ostatniej części tego rozdziału opisujemy modele z przemianą fazową(PT). Modele PT definiują odmiennie ruch drogowy dla dróg niezatłoczonych oraz dróg zatłoczonych. Z tego powodu rozważamy modele PT składające się z modelu LWR na zbiorze Ω_f odpowiadającym niezatłoczonym drogom oraz układu dwóch praw zachowania na zbiorze Ω_c odpowiadającym zatłoczonym drogom. Przedstawiamy dwie wersje modeli PT, oznaczone przez PT^a i PT^p i wprowadzone w [15, 53]. Następnie podajemy nasze uogólnienia [35] na przypadki odpowiednio bez fazy metastabilnej ($\Omega_f \cap \Omega_c = \emptyset$) oraz z fazą metastabilną ($\Omega_f \cap \Omega_c \neq \emptyset$). Następnie definiujemy rozwiązania dopuszczalne dla zagadnienia Riemanna oraz spełniające tę definicję rozwiązania zagadnienia Riemanna \mathcal{RS}_R i \mathcal{RS}_S . Rozdział kończymy propozycjami dotyczącymi niezmienniczości oraz ciągłości w przestrzeni L^1_{loc} funkcji lokalnie całkowalnych dla \mathcal{RS}_R i \mathcal{RS}_S .

W rozdziale trzecim opisujemy model LWR ze stałym ograniczeniem na przepływ. Innymi słowy, rozpatrujemy sytuację, w której maksymalny przepływ samochodów jest ograniczony w pewnym miejscu na drodze. Dzięki takim rozważaniom możemy modelować ruch drogowy na rogatkach, czy w miejscach robót drogowych. Definiujemy rozwiązanie zagadnienia Riemanna $\mathcal{CRS}_{\text{LWR}}$ oraz podajemy jego własności. Następnie definiujemy entropijne rozwiązanie zagadnienia Cauchy’ego oraz przypominamy twierdzenie o istnieniu jednoznacznego rozwiązania entropijnego zagadnienia Cauchy’ego.

Rozdział czwarty został poświęcony modelowi ARZ ze stałym ograniczeniem na przepływ oraz wynikiem własnym uzyskanym w [42]. W naszej pracy udowadniamy istnienie słabego rozwiązania zagadnienia Cauchy’ego w klasie funkcji o wahanii ograniczonym dla modelu ARZ ze stałym ograniczeniem na przepływ. W artykule rozpatrujemy rozwiązanie zagadnienia Riemanna dla którego warunek Rankine’a-Hugoniota nie jest spełniony dla drugiego równania. Dowód głównego twierdzenia opiera się na metodzie Wave Front Tracking. Mówiąc dokładniej, wprowadzamy siatkę i definiujemy przybliżone rozwiązanie zagadnienia Riemanna $\mathcal{CRS}_{\text{ARZ}}^n$ poprzez podział fali rozrzedzającej. Następnie, dzięki $\mathcal{CRS}_{\text{ARZ}}^n$ konstruujemy przybliżone rozwiązanie zagadnienia Cauchy’ego dla tego problemu. Przy pomocy malejącego w czasie funkcjonału Υ pokazujemy, że wahanie aproksymowanego rozwiązania jest ograniczone oraz liczba fal i interakcji między nimi jest skończona. Następnie, stosując twierdzenie Helly’ego otrzymujemy istnienie zbieżnego podciągu aproksymowanych rozwiązań. Ostatecznie wykazujemy, że funkcja graniczna jest rzeczywiście słabym rozwiązaniem zagadnienia Cauchy’ego dla modelu ARZ ze stałym ograniczeniem na przepływ.

W rozdziale piątym opisujemy modele PT^a i PT^p ze stałym ograniczeniem na

przepływ oraz podajemy wyniki własne zawarte w [10, 35]. Mówiąc dokładniej, wprowadzamy rozwiązania zagadnienia Riemanna \mathcal{CRS}_R i \mathcal{CRS}_S . Następnie w badamy ich zgodność, ciągłość w przestrzeni \mathbf{L}_{loc}^1 funkcji lokalnie całkowalnych oraz zbiory niezmiennicze. Pozostała część rozdziału została poświęcona wynikowi istnienia słabego rozwiązania entropijnego zagadnienia Cauchy’ego w klasie funkcji o wahanii ograniczonym dla modelu PT^a z fazą metastabilną. Dowód głównego twierdzenia opiera się na metodzie Wave Front Tracking. Podobnie do rozważań w poprzednim rozdziale, definiujemy siatkę, definiujemy przybliżone rozwiązanie zagadnienia Riemanna $\mathcal{CRS}_R^{p,n}$. Następnie wprowadzamy malejący w czasie funkcjonal T i pokazujemy, że wahanie przybliżonego rozwiązania jest ograniczone oraz liczba fal i interakcji między nimi jest skończona w skończonym czasie. Stosując twierdzenie Helly’ego otrzymujemy istnienie zbieżnego podciągu przybliżonych rozwiązań. Na koniec udowadniamy, że funkcja graniczna jest słabym rozwiązaniem entropijnym zagadnienia Cauchy’ego dla modelu PT^a z fazą metastabilną.

Rozdział szósty został poświęcony wynikom otrzymanym w materiałach konferencyjnych [34, 43]. W obu pracach rozważaliśmy modele makroskopowe na skrzyżowaniach drogowych. Pierwszym z wprowadzonych modeli jest LWR z ruchomym ograniczeniem na przepływ. Ruchome ograniczenie na przepływ pomaga nam modelować sytuacje, w których ciężarówka bądź inny wolniejszy pojazd redukuje przepływ w swoim otoczeniu. Z matematycznego punktu widzenia, ograniczenie jest dane przez równanie różniczkowe zwyczajne zależne od trajektorii tego pojazdu. Podajemy dokładny opis modelu dla drogi jednokierunkowej, wprowadzamy rozwiązanie zagadnienia Riemanna \mathcal{BRS}_{LWR} oraz uogólniamy je na przypadek skrzyżowania drogowego. Drugim rozważanym rodzajem modeli jest model PT wprowadzony w rozdziale drugim. Uogólniamy go do przypadku skrzyżowania drogowego poprzez wprowadzenie odpowiedniego rozwiązania zagadnienia Riemanna.

Ostatnią część pracy, dla zachowania przejrzystości tekstu, stanowią dodatki z dowodami twierdzeń pomocniczych.

Résumé

Durant ces 10 dernières années les embouteillages, les accidents de voiture, la pollution sont devenus des problèmes quotidiens. Afin de mieux comprendre et de mieux surmonter les problèmes de trafic routier, les scientifiques de tout domaine ont développé des modèles mathématiques avancés. Les modèles mathématiques aident à comprendre les phénomènes du trafic routier, à développer des réseaux de routes optimaux avec des circulations de véhicules efficaces et des problèmes d'embouteillage minimaux. Cette thèse est consacrée à la modélisation macroscopique du trafic routier où celle-ci décrit le trafic avec des variables moyennées sur plusieurs voitures : densité, vitesse et flux. Les modèles macroscopiques aboutissent naturellement aux lois de conservation, qui sont des équations aux dérivées partielles hyperboliques. Depuis ces récentes années, cette classe d'équations a davantage été considérée, cependant peu de résultats théoriques sont disponibles. Cela est dû à deux difficultés principales. La première est la nature hyperbolique non linéaire de ces équations, qui conduit à considérer la notion de solutions faibles, les instabilités et la diffusion de schémas numériques. La deuxième difficulté est la non unicité de la solution faible et la nécessité d'introduire de fonctionnelles exotiques permettant de sélectionner une unique solution physiquement raisonnable.

Dans le premier chapitre, nous introduisons les idées de base de la modélisation du trafic. Dans un premier temps, nous présentons les classifications principales des modèles mathématiques avec une attention particulière donnée au niveau des détails. Nous continuons par lister les différences entre la dynamique de trafic routier et celle des particules. Ensuite nous montrons les besoins minimaux pour construire un modèle de trafic macroscopique physiquement raisonnable. Nous définissons trois variables macroscopiques pour décrire le trafic, à savoir la densité (moyenne) ρ , la vitesse (moyenne) v et le flux moyen f . Nous tirons les relations de base qui les lient et nous formulons une loi de conservation scalaire. Le chapitre se termine par une présentation courte des modèles considérés, suivi de la présentation des résultats obtenus durant mes travaux de thèse.

Le second chapitre est dédié à une discussion détaillée des modèles macroscopiques de base dans le trafic. Le premier modèle présenté est le modèle proposé par Lightill, Witham [68] et Richards [81] (LWR). Il décrit la dynamique du trafic par une loi de conservation scalaire sous l'hypothèse $v = v(\rho)$. Nous définissons ce que sont une onde de détente, une onde de choc et un contact de discontinuité pour le modèle LWR, et nous définissons le solveur de Riemann. À la fin du chapitre, nous donnons une liste de défauts du modèle LWR. Le modèle considéré ensuite est celui

d'Aw, Rascle [7] et Zhang [85] (ARZ). Le modèle ARZ consiste en deux lois de conservation, exprimant la conservation du nombre de véhicules et la conservation du moment généralisé. Nous donnons les propriétés de base du système, telles que les valeurs, vecteurs propres et les marqueurs lagrangiens correspondants. Ensuite nous construisons le solveur de Riemann $\mathcal{RS}_{\text{ARZ}}$ en utilisant les ondes élémentaires. Enfin nous définissons les notions de solutions faibles pour le modèle ARZ associé à $\mathcal{RS}_{\text{ARZ}}$.

Dans la dernière partie de ce chapitre, nous décrivons le modèle de transition de phase (TP). le modèle TP traite de manière différente le trafic avec de faibles densité et de hautes densités sur la base d'études empiriques. C'est la raison pour laquelle, nous considérons le modèle TP décrit par le modèle LWR sur l'ensemble Ω_f correspondant aux faibles densités et à un système 2×2 de lois de conservation sur l'ensemble Ω_c correspondant aux hautes densités. Nous présentons deux modèles PT, notés PT^a et PT^p , et introduits dans [15, 53]. Ensuite à partir de notre papier [35], nous rappelons la généralisation de ces modèles aux cas avec une phase métastable ($\Omega_f \cap \Omega_c \neq \emptyset$). Ensuite, nous introduisons la notion de solution admissible pour les problèmes de Riemann et les solveurs de Riemann \mathcal{RS}_R and \mathcal{RS}_S . Le chapitre se termine avec des propositions sur la consistance et la continuité \mathbf{L}_{loc}^1 pour les solveurs de Riemann \mathcal{RS}_R and \mathcal{RS}_S .

Dans le troisième chapitre, nous décrivons le modèle LWR contenant une contrainte ponctuelle locale sur le flux. Plus précisément, nous considérons une situation dans laquelle le flux maximal de voitures est limité par un point qui reste fixe sur la route. Grâce à ces considérations, nous pouvons décrire le trafic à des postes de péage et à des chantiers. Nous définissons la solution entropique du problème de Cauchy et nous rappelons le résultat d'existence correspondant.

Le quatrième chapitre est dédié au modèle ARZ avec une contrainte ponctuelle locale sur le flux et à nos résultats obtenus dans [42]. Dans ces travaux, nous montrons l'existence de la solution faible correspondant au solveur de Riemann non conservatif dans la classe des fonctions à variations bornées. Le but est obtenu en montrant la convergence d'une suite de solutions approchées construites à partir de la méthode de Wave Front Tracking. Plus précisément nous introduisons un maillage, un solveur de Riemann approché $\mathcal{CRS}_{\text{ARZ}}^n$ en coupant une onde de détente et nous construisons des problèmes de Cauchy approchés. Grâce de la fonctionnelle Υ décroissante en temps, nous montrons que la variation totale des solutions accrochées est bornée uniformément. Grâce au théorème de Helly, nous obtenons la convergence la solution approchée et nous montrons que la limite est bien la solution faible du problème de Cauchy du modèle ARZ avec une contrainte ponctuelle locale sur le flux.

Dans le chapitre 5, nous décrivons les modèles PT^a et PT^p avec contrainte ponctuelle locale sur le flux et nous présentons les résultats obtenus dans [10, 35]. Plus précisément nous introduisons les solveurs de Riemann \mathcal{CRS}_R et \mathcal{CRS}_S , avec des phases métastable et non métastable. Ensuite nous étudions leurs consistances, leurs continuités \mathbf{L}_{loc}^1 et leurs domaines invariants. Le reste du chapitre

est dédié à l'existence d'une solution faible dans la classe des fonctions à variations bornées pour le modèle PT^p avec une phase métastable. Le but est obtenu en montrant la convergence d'une suite de solutions approchées construites par la méthode du Wave Front Tracking. De manière similaire aux résultats obtenus au chapitre précédent, nous définissons un maillage et un solveur de Riemann approché $\mathcal{CRS}_R^{p,n}$. Ensuite, nous introduisons la fonction T décroissante en temps et nous montrons que la solution approchée est à variations bornées, le nombre d'ondes et d'interactions est fini en temps fini. Nous appliquons le théorème de Helly et nous montrons que la limite est une solution entropique du problème de Cauchy PT^a avec phase métastable.

Le sixième chapitre est dédié aux résultats obtenus dans des actes de conférences [34, 43]. Nous y considérons deux modèles macroscopiques sur réseau. Le premier est le modèle LWR avec des contraintes mobiles sur le flux. Cette idée de contraintes mobiles sur le flux nous permet de modéliser la situation dans laquelle un camion (ou tout autre véhicule lent) réduit le flux à sa position. D'un point de vue mathématique, la contrainte est donnée par une équation différentielle ordinaire dépendant de la trajectoire du camion. Nous donnons une description détaillée du modèle pour une route unidimensionnelle, introduisant un solveur de Riemann \mathcal{BRS}_{LWR} et le généralisant à un réseau de routes. Le dernier modèle considéré est le modèle PT introduit dans le second chapitre. Nous le généralisons dans le cas d'un réseau de routes en introduisant un solveur de Riemann approprié.

Enfin, dans un souci de clarté et pour une plus facile compréhension, toutes les preuves techniques ont été déplacées dans l'annexe.

Table of Contents

Acknowledgments	iii
List of Figures	xvi
List of Tables	xviii
Chapter 1	
Vehicular traffic modelling	1
1.1 Introduction	1
1.2 Mathematical Models	2
1.3 The macroscopic traffic variables	4
1.4 The fundamental equations	7
Chapter 2	
Macroscopic models	14
2.1 Introduction	14
2.2 LWR model	15
2.2.1 The Riemann solver $\mathcal{RS}_{\text{LWR}}$	17
2.2.2 Drawbacks of the LWR model	21
2.3 ARZ model	21
2.3.1 ARZ model in Riemann invariant coordinates	22
2.3.2 The Riemann solver $\mathcal{RS}_{\text{ARZ}}$	24
2.3.3 Weak and entropy solutions	27
2.4 PT models	28
2.4.1 The general PT models	29
2.4.2 Main assumptions	34
2.4.3 The Riemann solvers \mathcal{RS}_{R} and \mathcal{RS}_{S} for PT models	36
Chapter 3	
Constrained LWR model	41
3.1 Introduction	41

3.1.1	The constrained Riemann solver \mathcal{RS}_{LWR}^c	41
3.2	The Constrained Cauchy Problem	43
Chapter 4		
	Constrained ARZ models	45
4.1	Introduction	45
4.2	Description of the model and notations	46
4.3	The main result	49
4.3.1	Wave Front Tracking	51
4.3.2	Proof of Theorem 4.1	55
4.4	A case study	58
Chapter 5		
	Constrained PT models	62
5.1	Introduction	62
5.2	Existence result for constrained PT^p model with metastable phase .	69
5.2.1	Notations, definitions and main result	69
5.2.1.1	The constrained Cauchy problem	71
5.2.2	The constrained Riemann problem	78
5.2.3	A case study	80
5.2.4	Proof of Theorem 5.2	83
Chapter 6		
	Networks	105
6.1	Introduction	105
6.2	LWR with moving bottleneck on networks	106
6.2.1	A single unidirectional road	106
6.2.2	Networks	109
6.2.3	A case study	113
6.3	PT models on networks	115
6.3.1	A case study	120
Appendix A		
	Technical proofs of Subsection 2.4.3	121
A.1	Proofs of the main properties of \mathcal{RS}_R	121
A.2	Proofs of the main properties of \mathcal{RS}_S	122
A.3	Proofs of the main properties of \mathcal{CRS}_S	123
A.4	Proofs of the main properties of \mathcal{CRS}_R	124
A.5	Proof of Proposition 5.7	127
A.6	Proof of Proposition 5.8	140

Appendix B	
Technical proofs of Subsection 4.3.1	141
B.1 Proof of Lemma 4.1	141
B.2 Proof of Lemma 4.2	142
Bibliography	154

List of Figures

1.1	The example of vehicles trajectories on a road.	5
1.2	Vehicles on a road section moving with the same speed v , having the same length L and headings d	6
2.1	Fundamental diagram for the LWR model.	16
2.2	The first column refers to the case $\Omega_f \cap \Omega_c = \emptyset$, namely $v_c < v_{\max}$, while the second column refers to the case $\Omega_f \cap \Omega_c \neq \emptyset$, i.e. $v_c = v_{\max}$. The first row refers to PT ^a and the second row to PT ^p . Above $Y_{1\pm}^f \doteq (r_{\pm}^f, r_{\pm}^f \cdot \mathbf{w}_{\pm})$, $Y_{1\pm}^c \doteq (r_{\pm}^c, r_{\pm}^c \cdot \mathbf{w}_{\pm})$, $Y_2^{\pm} \doteq \psi_2^{\pm}(Y_r)$, $Y_1^f \doteq \psi_1^f(Y_{\ell})$ and $Y_1^c \doteq \psi_1^c(Y_{\ell})$ defined in Subsection 2.4.1.	31
4.1	Basic notations in (ρ, f) -coordinates.	47
4.2	The grid \mathcal{G}_n with $n = 3$	52
4.3	The solution to Cauchy problem (4.1) with initial datum (4.9) constructed in Section 4.4. The shaded areas correspond to rarefactions.	59
4.4	The solution to Cauchy problem (4.1) with initial datum (4.9) constructed in Section 4.4. Darker colors correspond to higher values.	60
5.1	The selection criterion for \hat{U} and \check{U} given in Definition 5.3 in the case $(U_{\ell}, U_r) \in \mathcal{D}_2$. In the first picture U_{ℓ}^1, U_{ℓ}^2 represent the left state in two different cases and \hat{U}_1, \hat{U}_2 are the corresponding \hat{U} . In the second picture q_1, q_2 are q in two different cases, \hat{U}_1, \hat{U}_2 are the corresponding \hat{U} and \check{U}_1, \check{U}_2 are the corresponding \check{U}	65
5.2	The selection criterion for \hat{U} and \check{U} given in Definition 5.4.	66
5.3	Invariant domains \mathcal{I}_f (left) and \mathcal{I}_c (right) described in (ICR.1) and (ICR.2) of Proposition 5.4.	68
5.4	Notations introduced in Subsection 2.4 adapted to U -coordinates.	69
5.5	Representation of $\mathbf{w}_q, \mathbf{v}_q^{\pm}$ and h_q in the case $q \in (0, f^-)$. The curve in the figure on the left is the graph of h_q and corresponds to the horizontal solid segment in the figure on the right. In particular $w_* = h_q(v_*)$	71
5.6	The functions \hat{U} and \check{U} in the case $q \in (f^-, f^+)$ defined in (5.14).	76
5.7	The functions \hat{U} and \check{U} in the case $q \in (0, f^-)$ defined in (5.14).	77

5.8	The selection criterion for $\hat{U}_\ell \doteq \hat{U}(w_\ell, q)$ and $\check{U}_r \doteq \check{U}(v_r, q)$ in Definition 5.7 for $(U_\ell, U_r) \in \mathcal{D}_2$ and $q \in (0, f^-)$. In the first picture U_ℓ^1, U_ℓ^2 represent the left state in two different cases and $\hat{U}_\ell^1, \hat{U}_\ell^2$ are the corresponding \hat{U}_ℓ . Analogously in the second and third pictures for U_r^1, U_r^2 and $\check{U}_r^1, \check{U}_r^2$	80
5.9	The solution constructed in Section 5.2.3.	81
5.10	The solution constructed in Section 5.2.3.	82
5.11	The grid \mathcal{G}_n for $q \in (0, f^-)$ and $n = 2$. The curve in the figure on the left is the support of h_q , which corresponds to (a portion of) the horizontal line in the figure on the right.	85
5.12	$q \in (f^-, f^+)$, $v_{0,F}^\pm \doteq F/p^{-1}(\mathbf{W}(U_n(t, 0^\pm)) - k)$ and $v_0^\pm \doteq v_n(t, 0^\pm)$. The first two pictures show that if $v_0^- < k < v_0^+$, then $v_{0,F}^- < k$. In the last picture we consider the case $v_0^- < v_0^+ < k$ and show that $v_{0,F}^- < v_{0,F}^+ < k$	100
5.13	Above $q \in (0, f^-)$, $v_0^\pm \doteq v_n(t, 0^\pm)$ and $v_{0,q}^\pm \doteq q/p^{-1}(\mathbf{W}(U_n(t, 0^\pm)) - k)$. With the first two pictures we show that if $v_0^- < k < v_0^+$, then $v_{0,q}^- < k$. In the last picture we consider the case $v_0^- < v_0^+ < k$ and show that $v_{0,q}^- < v_{0,q}^+ < k$	101
6.1	Fundamental diagram with constraint. Left: Fixed reference frame. Right: Bus reference frame.	108
6.2	Left: the set \mathfrak{N} . Center: the fundamental diagram with initial datum. Right: the set \mathfrak{N}^b	114
6.3	Above we represent the densities at time $t = 1/5$ along the roads I_1, \dots, I_4 . In red the case with the bus and in blue the case without the bus.	116
B.1	Case A1	143
B.2	Case A2.a	144
B.3	Cases A2.b , A2.c and A3	145
B.4	Cases A4.a and A4.b	147
B.5	Cases A5.a , A5.b and A6	148
B.6	Cases A7 , A8.a and A8.b	149
B.7	Cases A9 , B1.a , B1.b and B2	151
B.8	Cases B3.a , B3.b and B3.c	152

List of Tables

5.1	The main properties of the Riemann solvers.	67
A.1	Overview of the interactions considered in the proof of Proposition 5.7.	129

Vehicular traffic modelling

1.1 Introduction

Traffic congestion is one of the most challenging problems for nowadays cities. Transportation problems are studied by scientists from different research fields, such as Mathematics, Physics, Engineering, Psychology and Sociology. Currently, owning a vehicle is not only a convenience, but often is a must. Indeed, the public transport is typically inappropriate and forces the daily use of individual cars. As a result, we observe a steady escalation in road congestion over the past decades. This deeply affects environmental pollution, stress level of the drivers and fuel consumption.

Traffic management systems based on mathematical models may contribute to solve some of the mentioned problems. Automatic control of traffic, thanks to real-time simulations, can improve the flow of the cars and optimize the routes of individual drivers. Therefore, building new roads to minimize traffic congestion, which is often not affordable, might be not necessary. However, building new roads not always diminishes roads congestion. As Braess' paradox shows [17], expansion of a road network redistribute traffic flow and by that may cause its general decline. This phenomenon was observed among others in Stuttgart (1960), where closing the section of Königsstraße street improved traffic flow in the area of Schlossplatz [61]. In general, such phenomena are not easily observable. Instead of experiment empirically on working roads to show particular behavior of the traffic, traffic engineers can use mathematical models.

For decades several approaches to traffic flow modelling were proposed to solve key transportation problems. The main author's interest during doctoral studies was macroscopic traffic flow modelling. The history of macroscopic modelling dates back to 1950s and arose from fluid dynamics concepts. The first macroscopic traffic flow model, proposed by Lighthill and Witham [68], is based on similarities between traffic flow and flood movements in rivers. Despite age and variety of approaches, this branch of science is still actively developing, raising new challenges and proposing new mathematical tools.

The following thesis contains the state of art on selected issues related to macroscopic traffic flow modelling and own contribution to the topic.

1.2 Mathematical Models

In this section, we briefly recall the main classification of mathematical models with a special focus on differences at the level of details. We show disparity between fluid and traffic flow. At last, we list the minimal requirements for physically reasonable traffic flow model.

According to [82], mathematical models can be classified based on the following:

- Level of details (microscopic, mesoscopic, macroscopic).
- Scale of the independent variables (continuous, discrete, semi-discrete).
- Representation of the processes (deterministic, stochastic).
- Operationalisation (analytical, simulation).
- Scale of application (networks, stretches, links, intersections).

Let us have a deeper look into the classification with respect to the level of details.

Microscopic models describe each vehicle independently, according to its speed and headings. It is often assumed that driver's decisions are made according to the traffic situation in front of his car. However, more complex models might take into account additional factors like interactions with other vehicles or driving style. The trajectory of each vehicle is given by an ordinary differential equation, whose solution gives the vehicle's trajectory. Due to the model's complexity and

the fact that the size of the system grows proportionally to the number of vehicles, online simulations are computationally very demanding. Moreover, solutions to system equations depend on each other, which makes parallel computation difficult to apply. The literature on microscopic models is broad and contains numerous number of models, like self-distance models [74, 79], stimulus-response models [22, 51] or cellular-automata models [57, 73].

Mesoscopic models fill the gap between microscopic and macroscopic models. The traffic flow is described in aggregate terms like in a probability distributions, however behavioral rules are considered for individual drivers. We distinguish three main kinds of mesoscopic models: headway distribution models [19, 67], cluster models [63] and gas-kinetic models [76, 80]. Mesoscopic models give a good compromise between the level of details and size of the area that can be analysed.

Macroscopic models describe traffic flow by variables averaged over multiple vehicles: density, velocity and flow. The solution can be often expressed in a closed analytical form. Online simulations are capable, relatively easy to optimize and calibrate.

Macroscopic modelling of traffic flow has roots in fluid dynamics. Though, it is intuitively clear that the dynamics of cars on a highway is different from that of flowing particles. We list below the main differences.

- The driving behaviour differs among people. It depends on their experience, preferred style of driving but also on mood and tiredness at the particular moment. Some behaviours can be also culturally conditioned and vary between countries. The fluid particles always follow physical laws.
- The number of cars is far smaller than a number of particles in a fluid.
- Fluid is isotropic, namely it has no directional preference and responds to stimuli from surrounding particles. Traffic flow is anisotropic, namely drivers move in one direction and they are influenced only by cars in front of them.

Differences between traffic flow and fluid flow require a different approach to modelling. Aw and Rascle in [7] proposed the following minimal requirement for physically reasonable macroscopic traffic flow model.

(A.1) The system must be hyperbolic.

- (A.2) The solution to arbitrary bounded nonnegative Riemann data in a suitable region of the plane must remain non-negative and bounded from above.
- (A.3) The speed of propagation of solution to any Riemann solver must be at most equal to the average speed.
- (A.4) The shock wave, whose propagation speed can be either negative or non-negative, are created due to breaking, whereas rarefaction waves are produced due to acceleration and satisfy (A.3).
- (A.5) Near the vacuum, the solution to the Riemann problem must be very sensitive to the data.

The condition (A.1) guarantees conservation of the number of cars, namely vehicles are not created nor destroyed. The condition (A.2) is a minimal requirement for any reasonable model. The condition (A.3) states that car travelling with a certain velocity receives no information from the rear. The condition (A.4) is necessary due to real life observation of traffic. The last condition (A.5) states that there is no continuous dependence with respect to initial data nearby vacuum.

1.3 The macroscopic traffic variables

We already briefly described different approaches to traffic flow modelling. Nevertheless, none of the models can be applied in a wide range if needed data are hard to collect. What kind of information are therefore useful and easy to reach? History of handling data of traffic flow dates back to Grenshild's studies in the 1930s, what involved photographing the road section on fixed time intervals.

According to [60] traffic can be observed from three perspectives:

- Local(fixed position): camera, loop detector or other devices which captures changes at a certain point on the road.
- Instantaneous(fixed time): camera or another device which capture longer road section at a certain time(e.g pictures from a helicopter).
- Trajectory(moving with vehicle): in-car devices allowing to determine the position of the vehicle.

Which variables can be obtained using or mixing the above techniques? Let us start from studying the case in the microscopic framework.

Consider a section of a multilane, unidirectional road without on-ramps and off-ramps. The position of the i -th vehicle at time $t \geq 0$ can be described by a unique pair $X_i(t) = (x_i(t), \ell_i(t)) \in \mathbb{R} \times \mathbb{N}$, where the first component gives the position on the road section and the latter, number of the lane. Therefore we can give a graphical description of the traffic by providing the space-time diagram.

For example, in Figure 1.1 the position of the vehicles is measured along the horizontal axis and time is represented on the vertical axis. The curved arrows correspond to trajectories of each car. We may observe that the driver starting from x_5 is rapidly accelerating and overtaking three cars while the rest are rather timid. Two cars (starting from x_7 and x_8) are moving along straight lines, namely their speed is constant and probably one following the other. The velocity of each car is given by $v = x'_i(t)$.

However, keeping track of every car might be problematic and very demanding for transportation systems. Instead of exact trajectories, we can study the velocity field $v = v(t, x, \ell)$. Since for a given time and position on the specified lane, only one car may exist, the velocity vector field is uniquely determined. We observe also that the velocity field satisfies the equation $v(t, X_i(t)) = x'_i(t)$.

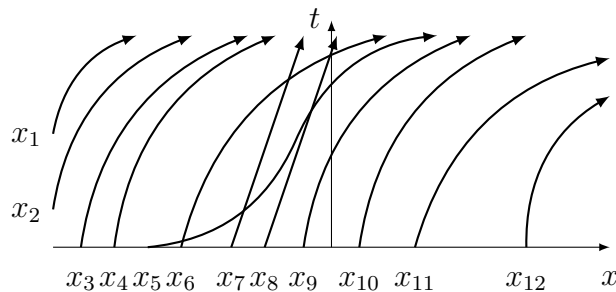


Figure 1.1: The example of vehicles trajectories on a road.

In the macroscopic framework the velocity v is averaged over multiple vehicles. We can easily find two other macroscopic variables. The first one is called traffic flow, that we will denote by f , and describes the number of cars passing through a point in a time unit. The second is called traffic density, denoted by ρ , and describes the number of cars observed at a fixed time per unit space.

Example 1.1. Consider one lane, unidirectional road section of the length 1, parametrized by a coordinate $x \in \mathbb{R}$, with vehicles moving in the direction of increasing x . Let us study the simplest situation, namely with identical cars of length L , moving with the same constant speed v such that the distance between two consecutive vehicles is constant and equals d , see Figure 1.2.

The traffic density, namely the number of vehicles per unit space, is constant in this case and expressed by

$$\rho = \frac{1}{L + d}.$$

The maximal density is achieved by taking $d = 0$, which is related in reality to the traffic jam with cars standing bumper to bumper, and therefore

$$\rho_{\max} = \frac{1}{L}.$$

The traffic flow illustrates the number of vehicles per unit time. Let place an observer, who is counting vehicles in front of him. Each vehicle passes him every $t = (L + d)/v$, hence the traffic flow computed in a time unit is represented as

$$f = \frac{v}{L + d}.$$

Again, the above expression takes its biggest value for $d = 0$. Such a situation is however unrealistic if the cars are in motion. The real traffic flow observation shows that $d = 0$ is related rather to cars stuck in a traffic jam with maximal traffic density ρ_{\max} .

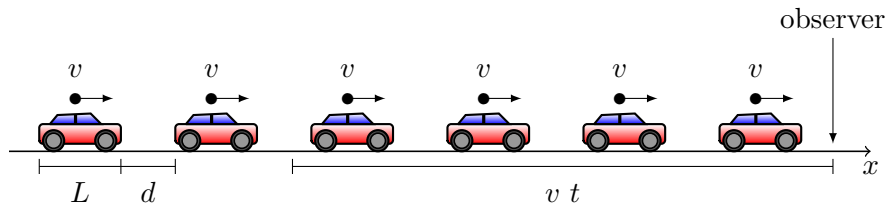


Figure 1.2: Vehicles on a road section moving with the same speed v , having the same length L and headings d .

1.4 The fundamental equations

In this section, we give a mathematical description of macroscopic variables, introduce the fundamental equation and present the derivation of a scalar conservation law. Example 1.1 gave us a good intuition on traffic density and traffic flow concepts. One could also observe the simple relation between macroscopic variables, namely

$$f(t, x) = \rho(t, x)v(t, x). \quad (1.1)$$

Nonetheless, our example is oversimplified and we may wonder whether it holds true in general. Consider the number of cars passing through the point $x = x_0$ in a small time interval $[t_0, t_0 + \Delta t]$. If we assume density and velocity functions to be continuous in time and space, then they might be approximated by constant values. Therefore, the number of cars passing through the point x_0 in a time Δt is approximately equal to $v(t, x)\rho(t, x)\Delta t$ and (1.1) is still valid. This construction can be done only on a long road section in a short time interval or analogously on the short road section and longer time interval. However, it is not sufficient to derive the evolution of traffic in real life.

Does formula (1.1) hold true for a more general framework? To answer this question, we need to define macroscopic variables at every point (x, t) . Therefore let us assume the number of cars $N(x, t)$ to be continuous and continuously differentiable. To find the local instantaneous density we take the road section $[x, x + \Delta x]$ at given time t and let $\Delta x \rightarrow 0$, namely

$$\rho(t, x) = \lim_{\Delta x \rightarrow 0} \frac{N(t, x + \Delta x) - N(t, x)}{\Delta x} = \partial_x N(x, t).$$

Similarly, we may introduce a local instantaneous traffic flow. Consider time interval $[t, t + \Delta t]$ at given space x and let $\Delta t \rightarrow 0$, namely

$$f(t, x) = \lim_{\Delta t \rightarrow 0} \frac{N(t + \Delta t, x) - N(t, x)}{\Delta t} = \partial_t N(x, t).$$

Velocity is a rate of change of vehicles position with respect to a frame of reference,

and is a function of time. By the above definitions we easily observe that for $\rho \neq 0$

$$v(t, x) = \frac{f(t, x)}{\rho(t, x)}.$$

Thanks to the above considerations we can study the simple situation of traffic evolution on a road section $[x_1, x_2]$ in a time interval $[t_1, t_2]$. For the road without entrances and exits, the following formula conserving the number of cars holds true

$$\int_{x_1}^{x_2} \rho(x, t_2) dx = \int_{x_1}^{x_2} \rho(x, t_1) dx + \int_{t_1}^{t_2} \rho(x_1, t)v(x_1, t) dt - \int_{t_1}^{t_2} \rho(x_2, t)v(x_2, t) dt. \quad (1.2)$$

Assuming the functions $\rho(x, t)$ and $v(x, t)$ to be differentiable we may write

$$\rho(x, t_2) - \rho(x, t_1) = \int_{t_1}^{t_2} \partial_t \rho(x, t) dt$$

and

$$\rho(x_2, t)v(x_2, t) - \rho(x_1, t)v(x_1, t) = \int_{x_1}^{x_2} \partial_x (\rho(x, t)v(x, t)) dx.$$

The equation (1.2) can be then written as

$$\int_{t_1}^{t_2} \int_{x_1}^{x_2} \{\partial_t \rho(x, t) + \partial_x (\rho(x, t)v(x, t))\} dx dt = 0.$$

Since a choice of a road section $[x_1, x_2]$ and a time interval $[t_1, t_2]$ is arbitrary, we conclude that integrand must be identically equal zero, namely

$$\partial_t \rho + \partial_x (\rho v) = 0. \quad (1.3)$$

This equation is a scalar conservation law in one space dimension. From the modelling point of view, it represents the conservation of the number of cars, namely vehicles are neither created nor destroyed.

Since we have one equation with two variables, additional informations are needed. In this sense traffic flow models based on conservation laws could be divided into two main groups:

- **Equilibrium traffic models** assume that the traffic velocity in (1.3) is a function of density, namely $v = v(\rho)$. Moreover, the dynamics of the traffic flow occurs along the equilibrium curve $\{(\rho, v(\rho)) : \rho \in [0, \rho_{\max}]\}$. They are also called first order models.
- **Non-equilibrium traffic models** add additional partial differential equations closing (1.3). They are also called higher order models.

The first equilibrium traffic flow model was proposed by Lighthill and Witham [68] and, independently, Richards [81] (LWR). The traffic dynamics is expressed by the scalar conservation law

$$\partial_t \rho + \partial_x f = 0, \quad f \doteq \rho v(\rho).$$

The function $v : [0, \rho_{\max}] \rightarrow [0, v_{\max}]$ is such that $v(0) = v_{\max}$ and $v(\rho_{\max}) = 0$. It is reasonable to assume also that v is \mathbf{C}^1 and non-increasing. The LWR model will be presented in details in Section 2.2.

In real life it has been observed that traffic is generally in non-equilibrium state. For small densities equilibrium models perform fairly good, however they do not describe correctly the dynamics of congested roads. This naturally leads to non-equilibrium models, which thanks to additional partial differential equation allow to consider non-equilibrium states.

The first non-equilibrium traffic flow model was introduced by Payne and Witham [77]. They closed the scalar conservation law (1.3) by the equation expressing traffic acceleration

$$v + v \partial_x v = \frac{v(\rho) - v}{\tau} - \frac{c^2}{\rho} \partial_x \rho, \quad (1.4)$$

where $v(\rho)$ is an equilibrium velocity, c^2 is a diffusion parameter and τ is a relaxation time. In the 1995 Daganzo in [32] pointed out drawbacks of higher order models based on fluid dynamics. For example, vehicles in Payne-Whitham model can move backwards at upstream jam fronts, which turns out the model to be non-realistic.

In 2000 Aw and Rascle in [7] and independently Zhang [85] proposed a new second-order model fixing flaws underlined by Daganzo. The Aw-Rascle-Zhang

model (ARZ) consists of the conservation of mass equation (1.2) and the equation that mimics the momentum equation. More precisely, instead of unrealistic space derivative of pressure from Payne-Witham model, ARZ uses the convective derivative $\partial_t + v\partial_x$. By the fact that there is no conservation of momentum in the car traffic, the pressure term has been substituted by an “anticipation factor” p , which describes drivers’ reaction to a variation of cars respect to the space. We may write the system in conservative form away from the vacuum as

$$\partial_t Y + \partial_x F(Y) = 0,$$

with

$$Y \doteq (\rho, y)^T \in \mathbb{R}_+^2 \setminus \{0\}, \quad F(Y) \doteq \left(\frac{y}{\rho} - p(\rho) \right) Y,$$

where the quantity y is a generalized momentum and $p(\rho)$ is an anticipation factor. The ARZ model will be presented in details in Section 2.3.

Nevertheless, none of the discussed construction is free of drawbacks. One of the main issue raised about the LWR model is infinite acceleration. In particular, when vehicles leave a congested road and enter an empty road, they immediately achieve their free flow speed. This can be solved by imposing additional term responsible for bounding acceleration, see [65]. Moreover, empirical studies show that the dynamics of traffic flow should be given on (ρ, f) -plane by a cloud of points rather than the equilibrium curve.

The ARZ model fails to show continuous dependency of a solution with respect to initial datum near the vacuum. Furthermore, the maximal speed of the vehicles on an empty road depends on an initial datum. The full list of drawbacks is postponed to another section, but the one mentioned here allow us to give a motivation for models with the phase transition.

The idea behind phase transition models is to solve some drawbacks related both to LWR and ARZ models. The phase transition model treats differently traffic with low and high densities. According to Greenshield studies [55], the relation between traffic velocity and traffic density is (almost)linear. For this reason, the LWR model performs well in free flow regime, namely in the region with low density

and high velocity. From experimental observations it appears that traffic in the congested regimes, namely sufficiently big densities, the fundamental diagram is 2-dimensional and should contain a cloud of points. Therefore, in the congested region, the traffic flow can be modelled by a 2×2 system of conservation laws. Phase transition models can be written as follows

$$\begin{array}{cc}
 \textbf{Free flow} & \textbf{Congested flow} \\
 \left\{ \begin{array}{l} Y \doteq (\rho, y) \in \Omega_f, \\ \partial_t \rho + \partial_x f(Y) = 0, \\ v(Y) = v(\rho), \end{array} \right. & \left\{ \begin{array}{l} Y \doteq (\rho, y) \in \Omega_c, \\ \partial_t \rho + \partial_x f(Y) = 0, \\ \partial_t y + \partial_x (y v(Y)) = 0, \end{array} \right. & f(Y) \doteq \rho v(Y).
 \end{array}$$

Above, $\rho \in [0, R]$ represents the density and $y \geq 0$ the generalized momentum of the vehicles. The sets Ω_f and Ω_c denote the invariant domains of the free and congested phases, respectively. Observe that in Ω_f the density ρ is the unique independent variable, so it is 1D while in Ω_c the independent variables are both ρ and y .

The models briefly introduced above can predict and control with success the traffic flow on a simple road sections. However, real life traffic flow is much more complicated, thus more tools are needed to apply traffic flow models in a broad sense. For instance let us consider a road with traffic lights, toll gates or construction sites. From the modelling point of view, all of them are "obstacles", reducing the traffic flow at fixed points on a road. We write such a constraint condition as

$$\rho(t, x_i) v(\rho(t, x_i)) \leq q_i(t),$$

where x_i are the "obstacles" positions, while $q_i(t)$ are the maximal flows allowed through them at time $t \geq 0$. The concept of macroscopic traffic flow models with flux constraints has been popular in recent years. However, the first time this idea was proposed in a crowd dynamics framework to model the evacuation of a corridor through the exit door [30]. In the framework of traffic flow modelling, the problem was studied first in [29] and have been developed in [5, 20, 25, 26, 37, 38].

The idea of local point constraints can be generalized. Consider, instead of fixed obstacle, a slow vehicle moving like a bus or a truck reducing the traffic

flow at its position. This type of constraint is called a "moving bottleneck". The traffic evolution can be described by a strongly coupled PDE-ODE system. The coupling of conservation laws with ODE has been widely studied in [16, 37–39, 64]. More precisely, a system of PDE describes the traffic evolution, while an ODE describes the trajectory of the slow vehicle. In the PDE part, we might consider the already mentioned models like LWR, ARZ or PT. The constraint condition is constructed by $X = x - y(t)$ change of coordinates, where $y(t)$ is the slow vehicle position at time $t \geq 0$. In (X, t) coordinates, the velocity of the bus equals zero and conservation of cars equation (1.3) becomes

$$\partial_t \rho + \partial_X (f(\rho) - \dot{y} \rho) = 0.$$

Therefore, the corresponding constraint condition might be written as

$$f(\rho) - \dot{y} \rho \leq F(\dot{y}(t)).$$

The following PhD thesis contains the main results obtained during author's doctoral studies. His main interests in this period concern macroscopic modelling of traffic flow with constraints. The outcome of collaborative work with supervisors and other collaborators are three journal articles and two conference proceedings. The main ideas of such papers are stated below.

In [42] we considered the ARZ model with fixed point constraint on the flow. We recall that the authors in [46] introduced two corresponding Riemann solvers, one fully conservative and one non-conservative. In our work we prove the existence of the weak solution, corresponding to the non-conservative Riemann solver, in the class of functions with bounded variation. The goal is obtained by showing the convergence of a sequence of approximate solution constructed via the Wave Front Tracking method [18, 59]. A case study to describe the qualitative features of the solutions is also presented.

The article [35] deals with a phase transition model with fixed local point constraint on the flow. We generalize the two PT models considered in [11, 12, 53] and [14, 15]. For more clarity, we consider two different PT models, both with metastable phases $\Omega_f \cap \Omega_c \neq \emptyset$ and non-metastable phases $\Omega_f \cap \Omega_c = \emptyset$. The main result consists in the definitions of two new Riemann solvers and the

study of their properties. More precisely, we study the total variation estimates and consistency of all Riemann solvers and their \mathbf{L}_{loc}^1 -continuity. A case study describing the qualitative features of the solutions is also presented.

In [10], we consider the constrained phase transition model with metastable phase. We prove the existence of a weak solutions in the class of function with bounded variation. The result is obtained via the Wave Front Tracking method. We point out that the main theorem distinguish two cases, namely when the constraint q is higher or lower than the flux related to minimal density in the congested phase. However, the latter case requires supplementary conditions. It is worth mentioning that the solutions satisfy the entropy inequality with entropy pairs introduced in [11].

The two conference proceedings [34, 43] concern traffic flow models on networks. The first is a generalization of the paper [35] to the case of the junction. The latter focuses on the LWR model with moving bottleneck. Both papers have a similar structure, namely, they define admissible solutions to the Riemann problem at the junction and introduce Riemann solvers generalized to the case of traffic networks. At last, we present a case study to give an intuition of solving the simple problems.

Macroscopic models

2.1 Introduction

This chapter is devoted to macroscopic traffic flow models. Their purpose is to describe the dynamics of traffic flow by using variables aggregated over road sections. We distinguish three main variables, namely (mean) density, (mean) velocity and (mean) flow, whose derivation is shown in Section 1.4. Macroscopic models are relatively simple and by that allow to real-time simulations of large traffic volumes and traffic on road networks. On the other hand, they are complex enough to capture traffic flow phenomena. Moreover, macroscopic models are able to reproduce important features like formation and dissipation of traffic queues or appearing of shocks. With that being said, macroscopic models are very applicable to controlling, predicting and optimizing traffic flow.

The available literature extensively describes the different approaches to macroscopic modelling. The traffic flow community actively develops new tools, both analytical and numerical, to solve problems motivated by real-life applications. In this section, we focus on issues related to the author's work during his doctoral studies. For information on different approaches we refer to state-of-art reports [9, 72, 78, 84] and books [48, 60, 82].

2.2 LWR model

The simplest and most widespread first order macroscopic model was derived by Lighthill and Witham [68] and independently Richards [81]. The dynamics of traffic is represented by a conservation of the number of cars equation, namely scalar conservation law

$$\partial_t \rho + \partial_x f(\rho) = 0, \quad (2.1)$$

where $\rho = \rho(t, x)$ is the (mean) density at time $t \geq 0$ and position $x \in \mathbb{R}$, $f \doteq \rho v$ is the flux and $v \doteq v(\rho)$ is the (mean) velocity. Equation (2.1) represents the fact that vehicles are neither created nor destroyed on a the road without entrances and exits. We recall that roads with entrances or exists could be considered by adding a source term, see for instance [8] and the references therein.

The equation is completed by a velocity-density relation $v = v(\rho)$. It implies that a traffic moves along an equilibrium curve $\{(\rho, v(\rho)) : \rho \in [0, R]\}$. This assumption does not match to the reality. It has been shown that for congested roads traffic flow data is more likely represented on (ρ, f) -plane by a cloud of points rather than a simple curve. Furthermore, it implies that a small change of the density causes an instantaneous change of velocity. Non-equilibrium models overcome this drawback by considering velocity as a fundamental variable, see for instance Section 2.3.

Whatsoever, in equilibrium models, only one averaged car population is considered. In reality, the roads are occupied, among others, both by fast (almost racing) cars and slow ones dedicated to city driving. For this reason the assumption that they share, for instance, the same maximal velocity seems to be disputable. For generalization to multi-class we refer the reader to [13].

The last issue we mention about assumptions of LWR model is that the overtaking is not allowed. A generalization to multi-lane case can be found in [24].

In the theory of traffic flow modelling it is convenient to consider the graph of the flux function $f(\rho) = \rho v(\rho)$, which is called fundamental diagram. Throughout the thesis we assume that the velocity and flux functions satisfy:

- $[0, R] \ni \rho \mapsto v(\rho) \in [0, \mathbf{v}_{\max}]$ is a non-increasing Lipschitz function such that $v(R) = 0$ and $v(0) = \mathbf{v}_{\max}$. (V)

- $[0, R] \ni \rho \mapsto f(\rho) \doteq \rho v(\rho) \in [0, f_{\max}]$ is a bell-shaped function, namely (F)
there exists $\rho_{\text{crit}} \in (0, R)$ such that $f'(\rho)(\rho - \rho_{\text{crit}}) \geq 0$ for a.e. $\rho \in [0, R]$.

The flux function f is not necessarily continuous; for models with discontinuous flux function we refer the reader to [41, 71]. By assumptions (V), (F) there exists maximal flow f_{\max} achieved at some "critical" density $\rho_{\text{crit}} \in (0, R)$, that is

$$f_{\max} = f(\rho_{\text{crit}}) = \rho_{\text{crit}} v(\rho_{\text{crit}}),$$

and moreover we have $f(0) = f(R) = 0$. The maximal flow f_{\max} is also known as a capacity flow. The critical density ρ_{crit} divides the fundamental diagram into two particular regions - free flow regime for $\rho \in [0, \rho_{\text{crit}}]$ and congested flow regime for $\rho \in (\rho_{\text{crit}}, R]$, see Figure 2.1. Observe that it is possible to have the same flow for different regimes and therefore for different velocities.

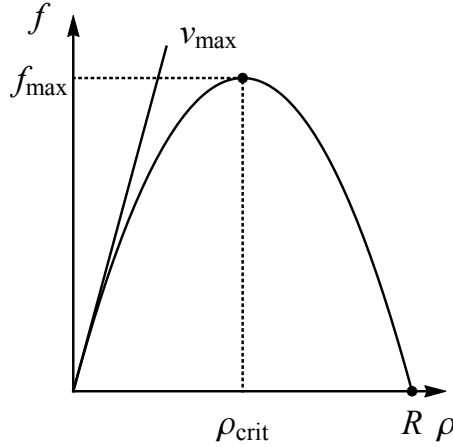


Figure 2.1: Fundamental diagram for the LWR model.

The expression of the velocity function v is chosen in order to fit best experimental data coming from the road under consideration. In the literature one may find the following expressions for the velocity functions satisfying (V), (F):

$$\text{Greenshields [54]} : \quad v(\rho) = v_{\max} - \frac{v_{\max}}{R} \rho, \quad (2.2)$$

$$\text{Daganzo [33]} : \quad v(\rho) = \begin{cases} v_{\max} & \text{if } \rho \in [0, \rho_{\text{crit}}), \\ \frac{\rho_{\text{crit}} v_{\max}}{R - \rho_{\text{crit}}} \left(\frac{R}{\rho} - 1 \right) & \text{if } \rho \in [\rho_{\text{crit}}, R], \end{cases} \quad (2.3)$$

$$\text{Smulders [83]} : \quad v(\rho) = \begin{cases} v_{\max} - \frac{v_{\max} - v_c}{\rho_{\text{crit}}} \rho & \text{if } \rho \in [0, \rho_{\text{crit}}), \\ \frac{\rho_{\text{crit}} v_{\max}}{R - \rho_{\text{crit}}} \left(\frac{R}{\rho} - 1 \right) & \text{if } \rho \in [\rho_{\text{crit}}, R], \end{cases} \quad (2.4)$$

for some $\rho_{\text{crit}} \in (0, R)$. Observe that the Greenshields' velocity (2.2) is expressed by a single linear, strictly decreasing function. Daganzo's velocity (2.3) is represented by a piecewise function such that the corresponding flux $f(\rho) = \rho v(\rho)$ is piecewise linear, with increasing part for low densities $[0, \rho_{\text{crit}})$ and decreasing part for high densities $[\rho_{\text{crit}}, R]$. The Smulders velocity function (2.4) is given by a decreasing linear function for low densities, while for high densities it has the same expression as Daganzo's velocity.

2.2.1 The Riemann solver $\mathcal{RS}_{\text{LWR}}$

In the theory of non-linear conservation laws has been shown, for example by the method of characteristics [18, 31], that even for smooth initial datum the solution may develop discontinuities (such as shocks) in finite time. Therefore it is convenient to consider problems with discontinuous initial data.

Let us study Riemann problems for the LWR model (2.1), namely the simplest Cauchy problem with Heavyside-like initial datum

$$\partial_t \rho + \partial_x f(\rho) = 0, \quad \rho(0, x) = \begin{cases} \rho_\ell & \text{if } x < 0, \\ \rho_r & \text{if } x \geq 0. \end{cases} \quad (2.5)$$

Below we give the detailed definition of the classical Riemann solver

$$\mathcal{RS}_{\text{LWR}} : [0, R]^2 \rightarrow \mathbf{C}^0(\mathbb{R}_+; \mathbf{BV}(\mathbb{R}; [0, R]))$$

corresponding to Riemann problem (2.5) for the case of \mathbf{C}^2 strictly concave flux functions and for the case corresponding to the Daganzo's velocity (2.3). We defer the reader to [1, 6, 18, 31] for informations about more general flux functions. We recall that $\mathcal{RS}_{\text{LWR}}$ associates to any initial datum $\rho_\ell, \rho_r \in [0, R]$ a self-similar solution $\rho(t, x) = \mathcal{RS}_{\text{LWR}}[\rho_\ell, \rho_r](x/t)$.

Definition 2.1. *Assume (\mathbf{V}) , (\mathbf{F}) and that f is a \mathbf{C}^2 strictly concave function.*

Then the Riemann solver $\mathcal{RS}_{\text{LWR}}: [0, R]^2 \rightarrow \mathbf{C}^0(\mathbb{R}_+; \mathbf{BV}(\mathbb{R}; [0, R]))$ is defined as follows:

(R.1) If $\rho_\ell < \rho_r$, then $\mathcal{RS}_{\text{LWR}}[\rho_\ell, \rho_r]$ is the shock wave

$$\mathcal{RS}_{\text{LWR}}[\rho_\ell, \rho_r](\xi) = \begin{cases} \rho_\ell & \text{if } \xi < \sigma(\rho_\ell, \rho_r), \\ \rho_r & \text{if } \xi \geq \sigma(\rho_\ell, \rho_r), \end{cases} \quad (2.6)$$

where the speed $\sigma(\rho_\ell, \rho_r)$ of propagation of the discontinuity satisfies the Rankine-Hugoniot condition

$$\sigma(\rho_\ell, \rho_r)(\rho_\ell - \rho_r) = f(\rho_\ell) - f(\rho_r). \quad (2.7)$$

(R.2) If $\rho_\ell \geq \rho_r$, then $\mathcal{RS}_{\text{LWR}}[\rho_\ell, \rho_r]$ is the rarefaction wave

$$\mathcal{RS}_{\text{LWR}}[\rho_\ell, \rho_r](\xi) = \begin{cases} \rho_\ell & \text{if } \xi < f'(\rho_\ell), \\ (f')^{-1}(\xi) & \text{if } f'(\rho_\ell) \leq \xi < f'(\rho_r), \\ \rho_r & \text{if } \xi \geq f'(\rho_r). \end{cases} \quad (2.8)$$

Observe that, from geometrical point of view, $\sigma(\rho_\ell, \rho_r)$ is the slope of the straight line passing through $(\rho_\ell, f(\rho_\ell))$ and $(\rho_r, f(\rho_r))$.

Definition 2.2. Assume **(V)**, **(F)** and that v is the Daganzo's velocity (2.3). Then the Riemann solver $\mathcal{RS}_{\text{LWR}}: [0, R]^2 \rightarrow \mathbf{C}^0(\mathbb{R}_+; \mathbf{BV}(\mathbb{R}; [0, R]))$ is defined as follows:

(R.1) If $\rho_\ell, \rho_r \in [0, \rho_{\text{crit}}]$, then $\mathcal{RS}_{\text{LWR}}[\rho_\ell, \rho_r]$ is the contact discontinuity wave

$$\mathcal{RS}_{\text{LWR}}[\rho_\ell, \rho_r](\xi) = \begin{cases} \rho_\ell & \text{if } \xi < \mathbf{v}_{\text{max}}, \\ \rho_r & \text{if } \xi \geq \mathbf{v}_{\text{max}}. \end{cases} \quad (2.9)$$

(R.2) If $\rho_\ell, \rho_r \in [\rho_{\text{crit}}, R]$, then $\mathcal{RS}_{\text{LWR}}[\rho_\ell, \rho_r]$ is the contact discontinuity wave

$$\mathcal{RS}_{\text{LWR}}[\rho_\ell, \rho_r](\xi) = \begin{cases} \rho_\ell & \text{if } \xi < -\frac{\rho_{\text{crit}} \mathbf{v}_{\text{max}}}{R - \rho_{\text{crit}}}, \\ \rho_r & \text{if } \xi \geq -\frac{\rho_{\text{crit}} \mathbf{v}_{\text{max}}}{R - \rho_{\text{crit}}}. \end{cases}$$

(R.3) If $\rho_r < \rho_{\text{crit}} < \rho_\ell$, then $\mathcal{RS}_{\text{LWR}}[\rho_\ell, \rho_r]$ is the juxtaposition of two contact

discontinuity waves

$$\mathcal{RS}_{\text{LWR}}[\rho_\ell, \rho_r](\xi) = \begin{cases} \rho_\ell & \text{if } \xi < \frac{\rho_{\text{crit}} \mathbf{v}_{\text{max}}}{R - \rho_{\text{crit}}}, \\ \rho_{\text{crit}} & \text{if } \frac{\rho_{\text{crit}} \mathbf{v}_{\text{max}}}{R - \rho_{\text{crit}}} \leq \xi < \mathbf{v}_{\text{max}}, \\ \rho_r & \text{if } \xi \geq \mathbf{v}_{\text{max}}. \end{cases}$$

(R.4) *If $\rho_\ell < \rho_{\text{crit}} < \rho_r$ then $\mathcal{RS}_{\text{LWR}}[\rho_\ell, \rho_r]$ is the shock wave given in (2.6), (2.7).*

Example 2.1. *Consider a barrier on the grade crossing placed at $x = 0$, which is closed at initial time $t = 0$. For simplicity let f be the flux function corresponding to Greenshields velocity (2.2) with $R = 1 = \mathbf{v}_{\text{max}}$, namely $f(\rho) = \rho(1 - \rho)$. Initially the traffic in $x < 0$ has density $\rho_\ell \in (0, 1)$ and velocity $v(\rho_\ell) = 1 - \rho_\ell$. The corresponding initial condition takes the form*

$$\rho(0, x) = \begin{cases} \rho_\ell & \text{if } x < 0, \\ 1 & \text{if } x > 0. \end{cases}$$

The above choice for $\rho_r = 1$ is to reproduce the effect in $x < 0$ of the closed barrier. Since $\rho_\ell < \rho_r = 1$, by (2.6) the solution is the shock wave

$$\rho(t, x) = \begin{cases} \rho_\ell & \text{if } x < \sigma(\rho_\ell, \rho_r) t, \\ 1 & \text{if } x \geq \sigma(\rho_\ell, \rho_r) t, \end{cases} \quad (2.10)$$

where $\sigma(\rho_\ell, \rho_r) < 0$ is given in (2.7).

The solution (2.10) represents a process of traffic jam formation with the discontinuity line $x = \sigma(\rho_\ell, \rho_r)t$ separating still moving vehicles from those already caught in the traffic jam.

A vehicle starting at the point $x(0) = x_0 < 0$ at time $t = 0$ has the following properties:

$$\text{position: } x(t) = \begin{cases} x_0 + v(\rho_\ell) t & \text{if } t < t_1, \\ \sigma(\rho_\ell, \rho_r) t_1 & \text{if } t \geq t_1, \end{cases}$$

$$\text{velocity: } x'(t) = \begin{cases} v(\rho_\ell) & \text{if } t < t_1, \\ 0 & \text{if } t \geq t_1, \end{cases}$$

$$\text{acceleration: } x''(t) \equiv 0,$$

where by definition

$$\sigma(\rho_\ell, \rho_r) = -\rho_\ell, \quad v(\rho_\ell) = 1 - \rho_\ell, \quad t_1 = -\frac{x_0}{v(\rho_\ell) - \sigma(\rho_\ell, \rho_r)} = -x_0.$$

Example 2.2. Let us consider here the same setting of the previous example, however with the assumption that the barrier opens at $t = 0$. The traffic in $x < 0$ has maximal density, while in $x > 0$ there are no cars, namely $\rho_\ell = 1$ and $\rho_r = 0$. In this case the initial condition takes the form

$$\rho(0, x) = \begin{cases} 1 & \text{if } x < 0, \\ 0 & \text{if } x \geq 0. \end{cases}$$

By (2.8) the solution is the rarefaction wave

$$\rho(t, x) = \begin{cases} 1 & \text{if } x < -t, \\ \frac{1}{2} \left(1 - \frac{x}{t}\right) & \text{if } -t \leq x < t, \\ 0 & \text{if } x \geq t. \end{cases}$$

From the modelling point of view, a rarefaction wave describes traffic acceleration and simultaneously gradual decrease of traffic density.

Again, consider the vehicle starting at $t = 0$ from $x_0 < 0$. Observe that this particular vehicle is stuck in the traffic jam until $t_1 = x_0/f'(\rho_\ell) = -x_0$. Then its trajectory $t \mapsto x(t)$ is given by the solution of the Cauchy problem

$$x'(t) = v(\rho(t, x(t))) = \frac{1}{2} \left(1 + \frac{x(t)}{t}\right), \quad x(t_1) = x_0.$$

The properties of the vehicle are the following:

$$\begin{aligned} \text{position:} & & x(t) &= \begin{cases} x_0 & \text{if } t < t_1, \\ t - 2\sqrt{t_1 t} & \text{if } t \geq t_1, \end{cases} \\ \text{velocity:} & & x'(t) &= \begin{cases} 0 & \text{if } t < t_1, \\ 1 - \sqrt{\frac{t_1}{t}} & \text{if } t \geq t_1, \end{cases} \end{aligned}$$

$$\text{acceleration:} \quad x''(t) = \begin{cases} 0 & \text{if } t < t_1, \\ \frac{1}{2t} \sqrt{\frac{t_1}{t}} & \text{if } t \geq t_1. \end{cases}$$

2.2.2 Drawbacks of the LWR model

The LWR model performs fairly well in some basic road situations. However, in most of the real situations car traffic is complex and simple models might not be able to reproduce important effects. In the articles [32, 69, 75] were listed some drawbacks of LWR model, what we give below:

- Vehicles are supposed to reach new velocity immediately after the change of a road density. The lack of any delay related to drivers' reaction implies an infinite acceleration.
- The LWR model (with passing allowed) does not recognize the distribution of desired velocities for light traffic but only the desired velocity of each vehicle. The velocity distribution across vehicles tends to spread a platoon linearly with time, while the variation within each vehicle with the square root of time.
- In contrast to reality, the transition from the free flow regime to the congested regime always occurs at the same density. This leads to the same outflow after breakdown.
- The velocity of the traffic depends only on the density what is empirically shown to be wrong. Moreover, only one velocity corresponds to a certain density.
- Equilibrium traffic flow models do not characterize the amplification of small disturbances in heavy traffic, called phantom jams [45, 56].
- Equilibrium models do not perform hysteresis phenomena, that is asymmetry between acceleration and deceleration behavior of driver-vehicle units. It is caused by retarded recovery of speed in deceleration-acceleration process.

2.3 ARZ model

To overcome drawbacks of LWR (2.1) and Payne-Whitham (1.3), (1.4) models, Aw and Rascle [7], and independently Zhang [85] proposed a new second order

model (ARZ). The model states the conservation of the total number cars and the conservation of the generalized momentum.

In this section, we first present the ARZ model both in conservative coordinates Y and Riemann invariants coordinates W . The reason for providing W coordinates is due to indefiniteness of the system in conservation form at the vacuum. The Riemann invariant coordinates are also handy to calculate total variation estimates and provide easy geometrical interpretations for solutions to Riemann problems. Next, we give the corresponding Riemann solver in W -coordinates. At last, we define weak and entropy solutions.

2.3.1 ARZ model in Riemann invariant coordinates

The ARZ model takes the form

$$\begin{cases} \partial_t \rho + \partial_x(\rho v) = 0, \\ \partial_t(v + p(\rho)) + v \partial_x(v + p(\rho)) = 0. \end{cases} \quad (2.11)$$

Above $\rho = \rho(t, x)$ and $v = v(t, x)$ are density and velocity functions at time $t \geq 0$ and position $x \in \mathbb{R}$, while $p(\rho)$ represents the anticipation factor accounting for drivers' reaction to the state of traffic downstream. We assume that

$$p(0) = 0 \quad \text{and} \quad p(\rho) > 0, \quad p'(\rho) > 0, \quad 2p'(\rho) + \rho p''(\rho) > 0 \quad \text{for any } \rho > 0. \quad (2.12)$$

Typical choice is $p(\rho) = \rho^\gamma$, $\gamma > 0$, see [7].

By assumption **(A.1)**, reasonable traffic flow models have to be expressed by hyperbolic systems of conservation laws. We show now that (2.11) can be rewritten as a hyperbolic systems of conservation laws. By multiplying the first equation of (2.11) by $v + p(\rho)$ and by adding the second equation in (2.11) multiplied by ρ we obtain

$$\partial_t y + \partial_x(vy) = 0,$$

where $y \doteq \rho(v + p(\rho))$ is the generalized momentum. As a result, system (2.11) is equivalent to the system of conservation laws

$$\partial_t Y + \partial_x F(Y) = 0, \quad (2.13)$$

with

$$Y \doteq (\rho, y)^T \in \mathbb{R}_+^2 \setminus \{0\}, \quad F(Y) \doteq \begin{bmatrix} y \\ \rho - p(\rho) \end{bmatrix} Y.$$

The Jacobian matrix of the flux function $F(Y)$ is given by

$$A(Y) = DF(Y) = \begin{pmatrix} -p(\rho) - \rho p'(\rho) & 1 \\ -\frac{y^2}{\rho^2} - yp'(\rho) & \frac{2y}{\rho} - p(\rho) \end{pmatrix}.$$

The eigenvalues of $A(Y)$ are

$$\lambda_1(Y) \doteq \frac{y}{\rho} - p(\rho) - \rho p'(\rho), \quad \lambda_2(Y) \doteq \frac{y}{\rho} - p(\rho),$$

with corresponding eigenvectors

$$r_1(Y) = Y, \quad r_2(Y) = (\rho, y + p^2 p'(\rho))^T.$$

By the assumptions in (2.12) we have that $\lambda_1(Y) < \lambda_2(Y)$ for every $\rho > 0$, so system (2.13) is hyperbolic away from the vacuum.

By direct computations we obtain

$$\nabla \lambda_1(Y) \cdot r_1(Y) = -\rho(2p'(\rho) + \rho p''(\rho)) < 0, \quad \nabla \lambda_2(Y) \cdot r_2(Y) = 0,$$

namely the first characteristic field is genuinely non-linear, while the second characteristic field is linearly degenerate.

We recall that the speed of propagation $\sigma \doteq \sigma(Y_\ell, Y_r)$ of any discontinuity (Y_ℓ, Y_r) satisfies the Rankine-Hugoniot conditions

$$(Y_r - Y_\ell) \sigma = F(Y_r) - F(Y_\ell). \quad (2.14)$$

In order to construct elementary waves, we use the Riemann invariant coordinates $U \doteq (v, w)^T$, which by definition [66] satisfies

$$\nabla_Y v \cdot r_2 \equiv 0, \quad \nabla_Y w \cdot r_1 \equiv 0.$$

Away from the vacuum $\rho = 0$ the Riemann invariant coordinates U are linked to the conservative coordinates Y by the identities

$$\begin{aligned} Y(U) &\doteq \begin{pmatrix} \rho(U) \\ y(U) \end{pmatrix} \doteq \begin{pmatrix} p^{-1}(w-v) \\ p^{-1}(w-v)w \end{pmatrix}, \\ U(Y) &\doteq \begin{pmatrix} v(Y) \\ w(Y) \end{pmatrix} = \begin{pmatrix} \frac{y}{\rho} - p(\rho) \\ \frac{y}{\rho} \end{pmatrix}. \end{aligned}$$

We recall that w is a Lagrangian marker. The Riemann invariant coordinates U are a good choice because in this coordinates the total variation of the solution does not increase in time [44].

For any element U of the space $\mathcal{U} \doteq \{U \in \mathbf{R}_+^2 : v \leq w\}$ we can define the corresponding density $\rho(U) \doteq p^{-1}(w-v)$, generalized momentum $y(U) \doteq p^{-1}(w-v)w$ and flow $f(U) \doteq p^{-1}(w-v)v$. The vacuum state $\rho = 0$ is described by a half-line $\mathcal{U}_0 \doteq \{U \in \mathcal{U} : v = w\}$ and non-vacuum state by $\mathcal{U}_0^c \doteq \mathcal{U} \setminus \mathcal{U}_0$.

2.3.2 The Riemann solver $\mathcal{RS}_{\text{ARZ}}$

In this section we present the Riemann solver for ARZ model (2.11). Consider Riemann problem

$$\begin{cases} \partial_t \rho + \partial_x f(U) = 0, \\ \partial_t w + v \partial_x w = 0, \\ U(0, x) = U_0(x), \end{cases} \quad (2.15)$$

with Riemann initial datum

$$U_0(x) = \begin{cases} U_\ell & \text{if } x < 0, \\ U_r & \text{if } x \geq 0, \end{cases} \quad (2.16)$$

where $U_\ell, U_r \in \mathcal{U}$ are constants.

Before we introduce elementary waves, let consider the inverse function $\Pi \in \mathbf{C}^0(\mathbb{R}_+; \mathbb{R}_+) \cap \mathbf{C}^1((0, +\infty); \mathbb{R}_+)$ of the function $\rho \mapsto p(\rho) + \rho p'(\rho)$. By the assumptions in (2.12) we have that $\Pi(0) = 0$ and Π is strictly increasing. The Riemann

solver $\mathcal{RS}_{\text{ARZ}}$ for problem (2.15), (2.16)

$$\begin{aligned} \mathcal{RS}_{\text{ARZ}} & : \quad \mathcal{U} \times \mathcal{U} & \rightarrow & \quad \mathbf{C}^0((0, +\infty); \mathbf{L}_{\text{loc}}^1(\mathbb{R}; \mathcal{U})), \\ & (U_\ell, U_r) & \mapsto & \quad \mathcal{RS}_{\text{ARZ}}[U_\ell, U_r], \end{aligned}$$

can be described in terms of the following three elementary waves.

- Take $U_\ell = (v_\ell, w_\ell)^T \in \mathcal{U}$, $U_r = (v_r, w_r)^T \in \mathcal{U}_0^c$, with $w_\ell = w_r$ and $v_r < v_\ell$. The elementary wave joining U_ℓ with U_r is the shock wave

$$S[U_\ell, U_r](\xi) \doteq \begin{cases} U_\ell & \text{if } \xi < \sigma(U_\ell, U_r), \\ U_r & \text{if } \xi > \sigma(U_\ell, U_r), \end{cases}$$

where

$$\sigma(U_\ell, U_r) \doteq \frac{f(U_r) - f(U_\ell)}{\rho(U_r) - \rho(U_\ell)}.$$

- Take $U_\ell \in \mathcal{U}_0^c$, $U_r \in \mathcal{U}$, with $w_\ell = w_r$ and $v_\ell < v_r$. The elementary wave joining U_ℓ with U_r is the rarefaction wave

$$R[U_\ell, U_r](\xi) \doteq \begin{cases} U_\ell & \text{if } \xi < \lambda_1(U_\ell), \\ \begin{pmatrix} w - p(\Pi(w - \xi)) \\ w \end{pmatrix} & \text{if } \lambda_1(U_\ell) < \xi < \lambda_1(U_r), \\ U_r & \text{if } \xi > \lambda_1(U_r), \end{cases}$$

where

$$\lambda_1(U) \doteq \begin{cases} v - \rho(U) p'(\rho(U)) & \text{if } U \in \mathcal{U}_0^c, \\ w & \text{if } U \in \mathcal{U}_0. \end{cases}$$

- Take $U_\ell, U_r \in \mathcal{U}_0^c$, with $w_\ell \neq w_r$ and $v_\ell = v_r$. The elementary wave joining U_ℓ with U_r is the contact discontinuity wave

$$C[U_\ell, U_r](\xi) \doteq \begin{cases} U_\ell & \text{if } \xi < v_{\ell,r}, \\ U_r & \text{if } \xi > v_{\ell,r}. \end{cases}$$

We stress that both shocks and contact discontinuities satisfy the Rankine-Hugoniot conditions (2.14). Indeed, any discontinuity (U_ℓ^*, U_r^*) with speed of prop-

agation $\sigma^* = \sigma(U_\ell^*, U_r^*)$ satisfies the Rankine-Hugoniot conditions (2.14), which in the U -coordinates take the form

$$\rho(U_r^*)(\sigma^* - v_r^*) = \rho(U_\ell^*)(\sigma^* - v_\ell^*), \quad \rho(U_r^*)(\sigma^* - v_r^*)w_r^* = \rho(U_\ell^*)(\sigma^* - v_\ell^*)w_\ell^*. \quad (2.17)$$

In particular away from the vacuum, namely for $U_\ell^*, U_r^* \in \mathcal{U}_0^c$, by (2.17) either $w_\ell^* = w_r^*$ or $v_\ell^* = \sigma^* = v_r^*$, which correspond to respectively shock and contact discontinuities waves.

Definition 2.3. For any $U_\ell = (v_\ell, w_\ell)^T, U_r = (v_r, w_r)^T \in \mathcal{U}$ with $U_\ell \neq U_r$ and $(U_\ell, U_r) \in \mathcal{U} \times \mathcal{U}$, we define $\mathcal{RS}_{\text{ARZ}}[U_\ell, U_r]$ as follows:

1. If $U_r \in \mathcal{U}_0^c$, $w_\ell = w_r$ and $v_r < v_\ell$, then $\mathcal{RS}_{\text{ARZ}}[U_\ell, U_r] \equiv \mathbf{S}[U_\ell, U_r]$.
2. If $U_\ell \in \mathcal{U}_0^c$, $w_\ell = w_r$ and $v_\ell < v_r$, then $\mathcal{RS}_{\text{ARZ}}[U_\ell, U_r] \equiv \mathbf{R}[U_\ell, U_r]$.
3. If $U_\ell, U_r \in \mathcal{U}_0^c$ and $v_\ell = v_r$, then $\mathcal{RS}_{\text{ARZ}}[U_\ell, U_r] \equiv \mathbf{C}[U_\ell, U_r]$.
4. If $U_\ell \in \mathcal{U}_0$ and $U_r \in \mathcal{U}_0^c$ with $w_\ell = w_r$, then

$$\mathcal{RS}_{\text{ARZ}}[U_\ell, U_r](\xi) = \begin{cases} U_\ell & \text{if } \xi < v_r, \\ U_r & \text{if } \xi > v_r. \end{cases}$$

5. If $U_\ell, U_r \in \mathcal{U}_0^c$ and $v_r < v_\ell < w_\ell$, then $\mathcal{RS}_{\text{ARZ}}[U_\ell, U_r]$ is the juxtaposition of $\mathbf{S}[U_\ell, U_m]$ and $\mathbf{C}[U_m, U_r]$, where $U_m = (v_r, w_\ell)^T \in \mathcal{U}_0^c$.
6. If $U_\ell, U_r \in \mathcal{U}_0^c$ and $v_\ell < v_r < w_\ell$, then $\mathcal{RS}_{\text{ARZ}}[U_\ell, U_r]$ is the juxtaposition of $\mathbf{R}[U_\ell, U_m]$ and $\mathbf{C}[U_m, U_r]$, where $U_m = (v_r, w_\ell)^T \in \mathcal{U}_0^c$.
7. If $U_\ell, U_r \in \mathcal{U}_0^c$ and $v_\ell < w_\ell \leq v_r < w_r$, then

$$\mathcal{RS}_{\text{ARZ}}[U_\ell, U_r](\xi) = \begin{cases} \mathbf{R}[U_\ell, U_m](\xi) & \text{if } \xi < v_r, \\ U_r & \text{if } \xi > v_r, \end{cases}$$

where $U_m = (w_\ell, w_\ell)^T \in \mathcal{U}_0$.

8. If $U_\ell \in \mathcal{U}_0^c$, $U_r \in \mathcal{U}_0$ and $w_\ell = w_r$, then $\mathcal{RS}_{\text{ARZ}}[U_\ell, U_r] \equiv \mathbf{R}[U_\ell, U_r]$.

9. If $U_\ell \in \mathcal{U}_0^c$, $U_r \in \mathcal{U}_0$ and $w_\ell \neq w_r$, we can define $\mathcal{RS}_{\text{ARZ}}[U_\ell, U_r] \equiv \mathbf{R}[U_\ell, U_m]$, where $U_m = (w_\ell, w_\ell)^T \in \mathcal{U}_0$.

At last, we define $\mathcal{RS}_{\text{ARZ}}[U_*, U_*] \equiv U_*$ for any $U_* \in \mathcal{U}$.

Remark 2.1. For any $U_\ell = (v_*, w_*)^T \in \mathcal{U}_0^c$ and $U_r = (v_*, v_*)^T \in \mathcal{U}_0$ then both

$$\begin{cases} U_\ell & \text{if } x < v_* t, \\ U_r & \text{if } x > v_* t, \end{cases}$$

and

$$\begin{cases} \mathbf{R}[U_\ell, U_m](x/t) & \text{if } x < w_* t, \\ U_r & \text{if } x > w_* t, \end{cases} \quad U_m = (w_*, w_*)^T \in \mathcal{U}_0,$$

are weak solutions for the corresponding Riemann problem. However, as already observed by Aw and Rascle [7], only the first solution is physically reasonable. This justifies the choice of the item **9.** in Definition 2.3.

2.3.3 Weak and entropy solutions

In this section we introduce the definition of solutions of the Cauchy problem

$$\begin{cases} \partial_t \rho + \partial_x(\rho v) = 0, \\ \partial_t w + v \partial_x w = 0, \\ U(0, x) = U_0(x), \end{cases} \quad (2.18)$$

where the initial datum U_0 is assumed to be in $\mathbf{L}^\infty(\mathbb{R}; \mathcal{U})$. Let $V_0 \doteq \|U_0\|_\infty$. We extend the flux F to the whole of \mathbb{R}_+ by taking $F(0) \doteq 0$.

Definition 2.4. Let $U_0 \in \mathbf{L}^\infty(\mathbb{R}; \mathcal{U})$. We say that a function

$$U \in \mathbf{L}^\infty(\mathbb{R}_+ \times \mathbb{R}; \mathcal{U}) \cap \mathbf{C}^0(\mathbb{R}_+; \mathbf{L}_{\text{loc}}^1(\mathbb{R}; \mathcal{U}))$$

is a weak solution of (2.18) if it satisfies the initial condition (2.18)₃ for a.e. $x \in \mathbb{R}$ and for any test function $\phi \in \mathbf{C}_c^\infty((0, +\infty) \times \mathbb{R}; \mathbb{R})$

$$\iint_{\mathbb{R}_+ \times \mathbb{R}} \rho(U) (\partial_t \phi + v \partial_x \phi) \begin{pmatrix} 1 \\ w \end{pmatrix} dx dt = 0.$$

Proposition 2.1 ([4]). *For any $(U_\ell, U_r) \in \mathcal{U} \times \mathcal{U}$ we have that*

$$U(t, x) \doteq \mathcal{RS}_{\text{ARZ}}[U_\ell, U_r](x/t)$$

is a weak solution of (2.18) with Riemann initial condition (2.16).

Conservation laws admit in general more than one weak solution. This motivates the introduction of an additional selection criterion, the so called entropy condition [66, 70]. As suggested in [4] we consider entropy pairs $(\mathcal{E}_k, \mathcal{Q}_k)$ defined for any fixed $k > 0$ as

$$\begin{aligned} \mathcal{E}_k(U) &= \begin{cases} 0 & \text{if } v \leq k, \\ 1 - \frac{p^{-1}(w-v)}{p^{-1}(w-k)} & \text{if } v > k, \end{cases} \\ \mathcal{Q}_k(U) &= \begin{cases} 0 & \text{if } v \leq k, \\ k - \frac{f(U)}{p^{-1}(w-k)} & \text{if } v > k. \end{cases} \end{aligned} \quad (2.19)$$

Definition 2.5 (Entropy solution for the ARZ model). *Fix $U_0 \in \mathbf{L}^\infty(\mathbb{R}; \mathcal{U})$. Let $U \in \mathbf{L}^\infty(\mathbb{R}_+ \times \mathbb{R}; \mathcal{U}) \cap \mathbf{C}^0(\mathbb{R}_+; \mathbf{L}_{\text{loc}}^1(\mathbb{R}; \mathcal{U}))$ be a weak solution of (2.18) in the sense of Definition 2.4. We say that U is an entropy solution if for any non-negative test function $\phi \in \mathbf{C}_c^\infty((0, +\infty) \times \mathbb{R}; \mathbb{R})$ and for any entropy pair (2.19) we have*

$$\iint_{\mathbb{R}_+ \times \mathbb{R}} \left(\mathcal{E}_k(U) \partial_t \phi + \mathcal{Q}_k(U) \partial_x \phi \right) dx dt \geq 0, \quad k \in (0, +\infty).$$

2.4 PT models

In this subsection we consider phase transition (PT) models of hyperbolic conservation laws for vehicular traffic. According to experimental data, the vehicular traffic flow acts differently depending on whether is free or congested. This leads to consider two regimes: free-flow phase Ω_f and congested phase Ω_c . The free-flow regime corresponds to low densities and can be approximated by a one-dimensional flux function, while the congested regime refers to high densities and the flow covers a two-dimensional domain, see [28, Figure 1.1] or [15, Figure 3.1]. Consequently, the traffic can be well described as a coupling of first order model (a scalar PDE)

in the free-flow regime and a second order model (a 2×2 system of PDEs) in the congested regime.

This two-phase approach was first introduced by Colombo in [28] and after exploited by other authors in [11, 14, 15, 53]. For instance, in [53] Goatin couples LWR model (2.1) for the free-flow phase Ω_f with ARZ model (2.13) for the congested phase Ω_c . Such model corrects drawbacks of LWR and ARZ models taken separately, see Subsection 2.2.2 and Remark 2.1.

In the paper [35] we generalize two PT models. The former one, denoted by PT^p , was studied in [11, 53] and describes the coupling of the LWR model with the ARZ model. The latter, denoted by PT^a , has been the subject of research in [14, 15] where the authors considered Greenshields' type flux functions in congested regime. The congested regime is treated there as an extension of the free flow regime. In [14, 15] the authors assume that the two phases have intersection, namely $\Omega_f \cap \Omega_c \neq \emptyset$, while in [11, 12, 53] the authors assume that $\Omega_f \cap \Omega_c = \emptyset$. In [35] we do not make any assumption on the intersection between free and congested phases. We suppose that the velocity in the free-flow regime is represented by a unique value, and coincides with the maximal velocity. This assumption is in order to avoid the loss of well-posedness, as observed in [28, Remark 2]. Therefore, in the free phase the velocity function coincides with Daganzo (2.3) velocity function. Moreover, in [14, 15] the authors assume that the flux function vanishes at a maximal density, namely that the vehicles have (almost) the same length, while in [11, 12, 53] the authors do not impose this requirement. In [35] we consider both the cases, as both are motivated by practical reasons.

2.4.1 The general PT models

In this section we recall the PT models we introduced in [35]. Throughout the thesis we ignore the superscripts p, a only when they are not necessary. The common fundamental parameters for the PT^p and the PT^a models are:

- $R > 0$ is the maximal value of the density;
- $v_{\max} > 0$ is the maximal velocity;
- $v_c \in (0, v_{\max}]$ is the maximal velocity in the congested phase.

The PT model can be written as

$$\begin{array}{cc}
 \text{Free flow} & \text{Congested flow} \\
 \left\{ \begin{array}{l} Y \doteq (\rho, y) \in \Omega_f, \\ \partial_t \rho + \partial_x f(Y) = 0, \\ v(Y) = \mathbf{v}_{\max}, \end{array} \right. & \left\{ \begin{array}{l} Y \doteq (\rho, y) \in \Omega_c, \\ \partial_t \rho + \partial_x f(Y) = 0, \\ \partial_t y + \partial_x (y v(Y)) = 0. \end{array} \right. \quad (2.20)
 \end{array}$$

Above, $\rho \in [0, R]$ is the density and y is the generalized momentum, while the domains Ω_f and Ω_c refers to the free and congested flow phases, respectively. The corresponding velocity $v(Y)$ and the flow $f(Y)$ are defined as follows:

$$v(Y) \doteq \begin{cases} v^a(Y) \doteq v_{eq}^a(\rho) (1 + y) & \text{for PT}^a, \\ v^p(Y) \doteq \frac{y}{\rho} - p(\rho) & \text{for PT}^p, \end{cases} \quad f(Y) \doteq \rho v(Y).$$

The term $(1 + y)$ in the definition of $v^a(Y)$ is a perturbation which corresponds to the thickness of fundamental diagram in the congested regime around the flux $f(\rho, 0) = \rho v_{eq}^a(\rho)$. The function $v_{eq}^a : (0, R] \rightarrow \mathbb{R}_+$ is the equilibrium velocity for PT^a model given by

$$v_{eq}^a(\rho) \doteq \left(\frac{R}{\rho} - 1 \right) \left(\frac{\mathbf{v}_{\max} r_0}{R - r_0} + a(r_0 - \rho) \right).$$

Above $a \in \mathbb{R}$ and $r_0 \in (0, R)$ are fixed parameters of the model. We point out that $v_{eq}^a(r) = \mathbf{v}_{\max}$ by definition. At last, we stress that the generalized momentum y has different physical meaning in the framework of PT^a and PT^p models.

We recall the notation and the main assumptions on the parameters discussed in [11, 15], see Figure 2.2. For PT^p we require that $p : (0, R] \rightarrow \mathbb{R}$ satisfies (2.12)

$$p(0) = 0 \quad \text{and} \quad p(\rho) > 0, \quad p'(\rho) > 0, \quad 2p'(\rho) + \rho p''(\rho) > 0 \quad \text{for any } \rho > 0.$$

Fix $y_- < y_+$ and r_{\pm}^f, r_{\pm}^c so that

$$\begin{array}{cc}
 0 < r_-^f < r_+^f < R, & v(r_{\pm}^f, r_{\pm}^f y_{\pm}/R) = \mathbf{v}_{\max}, \\
 0 < r_-^c < r_+^c < R, & v(r_{\pm}^c, r_{\pm}^c y_{\pm}/R) = \mathbf{v}_c.
 \end{array}$$

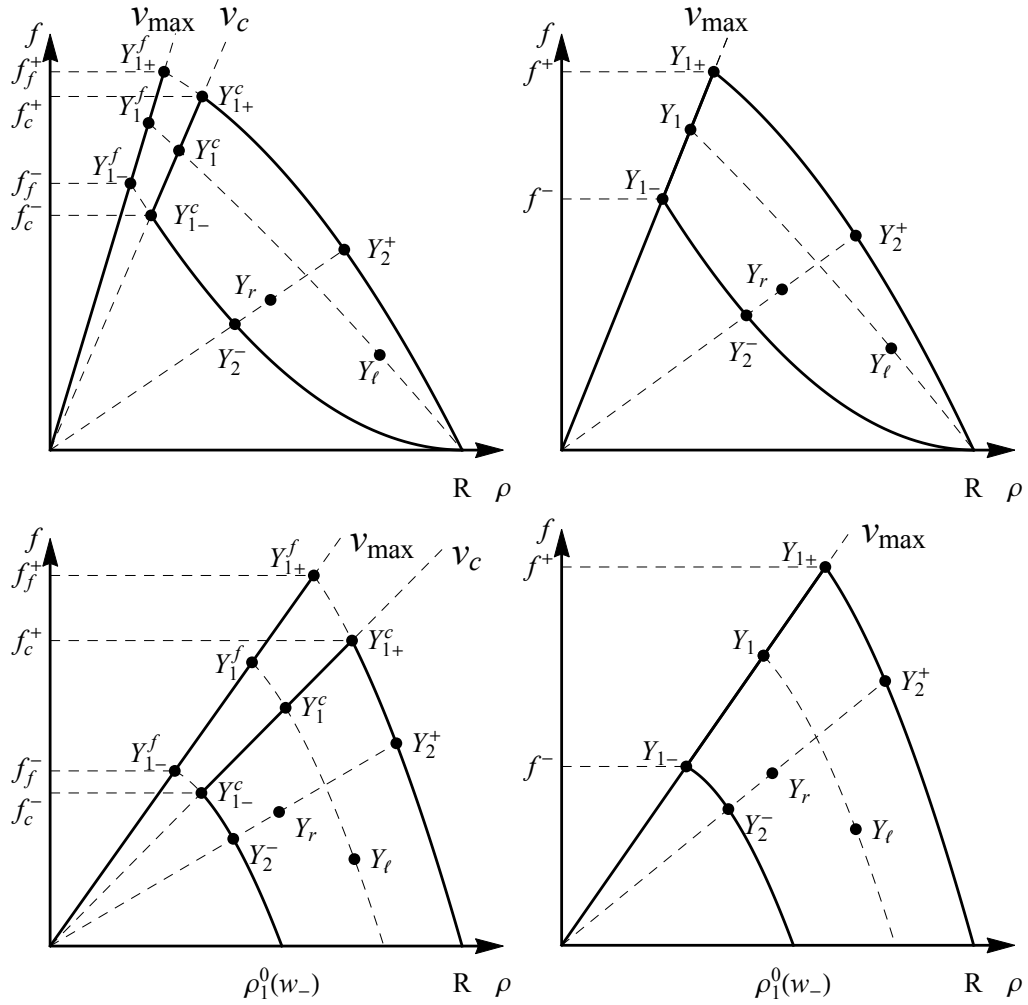


Figure 2.2: The first column refers to the case $\Omega_f \cap \Omega_c = \emptyset$, namely $v_c < v_{\max}$, while the second column refers to the case $\Omega_f \cap \Omega_c \neq \emptyset$, i.e. $v_c = v_{\max}$. The first row refers to PT^a and the second row to PT^p . Above $Y_{1\pm}^f \doteq (r_{\pm}^f, r_{\pm}^f \cdot w_{\pm})$, $Y_{1\pm}^c \doteq (r_{\pm}^c, r_{\pm}^c \cdot w_{\pm})$, $Y_2^{\pm} \doteq \psi_2^{\pm}(Y_r)$, $Y_1^f \doteq \psi_1^f(Y_{\ell})$ and $Y_1^c \doteq \psi_1^c(Y_{\ell})$ defined in Subsection 2.4.1.

Notice that $r_{\pm}^f \leq r_{\pm}^c$, with the equality holding if and only if $v_c = v_{\max}$. We can then explicitly characterize the free and congested regimes as

$$\Omega_f \doteq \left\{ Y \in [0, r_+^f] \times \mathbb{R} : y = Q(\rho) \right\},$$

$$\Omega_c \doteq \left\{ Y \in [r_-^c, R] \times \mathbb{R} : 0 \leq v(Y) \leq v_c, w_- \leq \frac{y}{\rho} \leq w_+ \right\},$$

where $w_{\pm} \doteq y_{\pm}/R$ and

$$Q(\rho) \doteq \begin{cases} \frac{(\rho - r_0)(a(R - \rho)(R - r_0) + v_{\max}R)}{(R - \rho)(a(r_0 - \rho)(R - r_0) + v_{\max}r_0)} & \text{for PT}^a, \\ \rho(v_{\max} + p(\rho)) & \text{for PT}^p. \end{cases}$$

Notice that $v(Y) = v_{\max}$ for any $Y \in \Omega_f$ and $w_{\pm} = Q(r_{\pm}^c)/r_{\pm}^c = Q(r_{\pm}^f)/r_{\pm}^f$. Moreover, we denote $\Omega \doteq \Omega_f \cup \Omega_c$ and

$$\begin{aligned} \Omega_f^- &\doteq \{Y \in \Omega_f : \rho \in [0, r_-^f]\}, & \Omega_f^+ &\doteq \{Y \in \Omega_f : \rho \in [r_-^f, r_+^f]\}, \\ \Omega_c^- &\doteq \Omega_c \setminus \Omega_f^+, & \Omega_c^{ex} &\doteq \{Y \in (0, R] \times \mathbb{R} : v(Y) \in [0, v_{\max}], w(Y) \in [w_-, w_+]\}, \end{aligned}$$

where

$$w(Y) \doteq \begin{cases} y/\rho & \text{if } u \in \Omega_c^{ex}, \\ w_- + \frac{\rho}{r_-^f} - 1 & \text{if } u \in \Omega_f^-. \end{cases}$$

Under the conditions stated above, we point out that

$$\begin{aligned} v_c = v_{\max} &\implies \Omega_f \cap \Omega_c = \Omega_f^+, & \Omega_c^- &\subset \Omega_c, & \Omega_c^{ex} &= \Omega_c, \\ v_c < v_{\max} &\implies \Omega_f \cap \Omega_c = \emptyset, & \Omega_c^- &= \Omega_c, & \Omega_c^{ex} &\supset \Omega_c \cup \Omega_f^+. \end{aligned}$$

Remark 2.2. *We underline that in the congested phase the variable w is a Lagrangian marker, namely the equation $\partial_t w(Y) + v(Y) \partial_x w(Y) = 0$ is satisfied, under the assumption that the weak solution Y to (2.20) takes values in Ω_c .*

We define functions that are useful to define the Riemann solvers given in the next subsections:

$$\begin{aligned} \rho_1^0: [w_-, w_+] &\rightarrow (0, R], & \rho_1^0(w) &\doteq \begin{cases} R & \text{for PT}^a, \\ p^{-1}(w) & \text{for PT}^p, \end{cases} \\ \psi_1^f: (\Omega_c \cup \Omega_f^+) &\rightarrow (\Omega_c \cup \Omega_f^+), & Y_1^f = \psi_1^f(Y_0) &\iff \begin{cases} w(Y_1^f) = w(Y_0), \\ v(Y_1^f) = v_{\max}, \end{cases} \end{aligned}$$

$$\begin{aligned} \psi_1^c: (\Omega_c \cup \Omega_f^+) &\rightarrow (\Omega_c \cup \Omega_f^+), & Y_1^c = \psi_1^c(Y_0) &\iff \begin{cases} w(Y_1^c) = w(Y_0), \\ v(Y_1^c) = \mathbf{v}_c, \end{cases} \\ \psi_2^\pm: \Omega &\rightarrow (\Omega_c \cup \Omega_f^+), & Y_2^\pm = \psi_2^\pm(Y_0) &\iff \begin{cases} w(Y_2^\pm) = \mathbf{w}_\pm, \\ v(Y_2^\pm) = v(Y_0). \end{cases} \end{aligned}$$

We stress that the maximal density is reached for $\rho_1^0(\mathbf{w}_+) = R$ both for the PT^a and PT^p models. Since the considered PT models are given by 2×2 system of conservation laws in the congested phase, then they have two Lax curves corresponding to each characteristic field in Ω_c , namely the curves along which the Riemann invariants are constant. We extend the Lax curves defined in Ω_c to Ω_c^{ex} as the graphs of the maps

$$\begin{aligned} [\rho_1^f(w(Y_0)), \rho_1^0(w(Y_0))] &\ni \rho \mapsto \mathcal{L}_{w(Y_0)}^1(\rho) \doteq f(\rho, w(Y_0)\rho), \\ [\rho_2^-(v(Y_0)), \rho_2^+(v(Y_0))] &\ni \rho \mapsto \mathcal{L}_{v(Y_0)}^2(\rho) \doteq v(Y_0)\rho, \end{aligned}$$

for any $Y_0 \in \Omega_c^{ex}$. Draw attention that the graphs of $\mathcal{L}_{w_-}^1$ and $\mathcal{L}_{w_+}^1$ belong to the boundary of Ω_c^{ex} in the (ρ, f) -plane. By using the Lax curves definition, we can give geometrical meaning of the functions introduced before, see Figure 2.2:

- $\psi_1^f(Y_0)$ is the intersection of Lax curve $\mathcal{L}_{w(Y_0)}^1$ and $\{Y \in \Omega : v(Y) = \mathbf{v}_{\max}\}$.
- $\psi_1^c(Y_0)$ is the intersection of Lax curve $\mathcal{L}_{w(Y_0)}^1$ and $\{Y \in \Omega : v(Y) = \mathbf{v}_c\}$.
- For any $w \in [\mathbf{w}_-, \mathbf{w}_+]$ the point $(\rho_1^0(w), \rho_1^0(w)w)$ is the intersection of the Lax curve \mathcal{L}_w^1 and $\{Y \in \Omega_c : v(Y) = 0\}$. More precisely, for any $w \in [\mathbf{w}_-, \mathbf{w}_+]$ we have $\rho_1^0(w) = p^{-1}(w)$ for PT^p , while $\rho_1^0(w) = R$ for PT^a .
- $\psi_2^\pm(Y_0)$ is the intersection of Lax curve $\mathcal{L}_{Y_0}^2$ and $\{Y \in \Omega : w(Y) = \mathbf{w}_\pm\}$.

At last, we define the maps

$$\rho_1^{f,c}: [\mathbf{w}_-, \mathbf{w}_+] \rightarrow [r_-^{f,c}, r_+^{f,c}] \quad \text{and} \quad \rho_2^\pm: [0, \mathbf{v}_{\max}] \rightarrow [r_\pm^f, \rho_1^0(\mathbf{w}_\pm)]$$

so that $\rho_1^{f,c}(w(Y_0))$ and $\rho_2^\pm(v(Y_0))$ are the ρ -components of $\psi_1^{f,c}(Y_0)$ and $\psi_2^\pm(Y_0)$.

2.4.2 Main assumptions

In this section we give eigenvalues, eigenvectors, Riemann invariants and main assumptions for the PT models in the congested phase. The eigenvalues in Ω_c are

$$\lambda_1^{\text{PT}}(Y) \doteq v(Y) + Y \cdot \nabla_Y v(Y), \quad \lambda_2^{\text{PT}}(Y) \doteq v(Y),$$

with corresponding eigenvectors

$$r_1^{\text{PT}}(Y) \doteq Y, \quad r_2^{\text{PT}}(Y) \doteq \begin{pmatrix} \partial_y v(Y) \\ -\partial_\rho v(Y) \end{pmatrix},$$

and Riemann invariants

$$w_1^{\text{PT}}(Y) \doteq w(Y), \quad w_2^{\text{PT}}(Y) \doteq v(Y).$$

The above functions naturally extend to Ω_c^{ex} . We can see that $\lambda_2^{\text{PT}}(Y) \geq 0$ for all $Y \in \Omega_c^{ex}$. We obtain by direct computation that

$$\begin{aligned} \nabla \lambda_1^{\text{PT}}(Y) \cdot r_1^{\text{PT}}(Y) &= 2Y \cdot \nabla v(Y) + \rho^2 \partial_\rho^2 v(Y) + 2\rho y \partial_\rho \partial_y v(Y) + y^2 \partial_y^2 v(Y), \\ \lambda_2^{\text{PT}}(Y) \cdot r_2^{\text{PT}}(Y) &= 0. \end{aligned}$$

As a consequence the second characteristic field is linearly degenerate.

For modelling consistency, we assume that for any $w \in [w_-, w_+]$ the flux is decreasing and has at most one inflection point. For this reason, in Ω_c the waves of the first and second characteristic families have respectively non-positive and non-negative speed of propagations. Therefore, the following assumptions will be needed in order to construct general PT model:

(H1) $\lambda_1^{\text{PT}}(Y) \leq 0$ for all $Y \in \Omega_c^{ex}$

(H2) the first characteristic field is genuinely non-linear in Ω_c^{ex} , except for the PT^0 model.

Notice that the first characteristic field for PT^0 model, namely PT^a with $a = 0$, is linearly degenerate along the Lax curve \mathcal{L}_0^1 and is genuinely non-linear along

any Lax curve \mathcal{L}_w^1 with $w \neq 0$. It is interesting to observe that if \mathcal{L}_w^1 vanishes in $Y \in \Omega_c^{ex}$, then **(H1)** and **(H2)** imply that $v(Y) \in \{0, \mathbf{v}_{\max}\}$.

Remark 2.3. *Regarding to the fact that for PT^p model, the p function satisfies $2p'(\rho) + \rho p''(\rho) > 0$ for every $\rho \in [r_-^f, r_+^f]$, **(H1)** reduces to the requirement $r_-^f p'(r_-^f) \geq \mathbf{v}_{\max}$. Moreover, by (2.12) we have $\nabla \lambda_1^{\text{PT}}(Y) \cdot r_1^{\text{PT}}(Y) = -\rho (2p'(\rho) + \rho p''(\rho)) < 0$ for every $\rho \in (0, R]$ and **(H2)** easily follows.*

*On the contrary, for PT^a in general assumptions **(H1)** and **(H2)** cannot be easily derived in terms of the parameters of the model. We just mention that in the simplest case $a = 0$ condition **(H1)**, as stated in [49], is guaranteed by*

$$-\frac{1}{R} < \mathbf{w}_- < 0 < \mathbf{w}_+ < \frac{1}{R}.$$

Remark 2.4. *The assumptions **(H1)** and **(H2)** can be reformulated with regard to the first Lax curves. Since $\frac{d}{d\rho} \mathcal{L}_w^1(\rho) = \lambda_1^{\text{PT}}(\rho, \rho w)$, then **(H1)** represents the fact that the first Lax curves are strictly decreasing. As a consequence the capacity drop in the passage from the free phase to the congested phase is ensured. Moreover, as a result of $\frac{d^2}{d\rho^2} \mathcal{L}_w^1(\rho) = \frac{1}{\rho} \nabla \lambda_1^{\text{PT}}(\rho, \rho w) \cdot r_1^{\text{PT}}(\rho, \rho w)$, we have that **(H2)** is equivalent to the fact that the first Lax curves are strictly concave or convex, except the case of PT^0 corresponding to $w = 0$. Point out that by (2.12) we have $\frac{d^2}{d\rho^2} \mathcal{L}_w^1(\rho) < 0$ for all $\rho \in [\rho_1^f(w), \rho_1^0(w)]$, hence the first Lax curves for PT^p are strictly concave.*

In the forthcoming subsections we recall the Riemann solvers corresponding to Riemann problems both with metastable phase $\Omega_f \cap \Omega_c \neq \emptyset$, and without metastable phase, that is $\Omega_f \cap \Omega_c = \emptyset$. We introduce now the admissible solutions to the Riemann problem for both problems. Consider the Riemann problem for PT model (2.20) with the initial datum

$$Y(0, x) = \begin{cases} Y_\ell & \text{if } x < 0, \\ Y_r & \text{if } x > 0. \end{cases} \quad (2.21)$$

Let us recall the definition of solution to (2.20), (2.21) introduced in [28].

Definition 2.6. *For any $Y_\ell, Y_r \in \Omega$ a self-similar function $Y \doteq (\rho, y): \mathbb{R}_+ \times \mathbb{R} \rightarrow \Omega$ is an admissible solution to (2.20), (2.21) if the following properties hold:*

C.1 If $Y_\ell, Y_r \in \Omega_f$, then $Y \doteq (\rho, y)$ with $y \equiv Q(\rho)$ and $\rho \equiv \mathcal{RS}_{\text{LWR}}[\rho_\ell, \rho_r]$ given by (2.9). The solution has no phase transition and attains values in Ω_f .

C.2 If $Y_\ell, Y_r \in \Omega_c$, then Y is the usual Lax solution to (2.20)₂, (2.21). The solution has no phase transition and attains values in Ω_c .

C.3 If $Y_\ell \in \Omega_f^-$ and $Y_r \in \Omega_c^-$, then there exists $\sigma \in \mathbb{R}$ such that:

(a) $Y(t, (-\infty, \sigma t)) \subseteq \Omega_f$ and $Y(t, (\sigma t, +\infty)) \subseteq \Omega_c$ for all $t > 0$.

(b) The first Rankine-Hugoniot condition is satisfied for all $t > 0$, namely

$$\sigma (\rho(t, \sigma t^+) - \rho(t, \sigma t^-)) = f(Y(t, \sigma t^+)) - f(Y(t, \sigma t^-)).$$

(c) The functions

$$(t, x) \mapsto \begin{cases} Y(t, x) & \text{if } x < \sigma t, \\ Y(t, \sigma t^-) & \text{if } x > \sigma t, \end{cases} \quad (t, x) \mapsto \begin{cases} Y(t, \sigma t^+) & \text{if } x < \sigma t, \\ Y(t, x) & \text{if } x > \sigma t, \end{cases}$$

are respectively the usual Lax solutions to the Riemann problems

$$\begin{cases} \partial_t \rho + \partial_x f(Y) = 0, \\ v(Y) = v_{\max}, \\ Y(0, x) = \begin{cases} Y_\ell & \text{if } x < 0, \\ Y(t, \sigma t^-) & \text{if } x > 0, \end{cases} \end{cases} \quad \begin{cases} \partial_t \rho + \partial_x f(Y) = 0, \\ \partial_t y + \partial_x (y v(Y)) = 0, \\ Y(0, x) = \begin{cases} Y(t, \sigma t^+) & \text{if } x < 0, \\ Y_r & \text{if } x > 0. \end{cases} \end{cases}$$

C.4 In the case of $Y_\ell \in \Omega_c^-$ and $Y_r \in \Omega_f^-$ analogous conditions to the previous case are required.

Notice that for the PT^p model, condition (C.2) states that $Y \equiv \mathcal{RS}_{\text{ARZ}}[Y_\ell, Y_r]$, where $\mathcal{RS}_{\text{ARZ}}$ is given by Definition 2.3.

2.4.3 The Riemann solvers \mathcal{RS}_R and \mathcal{RS}_S for PT models

In this section we introduce Riemann solvers \mathcal{RS}_R and \mathcal{RS}_S for the Riemann problems with metastable phase and without metastable phase, respectively. We

point out that these Riemann solvers are defined below according to Definition 2.6, in the sense that $(t, x) \mapsto \mathcal{RS}_R[Y_\ell, Y_r](x/t)$ and $(t, x) \mapsto \mathcal{RS}_S[Y_\ell, Y_r](x/t)$ are admissible solutions to the Riemann problem (2.20), (2.21).

Besides the elementary 1-waves, namely rarefactions R and shocks S, and 2-waves, namely contact discontinuities C, which are defined analogously to those introduced in Subsection 2.3.2 for the ARZ model, we need to introduce phase transitions (PT). A PT wave is a shock-like wave between states Y_ℓ and Y_r belonging to different regimes. More precisely, we distinguish the following types of PT waves:

- $Y_\ell \in \Omega_f^- \setminus \{(0, 0)\}$, $Y_r = \psi_2^-(Y_r) \in \Omega_c \setminus \Omega_f$;
- $Y_\ell = (0, 0)$, $Y_r \in \Omega_c \setminus \Omega_f$;
- $Y_\ell \in \Omega_f^+$, $Y_r \in \Omega_c^-$ with $f(Y_r) = \mathcal{L}_{w(Y_\ell)}^1(\rho_r)$ if $\Omega_c \cap \Omega_f = \emptyset$;
- $Y_\ell = \psi_1^c(Y_\ell) \in \Omega_c$, $Y_r = \psi_1^f(Y_\ell) \in \Omega_f^+$ if $\Omega_c \cap \Omega_f = \emptyset$.

Therefore, the PT wave can be defined as

$$\text{PT}[Y_\ell, Y_r](\xi) \doteq \begin{cases} Y_\ell & \text{if } \xi < \sigma(Y_\ell, Y_r), \\ Y_r & \text{if } \xi > \sigma(Y_\ell, Y_r), \end{cases}$$

where

$$\sigma(Y_\ell, Y_r) \doteq \frac{f(Y_\ell) - f(Y_r)}{\rho_\ell - \rho_r}.$$

Let us first consider a Riemann solver for the case with metastable phase, that is $\Omega_f \cap \Omega_c = \Omega_f^+ \neq \emptyset$. In this case the maximal velocities for both phases coincide, namely $v_{\max} = v_c$. We recall that $\psi_1^f \equiv \psi_1^c$, $r_\pm^f = r_\pm^c$ and for this reason we simply write ψ_1 and r_\pm . Moreover, we write below f_ℓ for $f(Y_\ell)$, v_ℓ for $v(Y_\ell)$, w_ℓ for $w(Y_\ell)$ and so on.

Definition 2.7. *The Riemann solver $\mathcal{RS}_R: \Omega^2 \rightarrow \mathbf{L}^\infty(\mathbb{R}; \Omega)$ associated to Riemann problem (2.20), (2.21) is defined as follows.*

(R.1) *If $Y_\ell, Y_r \in \Omega_f$, then $Y \doteq (\rho, y)$ with $y \equiv Q(\rho)$ and $\rho \equiv \mathcal{RS}_{\text{LWR}}[\rho_\ell, \rho_r]$ given by (2.9).*

- (**R.2**) If $Y_\ell, Y_r \in \Omega_c$ then $\mathcal{RS}_R[Y_\ell, Y_r]$ is the juxtaposition of possibly null 1-wave (Y_ℓ, Y_m) and possibly null $C[Y_m, Y_r]$, where $w_m = w_\ell$ and $v_m = v_r$.
- (**R.3**) If $Y_\ell \in \Omega_c^-$ and $Y_r \in \Omega_f^-$, then $\mathcal{RS}_R[Y_\ell, Y_r]$ is the juxtaposition of a 1-wave $(Y_\ell, \psi_1(Y_\ell))$ and $C[\psi_1(Y_\ell), Y_r]$.
- (**R.4**) If $Y_\ell \in \Omega_f^-, Y_r \in \Omega_c^-$ and $\sigma(Y_\ell, \psi_2^-(Y_r)) \geq \lambda_1^{\text{PT}}(\psi_2^-(Y_r))$, then $\mathcal{RS}_R[Y_\ell, Y_r]$ is the juxtaposition of $\text{PT}[Y_\ell, \psi_2^-(Y_r)]$ and possibly null $C[\psi_2^-(Y_r), Y_r]$.
- (**R.5**) If $Y_\ell \in \Omega_f^-, Y_r \in \Omega_c^-$ and $\sigma(Y_\ell, \psi_2^-(Y_r)) < \lambda_1^{\text{PT}}(\psi_2^-(Y_r))$, then $\mathcal{RS}_R[Y_\ell, Y_r]$ is the juxtaposition of $\text{PT}[Y_\ell, Y_p]$, $R[Y_p, \psi_2^-(Y_r)]$ and $C[\psi_2^-(Y_r), Y_r]$, where $Y_p = Y_p(Y_\ell)$ is the state satisfying $w_p = w_-$ and $\sigma(Y_\ell, Y_p) = \lambda_1^{\text{PT}}(Y_p)$.

We point out that if $\frac{d^2 \mathcal{L}_w^1}{d\rho^2}(r_-) \leq 0$, then $\sigma(Y_\ell, \psi_2^-(Y_r)) \geq \lambda_1^{\text{PT}}(\psi_2^-(Y_r))$ for all $Y_\ell \in \Omega_f^-$ and $Y_r \in \Omega_c^-$; thus case (**R.5**) never occurs. We recall that by Remark 2.4 the Lax curves of the first characteristic family for PT^p model are always concave.

Let consider now a Riemann solver for the case without metastable phase, that is $\Omega_f \cap \Omega_c = \emptyset$. In this case the maximal velocities of each phase do not coincide, namely $v_c < v_{\max}$. We introduce the states

$$Y_{1-}^c \doteq (r_-^c, w_- r_-^c), \quad Y_{1+}^c \doteq (r_+^c, w_+ r_+^c),$$

which represents the points in Ω_c with minimal ρ -coordinate and maximal f -coordinate, respectively, see Figure 2.2. The states

$$Y_{1-}^f \doteq (r_-^f, w_- r_-^f), \quad Y_{1+}^f \doteq (r_+^f, w_+ r_+^f),$$

represents the points in Ω_f^+ with minimal ρ -coordinate and maximal f -coordinate, respectively, see Figure 2.2. At last we define

$$f_{f,c}^\pm \doteq f(Y_{1\pm}^{f,c}).$$

Definition 2.8. *The Riemann solver $\mathcal{RS}_S: \Omega^2 \rightarrow \mathbf{L}^\infty(\mathbb{R}; \Omega)$ associated to (2.20), (2.21) is defined as follows.*

(S.1) We let $\mathcal{RS}_S[Y_\ell, Y_r] \doteq \mathcal{RS}_R[Y_\ell, Y_r]$ whenever

$$\begin{aligned} (Y_\ell, Y_r) \in & \Omega_f^2 \cup \Omega_c^2 \cup \left\{ (Y_\ell, Y_r) \in \Omega_c \times \Omega_f : \frac{d^2 \mathcal{L}_{w_\ell}^1}{d\rho^2}(\rho_\ell) \geq 0 \right\} \\ & \cup \left\{ (Y_\ell, Y_r) \in \Omega_f^- \times \Omega_c : \sigma(Y_\ell, Y_{1-}^c) \geq \lambda_1^{\text{PT}}(Y_{1-}^c) \right\} \\ & \cup \left\{ (Y_\ell, Y_r) \in \Omega_f^+ \times \Omega_c : \frac{d^2 \mathcal{L}_{w_\ell}^1}{d\rho^2}(\rho_\ell) \leq 0 \right\}. \end{aligned}$$

(S.2) If $Y_\ell \in \Omega_c$, $Y_r \in \Omega_f$ and $\frac{d^2 \mathcal{L}_{w_\ell}^1}{d\rho^2}(\rho_\ell) < 0$, then we let

$$\mathcal{RS}_S[Y_\ell, Y_r](\xi) \doteq \begin{cases} \mathcal{RS}_R[Y_\ell, \psi_1^c(Y_\ell)](\xi) & \text{for } \xi < \sigma(\psi_1^c(Y_\ell), \psi_1^f(Y_\ell)), \\ \mathcal{RS}_R[\psi_1^f(Y_\ell), Y_r](\xi) & \text{for } \xi \geq \sigma(\psi_1^c(Y_\ell), \psi_1^f(Y_\ell)). \end{cases}$$

(S.3) If $Y_\ell \in \Omega_f^-$, $Y_r \in \Omega_c$ and $\sigma(Y_\ell, Y_{1-}^c) < \lambda_1^{\text{PT}}(Y_{1-}^c)$, then we let

$$\mathcal{RS}_S[Y_\ell, Y_r](\xi) \doteq \begin{cases} Y_\ell & \text{for } \xi < \sigma(Y_\ell, Y_{1-}^c), \\ \mathcal{RS}_R[Y_{1-}^c, Y_r](\xi) & \text{for } \xi \geq \sigma(Y_\ell, Y_{1-}^c). \end{cases}$$

(S.4) If $Y_\ell \in \Omega_f^+$, $Y_r \in \Omega_c$ and $\frac{d^2 \mathcal{L}_{w_\ell}^1}{d\rho^2}(\rho_\ell) > 0$, then we let

$$\mathcal{RS}_S[Y_\ell, Y_r](\xi) \doteq \begin{cases} Y_\ell & \text{for } \xi < \sigma(Y_\ell, \psi_1^c(Y_\ell)), \\ \mathcal{RS}_R[\psi_1^c(Y_\ell), Y_r](\xi) & \text{for } \xi \geq \sigma(Y_\ell, \psi_1^c(Y_\ell)). \end{cases}$$

Remark 2.5. We point out that \mathcal{RS}_S differs from \mathcal{RS}_R only in the cases described in (S.2), (S.3) and (S.4), hence the Riemann solver $\mathcal{RS}_S[Y_\ell, Y_r]$ differs from $\mathcal{RS}_R[Y_\ell, Y_r]$ if and only if (Y_ℓ, Y_r) one of the following condition holds:

$$Y_\ell \in \Omega_c, \quad Y_r \in \Omega_f, \quad \frac{d^2 \mathcal{L}_{w_\ell}^1}{d\rho^2}(\rho_\ell) < 0, \quad (2.22)$$

$$Y_\ell \in \Omega_f^-, \quad Y_r \in \Omega_c, \quad \sigma(Y_\ell, Y_{1-}^c) < \lambda_1^{\text{PT}}(Y_{1-}^c), \quad (2.23)$$

$$Y_\ell \in \Omega_f^+, \quad Y_r \in \Omega_c, \quad \frac{d^2 \mathcal{L}_{w_\ell}^1}{d\rho^2}(\rho_\ell) > 0. \quad (2.24)$$

Observe also that for PT^p model we have that $\mathcal{RS}_S[Y_\ell, Y_r]$ differs from $\mathcal{RS}_R[Y_\ell, Y_r]$ if and only if $Y_\ell \in \Omega_c$ and $Y_r \in \Omega_f$. Moreover, this is also the case for PT^a model if $\frac{d^2 \mathcal{L}^1_{w_\ell}}{d\rho^2}(r_-^f) < 0$.

At last we define a Riemann solver consistency and then give results on \mathcal{RS}_S and \mathcal{RS}_R .

Definition 2.9. A Riemann solver $\mathcal{RS}: \Omega^2 \rightarrow \mathbf{L}^\infty(\mathbb{R}; \Omega)$ is consistent if the following conditions are satisfied for any $Y_\ell, Y_m, Y_r \in \Omega$ and $\bar{\xi} \in \mathbb{R}$:

$$\mathcal{RS}[Y_\ell, Y_r](\bar{\xi}) = Y_m \implies \begin{cases} \mathcal{RS}[Y_\ell, Y_m](\xi) = \begin{cases} \mathcal{RS}[Y_\ell, Y_r](\xi) & \text{if } \xi < \bar{\xi}, \\ Y_m & \text{if } \xi \geq \bar{\xi}, \end{cases} \\ \mathcal{RS}[Y_m, Y_r](\xi) = \begin{cases} Y_m & \text{if } \xi < \bar{\xi}, \\ \mathcal{RS}[Y_\ell, Y_r](x) & \text{if } \xi \geq \bar{\xi}, \end{cases} \end{cases} \quad (\text{I})$$

$$\left. \begin{array}{l} \mathcal{RS}[Y_\ell, Y_m](\bar{\xi}) = Y_m \\ \mathcal{RS}[Y_m, Y_r](\bar{\xi}) = Y_m \end{array} \right\} \implies \mathcal{RS}[Y_\ell, Y_r](\xi) = \begin{cases} \mathcal{RS}[Y_\ell, Y_m](\xi) & \text{if } \xi < \bar{\xi}, \\ \mathcal{RS}[Y_m, Y_r](\xi) & \text{if } \xi \geq \bar{\xi}. \end{cases} \quad (\text{II})$$

The advantage of using consistent Riemann solver lies in the fact that it is necessary condition for the \mathbf{L}^1 -continuity of the semigroup associated to the Riemann solver. We present then the following propositions, with proofs deferred to Section A.

Proposition 2.2. The Riemann solver \mathcal{RS}_R is $\mathbf{L}^1_{\text{loc}}$ -continuous and consistent.

Proposition 2.3. The Riemann solver \mathcal{RS}_S is $\mathbf{L}^1_{\text{loc}}$ -continuous and consistent.

Constrained LWR model

3.1 Introduction

In this chapter we describe LWR model (2.1), introduced in Section 2.2, with local point constraint on the flow. From the modelling point of view, the unilateral constraint on the flow can represent the reduction of car traffic caused, for instance, by toll gates, traffic lights or construction sites. The idea of conservation laws with unilateral constraint was introduced in the framework of traffic flow in [29] and then studied in [2, 5, 21].

3.1.1 The constrained Riemann solver $\mathcal{RS}_{\text{LWR}}^c$

We consider a Riemann problem (2.5) for the LWR model

$$\partial_t \rho + \partial_x f(\rho) = 0, \quad \rho(0, x) = \begin{cases} \rho_\ell & \text{if } x < 0, \\ \rho_r & \text{if } x \geq 0, \end{cases} \quad (3.1)$$

with additional condition

$$f(\rho(t, 0)) \leq q, \quad (3.2)$$

where $\rho_\ell, \rho_r \in [0, R]$ and the value of constraint $q \in [0, f_{\max}]$ are constant. Observe that the classical Riemann solver $\mathcal{RS}_{\text{LWR}}$ for the LWR model introduced in Definition 2.1 does not necessarily satisfy condition (3.2). For this reason in [29] the authors introduced the constrained Riemann solver $\mathcal{RS}_{\text{LWR}}^c$ defined below.

Definition 3.1. *Constrained LWR Riemann solver $\mathcal{RS}_{\text{LWR}}^c : [0, R]^2 \rightarrow \mathbf{C}^0(\mathbb{R}_+; \mathbf{BV}(\mathbb{R}; [0, R]))$ is defined as follows.*

1. *If $f(\mathcal{RS}_{\text{LWR}}[\rho_\ell, \rho_r])(0) \leq q$, then*

$$\mathcal{RS}_{\text{LWR}}^c[\rho_\ell, \rho_r](\xi) \doteq \mathcal{RS}_{\text{LWR}}[\rho_\ell, \rho_r](\xi).$$

2. *If $f(\mathcal{RS}_{\text{LWR}}[\rho_\ell, \rho_r])(0) > q$, then*

$$\mathcal{RS}_{\text{LWR}}^c[\rho_\ell, \rho_r](\xi) \doteq \begin{cases} \mathcal{RS}_{\text{LWR}}[\rho_\ell, \hat{\rho}](\xi) & \text{if } \xi < 0, \\ \mathcal{RS}_{\text{LWR}}[\check{\rho}, \rho_r](\xi) & \text{if } \xi \geq 0, \end{cases}$$

where

$$\check{\rho} \doteq \min\{\rho \in [0, R] : f(\rho) = q\}, \quad \hat{\rho} \doteq \max\{\rho \in [0, R] : f(\rho) = q\}.$$

Notice that $\check{\rho}$ and $\hat{\rho}$ coincide if and only if $q = f_{\max}$. On the contrary, if $q < f_{\max}$, namely the constraint is effective, the solution performs at $x = 0$ a stationary non-classical shock between $\hat{\rho}$ and $\check{\rho}$. Since $f(\check{\rho}) = f(\hat{\rho}) = q$, the non-classical shock satisfies the Rankine-Hugoniot condition (2.7). It can be proved that $[(t, x) \mapsto \mathcal{RS}_{\text{LWR}}^c[\rho_\ell, \rho_r](x/t)]$ is a weak solution, however it does not in general satisfy the Kruzhkov entropy condition [62].

The solution obtained by Riemann solver (3.1) can lead to significant increase of total variation, as it is shown in the following example:

Example 3.1. *Consider a constant initial datum $\rho(0, x) = \rho_0 \in [0, R]$ such that $f(\rho_0) > q$, hence $f(\mathcal{RS}_{\text{LWR}}[\rho_0, \rho_0])(0) > q$. In this case $\mathcal{RS}_{\text{LWR}}^c[\rho_\ell, \rho_r]$ has a shock $(\rho_0, \hat{\rho})$ with negative speed of propagation, followed by a stationary non-classical shock $(\hat{\rho}, \check{\rho})$ and a shock $(\check{\rho}, \rho_0)$ with positive speed of propagation. Its total variation jumps from 0 to $2(\hat{\rho} - \check{\rho})$.*

We recall now the proposition from [29] with the main properties of $\mathcal{RS}_{\text{LWR}}^c$.

Proposition 3.1. *The constrained Riemann solver $\mathcal{RS}_{\text{LWR}}^c$ has the following properties for any $\rho_\ell, \rho_r \in [0, R]$:*

- $\mathcal{RS}_{\text{LWR}}^c[\rho_\ell, \rho_r] \not\equiv \mathcal{RS}_{\text{LWR}}[\rho_\ell, \rho_r]$ if and only if $(\rho_\ell, \rho_r) \in (\check{\rho}, R] \times [0, \hat{\rho})$;

- $[(t, x) \mapsto \mathcal{RS}_{\text{LWR}}^c[\rho_\ell, \rho_r](x/t)]$ is a self similar weak solution to (3.1), (3.2);
- $\mathcal{RS}_{\text{LWR}}^c[\rho_\ell, \rho_r]$ satisfies the constraint (3.2) in the sense that

$$\lim_{x \rightarrow 0^+} f(\mathcal{RS}_{\text{LWR}}^c[\rho_\ell, \rho_r](x/t)) \leq q \quad \text{and} \quad \lim_{x \rightarrow 0^-} f(\mathcal{RS}_{\text{LWR}}^c[\rho_\ell, \rho_r](x/t)) \leq q;$$

- $\mathcal{RS}_{\text{LWR}}^c[\rho_\ell, \rho_r] \in \mathbf{BV}(\mathbb{R}; [0, R])$;
- $\mathcal{RS}_{\text{LWR}}^c : [0, R]^2 \rightarrow \mathbf{L}_{\text{loc}}^1(\mathbb{R}; \mathbb{R})$ is uniformly continuous.

3.2 The Constrained Cauchy Problem

We study now the constrained Cauchy problem

$$\partial_t \rho + \partial_x f(\rho) = 0, \quad \rho(0, x) = \rho_0(x), \quad (3.3)$$

with constraint condition

$$f(\rho(t, 0)) \leq q(t), \quad (3.4)$$

where $x = 0$ is the position of the obstacle and $q(t)$ is the maximal flow allowed at $x = 0$ at time $t > 0$. The definition of weak solution to constrained Cauchy problem (3.3), (3.4) is given as follows [29].

Definition 3.2. A function $\rho \in \mathbf{C}^0((0, +\infty); \mathbf{L}_{\text{loc}}^\infty(\mathbb{R}; [0, R]))$ is a weak entropy solution to constrained Cauchy problem (3.3), (3.4) if for every test function $\phi \in \mathbf{C}_c^\infty(\mathbb{R}^2; [0, +\infty))$ and for every $k \in [0, R]$ we have

$$\begin{aligned} 0 \leq & \iint_{\mathbb{R}_+ \times \mathbb{R}} (|\rho - k| \partial_t \phi + \text{sgn}(\rho - k) (f(\rho) - f(k)) \partial_x \phi) \, dx \, dt \\ & + \int_{\mathbb{R}} |\rho_0(x) - k| \phi(0, x) \, dx + 2 \int_{\mathbb{R}_+} \left(1 - \frac{q(t)}{f(\rho_{\text{crit}})}\right) f(k) \phi(t, 0) \, dt \end{aligned} \quad (3.5)$$

and $f(\rho(t, 0^-)) = f(\rho(t, 0^+)) \leq q(t)$ for almost every $t \in (0, +\infty)$.

Above the term $\rho(t, 0^\pm)$ expresses the measure theoretic trace implicitly defined

by

$$\begin{aligned} \lim_{\varepsilon \rightarrow 0^+} \frac{1}{\varepsilon} \iint_{\mathbb{R}_+ \times [0, \varepsilon]} |\rho(t, x) - \rho(t, 0^+)| \phi(t, x) \, dx \, dt &= 0, \\ \lim_{\varepsilon \rightarrow 0^+} \frac{1}{\varepsilon} \iint_{\mathbb{R}_+ \times [-\varepsilon, 0]} |\rho(t, x) - \rho(t, 0^-)| \phi(t, x) \, dx \, dt &= 0, \end{aligned}$$

for all $\phi \in \mathbf{C}_c^\infty(\mathbb{R}^2; \mathbb{R})$. It has been shown in [5, Theorem 2.2] that both traces at $x = 0$ exist and they are finite. We also point out that Definition 3.2 chooses the solution with maximal possible traffic flow through $x = 0$, however due to non-classical shock $(\hat{\rho}, \tilde{\rho})$ at $x = 0$, the solution turns out to be non-entropic [62].

Remark 3.1. *The first two addends in (3.5) correspond to the entropy condition of Cauchy problem (3.3) in the sense of Kruzkov [62]. The last addend accounts for constraint (3.4), see [29, Definitions 3.1 and 3.2]. The condition $f(\rho(t, 0^-)) = f(\rho(t, 0^+)) \leq q(t)$ chooses the solution described in Example 3.1 rather than the constant solution, which satisfies (3.5). Another equivalent formulations corresponding to unilateral constraints can be found in [5, Proposition 2.6].*

At last, we introduce the uniqueness theorem for constrained Cauchy problem (3.3)(3.4), proved in [29].

Theorem 3.1. *Assume that $f \in \mathbf{C}^{0,1}([0, R]; [0, f_{\max}])$ satisfy $f(0) = f(R) = 0$ and that there exists $\rho_{\text{crit}} \in (0, R]$ such that $(\rho_{\text{crit}} - \rho)f'(\rho) > 0$ for almost every $\rho \in [0, R]$. Assume that:*

1. $\rho_0 \in \mathbf{L}^1(\mathbb{R}; [0, R])$ is such that $\text{sgn}(\rho_0 - \rho_{\text{crit}})(f(\rho_{\text{crit}}) - f(\rho_0)) \in \mathbf{BV}(\mathbb{R}; \mathbb{R})$;
2. $q \in \mathbf{BV}((0, +\infty); [0, f(\rho_{\text{crit}})])$.

Then there exists unique entropy solution to constrained Cauchy problem (3.3), (3.4) in the sense of Definition 3.2. Moreover, $\rho(t, \cdot) \in \mathbf{L}^1(\mathbb{R}; [0, R])$ is such that $\text{sgn}(\rho(t, \cdot) - \rho_{\text{crit}})(f(\rho_{\text{crit}}) - f(\rho(t, \cdot))) \in \mathbf{BV}(\mathbb{R}; \mathbb{R})$. Furthermore, if $\tilde{\rho}$ is the solution of the Cauchy problem (3.3), (3.4) corresponding to the pair $(\tilde{\rho}_0, \tilde{q})$ which satisfies the above assumptions, then the following Lipschitz estimates holds true for all $t \in (0, +\infty)$

$$\|\rho(t, \cdot) - \tilde{\rho}(t, \cdot)\|_{\mathbf{L}^1(\mathbb{R}, \mathbb{R})} \leq \|\rho_0(x) - \tilde{\rho}_0(x)\|_{\mathbf{L}^1(\mathbb{R}, \mathbb{R})} + 2 \|q(t) - \tilde{q}(t)\|_{\mathbf{L}^1([0, t], \mathbb{R})}.$$

Constrained ARZ models

4.1 Introduction

In this chapter we consider the ARZ model described in Section 2.3 with point constraint on the flow. In [46] Garavello and Goatin proposed two distinct constrained Riemann solvers. The former is fully conservative, namely both the Rankine-Hugoniot conditions (2.14) hold. The latter is non-conservative and only the first Rankine-Hugoniot condition $(2.14)_1$ is satisfied, which ensures the conservation of the number of vehicles. In [4] the authors considered the fully conservative Riemann solver and proved the existence of the corresponding fully conservative solutions to general constrained Cauchy problems for ARZ model with initial data of bounded variation and piece-wise constant time depending constraint. The existence of non-fully conservative solutions to constrained Cauchy problems for ARZ model with constant constraints has been studied in [50], under the assumption that the waves of the first family have only negative propagation speeds. However, the assumption on the propagation speeds does not allow to take into account vacuum states, what is a drawback from application point of view.

In [42] we proved the existence of non-fully conservative solutions to general constrained Cauchy problems for ARZ model with initial data of bounded variation, without any restriction on the propagation speeds. The proof is based on the Wave Front Tracking method (see [18, 59] and the references therein). We provide a time decreasing functional Υ which allows to give uniform bound for the total variation of a sequence of approximate solutions constructed via the Wave Front

Tracking method. Then by Helly's theorem we get the existence of a convergent subsequence of the approximate solutions. At last we prove that the limit function is indeed a weak solution of the constrained Cauchy problem. These results are presented in Section 4.3.1.

4.2 Description of the model and notations

In this subsection we introduce notations and the definition of weak solution for the constrained Cauchy problem for ARZ model

$$\begin{cases} \partial_t Y + \partial_x F(Y) = 0, \\ f(U(t, 0^\pm)) \leq q, \\ Y(0, x) = \Psi(U_0(x)). \end{cases} \quad (4.1)$$

As in Section 2.3.1, above $\rho = \rho(t, x)$ is the density, $y = y(t, x)$ is the generalized momentum, $p(\rho)$ satisfies (2.12) and

$$\begin{aligned} Y &\doteq (\rho, y)^T \in \mathbb{R}_+^2 \setminus \{0\}, & F(Y) &\doteq \left(\frac{y}{\rho} - p(\rho) \right) Y, \\ U &\doteq \Psi^{-1}(Y), & f(U) &\doteq p^{-1}(w - v)v. \end{aligned}$$

The term $U(t, 0^\pm)$ expresses the measure theoretic traces along $x = 0$. The left and right measure theoretic trace are implicitly defined as

$$\begin{aligned} \lim_{\varepsilon \rightarrow 0^+} \frac{1}{\varepsilon} \iint_{\mathbb{R}_+ \times [-\varepsilon, 0]} |U(t, x) - U(t, 0^-)| \phi(t, x) dx dt &= 0 \\ \lim_{\varepsilon \rightarrow 0^+} \frac{1}{\varepsilon} \iint_{\mathbb{R}_+ \times [0, \varepsilon]} |U(t, x) - U(t, 0^+)| \phi(t, x) dx dt &= 0 \end{aligned}$$

for all $\phi \in \mathbf{C}_c^\infty(\mathbb{R}^2; \mathbb{R})$. The existence of measure theoretic traces for weak solutions guarantees suitable **BV** bounds, see [31, Lemma 1.3.3].

Define the physical domain in the Riemann invariant coordinates

$$\mathcal{D} \doteq \{U = (v, w)^T \in [0, V] \times [0, W] : v \leq w\},$$

where V and W are the maximal allowed speed and Lagrangian marker, respectively, with $W \geq V$. Denote by $\mathcal{D}_0 \doteq \{U \in \mathcal{D} : v = w\}$ the set of vacuum states and by $\mathcal{D} \setminus \mathcal{D}_0 = \{U \in \mathcal{D} : v < w\}$ the set of non-vacuum states.

We introduce the following notation, see Figure 4.1.

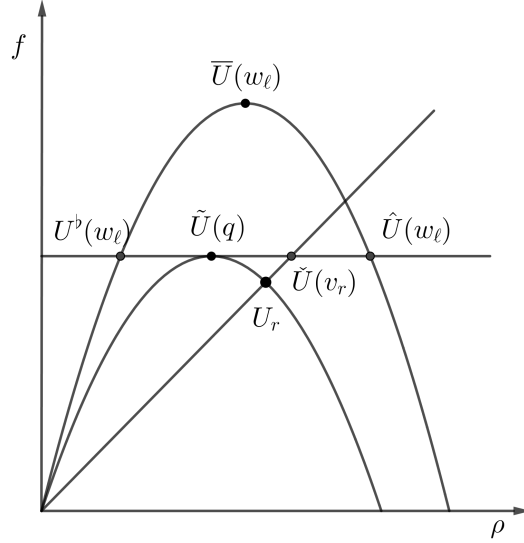


Figure 4.1: Basic notations in (ρ, f) -coordinates.

- For any $w_\ell \in (0, W]$, the state $\bar{U}(w_\ell) \doteq (\bar{v}_\ell, w_\ell)^T$ is such that $\bar{\rho} = p^{-1}(w_\ell - \bar{v}_\ell)$ is the maximum of $\rho \mapsto [w_\ell - p(\rho)]\rho$.
- Let $\tilde{U}(q) \doteq (\tilde{v}(q), \tilde{w}(q))^T \in \mathcal{D}$ be the unique state such that $f(\tilde{U}(q)) = q$ and $\bar{U}(\tilde{w}(q)) = \tilde{U}(q)$. We take $\tilde{U}(0) = (0, 0)^T$.
- The propagation speed of the discontinuity (U_ℓ, U_r) for $\rho_\ell \neq \rho_r$ is

$$\sigma(U_\ell, U_r) \doteq \frac{f(U_r) - f(U_\ell)}{\rho(U_r) - \rho(U_\ell)}, \quad (4.2)$$

where $\rho(U) = p^{-1}(w - v)$, as introduced in Section 2.3.1.

- We define

$$v^b(w_\ell) \doteq \begin{cases} \max \{v \in (0, w_\ell) : v + p(q/v) = w_\ell\} & \text{if } w_\ell > \tilde{w}(q), \\ \tilde{v}(q) & \text{if } w_\ell \leq \tilde{w}(q), \end{cases}$$

$$\hat{v}(w_\ell) \doteq \begin{cases} \min \{v \in (0, w_\ell) : v + p(q/v) = w_\ell\} & \text{if } w_\ell > \tilde{w}(q), \\ \tilde{v}(q) & \text{if } w_\ell \leq \tilde{w}(q), \end{cases}$$

and denote $U^\flat(w_\ell) \doteq (v^\flat(w_\ell), w_\ell)^T$, $\hat{U}(w_\ell) \doteq (\hat{v}(w_\ell), w_\ell)^T$. Notice that $w \mapsto v^\flat(w)$ is non-decreasing and $w \mapsto \hat{v}(w)$ is non-increasing.

- If $v_r > 0$, then we define $\check{U}(v_r) \doteq (\check{v}(v_r), \check{w}(v_r)) \doteq (v_r, v_r + p(q/v_r))$.

Definition 4.1. Consider the constrained Cauchy problem (4.1) with initial datum $U_0 \in \mathbf{BV}(\mathbb{R}; \mathcal{D})$. A function

$$U \in \mathbf{BV}(\mathbb{R}_+ \times \mathbb{R}; \mathcal{D}) \cap \mathbf{C}^0(\mathbb{R}_+; \mathbf{L}_{\text{loc}}^1(\mathbb{R}; \mathcal{D}))$$

is a weak solution of (4.1) if $Y = \Psi(U)$ satisfies the initial condition $Y(0, x) = \Psi(U_0(x))$ for a.e. $x \in \mathbb{R}$, for any test function $\phi \in \mathbf{C}_c^\infty((0, +\infty) \times \mathbb{R}; \mathbb{R})$

$$\iint_{\mathbb{R}_+ \times \mathbb{R}} (\rho \partial_t \phi + v \rho \partial_x \phi) \, dx \, dt = 0 \quad (4.3a)$$

and if $\phi(\cdot, 0) \equiv 0$ then

$$\iint_{\mathbb{R}_+ \times \mathbb{R}} (y \partial_t \phi + v y \partial_x \phi) \, dx \, dt = 0. \quad (4.3b)$$

Furthermore, the traces of Y at constraint $x = 0$ satisfy

$$f(U(t, 0^+)) = f(U(t, 0^-)) \leq q \quad \text{for a.e. } t > 0. \quad (4.4)$$

We point out that by the **BV** assumption the weak solutions admit traces in the classical sense.

Remark 4.1. Since we assume that $\phi(\cdot, 0) \equiv 0$ in (4.3b) but not in (4.3a), along $x = 0$ weak solutions satisfy the first Rankine-Hugoniot condition (2.17)₁ (with $\sigma^* = 0$, namely (4.4)), but not necessarily the second one (2.17)₂. We underline that in [4] the authors consider only weak solutions satisfying the second Rankine-Hugoniot condition (2.17)₂ (also along $x = 0$). Therefore such solutions are weak solutions also in the sense specified in Definition 4.1. This is in the same spirit

of the solutions considered in [12, 35, 38, 42, 46] for traffic through locations with reduced capacity.

Weak solutions given by the standard Riemann solver $\mathcal{RS}_{\text{ARZ}}$ (2.3) does not satisfy in general constraint condition in (4.1). Thus, let us introduce the following sets

$$\begin{aligned}\Omega_1 &\doteq \{(U_\ell, U_r) \in \mathcal{D} \times \mathcal{D} : f(\mathcal{RS}_{\text{ARZ}}[U_\ell, U_r])(0^\pm) \leq q\}, \\ \Omega_2 &\doteq \{(U_\ell, U_r) \in \mathcal{D} \times \mathcal{D} : f(\mathcal{RS}_{\text{ARZ}}[U_\ell, U_r])(0^\pm) > q\}.\end{aligned}$$

We conclude this subsection by recalling from [46] the definition of the non-conservative constrained Riemann solver

$$\begin{aligned}\mathcal{CRS}_{\text{ARZ}} & : \quad \mathcal{D} \times \mathcal{D} & \rightarrow & \quad \mathbf{C}^0((0, +\infty); \mathbf{L}_{\text{loc}}^1(\mathbb{R}; \mathcal{D})), \\ & (U_\ell, U_r) & \mapsto & \quad \mathcal{CRS}_{\text{ARZ}}[U_\ell, U_r].\end{aligned}$$

Definition 4.2. For any $U_\ell, U_r \in \mathcal{D}$, we define $\mathcal{CRS}_{\text{ARZ}}[U_\ell, U_r]$ as follows:

1. If $(U_\ell, U_r) \in \Omega_1$, then

$$\mathcal{CRS}_{\text{ARZ}}[U_\ell, U_r](\xi) \doteq \mathcal{RS}_{\text{ARZ}}[U_\ell, U_r](\xi).$$

2. If $(U_\ell, U_r) \in \Omega_2$, then

$$\mathcal{CRS}_{\text{ARZ}}[U_\ell, U_r](\xi) \doteq \begin{cases} \mathcal{RS}_{\text{ARZ}}[U_\ell, \hat{U}(w_\ell)](\xi) & \text{if } \xi < 0, \\ \mathcal{RS}_{\text{ARZ}}[\check{U}(v_r), U_r](\xi) & \text{if } \xi \geq 0. \end{cases}$$

Notice that if $(U_\ell, U_r) \in \Omega_2$, then $U(t, x) \doteq \mathcal{CRS}_{\text{ARZ}}[U_\ell, U_r](x/t)$ has a stationary non-classical shock $(\hat{U}(w_\ell), \check{U}(v_r))$ with $\hat{v}(w_\ell) < \check{v}(v_r) = v_r$.

4.3 The main result

In this subsection we present our main result from [42], that is we prove the existence of weak solution for constrained ARZ model (4.1). The proof is based

on Wave Front Tracking method, which is used to construct a globally defined approximate solution. Some technical proofs are postponed to Appendix B.

We introduce $\Upsilon: \mathbb{R}_+ \rightarrow \mathbb{R}$ defined by

$$\begin{aligned} \Upsilon(t) \doteq & \text{TV}(U(t, \cdot); \mathbb{R}) + 3\text{TV}(w(t, \cdot); \mathbb{R}_-) \\ & + 2[\text{TV}(\hat{v}(t); \mathbb{R}_-) + \text{TV}(v^b(t); \mathbb{R}_-) + W - \gamma(t) + \text{TV}_-(\tilde{\eta}(t, \cdot))], \end{aligned} \quad (4.5)$$

where

$$\hat{v}(t) \doteq \hat{v}(w(t, \cdot)), \quad v^b \doteq v^b(w(t, \cdot)),$$

and

$$\begin{aligned} \tilde{\eta}(t, x) \doteq & \begin{cases} \tilde{w}(v(t, x)) & \text{if } v(t, x) \in [\hat{v}(W), \tilde{v}(q)], \\ 0 & \text{otherwise,} \end{cases} \\ \gamma(t) \doteq & \begin{cases} \min\{v^b(w(t, 0^-)), v(t, 0^+)\} - v(t, 0^-) & \text{if } (U(t, 0^-), U(t, 0^+)) \in \Omega_2, \\ 0 & \text{otherwise.} \end{cases} \end{aligned}$$

Above, TV_- stands for the negative variation. By convention we assume that U is left continuous in time; therefore the maps $t \mapsto \text{TV}(v(t, \cdot)) + \text{TV}(w(t, \cdot))$ and $t \mapsto \Upsilon(t)$ are also left continuous.

Remark 4.2. *Some comments on the definition (4.5) of Υ are in order. The term $3\text{TV}(w(t, \cdot); \mathbb{R}_-) + 2[\text{TV}(\hat{v}(t); \mathbb{R}_-) + \text{TV}(v^b(t); \mathbb{R}_-)]$ is sensitive only for changes in w -coordinate, thus it measures the strength of the contact discontinuities in \mathbb{R}_- . Moreover $\text{TV}_-(\tilde{\eta}(t))$ measures the strength of the rarefaction waves and of non-classical shocks $(U(t, 0^-), U(t, 0^+))$. At last, γ is a compensation term and takes positive value if and only if the solution has a non-classical shock. Notice also that $\Upsilon(t) \geq 0$.*

We present now our main theorem from [42].

Theorem 4.1. *Assume that initial datum $U_0 \in \mathbf{BV}(\mathbb{R}; \mathcal{D})$ is such that $\Upsilon(0)$ is bounded. Then constrained Cauchy problem (4.1) admits a weak solution $U \in \mathbf{BV}(\mathbb{R}_+ \times \mathbb{R}; \mathcal{D}) \cap \mathbf{C}^0(\mathbb{R}_+; \mathbf{L}^1(\mathbb{R}; \mathcal{D}))$ in the sense of Definition 4.1 and for all $t, s \geq 0$*

it satisfies

$$\mathrm{TV}(U) \leq \Upsilon(0), \quad \|U(t, \cdot) - U(s, \cdot)\|_{\mathbf{L}^1(\mathbb{R})} \leq L|t - s|,$$

where $L \doteq \Upsilon(0) \cdot \max\{V, p^{-1}(W)p'(p^{-1}(W))\}$.

Remark 4.3. We underline that $\mathrm{TV}(U_0) < +\infty$ does not imply that $\Upsilon(0) < +\infty$. Indeed, the functions \hat{v} and v^b are not Lipschitz continuous close to $w = \tilde{w}(q)$ and $\tilde{\eta}(t, x)$ is discontinuous if $(t, x) \mapsto v(t, x)$ crosses the value $\tilde{v}(q)$ or $\hat{v}(W)$.

The proof of Theorem 4.1 bases on Wave Front Tracking method(see [18, 59] and references therein) and is described in the two forthcoming subsections. In the former one we describe the key tools to construct piecewise constant approximate solutions U^n to constrained Cauchy problem (4.1), namely a grid, an approximate constrained Riemann solver $\mathcal{CRS}_{\mathrm{ARZ}}^n$ and the functional Γ^n . In the latter subsection we give the proof of Theorem 4.1.

4.3.1 Wave Front Tracking

Grid construction

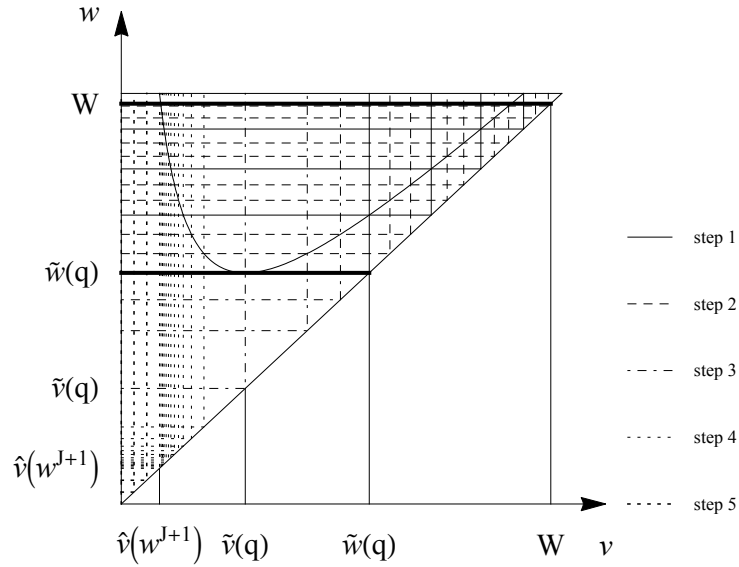
Fix $q \in (0, f_{\max}(W))$. We consider the grid $\mathcal{G}_n = (\mathcal{W}_n \times \mathcal{W}_n) \cap \mathcal{D}$, where $\mathcal{W}_n \doteq \{\omega_i^j\}_{i=0, \dots, n}^{j=-3-J, \dots, J}$ is a finite subset of $[0, W]$ constructed as follows, see Figure 4.2.

step 1 Consider the recursive sequence

$$\omega^j \doteq \begin{cases} \tilde{w}(q) & \text{if } j = 0, \\ \omega^{j-1} + p(q/\omega^{j-1}) & \text{if } j \in \mathbb{N} \setminus \{0\}, \end{cases}$$

which corresponds to the continuous lines in Figure 4.2. In other words, ω^j gives the w -coordinate of the intersection point between constraint curve $w = v + p(q/v)$ and $v = \omega^{j-1}$. We point out that there exists $J \leq (W - \tilde{w}(q))/p(q/W)$ such that $\omega^J \leq W < \omega^{J+1}$ and by monotonicity of p we have

$$\omega^j - \omega^{j-1} = p(q/\omega^{j-1}) \geq p(q/W).$$

Figure 4.2: The grid \mathcal{G}_n with $n = 3$.

step 2 Split $[\omega^0, \omega^1]$ into n subintervals of equal length with endpoints

$$\omega_i^0 = \omega^0 + i \frac{p(q/\tilde{w}(q))}{n}, \quad i \in \{0, \dots, n\},$$

and define recursive sequence

$$\omega_i^j = \omega_i^{j-1} + p(q/\omega_i^{j-1}) \in [\tilde{w}(q), \omega^{J+1}], \quad i \in \{0, \dots, n\}, \quad j \in \{1, \dots, J\},$$

corresponding to dashed lines in Figure 4.2. We point out that $\omega_n^j = \omega_0^{j+1} = \omega^{j+1}$.

step 3 In $[\tilde{v}(q), \tilde{w}(q)]$ we take

$$\omega_i^{-1} = v^b(\omega_i^0), \quad i \in \{0, \dots, n\},$$

corresponding to dot-dashed lines in Figure 4.2.

step 4 In $[\hat{v}(\omega^{J+1}), \tilde{v}(q)]$ we let

$$\omega_i^{-2-j} = \hat{v}(\omega_{n-i}^{J-j}), \quad i \in \{0, \dots, n\}, \quad j \in \{0, \dots, J\},$$

corresponding to thin dotted lines in Figure 4.2.

step 5 Split $[0, \hat{v}(\omega^{J+1})]$ into n subintervals of equal length with endpoints

$$\omega_i^{-3-J} = i \frac{\hat{v}(\omega^{J+1})}{n}, \quad i \in \{0, \dots, n\},$$

corresponding to thick dotted lines in Figure 4.2.

We show in the following lemma that the grid \mathcal{G}_n is well defined and the distance between two points of \mathcal{G}_n has a lower uniform bound; the proof is deferred to Appendix B.1. To simplify notation we write $\mathcal{W}_n = \{w_1, \dots, w_N\}$ for $w_i < w_{i+1}$.

Lemma 4.1. *Fix $n \in \mathbb{N}$ and $q \in (0, f_{\max}(W))$. The grid \mathcal{G}_n is well defined and*

$$\varepsilon_n \doteq \min_{i \in \{1, \dots, N\}} (w_{i+1} - w_i) > 0.$$

The cases $q = 0$ and $q = f_{\max}(W)$ are the straightforward generalizations.

Approximate Riemann solvers

To properly define in \mathcal{G}_n the approximate solutions U^n constructed via Wave Front Tracking method, we split rarefactions and introduce the approximate Riemann solver $\mathcal{RS}_{\text{ARZ}}^n : \mathcal{G}_n \times \mathcal{G}_n \rightarrow \mathbf{PC}(\mathbb{R}; \mathcal{G}_n)$. In more detail, for any $(U_\ell, U_r) \in \mathcal{G}_n \times \mathcal{G}_n$ with $w_\ell = w_r$ and $v_\ell = w_h < v_r = w_{h+k}$ we define

$$\mathcal{RS}_{\text{ARZ}}^n[U_\ell, U_r](\xi) = \begin{cases} U_\ell & \text{if } \xi \leq \sigma(U_\ell, U_1), \\ U_j & \text{if } \sigma(U_{j-1}, U_j) < \xi \leq \sigma(U_j, U_{j+1}), \quad 1 \leq j \leq k-1, \\ U_r & \text{if } \xi \geq \sigma(U_{k-1}, U_r), \end{cases}$$

where $U_0 = U_\ell$, $U_k = U_r$, $U_j = (w_{h+j}, w_\ell)^T$ and σ is defined in (4.2). The corresponding constrained approximate Riemann solver $\mathcal{CRS}_{\text{ARZ}}^n : \mathcal{G}_n \times \mathcal{G}_n \rightarrow \mathbf{PC}(\mathbb{R}; \mathcal{G}_n)$ is given as follows:

1. If $f(\mathcal{RS}_{\text{ARZ}}^n[U_\ell, U_r](0^\pm)) \leq q$, then

$$\mathcal{CRS}_{\text{ARZ}}^n[U_\ell, U_r] \doteq \mathcal{RS}_{\text{ARZ}}^n[U_\ell, U_r].$$

2. If $f(\mathcal{RS}_{\text{ARZ}}^n[U_\ell, U_r](0^\pm)) > q$, then

$$\mathcal{CRS}_{\text{ARZ}}^n[U_\ell, U_r](\xi) \doteq \begin{cases} \mathcal{RS}_{\text{ARZ}}^n[U_\ell, \hat{U}(w_\ell)](\xi) & \text{if } \xi < 0, \\ \mathcal{RS}_{\text{ARZ}}^n[\check{U}(v_r), U_r](\xi) & \text{if } \xi \geq 0. \end{cases}$$

Interaction estimates

We introduce now the Wave Front Tracking approximate solutions U^n and define the map $t \mapsto \Gamma^n(t) \doteq \Gamma^n(U^n(t))$. To shorten notation we omit the dependence on n , that is we write for instance U in place of U^n and ε for ε_n . Therefore, the non-negative map $\Gamma(U^n(t))$ has the following form

$$\begin{aligned} \Gamma(U(t)) &\doteq \text{TV}(U(t)) + 3\text{TV}(w(t); \mathbb{R}_-) + 2\text{TV}(\hat{v}(t); \mathbb{R}_-) + 2\text{TV}(v^b(t); \mathbb{R}_-) \\ &\quad + 2 \left(W - \gamma(t) + \sum_{x \in \mathbf{J}(t)} \eta(U(t, x^-), U(t, x^+)) \right). \end{aligned}$$

Above, $\hat{v}(t) = \hat{v}(w(t))$, $v^b(t) = v^b(w(t))$, $\mathbf{J}(t) \subset \mathbb{R}$ is the finite set of discontinuity points of $U(t, \cdot)$ and

$$\eta(U_-, U_+) = \begin{cases} \check{w}(v_-) - \check{w}(v_+) & \text{if } w_- = w_+ \text{ and } \hat{v}(W) \leq v_- < v_+ \leq \tilde{v}(q), \\ 0 & \text{otherwise.} \end{cases}$$

Remark 4.4. *We underline that the estimate*

$$\lim_{t \rightarrow 0^+} \left(\sum_{x \in \mathbf{J}(t)} \eta(U(t, x^-), U(t, x^+)) \right) \leq \sum_{x \in \mathbf{J}(0)} \eta(U_0(x^-), U_0(x^+))$$

does not hold true in general. For example we can take U_0 with a discontinuity (U_ℓ, U_r) away from $x = 0$ such that the following conditions are satisfied

$$w_\ell \neq w_r, \quad \hat{v}(W) \leq v_\ell < v_r \leq \tilde{v}(q).$$

However we have

$$\lim_{t \rightarrow 0^+} \left(\sum_{x \in \mathcal{J}(t)} \eta(U(t, x^-), U(t, x^+)) \right) \leq \text{TV}_-(\tilde{\eta}(U_0)).$$

These considerations show the difference between functionals Γ and Υ defined in (4.5). Moreover $t \mapsto \Upsilon(t)$ fails to satisfy the properties listed in Lemma 4.2 and thus giving motivation to introduce both functionals Γ and Υ .

Lemma 4.2. *For any $n \in \mathbb{N}$ let $U_0^n \in \mathbf{PC}(\mathbb{R}; \mathcal{G}_n)$ be an approximated initial datum, and U^n be a corresponding approximated solution constructed via Wave Front Tracking method. Then the map $t \mapsto \Gamma^n(U^n(t))$ is non-increasing and moreover decreases by at least ε_n if the number of waves increases.*

The proof of Lemma 4.2 is deferred to Appendix B.2.

4.3.2 Proof of Theorem 4.1

We approximate the initial datum U_0 with $U_0^n \in \mathbf{PC}(\mathbb{R}; \mathcal{G}_n)$ so that:

$$\|U_0^n\|_{\mathbf{L}^\infty(\mathbb{R})} \leq \|U_0\|_{\mathbf{L}^\infty(\mathbb{R})}, \quad \lim_{n \rightarrow +\infty} \|U_0 - U_0^n\|_{\mathbf{L}^1(\mathbb{R})} = 0, \quad \Gamma(U_0^n) \leq \Upsilon(0). \quad (4.6)$$

By Lemma 4.2 the map $t \rightarrow \Gamma(U^n(t))$ is non-increasing and as a consequence

$$\text{TV}(U^n(t, \cdot)) \leq \Gamma^n(U^n(t, \cdot)) \leq \Gamma^n(U_0^n) \leq \Upsilon(0).$$

By the standard application of Helly's Theorem, see [18, Theorem 2.4], we deduce that only finitely many interactions can occur at finite time. Therefore, the construction of approximated solution U^n can be extended globally in time.

We begin by straightforward observation that

$$\|U^n(t)\|_{\mathbf{L}^\infty(\mathbb{R})} \leq \|U_0\|_{\mathbf{L}^\infty(\mathbb{R})}$$

and the Lipschitz condition

$$\|U^n(t, \cdot) - U^n(s, \cdot)\|_{\mathbf{L}^1(\mathbb{R})} \leq L|t - s| \quad (4.7)$$

holds for $L \doteq \Upsilon(0) \cdot \max\{V, p^{-1}(W)p'(p^{-1}(W))\}$. More precisely, if there is no interaction between t and s , then

$$\begin{aligned} & \|U^n(t, \cdot) - U^n(s, \cdot)\|_{\mathbf{L}^1(\mathbb{R})} \\ &= \sum_{x \in \mathbf{J}(t^+)} \left\| (t-s)\sigma(U(t^+, x^-), U(t^+, x^+)) (U(t^+, x^-) - U(t^+, x^+)) \right\| \leq L|t-s|. \end{aligned}$$

Above, $\mathbf{J}(t^+) \subset \mathbb{R}$ is the finite set of discontinuity points of $U(t^+, \cdot)$ and σ is defined by (4.2). We point out that the map $t \mapsto U^n(t, \cdot)$ is \mathbf{L}^1 -continuous across interaction times.

By Helly's Theorem U^n converges (up to a subsequence) to some function U in $\mathbf{L}_{\text{loc}}^1(\mathbb{R}_+ \times \mathbb{R}; \mathcal{D})$ as $n \rightarrow +\infty$ and moreover the limit function U satisfies:

$$\begin{aligned} \text{TV}(U(t, \cdot)) &\leq \Upsilon(0), \\ \|U(t, \cdot) - U(s, \cdot)\|_{\mathbf{L}^1(\mathbb{R})} &\leq L|t-s|, \\ \|U(t, \cdot)\|_{\mathbf{L}^\infty(\mathbb{R})} &\leq \|U_0\|_{\mathbf{L}^\infty(\mathbb{R})}. \end{aligned}$$

It remains to prove that the limit function U is a weak solution of (4.1) in the sense of Definition 4.1.

We deduce that the initial condition of (4.1) is satisfied by (4.6)₂, (4.7) and $\mathbf{L}_{\text{loc}}^1$ -convergence of U^n to U . To prove that U is a weak solution of Cauchy problem (4.1) it is sufficient to show that condition (4.3) holds true, namely for any test function $\phi \in \mathbf{C}_c^\infty((0, +\infty) \times \mathbb{R}; \mathbb{R})$

$$\iint_{\mathbb{R}_+ \times \mathbb{R}} (\rho \partial_t \phi + v \rho \partial_x \phi) \, dx \, dt = 0$$

and if $\phi(\cdot, 0) \equiv 0$ then

$$\iint_{\mathbb{R}_+ \times \mathbb{R}} (y \partial_t \phi + v y \partial_x \phi) \, dx \, dt = 0.$$

Clearly $Y^n \doteq \Psi(U^n)$ and $v^n Y^n$ are uniformly bounded and we are reduced to show

$$\lim_{n \rightarrow +\infty} \iint_{\mathbb{R}_+ \times \mathbb{R}} (\rho^n \partial_t \phi + v^n \rho^n \partial_x \phi) \, dx \, dt = 0, \quad (4.8a)$$

and if $\phi(\cdot, 0) \equiv 0$

$$\lim_{n \rightarrow +\infty} \iint_{\mathbb{R}_+ \times \mathbb{R}} (y^n \partial_t \phi + v^n y^n \partial_x \phi) \, dx \, dt = 0. \quad (4.8b)$$

We take $T > 0$ so that $\phi(t, x) = 0$ for every $t \geq T$. By the Green-Gauss formula we write double integrals in (4.8) as

$$\int_0^T \sum_{x \in \mathcal{J}(t)} \left(\sigma(U^n(t, x^-), U^n(t, x^+)) \Delta Y^n(t, x) - \Delta F^n(t, x) \right) \phi(t, x) \, dt,$$

where

$$\begin{aligned} \Delta Y^n(t, x) &\doteq Y^n(t, x^+) - Y^n(t, x^-), \\ \Delta F^n(t, x) &\doteq v^n(t, x^+) Y^n(t, x^+) - v^n(t, x^-) Y^n(t, x^-). \end{aligned}$$

Notice that for any classical discontinuity at the point (t, x) Rankine-Hugoniot conditions (2.14) is satisfied and

$$\sigma(U^n(t, x^-), U^n(t, x^+)) \Delta Y^n(t, x) - \Delta F^n(t, x) = 0.$$

If a discontinuity is a (stationary) non-classical shock, then

$$\sigma(U^n(t, 0^-), U^n(t, 0^+)) \Delta Y^n(t, 0) - \Delta F^n(t, 0) = -\Delta F^n(t, 0).$$

However, in such a case $f(U(t, 0^-)) = f(U(t, 0^+))$ and then integral in (4.8a) equals zero. By the fact that the non-classical shocks occur only at $x = 0$ and thanks to assumption $\phi(\cdot, 0) \equiv 0$, we conclude that also the integral in (4.8b) is equal to zero.

The proof is completed by showing that U satisfies the constraint condition

$$f(U(t, 0^\pm)) \leq q.$$

To reach this goal we use the fact that both U and U^n are weak solutions of

$$\begin{cases} \partial_t Y + \partial_x F(Y) = 0, \\ Y(0, x) = \Psi(U_0(x)), \end{cases}$$

in $\mathbb{R}_+ \times \mathbb{R}_-$ and $\mathbb{R}_+ \times \mathbb{R}_+$. By the Wave Front Tracking approximation of U^n we have $f(U^n(t, 0^-)) = f(U^n(t, 0^+)) \leq q$ for all $t > 0$. We apply Gauss-Green formula to the weak formulation of $\partial_t \rho^n + \partial_x f(U^n) = 0$ and then obtain

$$\begin{aligned} q \int_{\mathbb{R}_+} \psi(t) dt &\geq \int_{\mathbb{R}_+} f(U^n(t, 0^-)) \psi(t) dt \\ &= \iint_{\mathbb{R}_+ \times \mathbb{R}_-} \left(\rho^n(t, x) \dot{\psi}(t) \xi(x) + f(U^n(t, x)) \psi(t) \dot{\xi}(x) \right) dx dt, \end{aligned}$$

where $\psi \in \mathbf{C}_c^\infty(\mathbb{R}_+; \mathbb{R})$ is an arbitrary time-dependent test function with compact support and $\xi \in \mathbf{C}_c^\infty(\mathbb{R}; \mathbb{R})$ is a space-dependent test function such that $\xi(0) = 1$.

We pass then to the limit $n \rightarrow +\infty$ in the term

$$\iint_{\mathbb{R}_+ \times \mathbb{R}_-} \left(\rho^n(t, x) \dot{\psi}(t) \xi(x) + f(U^n(t, x)) \psi(t) \dot{\xi}(x) \right) dx dt$$

and apply again the Green-Gauss formula. As a result we obtain

$$q \int_{\mathbb{R}_+} \psi(t) dt \geq \lim_{n \rightarrow +\infty} \int_{\mathbb{R}_+} f(U^n(t, 0^-)) \psi(t) dt = \int_{\mathbb{R}_+} f(U(t, 0^-)) \psi(t) dt.$$

Hence the trace $f(U^n(t, 0^-))$ weakly converges to the trace $f(U(t, 0^-))$ and moreover $f(U(t, 0^-)) \leq q$ for a.e. $t > 0$. At last, we repeat analogously the above procedure to $\mathbb{R}_+ \times \mathbb{R}_+$ and obtain $f(U(t, 0^+)) = f(U(t, 0^+)) \leq q$ for a.e. $t > 0$.

Summarizing, U^n can be extended globally in time and $\text{TV}(U^n(t)) \leq \Gamma^n(t) \leq \Gamma^n(0) \leq \Upsilon(0)$.

4.4 A case study

In this subsection we apply the Riemann solver $\mathcal{CRS}_{\text{ARZ}}$ to describe the evolution of traffic through a point constraint representing, for instance, a toll gate. Fix $x_A < x_B < 0$ and $w_1 < w_2$. Consider in $[x_A, 0)$ vehicles with zero velocity that are

bumper to bumper. We assume that they have different maximal densities $\rho_1 \doteq p^{-1}(w_1)$ and $\rho_2 \doteq p^{-1}(w_2)$ in $[x_A, x_B)$ and $[x_B, 0)$, respectively. This corresponds to consider constrained Cauchy problem (4.1) with piecewise constant initial datum.

$$U_0(x) = \begin{cases} (w_1, w_1) & \text{if } x < x_A, \\ (0, w_1) & \text{if } x_A \leq x < x_B, \\ (0, w_2) & \text{if } x_B \leq x < 0, \\ (w_2, w_2) & \text{if } x \geq x_B. \end{cases} \quad (4.9)$$

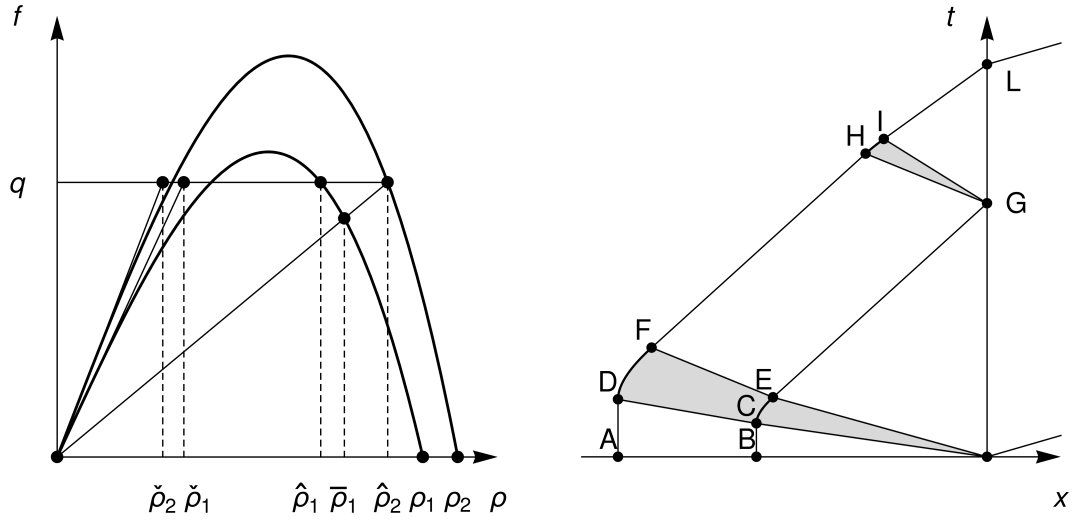


Figure 4.3: The solution to Cauchy problem (4.1) with initial datum (4.9) constructed in Section 4.4. The shaded areas correspond to rarefactions.

Define $\hat{U}_i \doteq \hat{U}(w_i)$ and let $\tilde{U}_1 \doteq \tilde{U}_1(\hat{U}_1, \hat{U}_2)$ be implicitly defined by

$$\tilde{v}_1 = \hat{w}_1 - p(\tilde{\rho}_1) = \hat{v}_2,$$

see Figure 4.3. Assume that q belongs to $(0, f_{\max}(w_1))$. The solution is constructed as follows. We first apply $\mathcal{RS}_{\text{ARZ}}$ at $A(0, x_A)$ and $B(0, x_B)$ and $\mathcal{CRS}_{\text{ARZ}}$ at $(0, 0)$. Two stationary contact discontinuities CD_A and CD_B start from A and B . From $(0, 0)$ we have a backward rarefaction R_0 , a stationary non-classical shock NS_0 and a forward contact discontinuity CD_0 . Denote by C and E the first and last interaction points between R_0 and CD_B . Denote by D and F the first and last

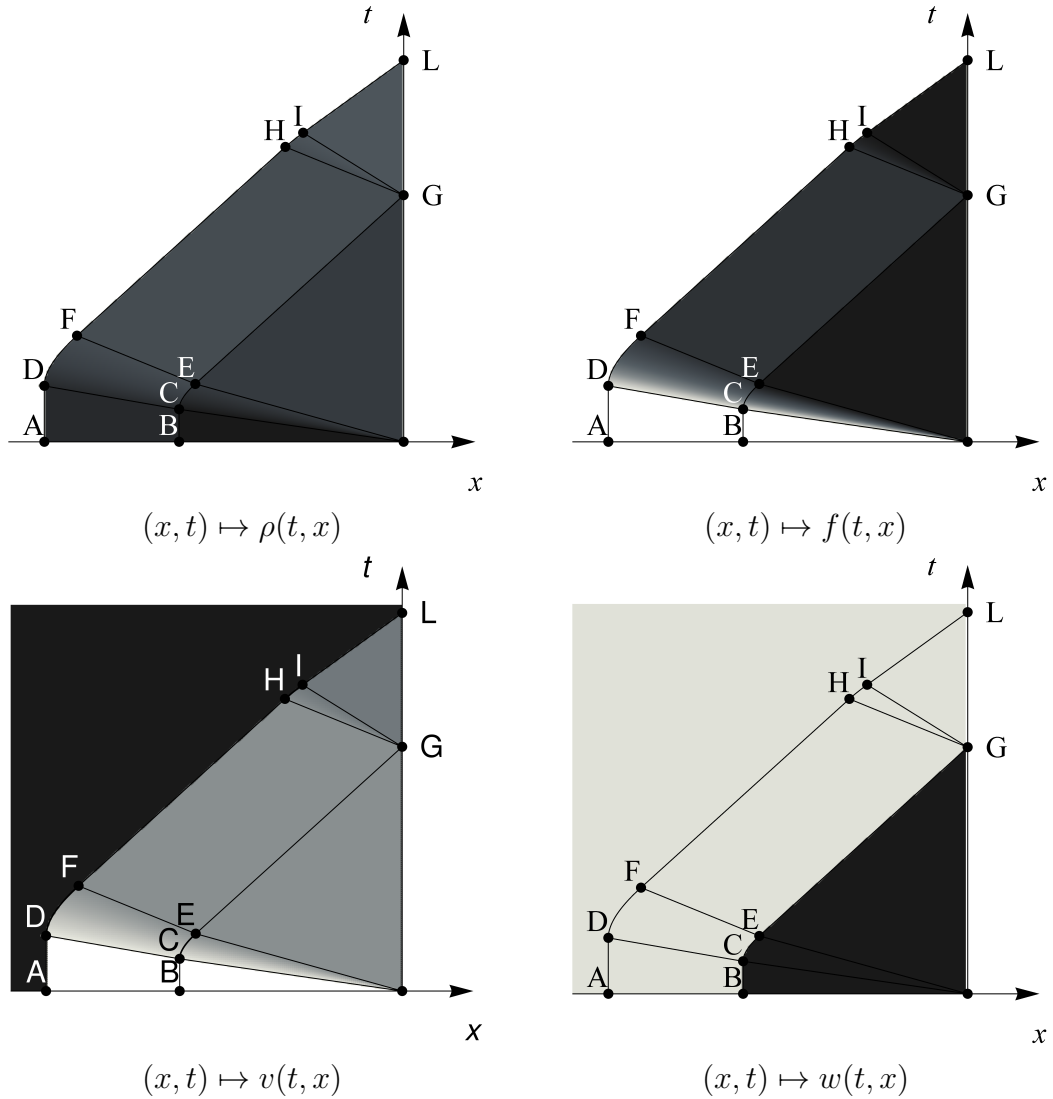


Figure 4.4: The solution to Cauchy problem (4.1) with initial datum (4.9) constructed in Section 4.4. Darker colors correspond to higher values.

interaction points between R_0 and CD_A . Notice that R_0 crosses CD_B ; on the other hand, R_0 does not cross CD_A and expires. Both CD_A and CD_B have speed of propagation $\tilde{v}_1 = \hat{v}_2$ after their interaction with R_0 . Once CD_B reaches $x = 0$ at $G = (t_G, 0)$, a backward rarefaction R_G is created and the left state of NS_0 varies from \hat{U}_2 to \hat{U}_1 . Let H and I be the first and last interaction points between CD_A and R_G . Observe that R_G does not cross CD_A and expires. CD_A moves with velocity \hat{v}_1 after time $t = t_I$, reaches $x = 0$ at $L = (t_L, 0)$ and then continues in

$(0, +\infty)$. CD_0 and CD_A do not interact because their speeds of propagation are w_2 and \tilde{v}_2 , respectively.

The solution above has the following physical interpretation. At time $t = 0$, the rightmost vehicle starts to move with constant maximal speed w_2 . The other vehicles start as soon as the following distance in front of them is safe. This acceleration is related to the rarefaction R_0 . Due to the presence of the toll gate, which hinders the flow at $x = 0$, the vehicles initially in $[x_B, 0)$ stop to accelerate once they reach the velocity \hat{v}_2 and flow q , which is the maximal capacity of the toll gate. On the other hand, the vehicles initially in $[x_A, x_B)$ stop to accelerate once they reach the velocity $\tilde{v}_1 = \hat{v}_2$ of the other vehicles in the upstream of the toll gates. Once all the vehicles initially in $[x_B, 0)$ have crossed the toll gate, namely at time $t = t_G$, the upstream vehicles accelerate and reach the velocity \hat{v}_1 and flow q . This acceleration corresponds to the rarefaction R_G . Finally, after time t_L all the vehicles have passed the toll gates.

In Figure 4.3 we represent the initial datum and an overall overview of the solution corresponding to

$$w_1 = 1, \quad w_2 = 6/5, \quad p(\rho) = \rho^2, \quad q = \sqrt{3}/5, \quad x_A = -8, \quad x_B = -5.$$

The quantitative evolution of the corresponding solution is represented in different coordinates in Figure 4.4. We finally observe that, once the overall picture of the solution is known, it is possible to express in a closed form the time at which the last vehicle passes through $x = 0$, indeed

$$t_L = [(x_B - x_A)p^{-1}(w_1) - x_B p^{-1}(w_2)]/q \approx 24.4716.$$

Constrained PT models

5.1 Introduction

In this chapter we consider the constrained versions of the PT^a and PT^p models introduced in Section 2.4.3 and study both the cases with and without metastable phase. We first introduce and describe in full details the corresponding constrained Riemann solvers. We then study their main properties we obtained in [35], namely $\mathbf{L}_{\text{loc}}^1$ -continuity with respect to the initial data and their invariant domains. Moreover, we show our existence result [10] for the constrained PT^p model with metastable phase.

As in Section 2.4.3 the Riemann solvers associated to the Riemann problem (2.20), (2.21) are denoted by \mathcal{RS}_R and \mathcal{RS}_S , respectively in the cases of intersecting and non-intersecting phases.

Besides the initial condition (2.21), in this chapter we enforce the local point constraint on the flow at $x = 0$, namely

$$f(U(t, 0^\pm)) \leq q, \quad (5.1)$$

where $q \in (0, f_f^+)$ is a given constant quantity. Admissible solutions to (2.20), (2.21) do not satisfy in general (5.1). Thus we introduce the following definition of admissible constrained solution to (2.20), (2.21), (5.1).

Definition 5.1. Fix $U_\ell, U_r \in \Omega$. A self-similar function $U \doteq (v, w) : \mathbb{R}_+ \times \mathbb{R} \rightarrow \Omega$ is an admissible constrained solution to constrained Riemann problem (2.20), (2.21),

(5.1) if for $U^- \doteq U(t, 0^-)$ and $U^+ \doteq U(t, 0^+)$ the following conditions hold true:

- The maps

$$(t, x) \mapsto \begin{cases} U(t, x) & \text{if } x < 0, \\ U^- & \text{if } x > 0, \end{cases} \quad (t, x) \mapsto \begin{cases} U^+ & \text{if } x < 0, \\ U(t, x) & \text{if } x > 0, \end{cases}$$

are admissible solutions to the Riemann problems for (2.20) with Riemann data respectively given by

$$U(0, x) = \begin{cases} U_\ell & \text{if } x < 0, \\ U^- & \text{if } x > 0, \end{cases} \quad U(0, x) = \begin{cases} U^+ & \text{if } x < 0, \\ U_r & \text{if } x > 0, \end{cases}$$

in the sense of Definition 2.6.

- The constrained condition $f(U^-) = f(U^+) \leq q$ is satisfied.

Remark 5.1. Notice that the linearized momentum y is in general not conserved across possible stationary discontinuities at $x = 0$. For this reason in the above definition we cannot impose $y(U^-)v^- = y(U^+)v^+$, even if $U^-, U^+ \in \Omega_c$. Therefore an admissible constrained solution to Riemann problem (2.20), (2.21), (5.1) taking values in Ω_c is not necessarily a weak solution.

We denote by \mathcal{CRS}_R and \mathcal{CRS}_S the constrained Riemann solvers associated to the Riemann problems (2.20), (2.21), (5.1), respectively for the cases with and without metastable phase. Their definitions given below are in accordance with Definition 5.1, in the sense that $(t, x) \mapsto \mathcal{CRS}_R[U_\ell, U_r](x/t)$ and $(t, x) \mapsto \mathcal{CRS}_S[U_\ell, U_r](x/t)$ are admissible constrained solutions.

We let (with a slight abuse of notation)

$$\begin{aligned} \mathcal{CRS}_R &\doteq \mathcal{RS}_R & \text{in} & \quad \mathcal{D}_1 \doteq \{(U_\ell, U_r) \in \Omega^2 : f(\mathcal{RS}_R[U_\ell, U_r](t, 0^\pm)) \leq q\}, \\ \mathcal{CRS}_S &\doteq \mathcal{RS}_S & \text{in} & \quad \mathcal{D}_1 \doteq \{(U_\ell, U_r) \in \Omega^2 : f(\mathcal{RS}_S[U_\ell, U_r](t, 0^\pm)) \leq q\}, \end{aligned}$$

and we denote $\mathcal{D}_2 \doteq \Omega^2 \setminus \mathcal{D}_1$.

We will also discuss their main properties, such as consistency, $\mathbf{L}_{\text{loc}}^1$ -continuity and invariant domains. In this regard, we recall the following definition.

Definition 5.2. *An invariant domain for a Riemann solver $\mathcal{RS}: \Omega^2 \rightarrow \mathbf{L}^\infty(\mathbb{R}; \Omega)$ is a set $\mathcal{I} \subseteq \Omega$ such that $\mathcal{RS}[\mathcal{I}, \mathcal{I}](\mathbb{R}) \subseteq \mathcal{I}$.*

Proposition 5.1. *Let $\mathcal{RS}: \Omega^2 \rightarrow \mathbf{L}^\infty(\mathbb{R}; \Omega)$ be a Riemann solver. If $(t, x) \mapsto \mathcal{RS}[U_\ell, U_r](x/t)$ satisfies (5.1) for all $U_\ell, U_r \in \Omega$, then \mathcal{RS} does not satisfy (I) of Definition 2.9, hence it is not consistent.*

Proof. Fix $U_\ell \doteq (v_{\max}, w_+) \doteq U_r$, see Figure 2.2. We have that $f(U_r) = f_f^+ > q$. By the finite speed of propagation of the waves we have $\mathcal{RS}[U_\ell, U_r](\bar{\xi}) = U_r$ for some $\bar{\xi} > 0$. Let $U_m \doteq U_r$. Assume by contradiction that $\mathcal{RS}[U_m, U_r](\xi) = U_m$ for any $\xi < \bar{\xi}$. Then $f(\mathcal{RS}[U_m, U_r](0^\pm)) = f(U_r) > q$ and this is contradictory to (5.1). We conclude that the property $\mathcal{RS}[U_m, U_r](x) = U_m$ for any $\xi < \bar{\xi}$ in (I) is not satisfied. \square

We define below the constrained Riemann solver for the case with metastable phase.

Definition 5.3. *Assume that $\Omega_f \cap \Omega_c \neq \emptyset$. The constrained Riemann solver $\mathcal{CRS}_R: \Omega^2 \rightarrow \mathbf{L}^\infty(\mathbb{R}; \Omega)$ associated to (2.20), (2.21), (5.1) is defined as*

$$\mathcal{CRS}_R[U_\ell, U_r](\xi) \doteq \begin{cases} \mathcal{RS}_R[U_\ell, U_r](\xi) & \text{if } (U_\ell, U_r) \in \mathcal{D}_1, \\ \begin{cases} \mathcal{RS}_R[U_\ell, \hat{U}](\xi) & \text{if } \xi < 0, \\ \mathcal{RS}_R[\check{U}, U_r](\xi) & \text{if } \xi > 0, \end{cases} & \text{if } (U_\ell, U_r) \in \mathcal{D}_2, \end{cases}$$

where $\hat{U} = \hat{U}(w_\ell, q) \in \Omega_c$ and $\check{U} = \check{U}(v_r, q) \in \Omega$ are uniquely selected by the conditions

$$f(\hat{U}) = f(\check{U}) = q, \quad \hat{w} = \max\{w_\ell, w_-\}, \quad \check{v} = \begin{cases} v_{\max} & \text{if } f(\psi_2^-(U_r)) > q, \\ v_r & \text{if } f(\psi_2^-(U_r)) \leq q. \end{cases}$$

In Figure 5.1 we present all possible choices of \hat{U} and \check{U} given by the above definition. It is worth noting that \hat{U} and \check{U} satisfy the following properties:

- if $(U_\ell, U_r) \in \mathcal{D}_2$, then $w_\ell > \check{w}$ and $v_r > \hat{v}$,
- if $(U_\ell, U_r) \in \mathcal{D}_2$ and $U_\ell \in \Omega_f^-$, then $\hat{w} = w_-$,

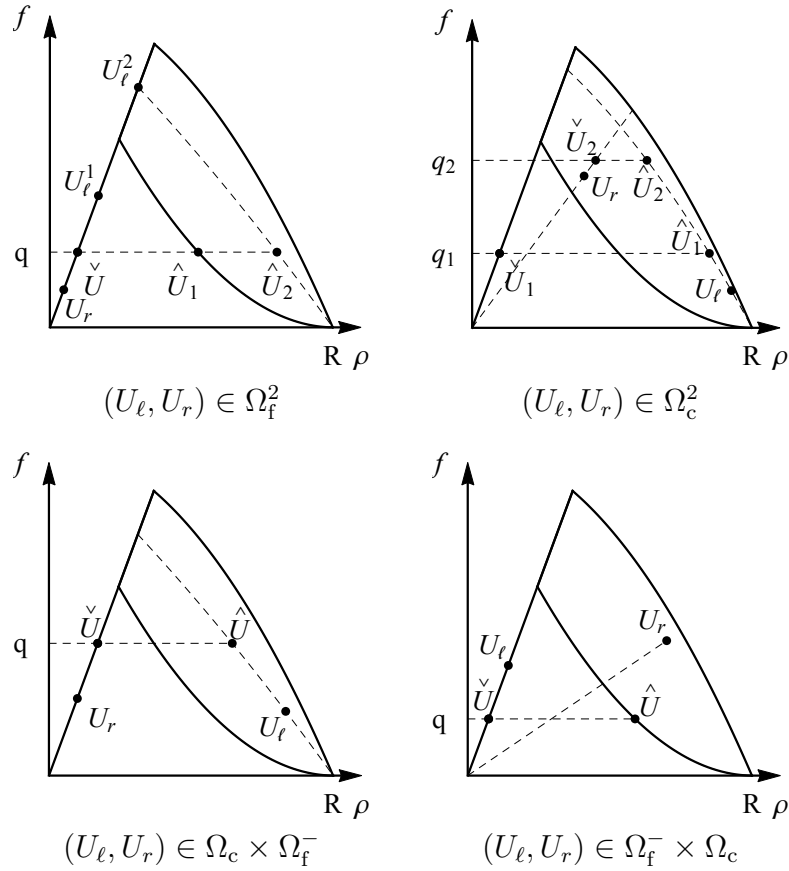


Figure 5.1: The selection criterion for \hat{U} and \check{U} given in Definition 5.3 in the case $(U_\ell, U_r) \in \mathcal{D}_2$. In the first picture U_ℓ^1, U_ℓ^2 represent the left state in two different cases and \hat{U}_1, \hat{U}_2 are the corresponding \hat{U} . In the second picture q_1, q_2 are q in two different cases, \hat{U}_1, \hat{U}_2 are the corresponding \hat{U} and \check{U}_1, \check{U}_2 are the corresponding \check{U} .

- if $(U_\ell, U_r) \in \mathcal{D}_2$ and $U_r \in \Omega_f$, then $\check{v} = v_{\max}$.

We define below the constrained Riemann solver for the case without metastable phase.

Definition 5.4. Assume that $\Omega_f \cap \Omega_c = \emptyset$. The constrained Riemann solver

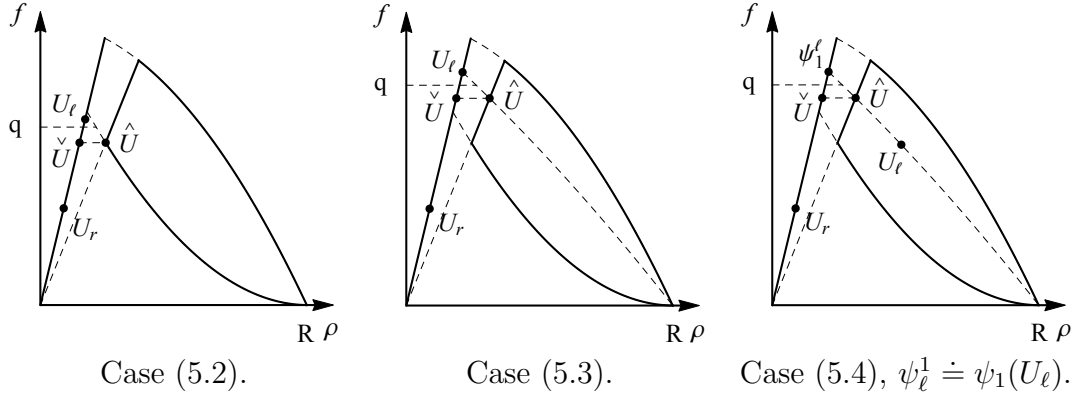


Figure 5.2: The selection criterion for \hat{U} and \check{U} given in Definition 5.4.

$\mathcal{CRS}_S: \Omega^2 \rightarrow \mathbf{L}^\infty(\mathbb{R}; \Omega)$ associated to (2.20), (2.21), (5.1) is defined as

$$\mathcal{CRS}_S[U_\ell, U_r](\xi) \doteq \begin{cases} \mathcal{RS}_S[U_\ell, U_r](\xi) & \text{if } (U_\ell, U_r) \in \mathcal{D}_1, \\ \begin{cases} \mathcal{RS}_S[U_\ell, \hat{U}](\xi) & \text{if } \xi < 0, \\ \mathcal{RS}_S[\check{U}, U_r](\xi) & \text{if } \xi > 0, \end{cases} & \text{if } (U_\ell, U_r) \in \mathcal{D}_2, \end{cases}$$

where $\hat{U} = \hat{U}(w_\ell, q) \in \Omega_c$ and $\check{U} = \check{U}(w_\ell, v_r, q) \in \Omega$ are uniquely selected by the conditions

$$f(\hat{U}) = f(\check{U}) = \max\{f(U) \leq q : U \in \Omega_c, w = \max\{w_\ell, w_-\}\},$$

$$\hat{w} = \max\{w_\ell, w_-\}, \quad \check{v} = \begin{cases} v_{\max} & \text{if } f(\psi_2^-(U_r)) > q, \\ v_r & \text{if } f(\psi_2^-(U_r)) \leq q. \end{cases}$$

Remark 5.2. In the case $(U_\ell, U_r) \in \mathcal{D}_2$, the choices of \hat{U} and \check{U} in Definitions 5.3 and 5.4 coincide if and only if one of the following conditions is satisfied

$$(U_\ell, U_r) \in \Omega_f^- \times \Omega_f, \quad q \in (f_c^-, f(U_\ell)), \quad (5.2)$$

$$(U_\ell, U_r) \in \Omega_f^+ \times \Omega_f, \quad q \in (f(\psi_1^c(U_\ell)), f(U_\ell)), \quad (5.3)$$

$$(U_\ell, U_r) \in \Omega_c \times \Omega_f, \quad q \in (f(\psi_1^c(U_\ell)), f(\psi_1(U_\ell))), \quad (5.4)$$

and in this case $f(\hat{U}) = f(\check{U}) < q$ and $\hat{v} = v_c$. The above cases are considered in

Figure 5.2. Thus $\mathcal{CRS}_R[U_\ell, U_r] \not\equiv \mathcal{CRS}_S[U_\ell, U_r]$ if and only if (U_ℓ, U_r) belongs to \mathcal{D}_1 and satisfies one of conditions (2.22), (2.24), (2.23), or (U_ℓ, U_r) belongs to \mathcal{D}_2 and satisfies one of conditions (5.2), (5.3), (5.4).

In the following propositions we give the main properties of the constrained Riemann solvers \mathcal{CRS}_R and \mathcal{CRS}_S . We point out that by Proposition 5.1 the constrained Riemann solvers \mathcal{CRS}_R and \mathcal{CRS}_S are not consistent; for this reason we consider in the next two proposition only condition (II) of Definition 2.9.

Proposition 5.2. \mathcal{CRS}_R is $\mathbf{L}_{\text{loc}}^1$ -continuous and satisfies (II) of Definition 2.9.

Proposition 5.3. \mathcal{CRS}_S is not $\mathbf{L}_{\text{loc}}^1$ -continuous and satisfies (II) of Definition 2.9.

The proofs of the above two propositions are deferred to Sections A.3 and A.4, respectively.

We summarize in Table 5.1 the $\mathbf{L}_{\text{loc}}^1$ -continuity and consistency properties of Riemann solvers considered in Section 2.4 and in the present chapter. We underline that the lack of $\mathbf{L}_{\text{loc}}^1$ -continuity of a Riemann solver does not prevent the study of the general Cauchy problem, see for instance [3, 27].

	metastable phase	$\mathbf{L}_{\text{loc}}^1$ -continuity	consistency	
			I	II
\mathcal{RS}_R	Yes	Yes	Yes	Yes
\mathcal{RS}_S	No	Yes	Yes	Yes
\mathcal{CRS}_R	Yes	Yes	No	Yes
\mathcal{CRS}_S	No	No	No	Yes

Table 5.1: The main properties of the Riemann solvers.

We complete this subsection with some remarks on the invariant domains. By construction Ω is an invariant domain for both \mathcal{CRS}_R and \mathcal{CRS}_S . The spaces Ω_f and Ω_c are invariant domains for \mathcal{CRS}_S , however not for \mathcal{CRS}_R . Therefore we look for the minimal (w.r.t. inclusion) invariant domains for \mathcal{CRS}_R containing Ω_f or Ω_c , see Figure 5.3.

Proposition 5.4. Let \mathcal{CRS}_R be the constrained Riemann solver introduced in Definition 5.7.

(ICR.1) The minimal invariant domain including Ω_f is $\mathcal{I}_f \doteq \Omega_f \cup \mathcal{I}_1 \cup \mathcal{I}_2$, where

$$\begin{aligned} \mathcal{I}_1 &\doteq \{U \in \Omega_c : f(U) \leq q \leq f(\psi_2^+(U))\}, \\ \mathcal{I}_2 &\doteq \left\{ U \in \Omega_c : f(U) > q, \frac{d^2 \mathcal{L}_w^1}{d\rho^2}(\rho(U)) > 0 \right\}. \end{aligned}$$

(ICR.2) The minimal invariant domain including Ω_c is

$$\mathcal{I}_c \doteq \Omega_c \cup \{(q/v_{\max}, Q(q/v_{\max}))\}.$$

The proof is deferred to Subsection A.4.

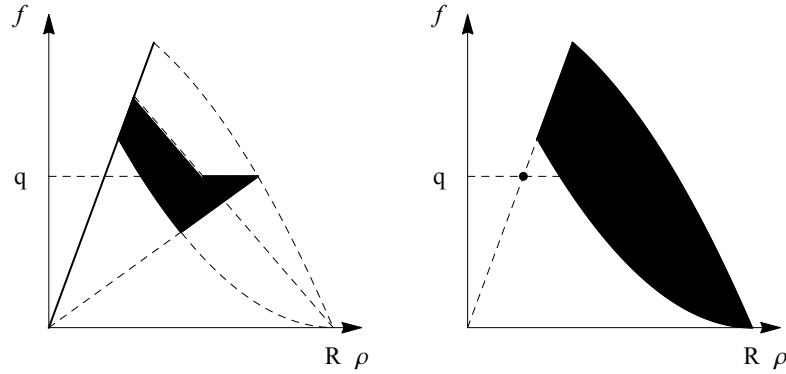


Figure 5.3: Invariant domains \mathcal{I}_f (left) and \mathcal{I}_c (right) described in (ICR.1) and (ICR.2) of Proposition 5.4.

We recall that the first Lax curves are strictly concave for the PT^p model and for the PT^a model under the assumption $\frac{d^2 \mathcal{L}_w^1}{d\rho^2}(r_-^c) \leq 0$. This implies $\mathcal{I}_2 = \emptyset$. At last, we give the minimal invariant domains for \mathcal{CRS}_S containing Ω_f or Ω_c .

Proposition 5.5. *Let \mathcal{CRS}_S be the constrained Riemann solver introduced in Definition 5.4.*

(ICS.1) The minimal invariant domain containing Ω_f is

$$\mathcal{I}_f \doteq \begin{cases} \mathcal{I}_f \text{ defined in (ICR.1) of Proposition 5.4} & \text{if } q < f_c^+, \\ \Omega_f \cup \{U \in \Omega_c : v = v_c\} & \text{if } q \geq f_c^+. \end{cases}$$

(ICS.2) The minimal invariant domain containing Ω_c is

$$\mathcal{I}_c \doteq \begin{cases} \Omega_c \cup \{(q/v_{\max}, Q(q/v_{\max}))\} & \text{if } q < f_c^-, \\ \Omega_c & \text{if } q \geq f_c^-. \end{cases}$$

Since the proof is analogous to that of Proposition 5.4, we skip it.

5.2 Existence result for constrained PT^p model with metastable phase

In this section we give our existence result [10] for the constrained PT^p model with metastable phase $\Omega_f^+ \doteq \Omega_f^- \cap \Omega_c$. For convenience we use the Riemann invariant coordinates $U \doteq (v, w)$. We adapt the notation introduced Subsection 2.4 to the U -coordinates, see Figure 2.2.

5.2.1 Notations, definitions and main result

In this subsection we reformulate in the U -coordinates the main assumptions on the parameters, adapt accordingly useful notations introduced in Subsection 2.4, see Figure 5.4, give the definition of solutions, state the main result in Theorem 5.2 and at last introduce the Riemann solvers.

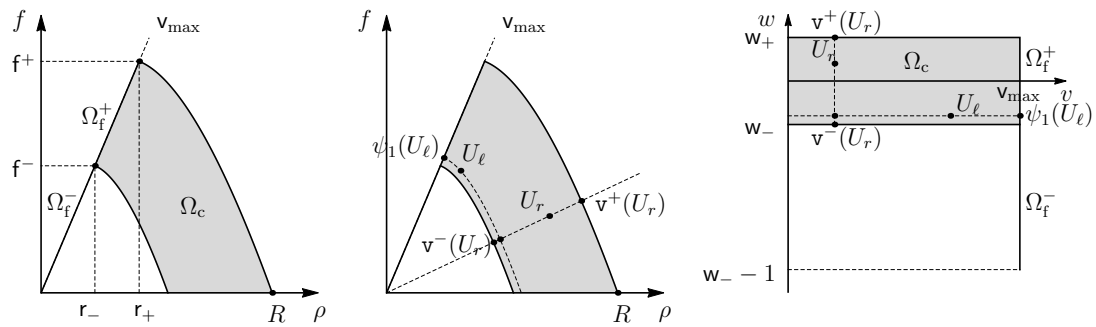


Figure 5.4: Notations introduced in Subsection 2.4 adapted to U -coordinates.

We consider the constrained Cauchy problem for PT^p model (2.20)

$$\begin{array}{cc} \text{Free flow} & \text{Congested flow} \\ \left\{ \begin{array}{l} U \doteq (v, w) \in \Omega_f, \\ \partial_t \rho(U) + \partial_x f(U) = 0, \\ v = \mathbf{v}_{\max}, \end{array} \right. & \left\{ \begin{array}{l} U \doteq (v, w) \in \Omega_c, \\ \partial_t \rho(U) + \partial_x f(U) = 0, \\ \partial_t w + v \partial_x w = 0, \end{array} \right. \end{array} \quad (5.5)$$

$$U(0, x) = U_0(x), \quad (5.6)$$

$$f(U(t, 0^\pm)) \leq q, \quad (5.7)$$

where $\rho(U) \doteq p^{-1}(w - v)$, $f(U) \doteq v \rho(U)$, and $q \in [0, \mathbf{f}^+]$ is a given constant quantity. Above, see Figure 5.4, in analogy with the notations introduced in Subsection 2.4, we define

$$\begin{aligned} \Omega_f &\doteq \{U = (v, w) : v = \mathbf{v}_{\max}, \mathbf{w}_- - 1 \leq w \leq \mathbf{w}_+\}, \\ \Omega_f^- &\doteq \{U = (v, w) : v = \mathbf{v}_{\max}, \mathbf{w}_- - 1 \leq w < \mathbf{w}_-\}, \\ \Omega_f^+ &\doteq \{U = (v, w) : v = \mathbf{v}_{\max}, \mathbf{w}_- \leq w \leq \mathbf{w}_+\}, \\ \Omega_c &\doteq \{U = (v, w) : 0 \leq v \leq \mathbf{v}_{\max}, \mathbf{w}_- \leq w \leq \mathbf{w}_+\}. \end{aligned}$$

We assume that requirements **(H1)** and **(H2)** are satisfied, therefore the first Lax curves are strictly decreasing and concave. The p function satisfies (2.12)

$$p(0) = 0, \quad p'(\rho) > 0, \quad 2p'(\rho) + p''(\rho)\rho > 0 \quad \text{for every } \rho > 0. \quad (5.8)$$

For later use we introduce the map $\mathbf{W}: \Omega \rightarrow [\mathbf{w}_-, \mathbf{w}_+]$ defined as

$$\mathbf{W}(U) \doteq \max\{\mathbf{w}_-, w\}.$$

Moreover, see Figure 5.5, let $\mathbf{v}_q^\pm \in [0, \mathbf{v}_{\max}]$ and $\mathbf{w}_q \in [\mathbf{w}_- - 1, \mathbf{w}_+]$ be defined as follows:

$$\begin{array}{ll} \text{if } q = \mathbf{f}^+ : & \mathbf{v}_q^+ \doteq \mathbf{v}_{\max}, \mathbf{v}_q^- \doteq \mathbf{v}_{\max}, \mathbf{w}_q \doteq \mathbf{w}_+, \\ \text{if } q \in [\mathbf{f}^-, \mathbf{f}^+) : & \mathbf{v}_q^+ \doteq \mathbf{v}_{\max}, \mathbf{v}_q^- + p\left(\frac{q}{\mathbf{v}_q^-}\right) = \mathbf{w}_+, \mathbf{w}_q \doteq p\left(\frac{q}{\mathbf{v}_{\max}}\right) + \mathbf{v}_{\max}, \end{array}$$

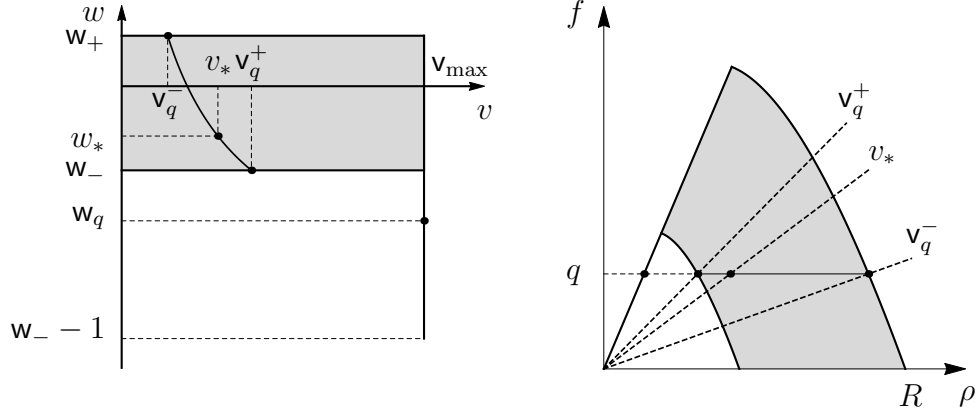


Figure 5.5: Representation of w_q , v_q^\pm and h_q in the case $q \in (0, f^-)$. The curve in the figure on the left is the graph of h_q and corresponds to the horizontal solid segment in the figure on the right. In particular $w_* = h_q(v_*)$.

$$\begin{aligned} \text{if } q \in (0, f^-) : \quad & v_q^+ + p\left(\frac{q}{v_q^+}\right) = w_-, \quad v_q^- + p\left(\frac{q}{v_q^-}\right) = w_+, \quad w_q \doteq w_- - 1 + \frac{q}{f^-}, \\ \text{if } q = 0 : \quad & v_q^+ \doteq 0, \quad v_q^- \doteq 0, \quad w_q \doteq w_- - 1. \end{aligned}$$

For any $q \in (0, f^+)$, let $h_q: [v_q^-, v_q^+] \rightarrow [w_-, w_+]$ be given by $h_q(v) \doteq v + p(q/v)$, see Figure 5.5. Notice that h_q is strictly decreasing by **(H1)** and is strictly convex by (5.8).

5.2.1.1 The constrained Cauchy problem

The notion of solution to Cauchy problem (5.5) is obtained by combining the notion of solutions of the LWR and ARZ models, and by choosing which phase transitions are admissible, see [11]. We recall that a discontinuity between states in Ω_f is entropic if and only if its speed of propagation is v_{\max} . Therefore we consider only the generalized entropy-entropy flux pair introduced in [4] for the ARZ model,

$$\mathbf{E}^k(U) \doteq \begin{cases} 0 & \text{if } v \geq k, \\ \frac{\rho(U)}{p^{-1}(W(U) - k)} - 1 & \text{if } v < k, \end{cases}$$

$$\mathbf{Q}^k(U) \doteq \begin{cases} 0 & \text{if } v \geq k, \\ \frac{f(U)}{p^{-1}(\mathbf{W}(U) - k)} - k & \text{if } v < k, \end{cases}$$

where $U \in \Omega$ and $k \in [0, \mathbf{v}_{\max}]$.

We introduce now the definition of solution to Cauchy problem (5.5), (5.6).

Definition 5.5. Fix $U_0 \in \mathbf{BV}(\mathbb{R}; \Omega)$. We say that a function

$$U \in \mathbf{L}^\infty((0, +\infty); \mathbf{BV}(\mathbb{R}; \Omega)) \cap \mathbf{C}^0(\mathbb{R}_+; \mathbf{L}_{\text{loc}}^1(\mathbb{R}; \Omega))$$

is a weak entropy solution to Cauchy problem (5.5), (5.6) if the following conditions hold:

(S.1) Initial condition (5.6) holds for a.e. $x \in \mathbb{R}$.

(S.2) For any test function $\phi \in \mathbf{C}_c^\infty((0, +\infty) \times \mathbb{R}; \mathbb{R})$ we have

$$\iint_{\mathbb{R}_+ \times \mathbb{R}} (\rho(U) \partial_t \phi + f(U) \partial_x \phi) \begin{pmatrix} 1 \\ \mathbf{W}(U) \end{pmatrix} dx dt = \begin{pmatrix} 0 \\ 0 \end{pmatrix}.$$

(S.3) For any $k \in [0, \mathbf{v}_{\max}]$ and $\phi \in \mathbf{C}_c^\infty((0, +\infty) \times \mathbb{R}; \mathbb{R})$ such that $\phi \geq 0$ we have

$$\iint_{\mathbb{R}_+ \times \mathbb{R}} (\mathbf{E}^k(U) \partial_t \phi + \mathbf{Q}^k(U) \partial_x \phi) dx dt \geq 0.$$

In [11, Theorem 2.8] the authors proved the existence of a weak entropy solution satisfying the above definition. We recall their result below.

Theorem 5.1. Assume that initial datum U_0 belongs to $\mathbf{L}^1 \cap \mathbf{BV}(\mathbb{R}; \Omega)$. Then Cauchy problem (5.5), (5.6) admits a weak entropy solution U in the sense of Definition 5.5. Furthermore there exist two constants C and L such that for any $t, s \geq 0$

$$\text{TV}(U(t)) \leq \text{TV}(U_0), \quad \|U(t)\|_{\mathbf{L}^\infty(\mathbb{R}; \Omega)} \leq C, \quad \|U(t) - U(s)\|_{\mathbf{L}^1(\mathbb{R}; \Omega)} \leq L|t - s|.$$

In the following definition we introduce the notion of solution to constrained Cauchy problem (5.5), (5.6), (5.7).

Definition 5.6. Fix $U_0 \in \mathbf{BV}(\mathbb{R}; \Omega)$. We say that $U \in \mathbf{L}^\infty((0, +\infty); \mathbf{BV}(\mathbb{R}; \Omega)) \cap \mathbf{C}^0(\mathbb{R}_+; \mathbf{L}_{\text{loc}}^1(\mathbb{R}; \Omega))$ is a weak entropy solution to constrained Cauchy problem (5.5), (5.6), (5.7) if the following holds:

(CS.1) Initial condition (5.6) holds for a.e. $x \in \mathbb{R}$.

(CS.2) For any $\phi \in \mathbf{C}_c^\infty((0, +\infty) \times \mathbb{R}; \mathbb{R})$ we have

$$\iint_{\mathbb{R}_+ \times \mathbb{R}} (\rho(U) \partial_t \phi + f(U) \partial_x \phi) \, dx dt = 0 \quad (5.9)$$

and if $\phi(\cdot, 0) \equiv 0$ then

$$\iint_{\mathbb{R}_+ \times \mathbb{R}} (\rho(U) \partial_t \phi + f(U) \partial_x \phi) \mathbf{W}(U) \, dx dt = 0. \quad (5.10)$$

(CS.3) For any $k \in [0, \mathbf{v}_{\max}]$ and $\phi \in \mathbf{C}_c^\infty((0, +\infty) \times \mathbb{R}; \mathbb{R})$ such that $\phi(\cdot, 0) \equiv 0$ and $\phi \geq 0$ we have

$$\iint_{\mathbb{R}_+ \times \mathbb{R}} (\mathbf{E}^k(U) \partial_t \phi + \mathbf{Q}^k(U) \partial_x \phi) \, dx dt \geq 0. \quad (5.11)$$

(CS.4) Constraint condition (5.7) holds for a.e. $t > 0$.

In the following proposition we state which discontinuities are admissible for the solutions to (5.5), (5.6), (5.7).

Proposition 5.6. Let U be a weak entropy solution to constrained Cauchy problem (5.5), (5.6), (5.7) in the sense of Definition 5.6. Then U has the following properties:

- Any discontinuity of U has speed of propagation σ satisfying the first Rankine-Hugoniot condition

$$\sigma(t) \left(\rho(U(t, \delta(t)^+)) - \rho(U(t, \delta(t)^-)) \right) = f(U(t, \delta(t)^+)) - f(U(t, \delta(t)^-)), \quad (5.12)$$

and away from $x = 0$ it satisfies also the second Rankine-Hugoniot condition

$$\begin{aligned} & \sigma(t) \left(\rho(U(t, \delta(t)^+)) \mathbf{W}(U(t, \delta(t)^+)) - \rho(U(t, \delta(t)^-)) \mathbf{W}(U(t, \delta(t)^-)) \right) \\ & = f(U(t, \delta(t)^+)) \mathbf{W}(U(t, \delta(t)^+)) - f(U(t, \delta(t)^-)) \mathbf{W}(U(t, \delta(t)^-)). \end{aligned} \quad (5.13)$$

- Any discontinuity of U away from $x = 0$ is classical, namely it satisfies the Lax entropy inequalities.
- Non-classical discontinuities of U may occur only at $x = 0$, and in this case the (density) flux at $x = 0$ satisfies (5.7).

Proof. These properties follow from **(CS.2)**, **(CS.3)** and **(CS.4)**. We underline that (5.12), (5.13) are equivalent to

$$\begin{aligned} & \left(v(t, 0^+) - \sigma(t) \right) \rho(U(t, 0^+)) = \left(v(t, 0^-) - \sigma(t) \right) \rho(U(t, 0^-)), \\ & \left(\mathbf{W}(U(t, 0^+)) - \mathbf{W}(U(t, 0^-)) \right) \left(v(t, 0^-) - \sigma(t) \right) \rho(U(t, 0^-)) = 0. \end{aligned}$$

The above equalities are satisfied by phase transitions and shocks because for them $\mathbf{W}(U(t, 0^+)) = \mathbf{W}(U(t, 0^-))$, and by contact discontinuities because for them $\sigma(t) = v(t, 0^\pm)$. \square

Remark 5.3. *Since we assume that $\phi(\cdot, 0) \equiv 0$ in (5.10) and in (5.11) but not in (5.9), along $x = 0$ weak entropy solutions satisfy the first Rankine-Hugoniot condition (5.12) (with $\sigma(t) = 0$), but not necessarily the second one (5.13). This is in the same spirit of Remark 4.1.*

Let $[\mathbf{w}_- - 1, \mathbf{w}_+] \ni w \mapsto \hat{\mathbf{U}}(w, q) = (\hat{\mathbf{v}}(w, q), \hat{\mathbf{w}}(w, q)) \in \Omega_c$ and $[0, \mathbf{v}_{\max}] \ni v \mapsto$

$\check{U}(v, q) = (\check{v}(v, q), \check{w}(v, q)) \in \Omega$ be defined by, see Figures 5.6 and 5.7,

$$\begin{aligned} (\hat{v}(w, q), \hat{w}(w, q)) &\doteq \begin{cases} (h_q^{-1}(w), w) & \text{if } w > \max\{\mathbf{w}_-, \mathbf{w}_q\}, \\ (\mathbf{v}_q^+, \mathbf{w}_-) & \text{if } \mathbf{w}_q < w \leq \mathbf{w}_-, \\ (\mathbf{v}_{\max}, \mathbf{w}_q) & \text{if } w \leq \mathbf{w}_q, \end{cases} \\ (\check{v}(v, q), \check{w}(v, q)) &\doteq \begin{cases} (\mathbf{v}_{\max}, \mathbf{w}_q) & \text{if } v > \mathbf{v}_q^+, \\ (v, h_q(v)) & \text{if } v \in [\mathbf{v}_q^-, \mathbf{v}_q^+], \\ (\mathbf{v}_q^-, \mathbf{w}_+) & \text{if } v < \mathbf{v}_q^-, \end{cases} \end{aligned} \quad (5.14)$$

where $\hat{w} \doteq w \circ \hat{U}$ and $\check{w} \doteq w \circ \check{U}$. As a consequence

$$\begin{aligned} \hat{r}(w, q) &= p^{-1}(\hat{w}(w, q) - \hat{v}(w, q)), \\ \check{r}(v, q) &= \begin{cases} p^{-1}(\check{w}(w, q) - \check{v}(w, q)) & \text{if } v \leq \mathbf{v}_q^+, \\ q/\mathbf{v}_{\max} & \text{if } v > \mathbf{v}_q^+. \end{cases} \end{aligned}$$

Remark 5.4. *By definition we have $f(\hat{U}(w, q)) = f(\check{U}(v, q)) = q$. Furthermore, $w \mapsto \hat{U}(w, q)$ and $v \mapsto \check{U}(v, q)$ are continuous if and only if $q \geq \mathbf{f}^-$, and in this case they are Lipschitz continuous. On the other hand, if $q < \mathbf{f}^-$, then $w \mapsto \hat{U}(w, q)$ and $v \mapsto \check{U}(v, q)$ are only left-continuous. Moreover $\hat{w}(w, q) \geq w$ and $\check{v}(v, q) \geq v$. At last, $w \mapsto \hat{w}(w, q)$ and $v \mapsto \check{v}(v, q)$ are non-decreasing, while $w \mapsto \hat{v}(w, q)$ and $v \mapsto \check{w}(v, q)$ are non-increasing.*

Let TV_+ and TV_- be the positive and negative total variations, respectively. For any $U: \mathbb{R} \rightarrow \Omega$ we let

$$\begin{aligned} \hat{Y}(U) &\doteq \text{TV}_+(\hat{v}(w, q); (-\infty, 0)) + \text{TV}_-(\hat{w}(w, q); (-\infty, 0)), \\ \check{Y}(U) &\doteq \text{TV}_+(\check{v}(v, q); (0, +\infty)) + \text{TV}_-(\check{w}(v, q); (0, +\infty)). \end{aligned} \quad (5.15)$$

For all $U \in \Omega$ and $k \in [0, \mathbf{v}_{\max}]$ we define

$$\mathbf{N}_q^k(U) \doteq \begin{cases} f(U) \left[\frac{k}{q} - \frac{1}{p^{-1}(\mathbf{W}(U) - k)} \right]_+ & \text{if } q \neq 0, \\ k & \text{if } q = 0, \end{cases}$$

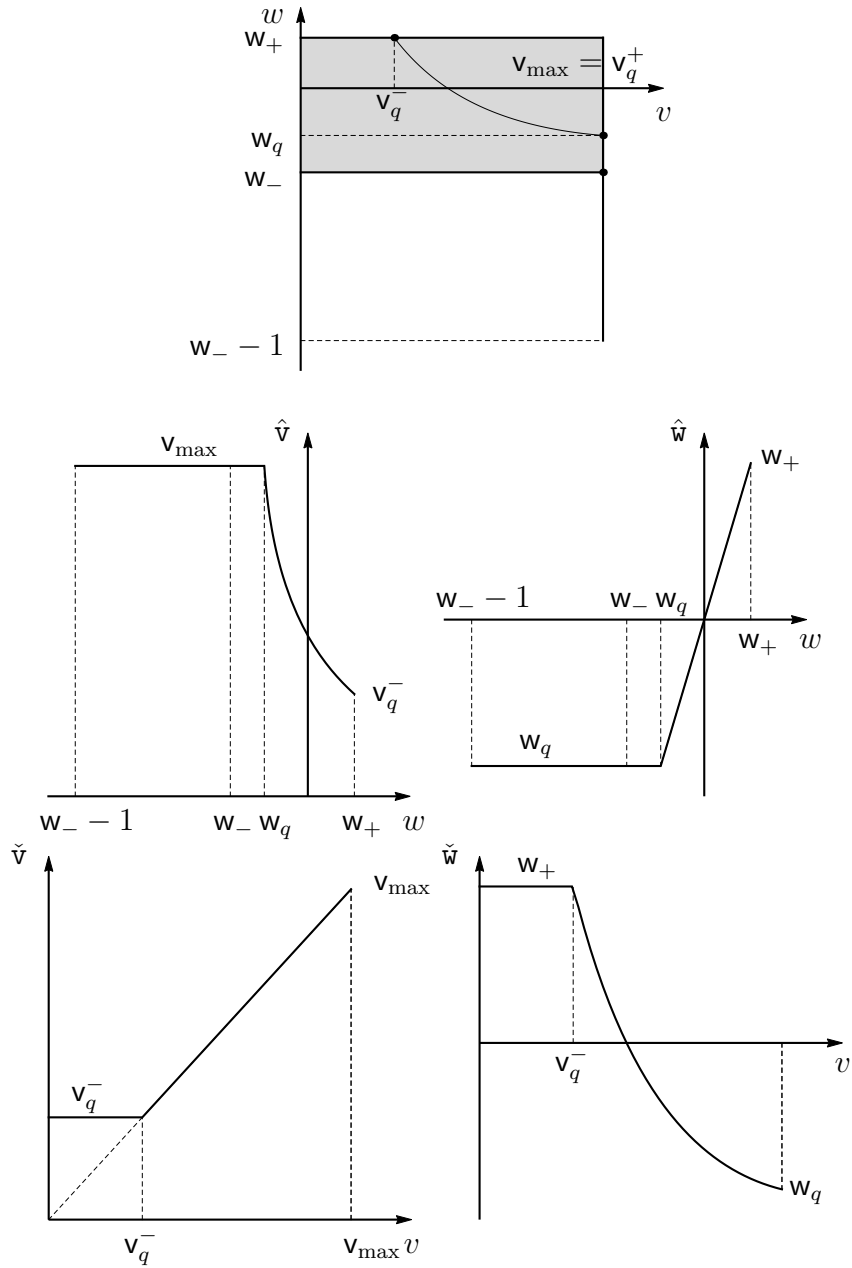


Figure 5.6: The functions \hat{U} and \check{U} in the case $q \in (f^-, f^+)$ defined in (5.14).

where

$$[w]_+ \doteq \begin{cases} w & \text{if } w > 0, \\ 0 & \text{otherwise.} \end{cases}$$

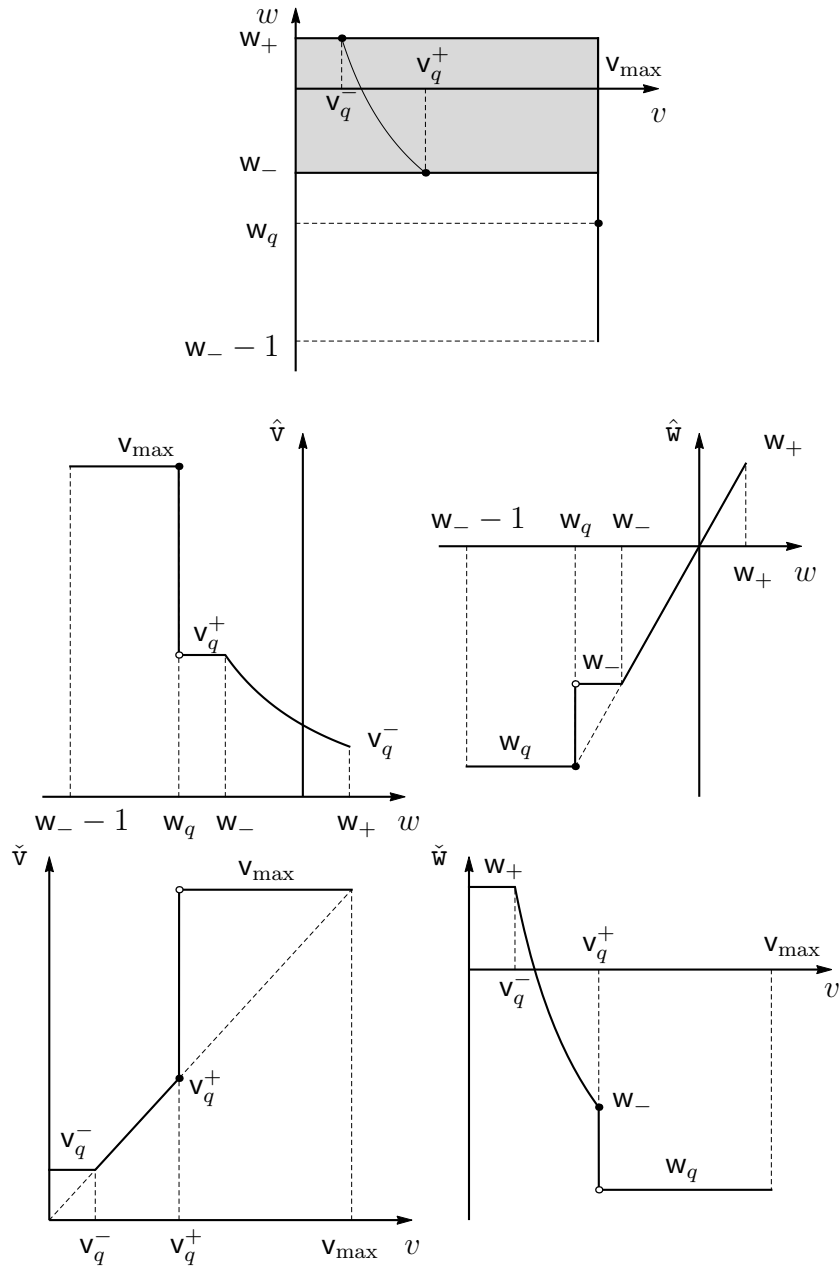


Figure 5.7: The functions \hat{U} and \check{U} in the case $q \in (0, f^-)$ defined in (5.14).

In the following theorem we give our main result obtained in [10].

Theorem 5.2. *Let $U_0 \in \mathbf{L}^1 \cap \mathbf{BV}(\mathbb{R}; \Omega)$ and $q \in [0, f^+]$ satisfy one of the following conditions:*

(H.1) $q \in [f^-, f^+]$;

(H.2) $q \in [0, f^-)$ and $\hat{\Upsilon}(U_0) + \check{\Upsilon}(U_0)$ is bounded.

Then the approximate solutions U_n constructed in Section 5.2.4 converge to a weak entropy solution $U \in \mathbf{C}^0(\mathbb{R}_+; \mathbf{BV}(\mathbb{R}; \Omega))$ of constrained Cauchy problem (5.5), (5.6), (5.7) in the sense of Definition 5.6. Moreover there exist constants C_q and L_q that depend on U_0 and q , such that for all $t, s > 0$

$$\mathrm{TV}(U(t)) \leq C_q, \quad \|U(t) - U(s)\|_{\mathbf{L}^1(\mathbb{R}; \Omega)} \leq L_q |t - s|, \quad \|U(t)\|_{\mathbf{L}^\infty(\mathbb{R}; \Omega)} \leq R + \mathbf{v}_{\max}. \quad (5.16)$$

Furthermore, non-classical discontinuities of U can occur only at $x = 0$, and if for any $k \in [0, \mathbf{v}_{\max}]$ and $\phi \in \mathbf{C}_c^\infty((0, +\infty) \times \mathbb{R}; \mathbb{R})$ such that $\phi \geq 0$ we have

$$\lim_{n \rightarrow +\infty} \int_0^T \mathbf{N}_q^k(U_n(t, 0^-)) \phi(t, 0) dt = \int_0^T \mathbf{N}_q^k(U(t, 0^-)) \phi(t, 0) dt, \quad (5.17)$$

then the (density) flow at $x = 0$ is the maximal flow q allowed by the constraint.

The proof is deferred to Section 5.2.4.

Remark 5.5. *If $q \in [f^-, f^+]$, then both $w \mapsto \hat{\mathbf{U}}(w, q)$ and $v \mapsto \check{\mathbf{U}}(v, q)$ are Lipschitz continuous, hence $\hat{\Upsilon}(U_0) + \check{\Upsilon}(U_0)$ is bounded for U_0 with bounded total variation.*

5.2.2 The constrained Riemann problem

This subsection deals with constrained Riemann problem (5.5), (5.7) with initial condition

$$U(0, x) = \begin{cases} U_\ell & \text{if } x < 0, \\ U_r & \text{if } x \geq 0. \end{cases} \quad (5.18)$$

Below we recall the definition of the constrained Riemann solver \mathcal{CRS}_R^p that we introduced in [35].

Let \mathcal{RS}_R^p be the Riemann solver for PT^p model given in Definition 2.7. We point out that in general $(t, x) \mapsto \mathcal{RS}_R^p[U_\ell, U_r](x/t)$ does not satisfy constraint condition (5.7). This motivates the introduction of the sets

$$\begin{aligned} \mathcal{D}_1 &\doteq \{(U_\ell, U_r) \in \Omega \times \Omega : f(\mathcal{RS}_R^p[U_\ell, U_r](0^\pm)) \leq q\} \\ &= \{(U_\ell, U_r) \in \Omega_f \times \Omega_f : f(U_\ell) \leq q\} \\ &\quad \cup \{(U_\ell, U_r) \in \Omega_c \times \Omega : f((v_r, (\mathbf{W}(U_\ell)))) \leq q\} \\ &\quad \cup \{(U_\ell, U_r) \in \Omega_f^- \times \Omega_c^- : \min\{f(U_\ell), f(\mathbf{v}^-(U_r))\} \leq q\}, \\ \mathcal{D}_2 &\doteq \Omega^2 \setminus \mathcal{D}_1, \end{aligned}$$

and the constrained Riemann solver \mathcal{CRS}_R^p given below.

Definition 5.7. *The constrained Riemann solver $\mathcal{CRS}_R^p: \Omega^2 \rightarrow \mathbf{L}^\infty(\mathbb{R}; \Omega)$ associated to constrained Riemann problem (5.5), (5.7), (5.18) is defined as*

$$\mathcal{CRS}_R^p[U_\ell, U_r](\xi) \doteq \begin{cases} \mathcal{RS}_R^p[U_\ell, U_r](\xi) & \text{if } (U_\ell, U_r) \in \mathcal{D}_1, \\ \begin{cases} \mathcal{RS}_R^p[U_\ell, \hat{U}_\ell](\xi) & \text{if } \xi < 0, \\ \mathcal{RS}_R^p[\check{U}_r, U_r](\xi) & \text{if } \xi > 0, \end{cases} & \text{if } (U_\ell, U_r) \in \mathcal{D}_2, \end{cases}$$

where $\hat{U}_\ell \doteq \hat{U}(w_\ell, q) \in \Omega_c$ and $\check{U}_r \doteq \check{U}(v_r, q) \in \Omega$ are given in (5.14).

Clearly, the above definition corresponds to Definition 5.3 for the PT^p model. In Figure 5.8 we clarify the selection criterion (5.14) for \hat{U}_ℓ and \check{U}_r in the case $(U_\ell, U_r) \in \mathcal{D}_2$. We point out that \hat{U}_ℓ and \check{U}_r satisfy the following general properties.

If $(U_\ell, U_r) \in \mathcal{D}_2$, then $w_\ell > \check{w}_r$ and $v_r > \hat{v}_\ell$.

If $(U_\ell, U_r) \in \mathcal{D}_2$ and $U_\ell \in \Omega_f^-$, then $\hat{w}_\ell = \mathbf{w}_-$.

If $(U_\ell, U_r) \in \mathcal{D}_2$ and $U_r \in \Omega_f$, then $\check{v}_r = \mathbf{v}_{\max}$.

We recall that the maps $(t, x) \mapsto \mathcal{RS}_R^p[U_\ell, U_r](x/t)$ and $(t, x) \mapsto \mathcal{CRS}_R^p[U_\ell, U_r](x/t)$ are solutions to Riemann problems (5.5), (5.18) and (5.5), (5.7), (5.18) in the sense of Definitions 5.5 and 5.6, respectively. Moreover both \mathcal{RS}_R^p and \mathcal{CRS}_R^p are $\mathbf{L}_{\text{loc}}^1$ -continuous, see Propositions 2.2 and 5.2.

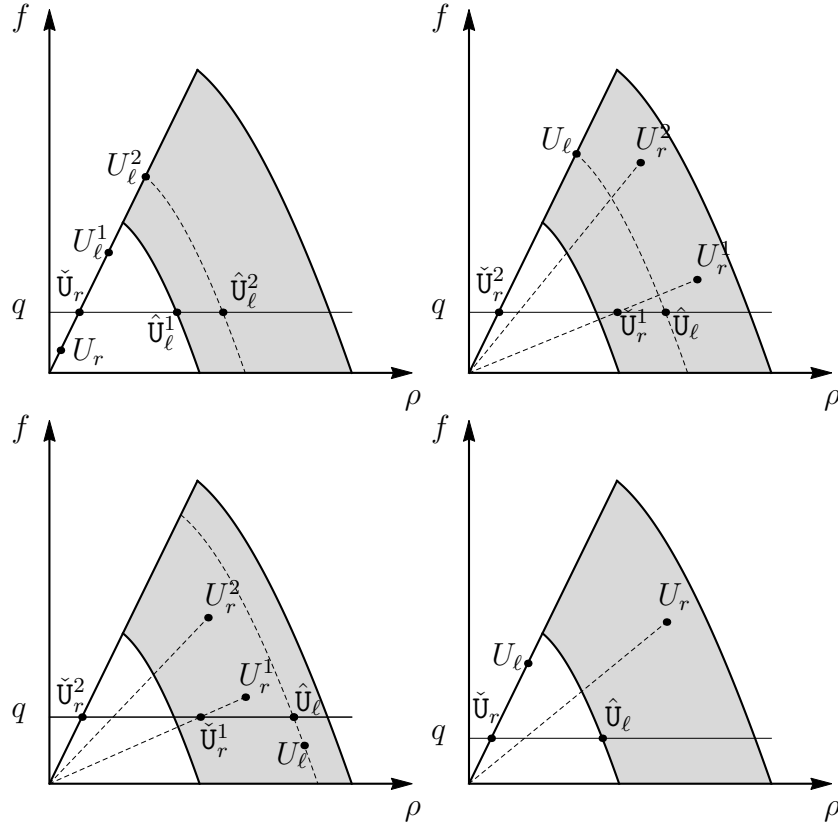


Figure 5.8: The selection criterion for $\hat{U}_\ell \doteq \hat{U}(w_\ell, q)$ and $\check{U}_r \doteq \check{U}(v_r, q)$ in Definition 5.7 for $(U_\ell, U_r) \in \mathcal{D}_2$ and $q \in (0, f^-)$. In the first picture U_ℓ^1, U_ℓ^2 represent the left state in two different cases and $\hat{U}_\ell^1, \hat{U}_\ell^2$ are the corresponding \hat{U}_ℓ . Analogously in the second and third pictures for U_r^1, U_r^2 and $\check{U}_r^1, \check{U}_r^2$.

5.2.3 A case study

In this subsection we simulate the traffic across a toll gate located at $x = 0$ and with capacity q by applying model (5.5), (5.6), (5.7). Let w_- and w_+ be the Lagrangian markers of vehicles that are at time $t = 0$ at rest in $[x_A, x_B)$ and $[x_B, 0)$, respectively. The corresponding initial condition is

$$U_0(x) \doteq \begin{cases} U_\ell & \text{if } x \in [x_A, x_B), \\ U_r & \text{if } x \in [x_B, 0), \\ U_0 & \text{if } x \in \mathbb{R} \setminus [x_A, 0), \end{cases}$$

with $U_0 \doteq (0, \mathbf{v}_{\max})$, $U_\ell \doteq (p^{-1}(\mathbf{w}_-), 0)$ and $U_r \doteq (p^{-1}(\mathbf{w}_+), 0)$, see Figure 5.9.

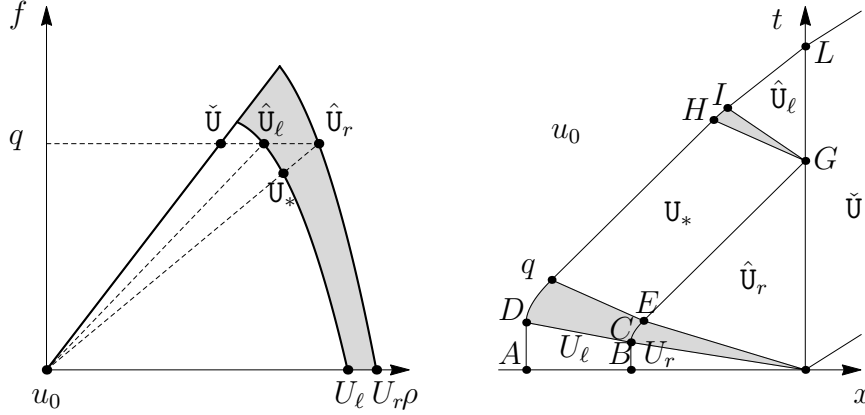


Figure 5.9: The solution constructed in Section 5.2.3.

The solution is constructed below by solving Riemann problems at the discontinuities of U_0 and by considering the interactions of the waves between themselves or with the point constraint $x = 0$. Put

$$\hat{U}_\ell \doteq \hat{U}(\mathbf{w}_-, q), \quad \hat{U}_r \doteq \hat{U}(\mathbf{w}_+, q), \quad \check{U} \doteq \check{U}(\mathbf{v}_{\max}, q), \quad U_* \doteq (\hat{v}_r, \mathbf{W}(U_\ell)).$$

At $x = 0$ we apply \mathcal{CRS}_R^p and obtain a backward rarefaction $R_0(U_r, \hat{U}_r)$, a stationary non-classical shock $NS_0(\hat{U}_r, \check{U})$ and a forward contact discontinuity $CD_0(\check{U}, u_0)$, which moves with speed \mathbf{v}_{\max} . At $x = x_B$ we apply \mathcal{RS}_R^p and obtain a stationary contact discontinuity $CD_B(U_\ell, U_r)$. Let C and E be the starting and final interaction points between CD_B and R_0 . During such interaction CD_B accelerates, while R_0 crosses CD_B and changes its values. After time $t = t_E$, CD_B has speed $\hat{v}_r > 0$ and interacts with NS_0 at G . At G we apply \mathcal{CRS}_R^p and obtain a backward rarefaction $R_G(u_*, \hat{U}_\ell)$ and a stationary non-classical shock $NS_G(\hat{U}_\ell, \check{U})$.

At $x = x_A$ we apply \mathcal{RS}_R^p and obtain a stationary phase transition $PT_A(u_0, U_\ell)$. Let D and q be the starting and final interaction points between PT_A and R_0 . During the time interval (t_D, t_q) we have that PT_A accelerates and R_0 starts to disappear. After time $t = t_F$ we have that PT_A has speed $\hat{v}_r > 0$. Let H and I be the starting and final interaction points between PT_A and R_G . During the time interval (t_H, t_I) , PT_A accelerates and R_G starts to disappear. After time $t = t_I$, PT_A moves with speed $\hat{v}_\ell > 0$. Finally, PT_A interacts with NS_G at L and then

moves with speed v_{\max} .

In Figure 5.10 we show the solution corresponding to $p(\rho) \doteq \rho^2$ and to the data

$$x_A = -8, \quad x_B = -5, \quad w_- = 1, \quad w_+ = 6/5, \quad v_{\max} = 3/5, \quad q = \sqrt{3}/5.$$

Such solution is obtained by the explicit analysis of the wave-fronts interactions with computer-assisted computation of the interaction times and front slopes.

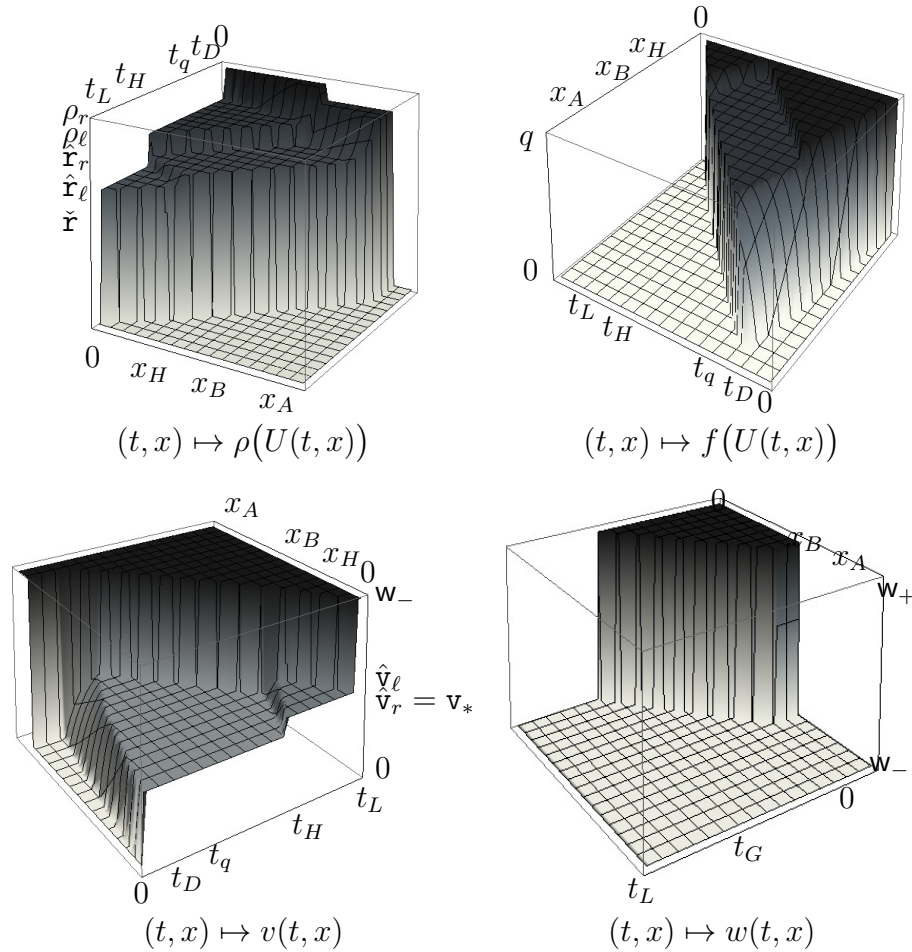


Figure 5.10: The solution constructed in Section 5.2.3.

Once the overall picture of the solution is known, it is possible to express in a closed form the time at which the last vehicle passes through $x = 0$, indeed

$$t_L = \frac{(x_B - x_A)\rho_\ell - x_B\rho_r}{q} \approx 24.4716.$$

5.2.4 Proof of Theorem 5.2

In this subsection we prove Theorem 5.2. The proof consists of the following steps. We start by constructing grid \mathcal{G}_n and defining approximate Riemann solvers $\mathcal{RS}_R^{p,n}$, $\mathcal{CRS}_R^{p,n}$ in \mathcal{G}_n . Therefore, we construct approximate solutions $U_n \doteq (v_n, w_n)$ via wave-front tracking method [18, 59] to constrained Cauchy problem (5.5), (5.6), (5.7) in the space \mathbf{PC} of piecewise constant functions. We show that U_n can be defined globally in time; this goal is achieved thanks to a non-increasing Temple functional \mathbf{T}_n , which decreases each time the number of discontinuities of U_n increases. Next, we prove that U_n converges to function U , which is a solution to (5.5), (5.6), (5.7) and satisfies the estimates listed in (5.16). At last we consider the flux density of the non-classical shocks.

Fix $n \in \mathbb{N}$ sufficiently large. We simplify the notation by letting

$$w_\ell \doteq w_\ell, \quad \hat{U}_\ell \doteq \hat{U}(w_\ell, q), \quad \check{U}_\ell \doteq \check{U}(v_\ell, q)$$

and so on, where \hat{u} and \check{u} are defined in (5.14).

The grid

Define $\mathcal{G}_n \doteq \Omega \cap \mathcal{P}$, see Figure 5.11, with \mathcal{P} given in the (v, w) -coordinates by

$$\left(\bigcup_{i=0}^{M \cdot 2^n} \{v^i\} \right) \times \left(\bigcup_{i=0}^{N \cdot 2^n} \{w^i\} \right),$$

where M , N , v^i and w^i , are defined as follows:

- If $q = 0$, then we let $M = 1$, $N = 2$,

$$v^i \doteq i 2^{-n} v_{\max} \quad \text{if } i \in \{0, \dots, 2^n\},$$

$$w^i \doteq \begin{cases} w_- - 1 + i 2^{-n} & \text{if } i \in \{0, \dots, 2^n\}, \\ w_- + (i - 2^n) 2^{-n} (w_+ - w_-) & \text{if } i \in \{2^n + 1, \dots, 2^{n+1}\}. \end{cases}$$

- If $q \in (0, f^-)$, then we let $M = 3$, $N = 3$,

$$v^i \doteq \begin{cases} i 2^{-n} \mathbf{v}_q^- & \text{if } i \in \{0, \dots, 2^n\}, \\ h_q^{-1}(w^{4 \cdot 2^n - i}) & \text{if } i \in \{2^n + 1, \dots, 2^{n+1}\}, \\ \mathbf{v}_q^+ + (i - 2^{n+1}) 2^{-n} (\mathbf{v}_{\max} - \mathbf{v}_q^+) & \text{if } i \in \{2^{n+1} + 1, \dots, 3 \cdot 2^n\}, \end{cases}$$

$$w^i \doteq \begin{cases} \mathbf{w}_- - 1 + i 2^{-n} (\mathbf{w}_q - \mathbf{w}_- + 1) & \text{if } i \in \{0, \dots, 2^n\}, \\ \mathbf{w}_q + (i - 2^n) 2^{-n} (\mathbf{w}_- - \mathbf{w}_q) & \text{if } i \in \{2^n + 1, \dots, 2^{n+1}\}, \\ \mathbf{w}_- + (i - 2 \cdot 2^n) 2^{-n} (\mathbf{w}_+ - \mathbf{w}_-) & \text{if } i \in \{2^{n+1} + 1, \dots, 3 \cdot 2^n\}. \end{cases}$$

- If $q \in [f^-, f^+]$, then we let $M = 2$, $N = 3$,

$$v^i \doteq \begin{cases} i 2^{-n} \mathbf{v}_q^- & \text{if } i \in \{0, \dots, 2^n\}, \\ h_q^{-1}(w^{2^{n+2} - i}) & \text{if } i \in \{2^n + 1, \dots, 2^{n+1}\}, \end{cases}$$

$$w^i \doteq \begin{cases} \mathbf{w}_- - 1 + i 2^{-n} & \text{if } i \in \{0, \dots, 2^n\}, \\ \mathbf{w}_- + (i - 2^n) 2^{-n} (\mathbf{w}_q - \mathbf{w}_-) & \text{if } i \in \{2^n + 1, \dots, 2^{n+1}\}, \\ \mathbf{w}_q + (i - 2^{n+1}) 2^{-n} (\mathbf{w}_+ - \mathbf{w}_q) & \text{if } i \in \{2^{n+1} + 1, \dots, 3 \cdot 2^n\}. \end{cases}$$

Notice that if $q \in \{f^-, f^+\}$, then not necessarily $w^i \neq w^{i+1}$.

The approximate Riemann solvers

To properly define in \mathcal{G}_n the approximate solutions U^n to (5.5), (5.6), (5.7) constructed via wave-front tracking method, we introduce the approximate Riemann solvers $\mathcal{RS}_R^{p,n}, \mathcal{CRS}_R^{p,n} : \mathcal{G}_n \times \mathcal{G}_n \rightarrow \mathbf{PC}(\mathbb{R}; \mathcal{G}_n)$ obtained by discretizing the rarefactions. In more detail, for any $(U_\ell, U_r) \in \mathcal{G}_n \times \mathcal{G}_n$ such that $w_\ell = w_r$ and $v_\ell = v^h < v_r = v^{h+k}$, we define

$$\mathcal{RS}_R^{p,n}[U_\ell, U_r](\xi) \doteq \begin{cases} U_\ell & \text{if } \xi \leq \sigma(U_\ell, U_1), \\ U_j & \text{if } \sigma(U_{j-1}, U_j) < \xi \leq \sigma(U_j, U_{j+1}), \quad 1 \leq j \leq k-1, \\ U_r & \text{if } \xi > \sigma(u_{k-1}, U_r), \end{cases}$$

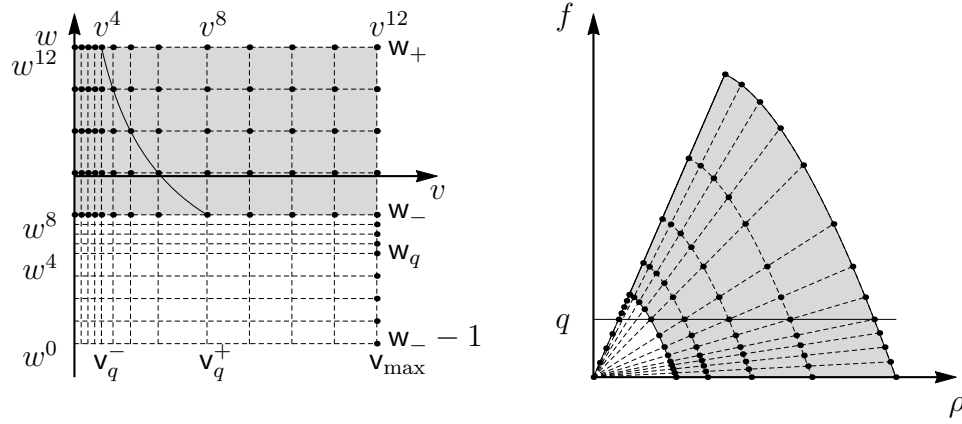


Figure 5.11: The grid \mathcal{G}_n for $q \in (0, f^-)$ and $n = 2$. The curve in the figure on the left is the support of h_q , which corresponds to (a portion of) the horizontal line in the figure on the right.

where $U_0 \doteq U_\ell$, $U_k \doteq U_r$ and $U_j \in \mathcal{G}_n$ is such that $v_j \doteq v^{h+j}$ and $w_j = w_\ell$. The approximate constrained Riemann solver $\mathcal{CRS}_R^{p,n}$ is defined as follows:

1. If $f(\mathcal{RS}_R^{p,n}[U_\ell, U_r](0^\pm)) \leq q$ then

$$\mathcal{CRS}_R^{p,n}[U_\ell, U_r] \doteq \mathcal{RS}_R^{p,n}[U_\ell, U_r].$$

2. If $f(\mathcal{RS}_R^{p,n}[U_\ell, U_r](0^\pm)) > q$ then

$$\mathcal{CRS}_R^{p,n}[U_\ell, U_r](\xi) \doteq \begin{cases} \mathcal{RS}_R^{p,n}[U_\ell, \hat{U}_\ell](\xi) & \text{if } \xi < 0, \\ \mathcal{RS}_R^{p,n}[\check{U}_r, U_r](\xi) & \text{if } \xi \geq 0. \end{cases}$$

The approximate solution

We give below the construction of the approximate solution $U_n \in \mathbf{PC}(\mathbb{R}_+ \times \mathbb{R}; \mathcal{G}_n)$ to (5.5), (5.6), (5.7). As a first step we approximate U_0 with $U_{0,n} \in \mathbf{PC}(\mathbb{R}; \mathcal{G}_n)$

such that

$$\begin{aligned}
\|v_n\|_{\mathbf{L}^\infty} &\leq \|v\|_{\mathbf{L}^\infty}, & \|w_n\|_{\mathbf{L}^\infty} &\leq \|w\|_{\mathbf{L}^\infty}, \\
\mathrm{TV}(v_n) &\leq \mathrm{TV}(v), & \mathrm{TV}(w_n) &\leq \mathrm{TV}(w), \\
\lim_{n \rightarrow +\infty} \|v_n - v\|_{\mathbf{L}_{\mathrm{loc}}^1} &= 0, & \lim_{n \rightarrow +\infty} \|w_n - w\|_{\mathbf{L}_{\mathrm{loc}}^1} &= 0, \\
\hat{\Upsilon}(U_{0,n}) &\leq C\hat{\Upsilon}(U_0), & \check{\Upsilon}(U_{0,n}) &\leq C\check{\Upsilon}(U_0),
\end{aligned} \tag{5.19}$$

for a constant C . The approximate solution U_n is then obtained by a wave-front tracking method, which exploits $\mathcal{CRS}_R^{p,n}$ at $x = 0$ and $\mathcal{RS}_R^{p,n}$ away from $x = 0$. We prove that only finitely many interactions may occur in finite time; this ensure the global (in time) existence of U_n . Then we show that $U_n \in \mathbf{PC}(\mathbb{R}_+ \times \mathbb{R}; \mathcal{G}_n)$. At last we demonstrate that U_n converges (up to a subsequence) in $\mathbf{L}_{\mathrm{loc}}^1$ to a limit U and show that U is a constrained weak entropy solution to (5.5), (5.6), (5.7) in the sense of Definition 5.6.

The Temple functional

Notice that any contact discontinuity (CD) has non-negative speed (of propagation), any shock (S) or rarefaction shock (RS) has negative speed, all the non-classical shocks (NSs) are stationary and the speed of all the possible phase transitions (PTs) ranges in the interval $(-f^-(p^{-1}(\mathbf{w}_-) - \mathbf{r}_-), \mathbf{v}_{\max})$. Below we say that (U_ℓ, U_r) is a null wave if $U_\ell = U_r$. Notice that if (U_ℓ, U_r) is a PT then $U_\ell \in \Omega_f^-$ and $U_r \in \Omega_c^-$, moreover if (U_ℓ, U_r) is a PT with $w_r > \mathbf{w}_-$ then $\rho_\ell = 0$.

Denote by $\sharp(t)$ the number of discontinuities of $U_n(t, \cdot)$ and introduce $\mathbf{T}_n: \mathbb{R}_+ \rightarrow \mathbb{R}_+$ defined as

$$\mathbf{T}_n(t) \doteq \mathrm{TV}(v_n(t, \cdot)) + \mathrm{TV}(w_n(t, \cdot)) + 2\hat{\Upsilon}_n(t) + 2\check{\Upsilon}_n(t),$$

where $\hat{\Upsilon}_n(t) \doteq \hat{\Upsilon}(U_n(t, \cdot))$ and $\check{\Upsilon}_n(t) \doteq \check{\Upsilon}(U_n(t, \cdot))$. Conventionally, we assume that U_n is left continuous in time, i.e. $U_n(t, \cdot) \equiv U_n(t_-, \cdot)$. Then also \mathbf{T}_n is left continuous in time. By the monotonicity of $w \mapsto \hat{v}(w)$, $w \mapsto \hat{w}(w)$, $v \mapsto \check{v}(v)$, $v \mapsto \check{w}(v)$, see Remark 5.4, and the definitions of $\hat{\Upsilon}$ and $\check{\Upsilon}$ given in (5.15), we have

that

$$\begin{aligned}
\hat{\Upsilon}_n(t) &= \text{TV}_+\left(\hat{v}(w_n(t, \cdot)); (-\infty, 0)\right) + \text{TV}_-\left(\hat{w}(w_n(t, \cdot)); (-\infty, 0)\right) \\
&= \sum_{x \in \text{CD}_n} [\hat{v}(w_n(t, x^+)) - \hat{v}(w_n(t, x^-))]_+ \\
&\quad + \sum_{x \in \text{CD}_n} [\hat{w}(w_n(t, x^-)) - \hat{w}(w_n(t, x^+))]_+, \\
\check{\Upsilon}_n(t) &= \text{TV}_+\left(\check{v}(v_n(t, \cdot), q); (0, +\infty)\right) + \text{TV}_-\left(\check{w}(v_n(t, \cdot), q); (0, +\infty)\right) \\
&= \sum_{x \in \text{RS}_n} [\check{v}(v_n(t, x^+), q) - \check{v}(v_n(t, x^-), q)]_+ \\
&\quad + \sum_{x \in \text{RS}_n} [\check{w}(v_n(t, x^-), q) - \check{w}(v_n(t, x^+), q)]_+,
\end{aligned}$$

where

$$\begin{aligned}
\text{CD}_n &\doteq \left\{ x \in \mathbb{R} : \begin{array}{l} (U_n(t, x^-), U_n(t, x^+)) \text{ is a CD in } x < 0 \text{ such} \\ \text{that } w_n(t, x^-) > \max\{w_n(t, x^+), w_q\} \end{array} \right\}, \\
\text{RS}_n &\doteq \left\{ x \in \mathbb{R} : \begin{array}{l} (U_n(t, x^-), U_n(t, x^+)) \text{ is a RS in } x > 0 \text{ such} \\ \text{that } v_n(t, x^+) > \max\{v_n(t, x^-), v_q^-\} \end{array} \right\}.
\end{aligned}$$

Let $\varepsilon_n > 0$ be the minimal (v, w) -distance between two points in the grid \mathcal{G}_n , namely

$$\varepsilon_n \doteq \min_{\substack{U^1, U^2 \in \mathcal{G}_n \\ U^1 \neq U^2}} \max\{|v^1 - v^2|, |w^1 - w^2|\}.$$

The next proposition ensures that the number of discontinuities of U_n is uniformly bounded in time. Moreover, it gives uniform bounds on the total variation of the approximate solution, which allows us to use Helly's Theorem.

Proposition 5.7. *For any fixed $n \in \mathbb{N}$ sufficiently large and $U_{0,n} \in \mathbf{PC}(\mathbb{R}; \mathcal{G}_n)$, we have that:*

- (a) *the map $t \mapsto \mathbf{T}_n(t)$ is non-increasing and decreases by at least ε_n any time the number of waves increases;*
- (b) *$U_n(t, \cdot) \in \mathbf{PC}(\mathbb{R}; \mathcal{G}_n)$ for all $t > 0$.*

The proof of Proposition 5.7 is deferred to Appendix A.5.

Beside the bound on the number of wave-fronts proved in Proposition 5.7, we need to bound also the number of interactions. This is the aim of the next proposition, which together with Proposition 5.7 ensure the global existence of U_n .

Proposition 5.8. *For any fixed $n \in \mathbb{N}$ sufficiently large and $U_{0,n} \in \mathbf{PC}(\mathbb{R}; \mathcal{G}_n)$, we have that the number of interactions in $(0, +\infty)$ is bounded. In particular U_n is globally defined.*

The proof is deferred to Appendix A.6.

We prove in Proposition 5.7 that U_n takes values in \mathcal{G}_n and we estimate $\text{TV}(U_n(t, \cdot))$ uniformly in n and t . This together with Proposition 5.8 guarantee that the number of interactions and the number of the discontinuities of U_n are both bounded globally in time.

Convergence

We first observe that

$$|\rho_\ell - \rho_r| \leq L(|v_\ell - v_r| + |w_\ell - w_r|)$$

where $L \doteq \max\{r_-, \|1/p'\|_{\mathbf{L}^\infty([p^{-1}(\mathbf{w}_-), p^{-1}(\mathbf{w}_+)];\mathbb{R})}\}$ because

$$\rho_{\ell,r} = \begin{cases} p^{-1}(w_{\ell,r} - v_{\ell,r}) & \text{if } w_{\ell,r} \in [\mathbf{w}_-, \mathbf{w}_+], \\ (w_{\ell,r} + 1 - \mathbf{w}_-)r_- & \text{if } w_{\ell,r} \in [\mathbf{w}_- - 1, \mathbf{w}_-]. \end{cases}$$

As a consequence $\text{TV}(\rho(U)) \leq L(\text{TV}(v) + \text{TV}(w))$, hence

$$\text{TV}(U) \leq (1 + L)(\text{TV}(v) + \text{TV}(w)).$$

Moreover, by Proposition 5.7 and (5.19) we have that for any $t > 0$

$$\begin{aligned} \text{TV}(v_n(t, \cdot)) + \text{TV}(w_n(t, \cdot)) &\leq \mathbf{T}_n(t) \leq \mathbf{T}_n(0) \\ &\leq \text{TV}(v) + \text{TV}(w) + 2C\left(\hat{\Upsilon}(U_0) + \check{\Upsilon}(U_0)\right). \end{aligned}$$

As a consequence $\text{TV}(U_n)$ is bounded by

$$C_q \doteq (1 + L) \left(\text{TV}(v) + \text{TV}(w) + 2C(\hat{\Upsilon}(U_0) + \check{\Upsilon}(U_0)) \right). \quad (5.20)$$

Since $U_{0,n}$ takes values in Ω , for any $t > 0$ we have that also $U_n(t, \cdot)$ takes values in Ω , hence

$$\|U_n(t, \cdot)\|_{\mathbf{L}^\infty(\mathbb{R}; \Omega)} \leq R + v_{\max}.$$

Moreover

$$\|U_n(t, \cdot) - U_n(s, \cdot)\|_{\mathbf{L}^1(\mathbb{R}; \Omega)} \leq L_q |t - s|, \quad (5.21)$$

with $L_q \doteq C_q \max\{v_{\max}, Rp'(R)\}$. Indeed, if no interaction occurs for times between t and s , then

$$\begin{aligned} & \|U_n(t, \cdot) - U_n(s, \cdot)\|_{\mathbf{L}^1(\mathbb{R}; \Omega)} \\ & \leq \sum_{i \in \mathbf{J}(t)} \left| (t - s) \delta_n^i(t) \left(\rho(U_n)(t, \delta_n^i(t)^-) - \rho(U_n)(t, \delta_n^i(t)^+) \right) \right| \\ & \quad + \sum_{i \in \mathbf{J}(t)} \left| (t - s) \delta_n^i(t) \left(v_n(t, \delta_n^i(t)^-) - v_n(t, \delta_n^i(t)^+) \right) \right| \\ & \leq L_q |t - s|, \end{aligned}$$

where $\delta_n^i(t) \in \mathbb{R}$, $i \in \mathbf{J}(t) \subset \mathbb{N}$, are the positions of the discontinuities of $U_n(t, \cdot)$. The case when one or more interactions take place for times between t and s is similar, because by the finite speed of propagation of the waves the map $t \mapsto U_n(t, \cdot)$ is \mathbf{L}^1 -continuous across interaction times.

Thus, by applying Helly's Theorem, the approximate solutions $(U_n)_n$ converge (up to a subsequence) in $\mathbf{L}_{\text{loc}}^1(\mathbb{R}_+ \times \mathbb{R}; \Omega)$ to a function

$$U \in \mathbf{L}^\infty(\mathbb{R}_+; \mathbf{BV}(\mathbb{R}; \Omega)) \cap \mathbf{C}^0(\mathbb{R}_+; \mathbf{L}_{\text{loc}}^1(\mathbb{R}; \Omega))$$

and the limit satisfies the estimates in (5.16).

Proposition 5.9. *Let $U_0 \in \mathbf{L}^1 \cap \mathbf{BV}(\mathbb{R}; \Omega)$ and $q \in [0, f^+]$ satisfy (H.1) or (H.2). If U is a limit of the approximate solutions $(U_n)_n$ constructed in Subsection 5.2.4, then U is a solution to constrained Cauchy problem (5.5), (5.6), (5.7) in the sense of Definition 5.6.*

Proof. We consider separately the conditions listed in Definition 5.6.

(CS.1) Initial condition (5.6) holds by (5.16), (5.21) and the $\mathbf{L}_{\text{loc}}^1$ -convergence of U_n to U .

(CS.2) We prove now (5.9), that is for any test function $\phi \in \mathbf{C}_c^\infty((0, +\infty) \times \mathbb{R}; \mathbb{R})$ we have

$$\iint_{\mathbb{R}_+ \times \mathbb{R}} \left(\rho(U) \partial_t \phi + f(U) \partial_x \phi \right) dx dt = 0.$$

Choose $T > 0$ such that $\phi(t, x) = 0$ whenever $t \geq T$. Since U_n is uniformly bounded and f is uniformly continuous on bounded sets, it is sufficient to prove that

$$\int_0^T \int_{\mathbb{R}} \left(\rho(U_n) \partial_t \phi + f(U_n) \partial_x \phi \right) dx dt \rightarrow 0. \quad (5.22)$$

By the Green-Gauss formula the double integral above can be written as

$$\int_0^T \sum_{i \in \mathbf{J}(t)} \left(\dot{\delta}_n^i(t) \Delta \rho(U_n)^i(t) - \Delta f_n^i(t) \right) \phi(t, \delta_n^i(t)) dt,$$

where

$$\begin{aligned} \Delta \rho(U_n)^i(t) &\doteq \rho(U_n)(t, \delta_n^i(t)^+) - \rho(U_n)(t, \delta_n^i(t)^-), \\ \Delta f_n^i(t) &\doteq f\left(U_n(t, \delta_n^i(t)^+)\right) - f\left(U_n(t, \delta_n^i(t)^-)\right). \end{aligned}$$

By construction any discontinuity of the approximate solution $U_n(t, \cdot)$ satisfies the first Rankine-Hugoniot condition (5.12), therefore

$$\dot{\delta}_n^i(t) \Delta \rho(U_n)^i(t) - \Delta f_n^i(t) = 0, \quad i \in \mathbf{J}(t),$$

and (5.22) is trivial.

The proof of (5.10) is analogous because by construction any discontinuity of $U_n(t, \cdot)$ away from $x = 0$ satisfies also the second Rankine-Hugoniot condition (5.13).

(CS.3) We prove now (5.11), namely that for any $k \in [0, v_{\max}]$ and test function

$\phi \in C_c^\infty((0, +\infty) \times \mathbb{R}; \mathbb{R})$ such that $\phi(\cdot, 0) \equiv 0$ and $\phi \geq 0$ we have

$$\iint_{\mathbb{R}_+ \times \mathbb{R}} \left(\mathbf{E}^k(U) \partial_t \phi + \mathbf{Q}^k(U) \partial_x \phi \right) dx dt \geq 0,$$

where

$$\mathbf{E}^k(U) \doteq \begin{cases} 0 & \text{if } v \geq k, \\ \frac{\rho(U)}{p^{-1}(\mathbf{W}(U) - k)} - 1 & \text{if } v < k, \end{cases}$$

$$\mathbf{Q}^k(U) \doteq \begin{cases} 0 & \text{if } v \geq k, \\ \frac{f(U)}{p^{-1}(\mathbf{W}(U) - k)} - k & \text{if } v < k. \end{cases}$$

Choose $T > 0$ such that $\phi(t, x) = 0$ whenever $t \geq T$. By the a.e. convergence of U_n to U and the uniform continuity of \mathbf{E}^k and \mathbf{Q}^k , it is sufficient to prove that

$$\liminf_{n \rightarrow +\infty} \int_0^T \int_{\mathbb{R}} \left(\mathbf{E}^k(U_n) \partial_t \phi + \mathbf{Q}^k(U_n) \partial_x \phi \right) dx dt \geq 0. \quad (5.23)$$

By the Green-Gauss formula the double integral above can be written as

$$\int_0^T \sum_{i \in \mathcal{J}(t)} \left(\dot{\delta}_n^i(t) \Delta \mathbf{E}_n^{k,i}(t) - \Delta \mathbf{Q}_n^{k,i}(t) \right) \phi(t, \delta_n^i(t)) dt,$$

where

$$\Delta \mathbf{E}_n^{k,i}(t) \doteq \mathbf{E}^k \left(U_n(t, \delta_n^i(t)^+) \right) - \mathbf{E}^k \left(U_n(t, \delta_n^i(t)^-) \right),$$

$$\Delta \mathbf{Q}_n^{k,i}(t) \doteq \mathbf{Q}^k \left(U_n(t, \delta_n^i(t)^+) \right) - \mathbf{Q}^k \left(U_n(t, \delta_n^i(t)^-) \right).$$

To estimate the above integral we have to distinguish the following cases.

- If the i th discontinuity is a PT, then we let $x \doteq \delta_n^i(t)$ and observe that

$$\rho(U_n(t, x^-)) < \min \{ \rho(U_n(t, x^+)), p^{-1}(\mathbf{w}_- - k) \},$$

$$v_n(t, x^-) = \mathbf{v}_{\max} > v_n(t, x^+),$$

$$\begin{aligned}\dot{\delta}_n^i(t) &= \sigma(U_n(t, x^-), U_n(t, x^+)), \\ \mathbf{W}(U_n(t, x^-)) &= \mathbf{w}_- \leq w_n(t, x^+) = \mathbf{W}(U_n(t, x^+)),\end{aligned}$$

hence

$$\begin{aligned}\Delta \mathbf{E}_n^{k,i}(t) &= \begin{cases} \frac{\rho(U_n(t, x^+))}{\rho_{n,+}^k} - 1 & \text{if } v_n(t, x^+) < k \leq \mathbf{v}_{\max}, \\ 0 & \text{if } k \leq v_n(t, x^+), \end{cases} \\ -\Delta \mathbf{Q}_n^{k,i}(t) &= \begin{cases} k - \frac{f(U_n(t, x^+))}{\rho_{n,+}^k} & \text{if } v_n(t, x^+) < k \leq \mathbf{v}_{\max}, \\ 0 & \text{if } k \leq v_n(t, x^+), \end{cases}\end{aligned}$$

where $\rho_{n,+}^k \doteq p^{-1}(w(U_n(t, x^+)) - k)$. If $v_n(t, x^+) < k \leq \mathbf{v}_{\max}$, then

$$\begin{aligned}& \dot{\delta}_n^i(t) \Delta \mathbf{E}_n^{k,i}(t) - \Delta \mathbf{Q}_n^{k,i}(t) \\ &= \sigma(U_n(t, x^-), U_n(t, x^+)) \left(\frac{\rho(U_n(t, x^+))}{\rho_{n,+}^k} - 1 \right) + k - \frac{f(U_n(t, x^+))}{\rho_{n,+}^k} \\ &= \underbrace{\left(\frac{\rho(U_n(t, x^+))}{\rho_{n,+}^k} - 1 \right)}_{>0} \underbrace{\left(\sigma(U_n(t, x^-), U_n(t, x^+)) - \sigma((\rho_{n,+}^k, k), U_n(t, x^+)) \right)}_{>0} \\ &> 0.\end{aligned}$$

- If the i th discontinuity is a CD, then we let $x \doteq \delta_n^i(t)$ and observe that $\dot{\delta}_n^i(t) = v_n(t, x^-) = v_n(t, x^+)$ implies that $\dot{\delta}_n^i(t) \Delta \mathbf{E}_n^{k,i}(t) - \Delta \mathbf{Q}_n^{k,i}(t) = 0$.
- If the i th discontinuity is a S, then we let $x \doteq \delta_n^i(t)$ and observe that

$$\begin{aligned}\rho(U_n(t, x^-)) &< \rho(U_n(t, x^+)), \\ v_n(t, x^-) &> v_n(t, x^+), \\ f(U_n(t, x^-)) &> f(U_n(t, x^+)), \\ \dot{\delta}_n^i(t) &= \sigma(U_n(t, x^-), U_n(t, x^+)) < 0, \\ \mathbf{w}_\pm &\doteq w_n(t, x^-) = w_n(t, x^+) \geq \mathbf{w}_-, \end{aligned}$$

hence

$$\Delta \mathbf{E}_n^{k,i}(t) = \begin{cases} \frac{\rho(U_n(t, x^+)) - \rho(U_n(t, x^-))}{p^{-1}(\mathbf{w}_\pm - k)} & \text{if } v_n(t, x^+) < v_n(t, x^-) < k, \\ \frac{\rho(U_n(t, x^+))}{p^{-1}(\mathbf{w}_\pm - k)} - 1 & \text{if } v_n(t, x^+) < k \leq v_n(t, x^-), \\ 0 & \text{if } k \leq v_n(t, x^+) < v_n(t, x^-), \end{cases}$$

$$-\Delta \mathbf{Q}_n^{k,i}(t) = \begin{cases} \frac{f(U_n(t, x^-)) - f(U_n(t, x^+))}{p^{-1}(\mathbf{w}_\pm - k)} & \text{if } v_n(t, x^+) < v_n(t, x^-) < k, \\ k - \frac{f(U_n(t, x^+))}{p^{-1}(\mathbf{w}_\pm - k)} & \text{if } v_n(t, x^+) < k \leq v_n(t, x^-), \\ 0 & \text{if } k \leq v_n(t, x^+) < v_n(t, x^-). \end{cases}$$

If $k > v_n(t, x^-)$ or $k \leq v_n(t, x^+)$, then obviously $\dot{\delta}_n^i(t) \Delta \mathbf{E}_n^{k,i}(t) - \Delta \mathbf{Q}_n^{k,i}(t) = 0$. Furthermore, if $v_n(t, x^+) < k \leq v_n(t, x^-)$, then

$$\begin{aligned} & \dot{\delta}_n^i(t) \Delta \mathbf{E}_n^{k,i}(t) - \Delta \mathbf{Q}_n^{k,i}(t) \\ &= \sigma(U_n(t, x^-), U_n(t, x^+)) \left(\frac{\rho(U_n(t, x^+))}{p^{-1}(\mathbf{w}_\pm - k)} - 1 \right) + k - \frac{f(U_n(t, x^+))}{p^{-1}(\mathbf{w}_\pm - k)} \\ &= \underbrace{\left(\frac{\rho(U_n(t, x^+))}{p^{-1}(\mathbf{w}_\pm - k)} - 1 \right)}_{>0} \\ & \quad \times \underbrace{\left(\sigma(U_n(t, x^-), U_n(t, x^+)) - \sigma\left((p^{-1}(\mathbf{w}_\pm - k), k), U_n(t, x^+) \right) \right)}_{>0} \\ &> 0. \end{aligned}$$

- If the i th discontinuity is a RS, then we let $x \doteq \delta_n^i(t)$ and observe that

$$\begin{aligned} \rho(U_n(t, x^-)) &> \rho(U_n(t, x^+)), \\ v_n(t, x^-) &< v_n(t, x^+), \\ f(U_n(t, x^-)) &< f(U_n(t, x^+)), \\ \dot{\delta}_n^i(t) &= \sigma(U_n(t, x^-), U_n(t, x^+)) < 0, \end{aligned}$$

$$\mathbf{w}_\pm \doteq w_n(t, x^-) = w_n(t, x^+) \geq \mathbf{w}_-,$$

hence

$$\Delta \mathbf{E}_n^{k,i}(t) = \begin{cases} \frac{\rho(U_n(t, x^+)) - \rho(U_n(t, x^-))}{p^{-1}(\mathbf{w}_\pm - k)} & \text{if } v_n(t, x^-) < v_n(t, x^+) < k, \\ \frac{\rho(U_n(t, x^-))}{p^{-1}(\mathbf{w}_\pm - k)} - 1 & \text{if } v_n(t, x^-) < k \leq v_n(t, x^+), \\ 0 & \text{if } k \leq v_n(t, x^-) < v_n(t, x^+), \end{cases}$$

$$-\Delta \mathbf{Q}_n^{k,i}(t) = \begin{cases} \frac{f(U_n(t, x^-)) - f(U_n(t, x^+))}{p^{-1}(\mathbf{w}_\pm - k)} & \text{if } v_n(t, x^-) < v_n(t, x^+) < k, \\ \frac{f(U_n(t, x^-))}{p^{-1}(\mathbf{w}_\pm - k)} - k & \text{if } v_n(t, x^-) < k \leq v_n(t, x^+), \\ 0 & \text{if } k \leq v_n(t, x^-) < v_n(t, x^+). \end{cases}$$

If $k > v_n(t, x^+)$ or $k \leq v_n(t, x^-)$, then obviously

$$\dot{\delta}_n^i(t) \Delta \mathbf{E}_n^{k,i}(t) - \Delta \mathbf{Q}_n^{k,i}(t) = 0.$$

Furthermore, if $v_n(t, x^-) < k \leq v_n(t, x^+)$, then

$$\begin{aligned} & \dot{\delta}_n^i(t) \Delta \mathbf{E}_n^{k,i}(t) - \Delta \mathbf{Q}_n^{k,i}(t) \\ &= \sigma(U_n(t, x^-), U_n(t, x^+)) \left(\frac{\rho(U_n(t, x^-))}{p^{-1}(\mathbf{w}_\pm - k)} - 1 \right) + \frac{f(U_n(t, x^-))}{p^{-1}(\mathbf{w}_\pm - k)} - k \\ &= \underbrace{\left(\frac{\rho(U_n(t, x^-))}{p^{-1}(\mathbf{w}_\pm - k)} - 1 \right)}_{>0} \\ & \quad \times \underbrace{\left(\sigma(U_n(t, x^-), U_n(t, x^+)) + \sigma(U_n(t, x^-), (p^{-1}(\mathbf{w}_\pm - k), k)) \right)}_{<0} \\ & \geq -\frac{2}{r_-} p^{-1}(\mathbf{w}_\pm) p'(p^{-1}(\mathbf{w}_\pm)) [\rho(U_n(t, x^-)) - \rho(U_n(t, x^+))] \end{aligned}$$

because $\rho(U_n(t, x^-)) > p^{-1}(\mathbf{w}_\pm - k) \geq \rho(U_n(t, x^+)) \geq r_-$ and because by

the concavity of $\mathcal{L}_{\mathbf{w}_{\pm}}^1$ we have

$$\begin{aligned}
0 &> \sigma(U_n(t, x^-), U_n(t, x^+)) > \sigma(U_n(t, x^-), (p^{-1}(\mathbf{w}_{\pm} - k), k)) \\
&> \frac{d\mathcal{L}_{\mathbf{w}_{\pm}}^1}{d\rho}(\rho(U_n(t, x^-))) \\
&= \mathbf{w}_{\pm} - p(\rho(U_n(t, x^-))) - \rho(U_n(t, x^-))p'(\rho(U_n(t, x^-))) \\
&\geq \frac{d\mathcal{L}_{\mathbf{w}_{\pm}}^1}{d\rho}(p^{-1}(\mathbf{w}_{\pm})) = -p^{-1}(\mathbf{w}_{\pm})p'(p^{-1}(\mathbf{w}_{\pm})).
\end{aligned}$$

The above case by case study shows that

$$\begin{aligned}
&\liminf_{n \rightarrow +\infty} \int_0^T \int_{\mathbb{R}} (\mathbf{E}^k(U_n) \partial_t \phi + \mathbf{Q}^k(U_n) \partial_x \phi) dx dt \\
&= \liminf_{n \rightarrow +\infty} \int_0^T \sum_{i \in \text{RS}_n(t)} (\delta_n^i(t) \Delta \mathbf{E}_n^{k,i}(t) - \Delta \mathbf{Q}_n^{k,i}(t)) \phi(t, \delta_n^i(t)) dt \\
&\geq -\frac{2}{r_-} \max_{\rho \in [p^{-1}(\mathbf{w}_-), R]} |\rho p'(\rho)| \\
&\quad \times \liminf_{n \rightarrow +\infty} \int_0^T \sum_{i \in \text{RS}_n(t)} (\rho(U_n(t, \delta_n^i(t)^-)) - \rho(U_n(t, \delta_n^i(t)^+))) \phi(t, \delta_n^i(t)) dt \\
&\geq -\frac{2T}{r_-} \|\phi\|_{\mathbf{L}^\infty} C_q \max_{\rho \in [r_-, R]} |\rho p'(\rho)| \doteq -M,
\end{aligned}$$

where $\delta_n^i(t) \in \mathbb{R}$, $i \in \text{RS}_n(t) \subset \mathbb{N}$, are the positions of the RSs of $U_n(t, \cdot)$ and C_q is defined in (5.20).

We claim that for any fixed $h > 0$, there exists a dense set \mathcal{K}_h of values of k in $[0, \mathbf{v}_{\max}]$ such that

$$\liminf_{n \rightarrow +\infty} \int_0^T \sum_{i \in \text{RS}_n(t)} (\delta_n^i(t) \Delta \mathbf{E}_n^{k,i}(t) - \Delta \mathbf{Q}_n^{k,i}(t)) \phi(t, \delta_n^i(t)) dt \geq -\frac{1}{h}.$$

To prove it we fix $a, b \in [0, \mathbf{v}_{\max}]$ with $a < b$ and show that there exists $k \in (a, b)$ such that the above estimate is satisfied. Let

$$l \doteq \left\lceil \frac{2(Mh + 1)}{b - a} \right\rceil$$

and introduce the set

$$\mathcal{K}_h \doteq \frac{2\mathbb{N} + 1}{l} \cap (a, b).$$

Let $\mathcal{E}_n > 0$ be the maximal (v, w) -distance between two “consecutive” points in the grid \mathcal{G}_n having the same w -coordinate, namely, with a slight abuse of notations, we let

$$\mathcal{E}_n \doteq \max_{\substack{(v^i, w), (v^{i+1}, w) \in \mathcal{G}_n \\ v^i \neq v^{i+1}}} (v^{i+1} - v^i).$$

Let $\mathbf{n}_h \in \mathbb{N}$ be sufficiently large so that $\mathcal{E}_{\mathbf{n}_h} < 2/l$. Take $n \geq \mathbf{n}_h$. We claim that for any $i \in \text{RS}_n(t)$ we have

$$\mathcal{K}_h \cap \left(v_n(t, \delta_n^i(t)^-), v_n(t, \delta_n^i(t)^+) \right)$$

has at most one element. Indeed, if \mathcal{K}_h has more than one element then for any $i \in \text{RS}_n(t)$ we have

$$v_n(t, \delta_n^i(t)^+) - v_n(t, \delta_n^i(t)^-) \leq \mathcal{E}_n < \frac{2}{l} = \min_{\substack{k^1, k^2 \in \mathcal{K}_h \\ k^1 \neq k^2}} |k^1 - k^2|.$$

As a consequence the sum

$$\sum_{k \in \mathcal{K}_h} \left(\delta_n^i(t) \Delta \mathbf{E}_n^{k,i}(t) - \Delta \mathbf{Q}_n^{k,i}(t) \right)$$

has at most one nonzero element; moreover

$$-m \left(\rho(U_n)(t, \delta_n^i(t)^-) - \rho(U_n)(t, \delta_n^i(t)^+) \right) \leq \sum_{k \in \mathcal{K}_h} \left(\delta_n^i(t) \Delta \mathbf{E}_n^{k,i}(t) - \Delta \mathbf{Q}_n^{k,i}(t) \right),$$

where

$$m \doteq \frac{2}{r_-} \max_{\rho \in [r_-, R]} |\rho p'(\rho)| = \frac{M}{T C_q \|\phi\|_{\mathbf{L}^\infty}}.$$

Therefore we find

$$\sum_{i \in \text{RS}_n(t)} \sum_{k \in \mathcal{K}_h} \left(\dot{\delta}_n^i(t) \Delta \mathbf{E}_n^{k,i}(t) - \Delta \mathbf{Q}_n^{k,i}(t) \right) \geq -mC_q.$$

By exchanging the sums, multiplying by the test function and integrating in time we get

$$\sum_{k \in \mathcal{K}_h} \int_0^T \sum_{i \in \text{RS}_n(t)} \left(\dot{\delta}_n^i(t) \Delta \mathbf{E}_n^{k,i}(t) - \Delta \mathbf{Q}_n^{k,i}(t) \right) \phi(t, \delta_n^i(t)) dt \geq -M.$$

Moreover, by construction we have that \mathcal{K}_h is a non-empty set with a finite number of elements (it has at most hM elements), hence

$$hM \max_{k \in \mathcal{K}_h} \left(\int_0^T \sum_{i \in \text{RS}_n(t)} \left(\dot{\delta}_n^i(t) \Delta \mathbf{E}_n^{k,i}(t) - \Delta \mathbf{Q}_n^{k,i}(t) \right) \phi(t, \delta_n^i(t)) dt \right) \geq -M.$$

In conclusion we proved that there exists $k \in \mathcal{K}_h \subseteq (a, b)$ such that the above estimate is satisfied for any $n \geq \mathbf{n}_h$; therefore, since \mathcal{K}_h has a finite number of elements, we have

$$\liminf_{n \rightarrow +\infty} \int_0^T \sum_{i \in \text{RS}_n(t)} \left(\dot{\delta}_n^i(t) \Delta \mathbf{E}_n^{k,i}(t) - \Delta \mathbf{Q}_n^{k,i}(t) \right) \phi(t, \delta_n^i(t)) dt \geq -\frac{1}{h}.$$

Since a and b are arbitrary, the above estimate holds true for a dense set of values of k in $[0, \mathbf{v}_{\max}]$.

Actually, the above estimate holds for any k in $[0, \mathbf{v}_{\max}]$ because the term in brackets in the above formula is continuous with respect to k . Finally, for the arbitrariness of h , we have that

$$\liminf_{n \rightarrow +\infty} \int_0^T \sum_{i \in \text{RS}_n(t)} \left(\dot{\delta}_n^i(t) \Delta \mathbf{E}_n^{k,i}(t) - \Delta \mathbf{Q}_n^{k,i}(t) \right) \phi(t, \delta_n^i(t)) dt \geq 0$$

and this concludes the proof of (5.23).

(CS.4) We prove now that (5.7) holds for a.e. $t > 0$, namely

$$f(U(t, 0^\pm)) \leq q \quad \text{for a.e. } t > 0.$$

By construction $f(U_n(t, 0^\pm)) \leq q$ for any $t > 0$, namely the approximate solutions satisfy (5.7). Since weak convergence preserves pointwise inequalities, it is sufficient to prove that $f(U_n(t, 0^\pm))$ weakly converges to $f(U(t, 0^\pm))$. If ϕ is a smooth test function of time with compact support in $(0, +\infty)$ and φ is a smooth test function of space with compact support and such that $\varphi(0) = 1$, then

$$\begin{aligned} & \int_{\mathbb{R}_+} f(U_n(t, 0^-)) \phi(t) dt \\ &= \int_{\mathbb{R}_+} \int_{-\infty}^0 \left(\rho(U_n(t, x)) \dot{\phi}(t) \varphi(x) + f(U_n(t, x)) \phi(t) \dot{\varphi}(x) \right) dx dt. \end{aligned}$$

The right-hand side passes to the limit, yielding the analogous expression with U_n replaced by U . By using again the Green-Gauss formula, one finally finds that

$$\lim_{n \rightarrow +\infty} \int_{\mathbb{R}_+} f(U_n(t, 0^-)) \phi(t) dt = \int_{\mathbb{R}_+} f(U(t, 0^-)) \phi(t) dt.$$

As a consequence $f(U_n(t, 0^-))$ weakly converges to $f(U(t, 0^-))$ and therefore $f(U(t, 0^-)) \leq q$ for a.e. $t > 0$. At last, since we already proved that U satisfies the first Rankine-Hugoniot condition, we have $f(U(t, 0^-)) = f(U(t, 0^+))$, hence $f(U(t, 0^\pm)) \leq q$ for a.e. $t > 0$. \square

The density flow through $x = 0$

Let U be the solution of constrained Cauchy problem (5.5), (5.6), (5.7) constructed in the previous section. By Propositions 5.6 and 5.9 we have that non-classical shocks of U can occur only at the constraint location $x = 0$, and in this case the (density) flow at $x = 0$ does not exceed the maximal flow q allowed by the constraint.

In the case of a constrained Riemann problem (5.5), (5.7), (5.18), we know

that U coincides with $(t, x) \mapsto \mathcal{CRS}_R^p[U_\ell, U_r](x/t)$, moreover if $(U_\ell, U_r) \in \mathcal{D}_2$ then the flow of the non-classical shock of U coincides with q . In the next proposition we show that also for a general constrained Cauchy problem the flow of the non-classical shocks of U coincides with q if the traces at $x = 0$ of the approximate solutions $(U_n)_n$ satisfy a technical condition.

Proposition 5.10. *Let $U_0 \in \mathbf{L}^1 \cap \mathbf{BV}(\mathbb{R}; \Omega)$, $F \in [0, f^+]$ satisfy (H.1) or (H.2) and U be a limit of the approximate solutions $(U_n)_n$. Assume that the traces at $x = 0$ of $(U_n)_n$ and U satisfy (5.17), that is for any $k \in [0, \mathbf{v}_{\max}]$ and $\phi \in \mathbf{C}_c^\infty((0, +\infty) \times \mathbb{R}; \mathbb{R})$ such that $\phi \geq 0$*

$$\lim_{n \rightarrow +\infty} \int_0^T \mathbf{N}_q^k(U_n(t, 0^-)) \phi(t, 0) dt = \int_0^T \mathbf{N}_q^k(U(t, 0^-)) \phi(t, 0) dt,$$

with

$$\mathbf{N}_q^k(U) \doteq \begin{cases} f(U) \left[\frac{k}{q} - \frac{1}{p^{-1}(\mathbf{W}(U) - k)} \right]_+ & \text{if } q \neq 0, \\ k & \text{if } q = 0. \end{cases}$$

If the limit U has a non-classical discontinuity at time $t_0 > 0$ then

$$f(U(t_0, 0^\pm)) = q.$$

Proof. We first prove that for any $k \in [0, \mathbf{v}_{\max}]$ and $\phi \in \mathbf{C}_c^\infty((0, +\infty) \times \mathbb{R}; \mathbb{R})$ such that $\phi \geq 0$ we have

$$\int_{\mathbb{R}_+} \left(\int_{\mathbb{R}} \left(\mathbf{E}^k(U) \partial_t \phi + \mathbf{Q}^k(U) \partial_x \phi \right) dx + \mathbf{N}_q^k(U(t, 0^-)) \phi(t, 0) \right) dt \geq 0. \quad (5.24)$$

We stress that (5.24) differs from (5.11) not only for an extra term involving $\mathbf{N}_q^k(\text{bigl}(U(t, 0^+))$, but also because here we do not require that $\phi(\cdot, 0) \equiv 0$.

Choose $T > 0$ such that $\phi(t, x) = 0$ whenever $t \geq T$. By (5.17), the a.e. convergence of U_n to U and the uniform continuity of \mathbf{E}^k and \mathbf{Q}^k , it is sufficient to prove that

$$\liminf_{n \rightarrow +\infty} \int_0^T \left(\int_{\mathbb{R}} \left(\mathbf{E}^k(U_n) \partial_t \phi + \mathbf{Q}^k(U_n) \partial_x \phi \right) dx + \mathbf{N}_q^k(U_n(t, 0^-)) \phi(t, 0) \right) dt \geq 0. \quad (5.25)$$

As already observed in the proof of Proposition 5.9, by the Green-Gauss formula the double integral above can be written as

$$\int_0^T \sum_{i \in J(t)} \left(\dot{\delta}_n^i(t) \Delta \mathbf{E}_n^{k,i}(t) - \Delta \mathbf{Q}_n^{k,i}(t) \right) \phi(t, \delta_n^i(t)) dt,$$

where

$$\begin{aligned} \Delta \mathbf{E}_n^{k,i}(t) &\doteq \mathbf{E}^k \left(U_n(t, \delta_n^i(t)^+) \right) - \mathbf{E}^k \left(U_n(t, \delta_n^i(t)^-) \right), \\ \Delta \mathbf{Q}_n^{k,i}(t) &\doteq \mathbf{Q}^k \left(U_n(t, \delta_n^i(t)^+) \right) - \mathbf{Q}^k \left(U_n(t, \delta_n^i(t)^-) \right). \end{aligned}$$

To estimate the above integral we can proceed as in the proof of Proposition 5.9, with the exception that here the i th discontinuity could also be a NS. In this case,

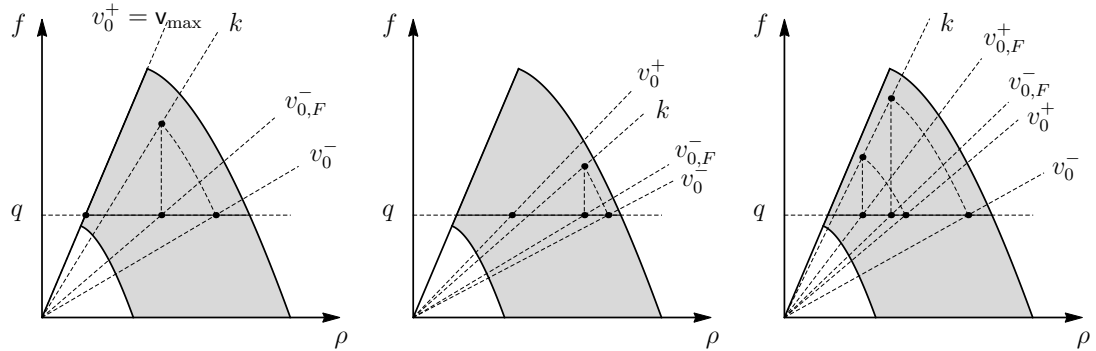


Figure 5.12: $q \in (f^-, f^+)$, $v_{0,F}^\pm \doteq F/p^{-1}(\mathbf{W}(U_n(t, 0^\pm)) - k)$ and $v_0^\pm \doteq v_n(t, 0^\pm)$. The first two pictures show that if $v_0^- < k < v_0^+$, then $v_{0,F}^- < k$. In the last picture we consider the case $v_0^- < v_0^+ < k$ and show that $v_{0,F}^- < v_{0,F}^+ < k$.

that is, if the i th discontinuity is a NS, then

$$\begin{aligned} \delta_n^i(t) &= 0, & f(U_n(t, 0^\pm)) &= q, & v_q^- &\leq v_n(t, 0^-) < v_n(t, 0^+), \\ \dot{\delta}_n^i(t) &= 0, & w_n(t, 0^-) &= \mathbf{W}(U_n(t, 0^-)) \geq \mathbf{W}(U_n(t, 0^+)), \end{aligned}$$

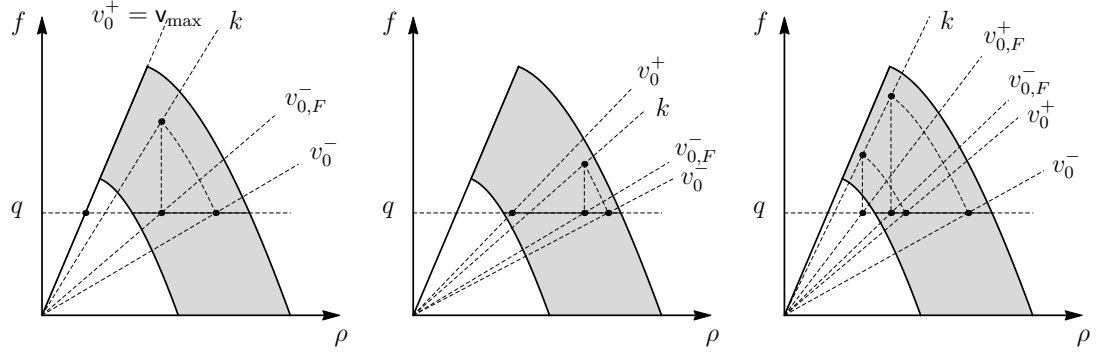


Figure 5.13: Above $q \in (0, f^-)$, $v_0^\pm \doteq v_n(t, 0^\pm)$ and $v_{0,q}^\pm \doteq q/p^{-1}(\mathbf{W}(U_n(t, 0^\pm)) - k)$. With the first two pictures we show that if $v_0^- < k < v_0^+$, then $v_{0,q}^- < k$. In the last picture we consider the case $v_0^- < v_0^+ < k$ and show that $v_{0,F}^- < v_{0,F}^+ < k$.

hence

$$-\Delta \mathbf{Q}_n^{k,i}(t) = \begin{cases} \frac{q}{p^{-1}(w_n(t, 0^-) - k)} - \frac{q}{p^{-1}(\mathbf{W}(U_n(t, 0^+)) - k)} & \text{if } v_n(t, 0^-) < v_n(t, 0^+) < k, \\ \frac{q}{p^{-1}(w_n(t, 0^-) - k)} - k & \text{if } v_n(t, 0^-) < k \leq v_n(t, 0^+), \\ 0 & \text{if } k \leq v_n(t, 0^-) < v_n(t, 0^+), \end{cases}$$

$$\mathbf{N}_q^k(U_n(t, 0^-)) = \begin{cases} \left[k - \frac{q}{p^{-1}(\mathbf{W}(U_n(t, 0^-)) - k)} \right]_+ & \text{if } q \neq 0, \\ k & \text{if } q = 0. \end{cases}$$

Notice that if $q = 0$, then $U_n(t, 0^+) = (0, \mathbf{v}_{\max})$ and $U_n(t, 0^-) \in [p^{-1}(\mathbf{w}_-), R] \times \{0\}$. We observe, see Figure 5.12 and Figure 5.13, that $-\Delta \mathbf{Q}_n^{k,i}(t) < 0$ and that $-\Delta \mathbf{Q}_n^{k,i}(t) + \mathbf{N}_q^k(U_n(t, 0^-)) \geq 0$ and therefore

$$\begin{aligned} & \left(\dot{\delta}_n^i(t) \Delta \mathbf{E}_n^{k,i}(t) - \Delta \mathbf{Q}_n^{k,i}(t) \right) \phi(t, \delta_n^i(t)) + \mathbf{N}_q^k(U(t, 0^-)) \phi(t, 0) \\ &= \left(-\Delta \mathbf{Q}_n^{k,i}(t) + \mathbf{N}_q^k(U_n(t, 0^-)) \right) \phi(t, 0) \geq 0. \end{aligned}$$

Thus, by proceeding as in the proof of Proposition 5.9 it is easy to see that (5.25)

holds true. Let us just underline that beside the NSs, the only possible stationary discontinuities at $x = 0$ are PTs and CDs, however in both of these cases we have $f(U_n(t, 0^-)) = 0$ and therefore $\mathbf{N}_q^k(U_n(t, 0^-)) = 0$.

We can now prove that if U has a non-classical discontinuity then $f(U(t, 0^\pm)) = q$. This is of course obvious if $q = 0$, due to **(CS.4)** and the fact that $f(U) \geq 0$. We can therefore assume that $q > 0$ and that $x \mapsto U(t_0, x)$ has a (stationary) non-classical shock (U_ℓ, U_r) , with $v_\ell < v_r$ and $f(U_\ell) = f(U_r) \doteq f \leq q$. We want to prove that $f = q$. Consider the test function

$$\phi(t, x) \doteq \left(\int_{|x|-\varepsilon}^{+\infty} \varphi_\varepsilon(z) dz \right) \left(\int_{t-t_0+\varepsilon}^{t-t_0+2\varepsilon} \varphi_\varepsilon(z) dz \right),$$

where φ_ε is a smooth approximation of the Dirac mass centred at 0^+ , $\delta_{0^+}^D$, namely

$$\varphi_\varepsilon \in \mathbf{C}_c^\infty(\mathbb{R}; \mathbb{R}_+), \quad \varepsilon > 0, \quad \text{supp}(\delta_\varepsilon) \subseteq [0, \varepsilon], \quad \|\varphi_\varepsilon\|_{\mathbf{L}^1(\mathbb{R}; \mathbb{R})} = 1, \quad \varphi_\varepsilon \rightarrow \delta_{0^+}^D.$$

Observe that as ε goes to zero

$$\begin{aligned} \phi(t_0, x) &\equiv 0 \rightarrow 0, \\ \phi(t, 0) &= \int_{t-t_0+\varepsilon}^{t-t_0+2\varepsilon} \varphi_\varepsilon(z) dz \rightarrow \delta_{t_0^-}^D(t), \\ \partial_t \phi(t, x) &= \left(\int_{|x|-\varepsilon}^{+\infty} \varphi_\varepsilon(z) dz \right) \left(\varphi_\varepsilon(t-t_0+2\varepsilon) - \varphi_\varepsilon(t-t_0+\varepsilon) \right) \rightarrow 0, \\ \chi_{\mathbb{R}_\pm}(x) \partial_x \phi(t, x) &\rightarrow \mp \delta_{0^\pm}^D(x) \delta_{t_0^-}^D(t). \end{aligned}$$

Then by (5.24) for all k belonging to the interval $(\hat{v}(w_\ell, q), \check{v}(v_r, q))$ we have

$$\begin{aligned} &\mathbf{Q}^k(U_\ell) - \mathbf{Q}^k(U_r) + f \left[\frac{k}{q} - \frac{1}{p^{-1}(\mathbf{W}(U_\ell) - k)} \right]_+ \\ &= \left(\frac{f}{p^{-1}(\mathbf{W}(U_\ell) - k)} - k \right) + f \left(\frac{k}{q} - \frac{1}{p^{-1}(\mathbf{W}(U_\ell) - k)} \right) = \left(\frac{f}{q} - 1 \right) k \geq 0. \end{aligned}$$

Since $f \leq q$, the above estimate implies that $f = q$ and this concludes the proof. \square

We underline that the entropy condition (5.11) “becomes” (5.24) if we do not require that the test function ϕ satisfy the condition $\phi(\cdot, 0) \equiv 0$. Even if it is not necessary for the proof of Theorem 5.2, we conclude this section by considering in (5.10) a test function ϕ which may not satisfy the condition $\phi(\cdot, 0) \equiv 0$.

Proposition 5.11. *Let $U_0 \in \mathbf{L}^1 \cap \mathbf{BV}(\mathbb{R}; \Omega)$, $q \in [0, f^+]$ satisfy (H.1) or (H.2) and U be a limit of the approximate solutions $(U_n)_n$. If the traces at $x = 0$ of $(U_n)_n$ and U satisfy for any $\phi \in \mathbf{C}_c^\infty((0, +\infty) \times \mathbb{R}; \mathbb{R})$*

$$\begin{aligned} & \lim_{n \rightarrow +\infty} \int_0^T f(U_n(t, 0^-)) \left[\mathbf{W}(U_n(t, 0^-)) - \mathbf{W}(U_n(t, 0^+)) \right]_+ \phi(t, 0) dt \\ &= \int_0^T f(U(t, 0^-)) \left[\mathbf{W}(U(t, 0^-)) - \mathbf{W}(U(t, 0^+)) \right]_+ \phi(t, 0) dt \end{aligned} \quad (5.26)$$

then U satisfies the following integral condition for any $\phi \in \mathbf{C}_c^\infty((0, +\infty) \times \mathbb{R}; \mathbb{R})$

$$\begin{aligned} & \iint_{\mathbb{R}_+ \times \mathbb{R}} (\rho(U) \partial_t \phi + f(U) \partial_x \phi) \mathbf{W}(U) dx dt \\ & - \int_{\mathbb{R}_+} f(U(t, 0^-)) \left[\mathbf{W}(U(t, 0^-)) - \mathbf{W}(U(t, 0^+)) \right]_+ \phi(t, 0) dt = 0. \end{aligned}$$

Proof. Choose $T > 0$ such that $\phi(t, x) = 0$ whenever $t \geq T$. By (5.26), since U_n is uniformly bounded and f is uniformly continuous on bounded sets, it is sufficient to prove that

$$\begin{aligned} & \int_0^T \int_{\mathbb{R}} (\rho(U_n) \partial_t \phi + f(U_n) \partial_x \phi) \mathbf{W}(U_n) dx dt \\ & - \int_0^T f(U_n(t, 0^-)) \left[\mathbf{W}(U_n(t, 0^-)) - \mathbf{W}(U_n(t, 0^+)) \right]_+ \phi(t, 0) dt \rightarrow 0. \end{aligned} \quad (5.27)$$

By the Green-Gauss formula the double integrals above can be written as

$$\int_0^T \sum_{i \in \mathcal{J}(t)} (\dot{\delta}_n^i(t) \Delta Y_n^i(t) - \Delta Q_n^i(t)) \phi(t, \delta_n^i(t)) dt,$$

where

$$\Delta Y_n^i(t) \doteq \rho(U_n(t, \delta_n^i(t)^+)) \mathbf{W}(U_n(t, \delta_n^i(t)^+)) - \rho(U_n(t, \delta_n^i(t)^-)) \mathbf{W}(U_n(t, \delta_n^i(t)^-)),$$

$$\Delta Q_n^i(t) \doteq f(U_n(t, \delta_n^i(t)^+)) \mathbf{W}(U_n(t, \delta_n^i(t)^+)) - f(U_n(t, \delta_n^i(t)^-)) \mathbf{W}(U_n(t, \delta_n^i(t)^-)).$$

If $U_n(t, \cdot)$ does not have a non-classical shock at $\delta_n^i(t)$, then by the Rankine-Hugoniot conditions

$$\dot{\delta}_n^i(t) \Delta Y_n^i(t) - \Delta Q_n^i(t) = 0;$$

moreover, if $\delta_n^i(t) = 0$ and $U_n(t, \cdot)$ has a stationary discontinuity at $x = 0$, namely a phase transition or a contact discontinuity, then $v_n(t, 0^+) = v_n(t, 0) = 0$ and therefore $\text{sign}(v_n(t, 0^+)) = 0$.

On the other hand, if $\delta_n^i(t) = 0$ and $U_n(t, \cdot)$ has a stationary non-classical shock at $x = 0$, then

$$\dot{\delta}_n^i(t) = 0, \quad f(U_n(t, 0^\pm)) = q, \quad \mathbf{W}(U_n(t, 0^-)) \geq \mathbf{W}(U_n(t, 0^+)),$$

and therefore

$$\begin{aligned} \dot{\delta}_n^i(t) \Delta Y_n^i(t) - \Delta Q_n^i(t) &= -q \left(\mathbf{W}(U_n(t, 0^+)) - \mathbf{W}(U_n(t, 0^-)) \right) \\ &= f(U_n(t, 0^-)) \left[\mathbf{W}(U_n(t, 0^-)) - \mathbf{W}(U_n(t, 0^+)) \right]_+. \end{aligned}$$

As a consequence (5.27) is trivial. □

Networks

6.1 Introduction

This chapter is devoted to our traffic flow models on networks presented in [34,43]. A network is a directed graph $(\mathcal{I}, \mathcal{J})$, where \mathcal{I} is a finite set of unidirectional roads and \mathcal{J} is a finite set of junctions.

Here we consider the basic case $\mathcal{J} = \{J\}$, and assume that the node J is placed at $x = 0$ with n incoming roads $I_i = (-\infty, 0) \in \mathcal{I}$, $i \in \mathbf{I} \doteq \{1, \dots, n\}$, and m outgoing roads $I_j = (0, +\infty) \in \mathcal{I}$, $j \in \mathbf{J} \doteq \{n+1, \dots, n+m\}$; the general case is analogous.

The evolution of traffic along the roads is described by the PT model in [43] and by the LWR model with moving constraint in [34]. At the junction $x = 0$ we propose accordingly two Riemann solvers. We recall that a Riemann problem at a junction is a Cauchy problem with constant initial data on each road. Several Riemann solvers at junction are available in the literature, see [23, 36, 58, 59]. For instance, in [23] the authors propose a Riemann solver for the case of a node having more exiting than entering roads, which is determined by applying the following rules:

- I) The percentages of drivers who come from the i -th incoming road and take the j -th outgoing road is given by fixed coefficients $\alpha_{ji} \in (0, 1)$ such that

$$\sum_{j=n+1}^{n+m} \alpha_{ji} = 1.$$

II) Drivers maximize the flow through the junction.

We underline that rules I) and II) are not sufficient for nodes having more entering than exiting arcs. A way out of this problem is proposed in [36, 49] for telecommunication networks: the authors design a Riemann solver that inverts the order of rules I) and II).

Differently from the previous chapters, for notational simplicity, each Riemann solver associates to any Riemann initial condition the traces at the junction of the corresponding weak solutions rather than the weak solution itself.

6.2 LWR with moving bottleneck on networks

In this section we consider the LWR model coupled with moving bottleneck [38] in the case of networks. A moving bottleneck models a slow vehicle, e.g a bus or a truck, which reduces the road capacity at its position. The road traffic with a slow-moving vehicle is described by the strongly coupled PDE-ODE system introduced in [38, 52]. More precisely, the PDE is a scalar conservation law (6.1) which models the evolution of traffic, while ODE (6.2) describes the trajectory of the slow-moving vehicle. For more informations on different approaches of coupled PDE-ODE systems, we refer the reader to [16, 37–39, 42, 64].

6.2.1 A single unidirectional road

We take the Greenshields' velocity (2.2) with $R = 1$, namely

$$v(\rho) = v_{\max}(1 - \rho).$$

Notice that $\rho_{\text{crit}} = 1/2$. Let $V_b \in [0, v_{\max})$ be the maximal speed of the bus and $y = y(t) \in \mathbb{R}$ be its position. Then, $\dot{y} \in \mathbb{R}$ is given by the function

$$\omega(\rho) \doteq \min\{v(\rho), V_b\}.$$

The LWR model with moving bottleneck takes the form

$$\partial_t \rho + \partial_x f(\rho) = 0, \quad t > 0, \quad x \in \mathbb{R}, \quad (6.1)$$

$$\dot{y}(t) = \omega(\rho(t, y(t)^+)), \quad t \geq 0, \quad (6.2)$$

$$f(\rho(t, y(t))) - \dot{y}(t)\rho(t, y(t)) \leq \frac{\alpha}{4\mathbf{v}_{\max}} (\mathbf{v}_{\max} - \dot{y}(t))^2, \quad t \geq 0. \quad (6.3)$$

Clearly, the trajectory of the bus is determined by the function $y : \mathbb{R}_+ \rightarrow \mathbb{R}$ satisfying (6.2). We underline that if $v(\rho(t, y(t)^+)) < V_b$, namely the road is highly congested at the bus position, then its speed coincides with the speed of surrounding cars.

Remark 6.1. *Condition (6.3) can be obtained by considering the bus reference frame, where the velocity of the bus is equal to zero. Indeed, by the change of coordinates $X = x - y(t)$, conservation law (6.1) becomes*

$$\partial_t \rho + \partial_X F(\rho, \dot{y}) = 0,$$

where the flux function F is defined by

$$F(\rho, \dot{y}) \doteq f(\rho) - \dot{y}\rho,$$

see Figure 6.1. Fix $\alpha \in (0, 1)$ and consider at $X = 0$ the reduced flux function

$$f_\alpha(\rho) = \mathbf{v}_{\max} \rho \left(1 - \frac{\rho}{\alpha}\right).$$

Notice that α is the reduction rate of the road capacity at the bus position $X = 0$, indeed $\max_\rho f_\alpha = \alpha \cdot \max_\rho f$. We correspondingly consider at $X = 0$ the reduced flux function

$$F_\alpha(\rho, \dot{y}) \doteq f_\alpha(\rho) - \dot{y}\rho.$$

Since

$$\max_\rho F_\alpha(\rho, \dot{y}) = \frac{\alpha}{4\mathbf{v}_{\max}} (\mathbf{v}_{\max} - \dot{y})^2,$$

it is reasonable to impose that at $X = 0$

$$F(\rho, \dot{y}) \leq \frac{\alpha}{4\mathbf{v}_{\max}} (\mathbf{v}_{\max} - \dot{y})^2,$$

namely (6.3). We point out that

$$\frac{\alpha}{4v_{\max}}(v_{\max} - y)^2 \in \left[\frac{\alpha}{4v_{\max}}(v_{\max} - V_b)^2, \frac{\alpha v_{\max}}{4} \right].$$

Let us consider initial datum with jump at $x = 0$, which is also assumed to be the initial point of the bus trajectory, namely

$$\rho(0, x) = \begin{cases} \rho_\ell & \text{if } x < 0, \\ \rho_r & \text{if } x \geq 0, \end{cases} \quad y(0) = 0. \quad (6.4)$$

We look for self-similar solutions of problem (6.1), (6.2), (6.3), (6.4), thus we let $y(t)$ to be piecewise-constant. The standard Riemann solver $\mathcal{RS}_{\text{LWR}}$ for the LWR model introduced in Section 2.2, does not necessarily satisfy constraint condition (6.3). For this reason in [38] the authors introduced the constrained Riemann solver $\mathcal{BRS}_{\text{LWR}}: [0, 1]^2 \rightarrow \mathbf{L}_{\text{loc}}^1(\mathbb{R}; [0, 1])$.

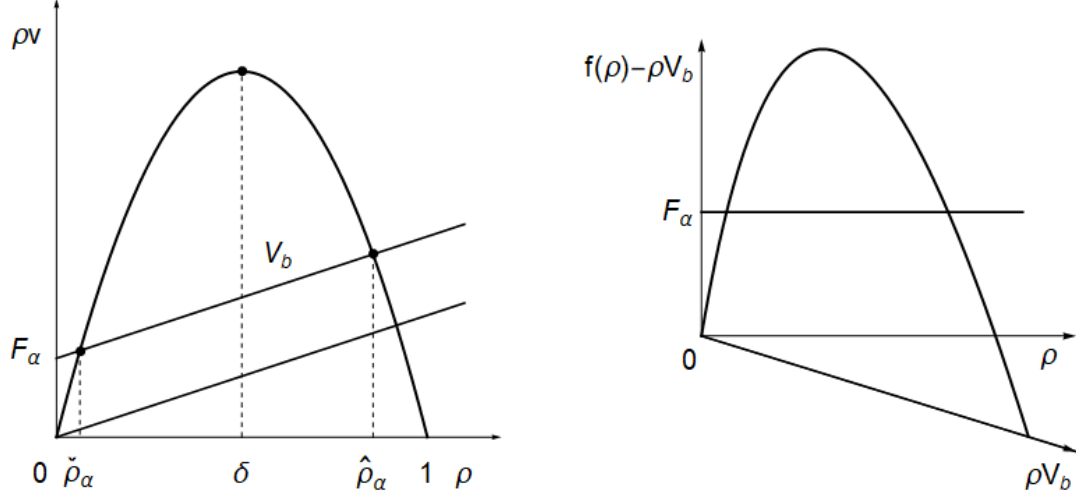


Figure 6.1: Fundamental diagram with constraint. Left: Fixed reference frame. Right: Bus reference frame.

Definition 6.1. Fix $F \doteq \frac{\alpha}{4v_{\max}}(v_{\max} - V_b)^2$. The constrained Riemann solver $\mathcal{BRS}_{\text{LWR}}: [0, 1]^2 \rightarrow \mathbf{L}_{\text{loc}}^1(\mathbb{R}; [0, 1])$ is defined as follows:

1. If $f((\mathcal{RS}_{\text{LWR}}[\rho_\ell, \rho_r](V_b)) \leq V_b \mathcal{RS}_{\text{LWR}}[\rho_\ell, \rho_r](V_b) + F$, then

$$\mathcal{BRS}_{\text{LWR}}[\rho_\ell, \rho_r] \doteq \mathcal{RS}_{\text{LWR}}[\rho_\ell, \rho_r] \quad \text{and} \quad y(t) = \omega(\rho_r)t.$$

2. If $f((\mathcal{RS}_{\text{LWR}}[\rho_\ell, \rho_r](V_b)) > V_b \mathcal{RS}_{\text{LWR}}[\rho_\ell, \rho_r](V_b) + \mathbf{F}$, then

$$\mathcal{BRS}_{\text{LWR}}[\rho_\ell, \rho_r](\xi) \doteq \begin{cases} \mathcal{RS}_{\text{LWR}}[\rho_\ell, \hat{\rho}_\alpha](\xi) & \text{if } \xi < V_b, \\ \mathcal{RS}_{\text{LWR}}[\check{\rho}_\alpha, \rho_r](\xi) & \text{if } \xi \geq V_b, \end{cases} \quad \text{and} \quad y(t) = V_b t,$$

where

$$\begin{aligned} \check{\rho}_\alpha &= \min\{\rho \in [0, 1] : f(\rho) = \rho V_b + \mathbf{F}\}, \\ \hat{\rho}_\alpha &= \max\{\rho \in [0, 1] : f(\rho) = \rho V_b + \mathbf{F}\}. \end{aligned}$$

We point out that if constraint condition (6.3) is not satisfied for classical Riemann solver $\mathcal{RS}_{\text{LWR}}$, then the solution has a non-classical shock $(\hat{\rho}_\alpha, \check{\rho}_\alpha)$ moving with speed of propagation equals V_b .

6.2.2 Networks

Let assign to each road of the junction I_h , for $h \in \mathbf{H} \doteq \mathbf{I} \cup \mathbf{J}$, the corresponding flux function $f_h(\rho) \doteq v_{\max}^h \rho(1 - \rho)$. The corresponding Riemann problem at the junction J is then

$$\begin{cases} \partial_t \rho_h + \partial_x f_h(\rho_h) = 0, & t > 0, x \in I_h, \\ \rho_h(0, x) = \rho_h^0, & x \in I_h, \end{cases} \quad h \in \mathbf{H}, \quad (6.5)$$

where $\rho_h^0 \in [0, 1]$ is the constant initial density along road I_h . If we further consider a bus initially at $x = 0$ and moving towards road I_k , $k \in \mathbf{J}$, then beside (6.5) we consider also

$$\begin{cases} y(t) = \omega(\rho_k(t, y(t)^+)), & t > 0, \\ y(0) = 0, \end{cases} \quad (6.6)$$

$$f_k(\rho_k(t, y(t))) - \dot{y}(t)\rho_k(t, y(t)) \leq \frac{\alpha_k}{4v_{\max}^k} (v_{\max}^k - \dot{y})^2, \quad t > 0.$$

Above, $y(t) \in I_k$ is the position of the bus at time $t \geq 0$ and $\alpha_k \in [0, 1]$ gives the reduction of the road capacity due to the presence of bus.

Before we introduce in Definition 6.5 our constrained Riemann solver $\mathcal{BRS}_{\text{LWR}}^J$ for (6.5), (6.6), we give the following definition of admissible constrained Riemann

solvers. We denote by $\mathcal{RS}_{\text{LWR}}^h$ the classical Riemann solver for the LWR model corresponding to the flux f_h , $h \in \mathbf{H}$. Moreover, let $\mathcal{BRS}_{\text{LWR}}$ be the constrained Riemann solver defined in Definition 6.1 and corresponding to road I_k .

Definition 6.2. *An admissible constrained Riemann solver at the junction $J \in \mathcal{J}$ for (6.5), (6.6) is a map $\mathcal{BRS}^J: [0, 1]^{n+m} \rightarrow [0, 1]^{n+m}$ such that for any initial datum $(\rho_1^0, \dots, \rho_{n+m}^0) \in [0, 1]^{n+m}$ we have that $(\bar{\rho}_1, \dots, \bar{\rho}_{n+m}) \doteq \mathcal{BRS}^J[\rho_1^0, \dots, \rho_{n+m}^0]$ satisfies the following conditions:*

- (A.1) *For every $i \in \mathbf{I}$, $\mathcal{RS}_{\text{LWR}}^i[\rho_i^0, \bar{\rho}_i]$ consists of waves propagating in $x \leq 0$.*
- (A.2) *For every $j \in \mathbf{J} \setminus \{k\}$, $\mathcal{RS}_{\text{LWR}}^j[\bar{\rho}_j, \rho_j^0]$ and $\mathcal{BRS}_{\text{LWR}}[\bar{\rho}_k, \rho_k^0]$ consists of waves propagating in $x \geq 0$.*
- (A.3) *The number of vehicles is conserved at the junction, namely*

$$\sum_{i=1}^n f_i(\bar{\rho}_i) = \sum_{j=n+1}^{n+m} f_j(\bar{\rho}_j).$$

- (A.4) *\mathcal{BRS}^J is consistent, that is*

$$\mathcal{BRS}^J[\bar{\rho}_1, \dots, \bar{\rho}_{n+m}] = (\bar{\rho}_1, \dots, \bar{\rho}_{n+m}).$$

By the last condition of the above definition, we can observe that the n -tuple traces at the junction is a fixed point for $\mathcal{BRS}_{\text{LWR}}^J$.

Since we wish to maximize the flow through the junction, we propose the possible traces and their ranges corresponding to a given initial datum $(\rho_1^0, \dots, \rho_{n+m}^0)$. Let us first define the following function.

Definition 6.3. *For any $h \in \mathbf{H}$, the function $\tau_h: [0, 1] \rightarrow [0, 1]$ is defined as follows:*

- $f_h(\tau_h(\rho)) = f_h(\rho)$ for every $\rho \in [0, 1]$;
- $\tau_h(\rho) \neq \rho$ for every $\rho \in [0, 1] \setminus \{1/2\}$.

The function τ_h is well defined, continuous and satisfies

$$0 \leq \rho \leq 1/2 \iff 1/2 \leq \tau_h(\rho) \leq 1, \quad 1/2 \leq \rho \leq 1 \iff 0 \leq \tau_h(\rho) \leq 1/2.$$

Proposition 6.1. *Let ρ_i^0 be the initial datum on the incoming road I_i for $i \in \mathbb{I}$. The set of reachable fluxes $f_i(\bar{\rho}_i)$ for an admissible constrained Riemann solver is*

$$\mathfrak{R}_i(\rho_i^0) = \begin{cases} [0, f_i(\rho_i^0)] & \text{if } \rho_i^0 \in [0, 1/2], \\ [0, f_i(1/2)] & \text{if } \rho_i^0 \in (1/2, 1]. \end{cases}$$

Proof. We apply the construction done in [47, Proposition 4.3.3]. We consider the case $\rho_i^0 \in [0, 1/2]$; the case $\rho_i^0 \in (1/2, 1]$ is analogous. By **(A.1)** we have that $\mathcal{RS}_{\text{LWR}}^i[\rho_i^0, \bar{\rho}_i]$ must have only waves propagating in $x \leq 0$. If $\bar{\rho}_i \in \{\rho_i^0\} \cup (\tau_i(\rho_i^0), 1]$ then $\mathcal{RS}_{\text{LWR}}^i[\rho_i^0, \bar{\rho}_i]$ is either constant or has a single shock with negative speed. On the contrary, if $\bar{\rho}_i \in [0, \tau_i(\rho_i^0)] \setminus \{\rho_i^0\}$ then $\mathcal{RS}_{\text{LWR}}^i[\rho_i^0, \bar{\rho}_i]$ is either a rarefaction or a single shock, however both of them propagate in $x \leq 0$, which concludes the proof. \square

From the above proposition the following conclusion is clear.

Corollary 6.1. *The maximal flow of the incoming road I_i at the junction J is*

$$\gamma_i^{\max}(\rho_i^0) = \begin{cases} f_i(\rho_i^0) & \text{if } \rho_i^0 \in [0, 1/2], \\ f_i(1/2) & \text{if } \rho_i^0 \in (1/2, 1]. \end{cases}$$

We observe that there exists a unique $\bar{\rho}_i \in [0, 1]$ so that $f_i(\bar{\rho}_i) = \gamma_i^{\max}(\rho_i^0)$ and $\mathcal{RS}_{\text{LWR}}^i[\rho_i^0, \bar{\rho}_i]$ has waves propagating in $x \leq 0$.

Proposition 6.2. *Let $j \in \mathbb{J}$ and ρ_j^0 be the initial datum on the outgoing road I_j . The set of reachable fluxes $f_j(\bar{\rho}_j)$ for an admissible constrained Riemann solver is*

$$\mathfrak{R}_j(\rho_j^0) = \begin{cases} \begin{cases} [0, f_j(1/2)] & \text{if } \rho_j^0 \in [0, 1/2] \text{ and } j \neq k, \\ [0, f_j(\rho_j^0)] & \text{if } \rho_j^0 \in (1/2, 1] \text{ and } j \neq k, \end{cases} \\ \begin{cases} [0, f_k(\hat{\rho}_{\alpha_k})] & \text{if } \rho_k^0 \in [0, \hat{\rho}_{\alpha_k}], \\ [0, f_k(\rho_k^0)] & \text{if } \rho_k^0 \in (\hat{\rho}_{\alpha_k}, 1]. \end{cases} \end{cases}$$

Proof. Except for the case $j \neq k$, the proof is analogous to proof of Proposition 6.1. Consider $j = k$ and $\rho_k^0 \in [0, \hat{\rho}_{\alpha_k}]$. We observe that $\bar{\rho}_k \in [0, \check{\rho}_{\alpha_k}]$ can be joined with ρ_k^0 by a classical wave. If $\bar{\rho}_k \in (\check{\rho}_{\alpha_k}, \tau_k(\hat{\rho}_{\alpha_k})) \cup \{\hat{\rho}_{\alpha_k}\}$ then $\mathcal{BRS}_{\text{LWR}}[\bar{\rho}_k, \rho_k^0]$ has a possibly null shock $(\bar{\rho}_k, \hat{\rho}_{\alpha_k})$, followed by a non-classical shock $(\hat{\rho}_{\alpha_k}, \check{\rho}_{\alpha_k})$ and a

shock $(\check{\rho}_{\alpha_k}, \rho_k^0)$. We point out that $\bar{\rho}_k \in [\tau(\hat{\rho}_{\alpha_k}), \hat{\rho}_{\alpha_k})$ cannot be connected with $\hat{\rho}_{\alpha_k}$ by a wave propagating in $x \leq 0$. At last, the case $j = k$ and $\rho_k^0 \in (\hat{\rho}_{\alpha_k}, 1]$ is analogous to the situation when $j \neq k$ and $\rho_j^0 \in (1/2, 1]$. \square

Corollary 6.2. *The maximal flow of the outgoing road I_j at the junction J is*

$$\gamma_j^{\max}(\rho_j^0) = \begin{cases} \left\{ \begin{array}{l} f_j(1/2) \text{ if } \rho_j^0 \in [0, 1/2] \text{ and } j \neq k, \\ f_j(\rho_j^0) \text{ if } \rho_j^0 \in (1/2, 1] \text{ and } j \neq k, \end{array} \right. \\ \left\{ \begin{array}{l} f_k(\hat{\rho}_{\alpha_k}) \text{ if } \rho_k^0 \in [0, \hat{\rho}_{\alpha_k}], \\ f_k(\rho_k^0) \text{ if } \rho_k^0 \in (\hat{\rho}_{\alpha_k}, 1]. \end{array} \right. \end{cases}$$

Additionally, for any $j \neq k$ there exists a unique $\bar{\rho}_j \in [0, 1]$ so that $f_j(\bar{\rho}_j) = \gamma_j^{\max}(\rho_j^0)$ and $\mathcal{RS}_{\text{LWR}}^j[\bar{\rho}_j, \rho_j^0]$ has waves propagating in $x \geq 0$. Analogously there exists a unique $\bar{\rho}_k \in [0, 1]$ so that $f_k(\bar{\rho}_k) = \gamma_k^{\max}(\rho_k^0)$ and $\mathcal{BRS}_{\text{LWR}}[\bar{\rho}_k, \rho_k^0]$ has waves propagating in $x \geq 0$.

For each junction we define a traffic distribution matrix, namely the matrix representing the percentage of cars from incoming road I_i moving towards outgoing road I_j .

Definition 6.4. *A distribution matrix $A_{m \times n}$ for the junction $J \in \mathcal{J}$ is given by*

$$A_{m \times n} = \begin{pmatrix} \alpha_{n+1,1} & \cdots & \alpha_{n+1,n} \\ \vdots & \ddots & \vdots \\ \alpha_{n+m,1} & \cdots & \alpha_{n+m,n} \end{pmatrix},$$

where $\alpha_{j,i} \geq 0$ for every i, j and $\sum_{j=n+1}^{n+m} \alpha_{j,i} = 1$ for every i .

More precisely, if C is the number of cars coming from road I_i , then $C\alpha_{j,i}$ is the number of cars moving from I_i towards I_j .

We conclude this subsection by defining our admissible constrained Riemann solver at the junction J .

Definition 6.5. *Fix a distribution matrix $A_{m \times n}$. The associated constrained Riemann solver $\mathcal{BRS}_{\text{LWR}}^J: [0, 1]^{n+m} \rightarrow [0, 1]^{n+m}$ is defined as follows for any initial datum $(\rho_1^0, \dots, \rho_{n+m}^0) \in [0, 1]^{n+m}$:*

1. Consider the closed, convex and non-empty set

$$\mathfrak{N} = \{(\gamma_1, \dots, \gamma_n) \in \mathfrak{N}_1 \times \dots \times \mathfrak{N}_n : A(\gamma_1, \dots, \gamma_n)^T \in \mathfrak{N}_{n+1} \times \dots \times \mathfrak{N}_{n+m}\},$$

where $\mathfrak{N}_i \doteq \mathfrak{N}_i(\rho_i^0) = [0, \gamma_i^{\max}(\rho_i^0)]$ and $\mathfrak{N}_j \doteq \mathfrak{N}_j(\rho_j^0) = [0, \gamma_j^{\max}(\rho_j^0)]$ are respectively defined in Propositions 6.1 and 6.2, see also Corollaries 6.1 and 6.2.

2. Let $(\bar{\gamma}_1, \dots, \bar{\gamma}_n) \in \mathfrak{N}$ be such that

$$\sum_{i=1}^n \bar{\gamma}_i = \max_{(\gamma_1, \dots, \gamma_n) \in \mathfrak{N}} \sum_{i=1}^n \gamma_i \quad (6.7)$$

and for any $i \in \mathbb{I}$ consider the unique $\bar{\rho}_i \in [0, 1]$ so that $f_i(\bar{\rho}_i) = \bar{\gamma}_i$ and $\mathcal{RS}_{\text{LWR}}^i[\rho_i^0, \bar{\rho}_i]$ has waves propagating in $x \leq 0$.

3. Define

$$(\bar{\gamma}_{n+1}, \dots, \bar{\gamma}_{n+m})^T \doteq A(\bar{\gamma}_1, \dots, \bar{\gamma}_n)^T.$$

Then for any $j \in \mathbb{J}$ consider the unique $\bar{\rho}_j \in [0, 1]$ so that $f_j(\bar{\rho}_j) = \bar{\gamma}_j$ and $\mathcal{RS}_{\text{LWR}}^j[\bar{\rho}_j, \rho_j^0]$ has waves propagating in $x \geq 0$.

4. At last, define $\mathcal{BRS}_{\text{LWR}}^J[\rho_1^0, \dots, \rho_{n+m}^0] \doteq (\bar{\rho}_1, \dots, \bar{\rho}_{n+m})$.

Remark 6.2. We underline that problem (6.7) may have more than one solution. In such a case, we can impose additional requirements on the distribution matrix A as in [47, Section 5.1], or introduce the priority vector, see [40].

6.2.3 A case study

We study a junction having two incoming ($n = 2$) and two outgoing ($m = 2$) roads with corresponding flux functions $f_h(\rho) = 4\rho(1 - \rho)$, $h \in \{1, \dots, 4\}$. Consider constant initial density $(\rho_1^0, \dots, \rho_4^0) \in [0, 1]^4$, see Figure 6.2, center, as follows:

$$\begin{aligned} 0 < \rho_1^0 < 1/2, & \quad 1/2 < \rho_2^0 < 1, & \quad 1/2 < \rho_3^0 < 1, & \quad 1/2 < \rho_4^0 < 1, \\ f(\rho_1^0) = 1/2, & \quad f(\rho_2^0) = 2/5, & \quad f(\rho_3^0) = 7/10, & \quad f(\rho_4^0) = 1/2. \end{aligned}$$

Let us choose the parameter α_3 appropriately to obtain $f(\hat{\rho}_{\alpha_3}) = 7/20$ and consider the distribution matrix

$$A = \begin{pmatrix} 1/2 & 1/3 \\ 1/2 & 2/3 \end{pmatrix}.$$

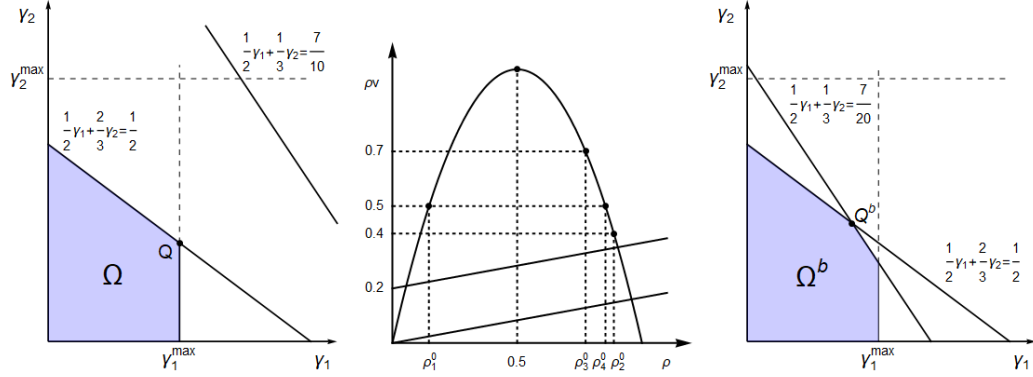


Figure 6.2: Left: the set \mathfrak{N} . Center: the fundamental diagram with initial datum. Right: the set \mathfrak{N}^b .

We consider two cases. The former one describes a junction without bus, while the latter describes a bus with maximal velocity $V_b = 1/6$ entering road I_3 . By Propositions 6.1 and 6.2, the sets of admissible fluxes at the junction are

$$\mathfrak{N}_1 = \mathfrak{N}_4 = [0, 1/2], \quad \mathfrak{N}_2 = [0, 1], \quad \mathfrak{N}_3 = [0, 7/10], \quad \mathfrak{N}_3^b = [0, 7/20].$$

Above, \mathfrak{N}_3^b and \mathfrak{N}_3 correspond to the cases when the bus is present or not, respectively.

In the case without the bus at the junction we have

$$\mathfrak{N} = \{(\gamma_1, \gamma_2) \in \mathfrak{N}_1 \times \mathfrak{N}_2 : A(\gamma_1, \gamma_2)^T \in \mathfrak{N}_3 \times \mathfrak{N}_4\}.$$

The maximal admissible flow through junction $\max_{(\gamma_1, \gamma_2) \in \mathfrak{N}}(\gamma_1 + \gamma_2)$ is achieved at the point $Q = (1/2, 3/8) \in \mathfrak{N}$, see Figure 6.2, left, therefore

$$BRS_{LWR}^J[\rho_1^0, \dots, \rho_4^0] = (1/2, 3/8, 3/8, 1/2).$$

The solution of Riemann problem at the junction for (6.5) is then completely

determined.

In the case with the bus, the set of reachable fluxes is given by

$$\mathfrak{N}^b = \{(\gamma_1, \gamma_2) \in \mathfrak{N}_1 \times \mathfrak{N}_2 : A(\gamma_1, \gamma_2)^T \in \mathfrak{N}_3^b \times \mathfrak{N}_4\}.$$

The maximal admissible flow through the junction $\max_{(\gamma_1, \gamma_2) \in \mathfrak{N}^b} (\gamma_1 + \gamma_2)$ is achieved at the point $Q^b = (2/5, 9/20) \in \mathfrak{N}^b$, see Figure 6.2, right, thus

$$\begin{aligned} 1/2 < \bar{\rho}_1 < 1, & & 1/2 < \bar{\rho}_2 < 1, & & \bar{\rho}_3 = \hat{\rho}_{\alpha_3}, & & \bar{\rho}_4 = \rho_4^0, \\ f(\bar{\rho}_1) = 2/5, & & f(\bar{\rho}_2) = 9/20, & & f(\bar{\rho}_3) = 7/20, & & f(\bar{\rho}_4) = 1/2. \end{aligned}$$

The solution of Riemann problem at the junction (6.5), (6.6) is completely determined.

In Figure 6.3 we display both solutions at time $t = 1/5$. The blue line describes the solution for the problem (6.5) without the bus. We point out that in this case the solution is constant along roads I_1 and I_4 , while along each road I_2 and I_3 it has a single shock. The red line in Figure 6.3 describes the solution of problem (6.5), (6.6) in presence of the bus. Notice that in this case the solution has a single shock along road I_1 , a single rarefaction along road I_2 , a non-classical shock followed by a shock along road I_3 , and it is constant along road I_4 .

6.3 PT models on networks

In this section we adapt the Riemann solvers for PT models described in Section 2.4 to the case of road networks. More precisely, we introduce a Riemann solver at the junction $\mathcal{RS}_{\text{PT}}^J$ obtained by adapting the Riemann solver \mathcal{RS}_{PT} . Here we use \mathcal{RS}_{PT} to indicate the Riemann solvers \mathcal{RS}_R^a , \mathcal{RS}_R^p , \mathcal{RS}_S^a and \mathcal{RS}_S^p defined in Subsection 2.4.3.

The Riemann problem at J is

$$\begin{cases} \text{PT model} & t > 0, x \in I_h, \\ Y_h(0, x) = Y_h^0 & x \in I_h, \end{cases} \quad (6.8)$$

where $(Y_1^0, \dots, Y_{n+m}^0) \in \Omega^{n+m}$ and ‘‘PT model’’ stands for phase transition model

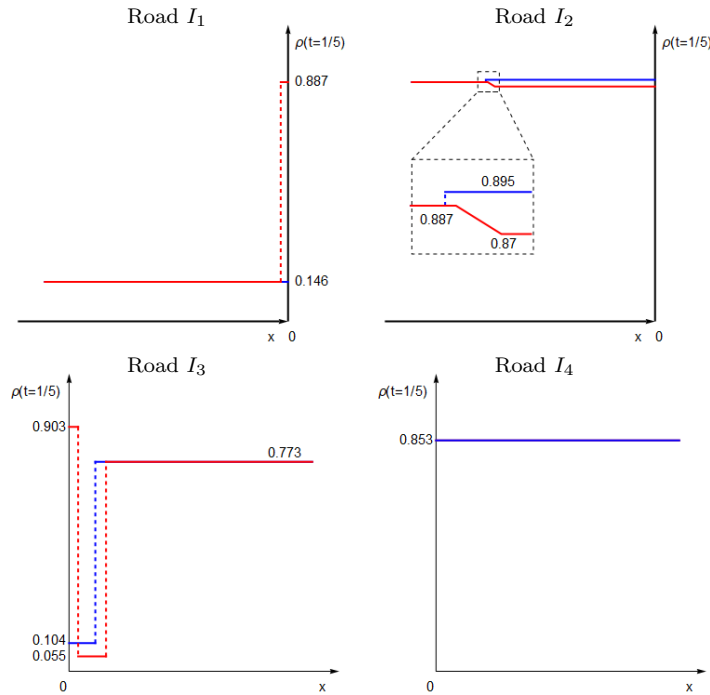


Figure 6.3: Above we represent the densities at time $t = 1/5$ along the roads I_1, \dots, I_4 . In red the case with the bus and in blue the case without the bus.

(2.20). In particular the traffic evolution along each road I_h , $h \in \{1, \dots, n + m\}$, is described by PT model (2.20).

As in the previous section, before stating our Riemann solver at the junction \mathcal{RS}_{PT} for (6.8) we give the definition of admissible Riemann solvers.

Definition 6.6. *An admissible Riemann solver at the junction $J \in \mathcal{J}$ for (6.8) is a map $\mathcal{RS}^J: \Omega^{n+m} \rightarrow \Omega^{n+m}$ such that for any initial datum $(Y_1^0, \dots, Y_{n+m}^0) \in \Omega^{n+m}$ we have that $(\bar{Y}_1, \dots, \bar{Y}_{n+m}) \doteq \mathcal{RS}^J[Y_1^0, \dots, Y_{n+m}^0]$ satisfies the following conditions:*

- For every $i \in I$ we have that $\mathcal{RS}_{PT}^i[Y_i^0, \bar{Y}_i]$ consists of waves propagating in $x \leq 0$.
- For every $j \in J$ we have that $\mathcal{RS}_{PT}^j[\bar{Y}_j, Y_j^0]$ consists of waves propagating in $x \geq 0$.

- The number of vehicles is conserved at the junction, namely

$$\sum_{i=1}^n f(\bar{Y}_i) = \sum_{j=n+1}^{n+m} f(\bar{Y}_j).$$

- \mathcal{RS}^J is consistent, that is

$$\mathcal{RS}^J[\bar{Y}_1, \dots, \bar{Y}_{n+m}] = (\bar{Y}_1, \dots, \bar{Y}_{n+m}).$$

As in the previous section we study the possible traces and their ranges corresponding to a given initial datum $(Y_1^0, \dots, Y_{n+m}^0)$.

Proposition 6.3. Fix initial datum $(Y_1^0, \dots, Y_{n+m}^0) \in \Omega^{n+m}$.

- If $\Omega_f \cap \Omega_c \neq \emptyset$, then the set of reachable fluxes is given by

$$\mathcal{O}_i(Y_i^0) \doteq \begin{cases} [0, f(Y_i^0)] & \text{if } Y_i^0 \in \Omega_f, \\ [0, f(\psi_1^f(Y_i^0))] & \text{if } Y_i^0 \in \Omega_c. \end{cases}$$

- If $\Omega_f \cap \Omega_c = \emptyset$, then the set of reachable fluxes is given by

$$\mathcal{O}_i(Y_i^0) \doteq \begin{cases} [0, f(Y_i^0)] & \text{if } Y_i^0 \in \Omega_f^- \text{ and } f(Y_i^0) < f_c^-, \\ [0, f_c^-] & \text{if } Y_i^0 \in \Omega_f^- \text{ and } f(Y_i^0) \geq f_c^-, \\ [0, f(\psi_1^c(Y_i^0))] \cup \{f(Y_i^0)\} & \text{if } Y_i^0 \in \Omega_f^+, \\ [0, f(\psi_1^c(Y_i^0))] \cup \{f(\psi_1^f(Y_i^0))\} & \text{if } Y_i^0 \in \Omega_c. \end{cases}$$

Proof. It suffices to make the observation that waves with negative speed can be of three types:

- waves of the first characteristic family,
- phase transitions $(Y_\ell, Y_r) \in \Omega_f^- \times \Omega_c^-$ with $f(Y_\ell) > f(Y_r)$ and $w_\ell < w_r = \mathbf{w}_-$,
- phase transitions $(Y_\ell, Y_r) \in (\Omega_f^+ \times \Omega_c^-) \cup (\Omega_c^- \times \Omega_f^+)$ with $w_\ell = w_r$ (in the case $\Omega_f \cap \Omega_c = \emptyset$).

□

The set $\mathcal{O}_i(Y_i^0)$ is non-convex, therefore we do not consider the metastable states in the definition of the corresponding maximum flows. Hence, we let

$$\gamma_i^{\max}(Y_i^0) \doteq \begin{cases} \begin{cases} f(Y_i^0) & \text{if } Y_i^0 \in \Omega_f, \\ f(\psi_1^f(Y_i^0)) & \text{if } Y_i^0 \in \Omega_c, \end{cases} & \text{if } \Omega_f \cap \Omega_c \neq \emptyset, \\ \begin{cases} f(Y_i^0) & \text{if } Y_i^0 \in \Omega_f^- \text{ and } f(Y_i^0) < f_c^-, \\ f_c^- & \text{if } Y_i^0 \in \Omega_f^- \text{ and } f(Y_i^0) \geq f_c^-, \end{cases} & \text{if } \Omega_f \cap \Omega_c = \emptyset. \\ f(\psi_1^c(Y_i^0)) & \text{if } Y_i^0 \in \Omega_f^+ \cup \Omega_c, \end{cases}$$

Corollary 6.3. *For any initial datum $Y_i^0 \in \Omega$ and $\bar{\gamma}_i \in \mathcal{O}_i(Y_i^0)$, there exists a unique $\bar{Y}_i \in \Omega$ such that $\mathcal{RS}_{\text{PT}}[Y_i^0, \bar{Y}_i]$ consists of waves propagating in $x \leq 0$.*

Proposition 6.4. *Fix initial datum $Y_j^0 \in \Omega$ for $j \in J$. The set of reachable flows is given by*

$$\mathcal{O}_j(Y_j^0) \doteq \begin{cases} [0, f_f^+] & \text{if } Y_j^0 \in \Omega_f, \\ [0, f(\psi_2^+(Y_j^0))] & \text{if } Y_j^0 \in \Omega_c. \end{cases}$$

Proof. It suffices to make the observation that waves with positive speed can be of two types:

- contact discontinuities,
- phase transitions $(Y_\ell, Y_r) \in \Omega_f^- \times \Omega_c^-$ with $f_\ell < f_r$ and $w(Y_\ell) < w_r = w_-$. \square

We point out that in Proposition 6.4 we do not have to distinguish between the cases of intersecting and non-intersecting phases. The set $\mathcal{O}_j(Y_j^0)$ is convex and we denote its maximum as

$$\gamma_j^{\max}(Y_j^0) \doteq \begin{cases} f_f^+ & \text{if } Y_j^0 \in \Omega_f, \\ f(\psi_2^+(Y_j^0)) & \text{if } Y_j^0 \in \Omega_c. \end{cases}$$

Corollary 6.4. *For any initial datum $Y_j^0 \in \Omega$ and $\bar{\gamma}_j \in \mathcal{O}_j(Y_j^0)$, there exists a unique $\bar{Y}_j \in \Omega$ such that $\mathcal{RS}_{\text{PT}}[Y_j^0, \bar{Y}_j]$ consists of waves propagating in $x \geq 0$.*

We introduce now the definition of our admissible Riemann solver at the junction J .

Definition 6.7. Fix an $(n+m)$ -tuple of priority parameters $(\theta_1, \dots, \theta_{n+m}) \in \mathbb{R}^{n+m}$ such that $\theta_h > 0$ for all $h \in \mathbf{H}$ and

$$\sum_{i=1}^n \theta_i = \sum_{j=n+1}^{n+m} \theta_j = 1.$$

The associated admissible Riemann solver $\mathcal{RS}_{\text{PT}}^J: \Omega^{n+m} \rightarrow \Omega^{n+m}$ is defined as follows for any initial datum $(Y_1^0, \dots, Y_{n+m}^0) \in \Omega^{n+m}$.

1. Define the maximal possible through-flow at the junction, namely

$$\Gamma \doteq \min \left\{ \sum_{i=1}^n \gamma_i^{\max}(Y_i^0), \sum_{j=n+1}^{n+m} \gamma_j^{\max}(Y_j^0) \right\}.$$

2. Consider the closed, convex and non-empty sets

$$\begin{aligned} \mathcal{C}_{\text{inc}} &\doteq \left\{ (\gamma_1, \dots, \gamma_n) \in \prod_{i=1}^n [0, \gamma_i^{\max}(Y_i^0)] : \sum_{i=1}^n \gamma_i = \Gamma \right\}, \\ \mathcal{C}_{\text{out}} &\doteq \left\{ (\gamma_{n+1}, \dots, \gamma_{n+m}) \in \prod_{j=n+1}^{n+m} [0, \gamma_j^{\max}(Y_j^0)] : \sum_{j=n+1}^{n+m} \gamma_j = \Gamma \right\}. \end{aligned}$$

3. Denote by $(\bar{\gamma}_1, \dots, \bar{\gamma}_n)$ the projection of the point $(\Gamma\theta_1, \dots, \Gamma\theta_n)$ on the convex set \mathcal{C}_{inc} and by $(\bar{\gamma}_{n+1}, \dots, \bar{\gamma}_{n+m})$ the projection of $(\Gamma\theta_{n+1}, \dots, \Gamma\theta_{n+m})$ on the convex set \mathcal{C}_{out} .

4. For every $h \in \mathbf{H}$, set

$$\bar{Y}_h \doteq \begin{cases} Y_{h,0} & \text{if } f(Y_{h,0}) = \bar{\gamma}_h, \\ Y_h & \text{otherwise,} \end{cases}$$

where Y_h is the unique solution to the equation $f(Y) = \bar{\gamma}_h$ given by Corollary 6.3 or Corollary 6.4.

5. At last, let $\mathcal{RS}_{\text{PT}}^J(Y_1^0, \dots, Y_{n+m}^0) \doteq (\bar{Y}_1, \dots, \bar{Y}_{n+m})$.

We point out that $\mathcal{RS}_{\text{PT}}^J$ is admissible in the sense of Definition 6.6.

6.3.1 A case study

Consider a simple network made of two incoming roads $i = 1, 2$ and one outgoing road $j = 3$ that meet at $x = 0$. Assume that the traffic on each road is described by either PT^a or PT^p . Once the initial data $(Y_1^0, Y_2^0, Y_3^0) \in \Omega^3$ is chosen, we can determine the maximum flows $\gamma_1^{\max}(Y_1^0)$, $\gamma_2^{\max}(Y_2^0)$, $\gamma_3^{\max}(Y_3^0)$. Then, we define $\Gamma \doteq \min\{\gamma_1^{\max} + \gamma_2^{\max}, \gamma_3^{\max}\}$ and fix $(\theta_1, \theta_2, \theta_3) = (\theta, 1 - \theta, 1)$, for some $\theta \in (0, 1)$. We have

$$\mathcal{C}_{\text{inc}} = \{(\gamma_1, \gamma_2) \in [0, \gamma_1^{\max}(Y_1^0)] \times [0, \gamma_2^{\max}(Y_2^0)]: \gamma_1 + \gamma_2 = \Gamma\}, \quad \mathcal{C}_{\text{out}} = \{\Gamma\}.$$

Then, we take $\bar{\gamma}_3 = \Gamma$. We have to distinguish two possible cases: either $\gamma_1^{\max}(Y_1^0) + \gamma_2^{\max}(Y_2^0) = \Gamma \leq \gamma_3^{\max}(Y_3^0)$ or $\gamma_1^{\max}(Y_1^0) + \gamma_2^{\max}(Y_2^0) > \Gamma = \gamma_3^{\max}(Y_3^0)$. In the first case, we take $(\bar{\gamma}_1, \bar{\gamma}_2) \doteq (\gamma_1^{\max}(Y_1^0), \gamma_2^{\max}(Y_2^0))$. In the second case, let $(\bar{\gamma}_1, \bar{\gamma}_2)$ be the point of intersection of the sets $\{(\gamma_1, \gamma_2) \in \mathbb{R}^+ \times \mathbb{R}^+ : \gamma_1 + \gamma_2 = \Gamma\}$ and $\{(\gamma_1, \gamma_2) \in \mathbb{R}^+ \times \mathbb{R}^+ : \gamma_2 = ((1 - \theta)/\theta)\gamma_1\}$. If $(\bar{\gamma}_1, \bar{\gamma}_2) \in [0, \gamma_1^{\max}(Y_1^0)] \times [0, \gamma_2^{\max}(Y_2^0)]$, then we take $(\bar{\gamma}_1, \bar{\gamma}_2) = (\bar{\gamma}_1, \bar{\gamma}_2)$. Otherwise, $(\bar{\gamma}_1, \bar{\gamma}_2)$ is the projection of $(\bar{\gamma}_1, \bar{\gamma}_2)$ on \mathcal{C}_{inc} . Finally, we can find the traces at the junction $(\bar{Y}_1, \bar{Y}_2, \bar{Y}_3)$ by Corollary 6.3 and Corollary 6.4.

Technical proofs of Subsection 2.4.3

In this section we collect the proofs concerning the properties of the Riemann solvers \mathcal{RS}_R and \mathcal{RS}_S .

A.1 Proofs of the main properties of \mathcal{RS}_R

Proposition 2.2 follows from the following two lemmas.

Lemma A.1. \mathcal{RS}_R is $\mathbf{L}_{\text{loc}}^1$ -continuous in Ω^2 .

Proof. Assume that $(Y_\ell^\varepsilon, Y_r^\varepsilon)$ converges to (Y_ℓ, Y_r) in Ω^2 as $\varepsilon \rightarrow 0$. We claim that $\mathcal{RS}_R[Y_\ell^\varepsilon, Y_r^\varepsilon] \rightarrow \mathcal{RS}_R[Y_\ell, Y_r]$ in $\mathbf{L}_{\text{loc}}^1$. We consider only the case where $\mathcal{RS}_R[Y_\ell, Y_r]$ is just one PT, namely the case described in **(R.4)** of Definition 2.7; for the remaining cases it is sufficient to apply the continuity of $\mathcal{RS}_{\text{LWR}}$ and $\mathcal{RS}_{\text{ARZ}}$. Observe that $\mathcal{RS}_R[Y_\ell^\varepsilon, Y_r^\varepsilon]$ is the juxtaposition of $\mathcal{RS}_R[Y_\ell^\varepsilon, \psi_2^-(Y_r^\varepsilon)]$ and $\mathcal{RS}_R[\psi_2^-(Y_r^\varepsilon), Y_r^\varepsilon]$. Therefore we have to consider only the following cases.

- Assume that $\rho_\ell = 0$. If $\psi_2^-(Y_r^\varepsilon) \rightarrow \psi_2^-(Y_r)$, then $\sigma(Y_\ell^\varepsilon, \psi_2^-(Y_r^\varepsilon)) \rightarrow v(Y_r)$. Then we can conclude by observing that $v(Y_r^\varepsilon) \rightarrow v(Y_r)$.
- Assume that $\rho_\ell \neq 0$ and $Y_r \neq Y_p(Y_\ell)$, with Y_p defined in **(R.5)**. In this case $w_r = w_-$, therefore $\psi_2^-(Y_r^\varepsilon) \rightarrow Y_r$, which implies that $\sigma(Y_\ell^\varepsilon, \psi_2^-(Y_r^\varepsilon)) \rightarrow \sigma(Y_\ell, Y_r)$. Then we can conclude by observing that $v(Y_r^\varepsilon) \rightarrow v(Y_r)$.
- Assume that $\rho_\ell \neq 0$ and $Y_r = Y_p(Y_\ell)$. In this case $w_r = w_-$ and $\mathcal{RS}_R[Y_\ell^\varepsilon, Y_r^\varepsilon]$ is described by either **(R.4)** or **(R.5)**. The former case is analogous to the previous

one. For the latter case, by $Y_p(Y_\ell^\varepsilon) \rightarrow Y_r$ and $\psi_2^-(Y_r^\varepsilon) \rightarrow Y_r$ we have that both $\sigma(Y_\ell^\varepsilon, u_p(Y_\ell^\varepsilon))$ and $\lambda_1^{\text{PT}}(\psi_2^-(Y_r^\varepsilon))$ converge to $\sigma(Y_\ell, Y_r) = \lambda_1^{\text{PT}}(Y_r)$, then it is easy to conclude. \square

Lemma A.2. *The Riemann solver \mathcal{RS}_R is consistent.*

Proof. Since $\mathcal{RS}_R[z, z] = z$ for all $z \in \Omega$, we can assume that Y_ℓ, Y_m and Y_r are all distinct. The Lax Riemann solver is consistent, hence it is enough to consider $\mathcal{RS}_R[Y_\ell, Y_r]$ with at least one PT. In this case by definition \mathcal{RS}_R has exactly one PT and it goes from Ω_f^- to Ω_c^- . Moreover, $\mathcal{RS}_R[Y_\ell, Y_m]$ does not contain any C. Hence, to prove (I) or (II) of Definition 2.9 it is sufficient to consider the cases described in (R.4) or (R.5), $\rho_\ell \neq 0$ and $w_m = w_-$. The result then easily follows. \square

A.2 Proofs of the main properties of \mathcal{RS}_S

Proposition 2.3 follows from the following two lemmas.

Lemma A.3. *The Riemann solver \mathcal{RS}_S is $\mathbf{L}_{\text{loc}}^1$ -continuous.*

Proof. By the analysis done in Lemma A.1 and Remark 2.5, it is sufficient to consider the case in which $\mathcal{RS}_S[Y_\ell, Y_r] \equiv \text{PT}[Y_\ell, Y_r]$ and one of the conditions (2.22),(2.24),(2.23) holds true. Let $(Y_\ell^\varepsilon, Y_r^\varepsilon) \rightarrow (Y_\ell, Y_r)$ in Ω^2 and consider the following cases.

- Assume that (Y_ℓ, Y_r) satisfies (2.22) with $Y_r = \psi_1^f(Y_\ell)$ and $v(Y_\ell) = v_c$. In this case it is sufficient to observe that $\psi_1^c(Y_\ell^\varepsilon) \rightarrow Y_\ell$ and $\psi_1^f(Y_\ell^\varepsilon) \rightarrow Y_r$, thus both $\lambda_1^{\text{PT}}(Y_\ell^\varepsilon)$ and $\lambda_1^{\text{PT}}(\psi_1^c(Y_\ell^\varepsilon))$ converge to $\lambda_1^{\text{PT}}(Y_\ell)$ and $\sigma(\psi_1^c(Y_\ell^\varepsilon), \psi_1^f(Y_\ell^\varepsilon)) \rightarrow \sigma(Y_\ell, Y_r)$.
- Assume that (Y_ℓ, Y_r) satisfies (2.23) with $Y_r = Y_c^-$. In this case, it is sufficient to observe that $\psi_2^-(Y_r^\varepsilon) \rightarrow Y_r$, $\lambda_1^{\text{PT}}(\psi_2^-(Y_r^\varepsilon)) \rightarrow \lambda_1^{\text{PT}}(Y_r)$ and $\sigma(Y_\ell^\varepsilon, Y_r) \rightarrow \sigma(Y_\ell, Y_r)$.
- Assume that (Y_ℓ, Y_r) satisfies (2.24) with $Y_\ell = \psi_1^f(Y_r)$ and $v(Y_r) = v_c$. Let Y_*^ε be the intersection point of $\mathcal{L}_{w_\ell^\varepsilon}^1$ and $\mathcal{L}_{v_\varepsilon}^2$. In this case it is sufficient to observe that $\psi_1^c(Y_\ell^\varepsilon) \rightarrow Y_r$ and $Y_*^\varepsilon \rightarrow Y_r$ to obtain that both $\lambda_1^{\text{PT}}(\psi_1^c(Y_\ell^\varepsilon))$ and $\lambda_1^{\text{PT}}(Y_*^\varepsilon)$ converge to $\lambda_1^{\text{PT}}(Y_r)$, and $\sigma(Y_\ell^\varepsilon, \psi_1^c(Y_\ell^\varepsilon)) \rightarrow \sigma(Y_\ell, Y_r)$. \square

Lemma A.4. *The Riemann solver \mathcal{RS}_S is consistent.*

Proof. Since $\mathcal{RS}_S[z, z] = z$ for all $z \in \Omega$, it is not restrictive to assume that Y_ℓ , Y_m and Y_r are all distinct. Furthermore, $\mathcal{RS}_S[Y_\ell, Y_m]$ does not contain any \mathbf{C} . By Lemma A.2 and Remark 2.5, to prove (I) or (II) of Definition 2.9 we are left to consider the following cases:

- (Y_ℓ, Y_r) satisfies (2.22) with Y_m such that $\mathbf{w}_m = \mathbf{w}_\ell$ and $v_m > v_\ell$;
- (Y_ℓ, Y_r) satisfies (2.23) with Y_m such that $\mathbf{w}_m = \mathbf{w}_-$ and $v_m \geq v_r$;
- (Y_ℓ, Y_r) satisfies (2.24) with Y_m such that $\mathbf{w}_m = \mathbf{w}_\ell$ and $v_m \geq v_r$.

The analysis of the above cases is straightforward, and the result easily follows. \square

A.3 Proofs of the main properties of \mathcal{CRS}_S

In this final section, we accomplish the proof of Proposition 5.3. Recall that the same constrained Riemann solver for PT^p has already been studied in [12].

Example A.1. *The constrained Riemann solver \mathcal{CRS}_S is not $\mathbf{L}_{\text{loc}}^1$ -continuous. Indeed, take $F > f(u_-^c)$ and consider $U_\ell, U_r, U_\ell^\varepsilon \in \Omega_f$ with $f(U_\ell) = q < f(U_\ell^\varepsilon)$ and $U_\ell^\varepsilon \rightarrow U_\ell$. In this case $\mathcal{CRS}_S[U_\ell^\varepsilon, U_r]$ does not converge to $\mathcal{CRS}_S[U_\ell, U_r]$ in $\mathbf{L}_{\text{loc}}^1$, since $\mathcal{CRS}_S[U_\ell, U_r] = U_\ell$ in \mathbb{R}_- and the restriction of $\mathcal{CRS}_S[U_\ell^\varepsilon, U_r]$ to \mathbb{R}_- converges to*

$$\begin{cases} U_\ell & \text{if } x < \sigma(U_\ell, z_\#), \\ z_\# & \text{if } \sigma(U_\ell, z_\#) < x < 0, \end{cases}$$

where $z_\# \doteq u_-^c$ if $U_\ell \in \Omega_f^-$ and $z_\# \doteq \psi_1^c(U_\ell)$ if $U_\ell \in \Omega_f^+$.

Lemma A.5. *The constrained Riemann solver \mathcal{CRS}_S satisfies (II) of Definition 2.9.*

Proof. Assume that $\mathcal{CRS}_S[U_\ell, U_m](\bar{x}) = U_m = \mathcal{CRS}_S[U_m, U_r](\bar{x})$, for some $\bar{x} \in \mathbb{R}$. Since by Lemma A.4 and Lemma A.7 the Riemann solvers \mathcal{RS}_S and \mathcal{CRS}_R already satisfy (II), by Remark 5.2 we have to consider the cases where at least one among (U_ℓ, U_r) , (U_ℓ, U_m) and (U_m, U_r) belong to \mathcal{D}_2 and satisfy one of the conditions (5.2),(5.3),(5.4). We observe that $\mathcal{CRS}_S[U_\ell, U_m]$ cannot present any contact discontinuity, otherwise it would not be possible to juxtapose $\mathcal{CRS}_S[U_\ell, U_m]$ and

$\mathcal{CRS}_S[U_m, U_r]$. Hence, we are left to consider $(U_\ell, U_r) \in \mathcal{D}_2$ satisfying (5.2) with $U_m \in \{\hat{U}, \check{U}\}$, or (5.3) with $U_m \in \{\hat{U}, \check{U}\}$, or (5.4) with $U_m \in \{\check{U}\} \cup \mathcal{CRS}_S[U_\ell, \hat{U}](\mathbb{R}_-)$. In all these cases, it is easy to see that (II) holds true. \square

A.4 Proofs of the main properties of \mathcal{CRS}_R

In the next lemmas we prove Proposition 5.2.

Lemma A.6. *The constrained Riemann solver \mathcal{CRS}_R is $\mathbf{L}_{\text{loc}}^1$ -continuous.*

Proof. By the $\mathbf{L}_{\text{loc}}^1$ -continuity of \mathcal{RS}_R , it suffices to consider $(U_\ell^\varepsilon, U_r^\varepsilon) \rightarrow (U_\ell, U_r)$ with $(U_\ell^\varepsilon, U_r^\varepsilon) \in \mathcal{D}_2$ and to prove that $\mathcal{RS}_R[U_\ell^\varepsilon, \hat{U}^\varepsilon] \rightarrow \mathcal{RS}_R[U_\ell, U_r]$ in \mathbb{R}_- and $\mathcal{RS}_R[\check{U}^\varepsilon, U_r^\varepsilon] \rightarrow \mathcal{RS}_R[U_\ell, U_r]$ in \mathbb{R}_+ , where $\hat{U}^\varepsilon \doteq \hat{U}(w(U_\ell^\varepsilon), F)$ and $\check{U}^\varepsilon \doteq \check{U}(v(U_r^\varepsilon), F)$. For notational simplicity, below we denote $\hat{U} \doteq \hat{U}(w(U_\ell), F)$, $\check{U} \doteq \check{U}(v(U_r), F)$ and $u_* \doteq u_*(U_\ell, U_r)$.

We first consider the cases with $(U_\ell, U_r) \in \mathcal{D}_1$.

- Assume $U_\ell, U_r \in \Omega_f$ and $f(U_\ell) = q$. Then, either $U_\ell \in \Omega_f^-$ or $U_\ell \in \Omega_f^+$. In the first case, $\sigma(U_\ell^\varepsilon, \hat{U}^\varepsilon) \rightarrow 0$ and $\mathcal{RS}_R[U_\ell^\varepsilon, \hat{U}^\varepsilon] \rightarrow U_\ell$ in \mathbb{R}_- , while in the latter $\hat{U}^\varepsilon \rightarrow U_\ell$ and $\mathcal{RS}_R[U_\ell^\varepsilon, \hat{U}^\varepsilon] \rightarrow \mathcal{RS}_R[U_\ell, U_\ell] = U_\ell$. Moreover, in both cases $\check{U}^\varepsilon \rightarrow U_\ell$ and $\mathcal{RS}_R[\check{U}^\varepsilon, U_r^\varepsilon] \rightarrow \mathcal{RS}_R[U_\ell, U_r]$.
- Assume $U_\ell, U_r \in \Omega_c$ and $f(u_*) = q$. Then, $\hat{U}^\varepsilon \rightarrow u_*$ and $\mathcal{RS}_R[U_\ell^\varepsilon, \hat{U}^\varepsilon] \rightarrow \mathcal{RS}_R[U_\ell, u_*]$. Moreover, it is sufficient to consider the cases $\check{U}^\varepsilon \in \Omega_f^-$ and $\check{U}^\varepsilon \in \Omega_c$. In the first case $\psi_2^-(U_r^\varepsilon) \rightarrow u_*$, $\sigma(\check{U}^\varepsilon, \psi_2^-(U_r^\varepsilon)) \rightarrow 0$ and $\mathcal{RS}_R[\check{U}^\varepsilon, U_r^\varepsilon] \rightarrow \mathcal{RS}_R[u_*, U_r]$ in \mathbb{R}_+ , while in the latter $\check{U}^\varepsilon \rightarrow u_*$ and $\mathcal{RS}_R[\check{U}^\varepsilon, U_r^\varepsilon] \rightarrow \mathcal{RS}_R[u_*, U_r]$.
- Assume $U_\ell \in \Omega_c^-, U_r \in \Omega_f^-$ and $f(\psi_1(U_\ell)) = q$. Then, $\hat{U}^\varepsilon \rightarrow \psi_1(U_\ell)$ and $\check{U}^\varepsilon = \psi_1(U_\ell)$. As a consequence, $\mathcal{RS}_R[U_\ell^\varepsilon, \hat{U}^\varepsilon] \rightarrow \mathcal{RS}_R[U_\ell, \psi_1(U_\ell)]$ and $\mathcal{RS}_R[\check{U}^\varepsilon, U_r^\varepsilon] \rightarrow \mathcal{RS}_R[\psi_1(U_\ell), U_r]$.
- Assume $U_\ell \in \Omega_f^-, U_r \in \Omega_c^-$ and $f(U_\ell) > f(\psi_2^-(U_r)) = q$. Then, $\hat{U}^\varepsilon = \psi_2^-(U_r)$ and therefore $\mathcal{RS}_R[U_\ell^\varepsilon, \hat{U}^\varepsilon] \rightarrow \mathcal{RS}_R[U_\ell, \psi_2^-(U_r)]$. Moreover, $\sigma(\check{U}^\varepsilon, \psi_2^-(U_r^\varepsilon)) \rightarrow 0$ and therefore $\mathcal{RS}_R[\check{U}^\varepsilon, U_r^\varepsilon] \rightarrow \mathcal{RS}_R[\psi_2^-(U_r), U_r]$ in \mathbb{R}_+ .
- Assume $U_\ell \in \Omega_f^-, U_r \in \Omega_c^-$ and $f(\psi_2^-(U_r)) \geq f(U_\ell) = q$. In this case, $\sigma(U_\ell^\varepsilon, \hat{U}^\varepsilon) \rightarrow 0$ and $\mathcal{RS}_R[U_\ell^\varepsilon, \hat{U}^\varepsilon] \rightarrow U_\ell$ in \mathbb{R}_- . Moreover, $\check{U}^\varepsilon = U_\ell$ and $\mathcal{RS}_R[\check{U}^\varepsilon, U_r^\varepsilon] \rightarrow \mathcal{RS}_R[U_\ell, U_r]$.

We finally consider the cases with $(U_\ell, U_r) \in \mathcal{D}_2$.

- Assume $U_\ell, U_r \in \Omega_f$ and $f(U_\ell) > q$. Then, $\hat{U}^\varepsilon \rightarrow \hat{U}$ and $\check{U}^\varepsilon \rightarrow \check{U}$. As a consequence, $\mathcal{RS}_R[U_\ell^\varepsilon, \hat{U}^\varepsilon] \rightarrow \mathcal{RS}_R[U_\ell, \hat{U}]$ and $\mathcal{RS}_R[\check{U}^\varepsilon, U_r^\varepsilon] \rightarrow \mathcal{RS}_R[\check{U}, U_r]$.
- Assume $U_\ell, U_r \in \Omega_c$ and $f(u_*(U_\ell, U_r)) > q$. Then, $\hat{U}^\varepsilon \rightarrow \hat{U}$ and therefore $\mathcal{RS}_R[U_\ell^\varepsilon, \hat{U}^\varepsilon] \rightarrow \mathcal{RS}_R[U_\ell, \hat{U}]$. Moreover, it is sufficient to consider the cases $\check{U}^\varepsilon \in \Omega_c$ and $\check{U}^\varepsilon \in \Omega_f^-$. In the first case $\check{U}^\varepsilon \rightarrow \check{U}$ and $\mathcal{RS}_R[\check{U}^\varepsilon, U_r^\varepsilon] \rightarrow \mathcal{RS}_R[\check{U}, U_r]$, while in the latter (whether $\check{U} = \psi_2^-(U_r)$ or $\check{U} = \check{U}^\varepsilon$) we have $\psi_2^-(U_r^\varepsilon) \rightarrow \psi_2^-(U_r)$ and $\mathcal{RS}_R[\check{U}^\varepsilon, U_r^\varepsilon] \rightarrow \mathcal{RS}_R[\check{U}, U_r]$ in \mathbb{R}_+ .
- Assume $U_\ell \in \Omega_c^-, U_r \in \Omega_f^-$ and $f(\psi_1(U_\ell)) > q$. Then, $\hat{U}^\varepsilon \rightarrow \hat{U}$ and $\check{U}^\varepsilon = \check{U}$. As a consequence, we have $\mathcal{RS}_R[U_\ell^\varepsilon, \hat{U}^\varepsilon] \rightarrow \mathcal{RS}_R[U_\ell, \hat{U}]$ and $\mathcal{RS}_R[\check{U}^\varepsilon, U_r^\varepsilon] \rightarrow \mathcal{RS}_R[\check{U}, U_r]$.
- Assume $U_\ell \in \Omega_f^-, U_r \in \Omega_c^-$ and $\min\{f(U_\ell), f(\psi_2^-(U_r))\} > q$. Then, $\hat{U}^\varepsilon = \hat{U}$ and $\check{U}^\varepsilon = \check{U}$. As a consequence, $\mathcal{RS}_R[U_\ell^\varepsilon, \hat{U}^\varepsilon] \rightarrow \mathcal{RS}_R[U_\ell, \hat{U}]$ and $\mathcal{RS}_R[\check{U}^\varepsilon, U_r^\varepsilon] \rightarrow \mathcal{RS}_R[\check{U}, U_r]$.

This concludes the proof. \square

Lemma A.7. *The constrained Riemann solver \mathcal{CRS}_R satisfies condition (II) of Definition 2.9.*

Proof. We assume

$$\mathcal{CRS}_R[U_\ell, U_m](\bar{x}) = U_m = \mathcal{CRS}_R[U_m, U_r](\bar{x}), \quad \text{for } \bar{x} \in \mathbb{R}. \quad (\text{Z1})$$

Since by Lemma A.2 the Riemann solver \mathcal{RS}_R satisfies (II), it is not restrictive to assume that

$$\{(U_\ell, U_r), (U_\ell, U_m), (U_m, U_r)\} \cap \mathcal{D}_2 \neq \emptyset. \quad (\text{Z2})$$

We also observe that (Z1) implies

$$\mathcal{CRS}_R[U_\ell, U_m] \text{ does not contain any contact discontinuity,} \quad (\text{Z3})$$

because otherwise it is not possible to juxtapose $\mathcal{CRS}_R[U_\ell, U_m]$ and $\mathcal{CRS}_R[U_m, U_r]$. We are then left to consider the following cases.

- Assume $U_\ell, U_m \in \Omega_f$. In this case, by (Z3) we have $(U_\ell, U_m) \in \mathcal{D}_2$ and $U_m = \check{U}(v(U_m), F)$, namely $f(U_\ell) > q = f(U_m)$. Then, by (Z1) we have that either $U_m \in \Omega_f^-$ and $f(\psi_2^-(U_r)) > q$ or $U_m \in \Omega_f^+$ and $U_r \in \Omega_f$. In both cases it is easy to conclude.
- Assume $U_\ell, U_m \in \Omega_c$. In this case, by (Z3) we have either $(U_\ell, U_m) \in \mathcal{D}_2$ or $(U_\ell, U_m) \in \mathcal{D}_1$ and $w(U_\ell) = \mathbf{w}_m$. In the first case, whether $\check{U}(v(U_m), F) \in \Omega_c$, $U_m = \check{U}(v(U_m), F)$ and $\mathbf{w}_m < w(U_\ell)$ or $\check{U}(v(U_m), F) \in \Omega_f^-$, $\mathbf{w}_m = \mathbf{w}_- \leq w(U_\ell)$ and $f(U_m) > q$, by (Z1) we have that $v(U_r) = v(U_m)$. In the latter case, by (Z1) and (Z2) we have that $f(U_m) = q$, $v(U_r) > v(U_m)$ and $(U_m, U_r) \in \mathcal{D}_2$. In both cases it is easy to conclude.
- Assume $U_\ell \in \Omega_c^-$ and $U_m \in \Omega_f^-$. In this case, by (Z3) we have $(U_\ell, U_m) \in \mathcal{D}_2$ and $U_m = \check{U}(v(U_m), F)$. Then, by (Z1) we have that U_r has to satisfy $f(\psi_2^-(U_r)) > q$. Hence, it is easy to conclude.
- Assume $U_\ell \in \Omega_f^-$ and $U_m \in \Omega_c^-$. In this case, by (Z3) we have $\mathbf{w}_m = \mathbf{w}_-$. Moreover, by (Z2) and (Z3) we have either $f(U_m) = q < f(U_\ell)$ and $v(U_r) > v(U_m)$ or $f(U_m) > q$ and $v(U_r) = v(U_m)$. In both cases it is easy to conclude.

This concludes the proof. \square

Finally, we accomplish the proof of Proposition 5.4 on the minimal invariant domains for \mathcal{CRS}_R . We remark that $(q/V, Q(q/V))$ is the point of intersection between the lines $\{U \in \Omega : f(U) = q\}$ and Ω_f : if $q \geq V\sigma_-$, this point belongs to the region Ω_c , otherwise it is in Ω_f^- .

Proof of Proposition 5.4. Let us first prove (ICR.1). The invariance of \mathcal{I}_f is an easy consequence of Definition 5.7, hence we are left to prove the minimality of \mathcal{I}_f . Let \mathcal{I} be an invariant domain for \mathcal{CRS}_R containing Ω_f . Then, \mathcal{I} has to contain

$$\mathcal{CRS}_R[\{(U_\ell, U_r) \in \Omega_f^2 : f(U_\ell) > q\}](\mathbb{R}) = \Omega_f \cup \{U \in \Omega_c : f(U) = q\} \cup \mathcal{I}_2.$$

As a consequence, \mathcal{I} has to contain also

$$\mathcal{CRS}_R[\{(U_\ell, U_r) \in \Omega_c^2 : f(U_\ell) = f(U_r) = q, v(U_\ell) > v(U_r)\}](\mathbb{R})$$

$$= \begin{cases} \mathcal{I}_1 & \text{if } q \leq V \sigma_-, \\ \{U \in \mathcal{I}_1 : f(\psi_1(U)) \geq q\} & \text{if } q > V \sigma_-. \end{cases}$$

Finally, if $q > V \sigma_-$, then \mathcal{I} has to contain also

$$\mathcal{CRS}_R[\{(U_\ell, U_r) \in \Omega_f^+ \times \Omega_c : f(U_\ell) \leq q = f(U_r)\}](\mathbb{R}) = \{U \in \mathcal{I}_1 : f(\psi_1(U)) \leq q\}.$$

In conclusion we proved that $\mathcal{I} \supseteq \mathcal{I}_f$.

Now, to prove (ICR.2) it is sufficient to observe that by Definition 5.7 we have that there exist $U_\ell, U_r \in \Omega_c$ such that the values attained by $\mathcal{CRS}_R[U_\ell, U_r]$ exit Ω_c if and only if $q < V \sigma_-$, and in this case

$$\begin{aligned} \mathcal{CRS}_R[\Omega_c^2](\mathbb{R}) \setminus \Omega_c &= \mathcal{CRS}_R[\{(U_\ell, U_r) \in \Omega_c^2 : f(\psi_2^-(U_r)) > q\}](\mathbb{R}) \setminus \Omega_c \\ &= \{(q/V, Q(q/V))\} \subset \Omega_f^-. \end{aligned}$$

This concludes the proof. □

A.5 Proof of Proposition 5.7

By construction, for any $t > 0$ sufficiently small $U_n(t, \cdot)$ belongs to the space $\mathbf{PC}(\mathbb{R}; \mathcal{G}_n)$, more precisely it is piecewise constant with jumps along a finite number of straight lines. If at time $t > 0$ an interaction occurs, namely two waves meet or a wave reaches $x = 0$, then the involved waves may change speed or strength, while new waves may be created. To prove that $U_n(t, \cdot)$ belongs to $\mathbf{PC}(\mathbb{R}; \mathcal{G}_n)$ we have to provide an a priori upper bound for the number of waves, which follows from **(a)**.

Clearly, if at time $t > 0$ no interaction occurs then $\mathcal{T}_n(t) = \mathcal{T}_n(t_+)$. For this reason we consider below all the possible interactions and distinguish the following main cases:

- a single wave reaches $x = 0$ and no NS is involved;
- a single wave reaches $x = 0$ and a NS is involved;
- two waves interact away from $x = 0$;

- two waves interact at $x = 0$ and no NS is involved;
- two waves interact at $x = 0$ and a NS is involved.

For completeness we estimate

$$\begin{aligned}\Delta\text{TV}_v &\doteq \text{TV}(v_n(t_+, \cdot)) - \text{TV}(v_n(t, \cdot)), & \Delta\hat{\Upsilon}_n &\doteq \hat{\Upsilon}_n(\mathbf{w}_n(t_+, \cdot)) - \hat{\Upsilon}_n(\mathbf{w}_n(t, \cdot)), \\ \Delta\text{TV}_w &\doteq \text{TV}(\mathbf{w}_n(t_+, \cdot)) - \text{TV}(\mathbf{w}_n(t, \cdot)), & \Delta\check{\Upsilon}_n &\doteq \check{\Upsilon}_n(v_n(t_+, \cdot)) - \check{\Upsilon}_n(v_n(t, \cdot)),\end{aligned}$$

and

$$\Delta\sharp \doteq \sharp(t_+) - \sharp(t_-), \quad \Delta\mathcal{T}_n \doteq \mathcal{T}_n(t_+) - \mathcal{T}_n(t_-).$$

For simplicity in the exposition, whenever a NS is involved we consider separately the cases $q \in [f^-, f^+)$ and $q \in [0, f^-)$. Notice that $\mathbf{w}^- > \mathbf{w}_q$ if and only if $q < f^-$, or equivalently $\mathbf{v}_{\max} \neq \mathbf{v}_q^+$. Notice also that if $q = f^+$ then $\mathcal{D}_2 = \emptyset$, while if $q = 0$ then $\mathcal{D}_1 = \emptyset$. At last, notice that if $q \in [f^-, f^+)$ and $(U_\ell, U_r) \in \mathcal{D}_2$, then $\hat{\mathbf{w}}_\ell = \mathbf{w}_\ell$ and $\check{\mathbf{v}}_r = v_r$.

In Table A.1 we collect the most relevant possible interactions considered in this section and list the corresponding possible results in terms of wave types, $\Delta\sharp$ and $\Delta\mathcal{T}_n$.

We start with the interaction estimates.

- If a wave (U_ℓ, U_r) reaches $x = 0$, $U_n(t, 0^-) = U_n(t, 0^+)$ and $(U_\ell, U_r) \in \mathcal{D}_1$, then the constraint has no influence on the wave and $0 = \Delta\text{TV}_v = \Delta\text{TV}_w = \Delta\sharp$. Since any CD has non-negative speed, we have that $\Delta\hat{\Upsilon}_n \leq 0$. Since any RS has negative speed, we have that $\Delta\check{\Upsilon}_n \leq 0$. As a consequence $\Delta\mathcal{T}_n \leq 0$.

- Assume that a wave (U_ℓ, U_r) reaches $x = 0$, $U_n(t, 0^-) = U_n(t, 0^+)$ and $(U_\ell, U_r) \in \mathcal{D}_2$.

If $q \in [f^-, f^+)$, then one of the following cases occurs:

CD_q⁺ (U_ℓ, U_r) is a CD. In this case $\hat{\mathbf{v}}_r \geq v_\ell = v_r = \check{\mathbf{v}}_r > \hat{\mathbf{v}}_\ell$, $\mathbf{w}_\ell = \hat{\mathbf{w}}_\ell > \check{\mathbf{w}}_r \geq \hat{\mathbf{w}}_r \geq \mathbf{w}_r$ and $f(U_\ell) > q \geq f(U_r)$. $\mathcal{CRS}_R^n[U_\ell, U_r]$ has at most three waves $(U_\ell, \hat{\mathbf{U}}_\ell)$, $(\hat{\mathbf{U}}_\ell, \check{\mathbf{U}}_r)$ and $(\check{\mathbf{U}}_r, U_r)$ that are a S, a NS and a possibly null CD, respectively. As a

Interaction	Result	$\Delta\sharp$	$\Delta\mathcal{T}_n$
CD_q^+	(S,NS,CD), (S,NS)	$\in \{1, 2\}$	< 0
RS_q^+	(NS,CD)	$= 1$	< 0
CD_q^-	(S,NS,CD), (S,NS), (PT,NS,CD), (PT,NS)	$\in \{1, 2\}$	< 0
RS_q^-	(NS,PT), (NS,CD)	$= 1$	< 0
CD-S	(S,CD), (PT,CD), PT	≤ 0	$= 0$
CD-RS	(RS,CD)	$= 0$	$= 0$
CD-PT	(PT,CD), PT, (S,CD), S	≤ 0	≤ 0
S-S	S	< 0	$= 0$
S-RS	S	< 0	< 0
RS-S	S	< 0	< 0
PT-S	PT	< 0	$= 0$
PT-RS	PT, CD	< 0	< 0
CD-S ₀	(S,CD), (PT,CD), PT	≤ 0	≤ 0
CD-RS ₀	(RS,CD)	$= 0$	≤ 0
CD-NS ₀	(RSs,CD), RSs	$\in [-1, 2^n - 1]$	< 0
CD-PT ₀	(PT,CD), PT, (S,CD), S	≤ 0	≤ 0
S-S ₀	S	< 0	$= 0$
S-RS ₀	S	< 0	< 0
RS-S ₀	S	< 0	< 0
NS-S ₀	(S,CD), CD	≤ 0	< 0
NS-PT ₀	(S,CD), S, CD	≤ 0	< 0
PT-S ₀	PT	< 0	$= 0$
PT-RS ₀	PT, CD	< 0	< 0
PT-NS ₀	CD, PT	< 0	< 0
CD-S _{q}^+}	(S,NS,CD)	$= 1$	< 0
CD-RS _{q}^+}	(S,NS,CD), (NS,CD), (S,NS), NS	$\in \{-1, 0, 1\}$	< 0
CD-NS _{q}^+}	(RSs,NS), (S,NS)	$\in [0, 2^n - 2]$	< 0
CD-PT _{q}^+}	(S,NS,CD)	$= 1$	< 0
NS-S _{q}^+}	(NS,CD)	$= 0$	< 0
NS-RS _{q}^+}	(NS,CD)	$= 0$	< 0
CD-S _{q}^-}	(S,NS,CD)	$= 1$	< 0
CD-RS _{q}^-}	(S,NS,CD), (S,NS,PT), (NS,CD), (NS,PT), (S,NS), NS	$\in \{-1, 0, 1\}$	< 0
CD-NS _{q}^-}	(RSs,NS), (S,NS)	$\in [0, 2^n - 2]$	< 0
CD-PT _{q}^-}	(S,NS,CD), (S,NS)	$\in \{0, 1\}$	< 0
NS-S _{q}^-}	(NS,CD)	$= 0$	< 0
NS-RS _{q}^-}	(NS,PT), (NS,CD)	$= 0$	< 0
NS-PT _{q}^-}	(NS,CD)	$= 0$	< 0

Table A.1: Overview of the interactions considered in the proof of Proposition 5.7.

consequence

$$\Delta TV_v = 2(v_\ell - \hat{v}_\ell) > 0,$$

$$\Delta TV_w = 0,$$

$$\Delta \hat{Y}_n = -[\hat{v}_r - \hat{v}_\ell]_+ - [\hat{w}_\ell - \hat{w}_r]_+ < -(\hat{v}_r - \hat{v}_\ell) < 0,$$

$$\Delta \tilde{Y}_n = 0,$$

therefore $\Delta\sharp \in \{1, 2\}$ and $\Delta\mathcal{T}_n < -2(\hat{v}_r - v_\ell) \leq 0$.

\mathbf{RS}_q^+ (U_ℓ, U_r) is a RS. In this case $v_\ell = \check{v}_\ell < v_r = \check{v}_r$, $\check{w}_r < w_\ell = \check{w}_\ell = w_r$, $f(U_\ell) = q < f(U_r)$ and $U_\ell, U_r \in \Omega_c$. $\mathcal{CRS}_R^n[U_\ell, U_r]$ has two waves (U_ℓ, \check{U}_r) and (\check{U}_r, U_r) that are a NS and a CD, respectively. As a consequence

$$\begin{aligned}\Delta\text{TV}_v &= 0, \\ \Delta\text{TV}_w &= 2(w_\ell - \check{w}_r) > 0, \\ \Delta\hat{Y}_n &= 0, \\ \Delta\check{Y}_n &= -[\check{v}_r - \check{v}_\ell]_+ - [\check{w}_\ell - \check{w}_r]_+ = -(v_r - v_\ell) - (w_\ell - \check{w}_r) < 0,\end{aligned}$$

therefore $\Delta\sharp = 1$ and $\Delta\mathcal{T}_n = -2(v_r - v_\ell) < 0$.

If $q \in [0, f^-)$, then one of the following cases occurs:

\mathbf{CD}_q^- (U_ℓ, U_r) is a CD. In this case $\hat{v}_r \geq v_\ell = v_r = \check{v}_r > \hat{v}_\ell$, $\hat{w}_\ell \geq w_\ell > \check{w}_r \geq \hat{w}_r \geq w_r$ and $f(U_\ell) > q \geq f(U_r)$. $\mathcal{CRS}_R^n[U_\ell, U_r]$ has at most three waves (U_ℓ, \hat{U}_ℓ) , $(\hat{U}_\ell, \check{U}_r)$ and (\check{U}_r, U_r) that are a S or a PT, a NS and a possibly null CD, respectively. As a consequence

$$\begin{aligned}\Delta\text{TV}_v &= 2(v_\ell - \hat{v}_\ell) > 0, \\ \Delta\text{TV}_w &= 2(\hat{w}_\ell - w_\ell) \geq 0, \\ \Delta\hat{Y}_n &= -[\hat{v}_r - \hat{v}_\ell]_+ - [\hat{w}_\ell - \hat{w}_r]_+ = -(\hat{v}_r - \hat{v}_\ell) - (\hat{w}_\ell - \hat{w}_r) < 0, \\ \Delta\check{Y}_n &= 0,\end{aligned}$$

therefore $\Delta\sharp \in \{1, 2\}$ and $\Delta\mathcal{T}_n = -2(\hat{v}_r - v_\ell) - 2(w_\ell - \hat{w}_r) < 0$.

\mathbf{RS}_q^- (U_ℓ, U_r) is a RS. In this case $v_\ell < v_r \leq \check{v}_r$, $w_q \leq \check{w}_r < w_r = w_\ell = \check{w}_\ell$, $f(U_\ell) = q < f(U_r)$ and $U_\ell, U_r \in \Omega_c$. $\mathcal{CRS}_R^n[U_\ell, U_r]$ has two waves (U_ℓ, \check{U}_r) and (\check{U}_r, U_r) that are a NS and a PT or a CD, respectively. As a consequence

$$\begin{aligned}\Delta\text{TV}_v &= 2(\check{v}_r - v_r) \geq 0, \\ \Delta\text{TV}_w &= 2(w_\ell - \check{w}_r) > 0, \\ \Delta\hat{Y}_n &= 0, \\ \Delta\check{Y}_n &= -[\check{v}_r - \check{v}_\ell]_+ - [\check{w}_\ell - \check{w}_r]_+ = -(\check{v}_r - v_\ell) - (w_\ell - \check{w}_r) < 0,\end{aligned}$$

therefore $\Delta\sharp = 1$ and $\Delta\mathcal{T}_n = -2(v_r - v_\ell) < 0$. Notice that $\check{v}_r > v_r$ if and only if $\mathbf{w}_\ell = \mathbf{w}_r = \mathbf{w}^-$ and $v_r > v_\ell = \mathbf{v}_q^+$.

Assume that two waves (U_ℓ, U_m) and (U_m, U_r) interact at time $t > 0$. Let $\mathbf{U}_* \doteq \mathbf{U}_*(U_\ell, U_r)$. Notice that $\mathbf{U}_* = U_r$ if and only if (U_ℓ, U_m) is a S or a RS, while $\mathbf{U}_* = U_\ell$ if and only if (U_ℓ, U_m) is a CD.

- If the interaction occurs at $x \neq 0$, then one of the following cases occurs:

CD-S (U_ℓ, U_m) is a CD and (U_m, U_r) is a S. In this case $v_\ell = v_m > v_r = v_*$, $\mathbf{w}_m = \mathbf{w}_r$, \mathbf{w}_* belongs to the closed interval between \mathbf{w}_ℓ and \mathbf{w}_r , $\mathbf{W}(U_\ell) = \mathbf{W}(\mathbf{U}_*)$, $\mathbf{w}_m = \mathbf{w}_r$, $f(U_m) > f(U_r)$ and $U_m, U_r \in \Omega_c$. $\mathcal{RS}_R^n[U_\ell, U_r]$ has at most two waves (U_ℓ, \mathbf{U}_*) and (\mathbf{U}_*, U_r) that are respectively either a S and a CD, or a PT and a possibly null CD. As a consequence $0 = \Delta\text{TV}_v = \Delta\text{TV}_w = \Delta\hat{\Upsilon}_n = \Delta\check{\Upsilon}_n$, therefore $\Delta\sharp \leq 0$ and $\Delta\mathcal{T}_n = 0$.

CD-RS (U_ℓ, U_m) is a CD and (U_m, U_r) is a RS. In this case $v_\ell = v_m < v_r = v_*$, $\mathbf{w}_\ell = \mathbf{w}_*$, $\mathbf{w}_m = \mathbf{w}_r$, $f(U_\ell) < f(\mathbf{U}_*)$, $f(U_m) < f(U_r)$ and $U_\ell, U_m, \mathbf{U}_*, U_r \in \Omega_c$. $\mathcal{RS}_R^n[U_\ell, U_r]$ has two waves (U_ℓ, \mathbf{U}_*) and (\mathbf{U}_*, U_r) that are a RS and a CD, respectively. As a consequence $0 = \Delta\text{TV}_v = \Delta\text{TV}_w = \Delta\hat{\Upsilon}_n = \Delta\check{\Upsilon}_n$, therefore $\Delta\sharp = 0$ and $\Delta\mathcal{T}_n = 0$.

CD-PT (U_ℓ, U_m) is a CD and (U_m, U_r) is a PT. In this case $v_\ell = v_m = \mathbf{v}_{\max} > v_r = v_*$, $\mathbf{w}_m < \mathbf{w}^- \leq \mathbf{w}_r$, \mathbf{w}_* belongs to the closed interval between \mathbf{w}_ℓ and \mathbf{w}_r , $U_\ell \in \Omega_f$, $U_m \in \Omega_f^-$ and $\mathbf{U}_*, U_r \in \Omega_c$. $\mathcal{RS}_R^n[U_\ell, U_r]$ has at most two waves (U_ℓ, \mathbf{U}_*) and (\mathbf{U}_*, U_r) that are either a PT or a S and a possibly null CD, respectively. As a consequence

$$\begin{aligned} \Delta\text{TV}_v &= 0, & \Delta\hat{\Upsilon}_n &\leq 0, \\ \Delta\text{TV}_w &= |\mathbf{w}_\ell - \mathbf{w}_r| - (|\mathbf{w}_\ell - \mathbf{w}_m| + |\mathbf{w}_m - \mathbf{w}_r|) \leq 0, & \Delta\check{\Upsilon}_n &= 0, \end{aligned}$$

therefore $\Delta\sharp \leq 0$ and $\Delta\mathcal{T}_n \leq 0$.

S-S (U_ℓ, U_m) and (U_m, U_r) are Ss. In this case $v_\ell > v_m > v_r$, $\mathbf{w}_\ell = \mathbf{w}_m = \mathbf{w}_r \geq \mathbf{w}^-$ and $U_\ell, U_m, U_r \in \Omega_c$. $\mathcal{RS}_R^n[U_\ell, U_r]$ has one wave (U_ℓ, U_r) , which is a S. As a consequence $0 = \Delta\text{TV}_v = \Delta\text{TV}_w = \Delta\hat{\Upsilon}_n = \Delta\check{\Upsilon}_n$, therefore $\Delta\sharp = -1$ and $\Delta\mathcal{T}_n = 0$.

S-RS (U_ℓ, U_m) is a S and (U_m, U_r) is a RS. In this case $v_\ell > v_r > v_m$, $\mathbf{w}_\ell = \mathbf{w}_m = \mathbf{w}_r \geq \mathbf{w}^-$ and $U_\ell, U_m, U_r \in \Omega_c$. $\mathcal{RS}_R^n[U_\ell, U_r]$ has one wave (U_ℓ, U_r) , which is a S. As a consequence

$$\begin{aligned}\Delta\text{TV}_v &= -2(v_r - v_m) < 0, & \Delta\hat{\mathbf{Y}}_n &= 0, \\ \Delta\text{TV}_w &= 0, & \Delta\check{\mathbf{Y}}_n &\leq 0,\end{aligned}$$

therefore $\Delta\sharp = -1$ and $\Delta\mathcal{T}_n < 0$.

RS-S (U_ℓ, U_m) is a RS and (U_m, U_r) is a S. In this case $v_m > v_\ell > v_r$, $\mathbf{w}_\ell = \mathbf{w}_m = \mathbf{w}_r \geq \mathbf{w}^-$ and $U_\ell, U_m, U_r \in \Omega_c$. $\mathcal{RS}_R^n[U_\ell, U_r]$ has one wave (U_ℓ, U_r) , which is a S. As a consequence

$$\begin{aligned}\Delta\text{TV}_v &= -2(v_m - v_\ell) < 0, & \Delta\hat{\mathbf{Y}}_n &= 0, \\ \Delta\text{TV}_w &= 0, & \Delta\check{\mathbf{Y}}_n &\leq 0,\end{aligned}$$

therefore $\Delta\sharp = -1$ and $\Delta\mathcal{T}_n < 0$.

PT-S (U_ℓ, U_m) is a PT and (U_m, U_r) is a S. In this case $v_\ell = \mathbf{v}_{\max} > v_m > v_r$, $\mathbf{w}_\ell < \mathbf{w}^- \leq \mathbf{w}_m = \mathbf{w}_r$, $U_\ell \in \Omega_f^-$ and $U_m, U_r \in \Omega_c$. $\mathcal{RS}_R^n[U_\ell, U_r]$ has one wave (U_ℓ, U_r) , which is a PT. As a consequence $0 = \Delta\text{TV}_v = \Delta\text{TV}_w = \Delta\hat{\mathbf{Y}}_n = \Delta\check{\mathbf{Y}}_n$, therefore $\Delta\sharp = -1$ and $\Delta\mathcal{T}_n = 0$.

PT-RS (U_ℓ, U_m) is a PT and (U_m, U_r) is a RS. In this case $v_\ell = \mathbf{v}_{\max} \geq v_r > v_m$, $\mathbf{w}_\ell < \mathbf{w}^- \leq \mathbf{w}_m = \mathbf{w}_r$, $U_\ell \in \Omega_f^-$ and $U_m, U_r \in \Omega_c$. $\mathcal{RS}_R^n[U_\ell, U_r]$ has one wave (U_ℓ, U_r) , which is either a PT or a CD. As a consequence

$$\begin{aligned}\Delta\text{TV}_v &= -2(v_r - v_m) < 0, & \Delta\hat{\mathbf{Y}}_n &= 0, \\ \Delta\text{TV}_w &= 0, & \Delta\check{\mathbf{Y}}_n &\leq 0,\end{aligned}$$

therefore $\Delta\sharp = -1$ and $\Delta\mathcal{T}_n < 0$.

- If the interaction occurs at $x = 0$ and $(U_\ell, U_r) \in \mathcal{D}_1$, then one of the following cases occurs:

CD-S₀ (U_ℓ, U_m) is a CD and (U_m, U_r) is a S. In this case $v_\ell = v_m > v_r = v_*$, $\mathbf{w}_m = \mathbf{w}_r, \mathbf{w}_*$ belongs to the closed interval between \mathbf{w}_ℓ and \mathbf{w}_r , $\mathbf{W}(U_\ell) = \mathbf{W}(U_*)$, $\mathbf{w}_m = \mathbf{w}_r$,

$f(U_r) < (U_m) \leq q$, $\min\{f(U_\ell), f(\mathbf{U}_*)\} \leq q$ and $U_m, U_r \in \Omega_c$. $\mathcal{CRS}_R^n[U_\ell, U_r]$ has at most two waves (U_ℓ, \mathbf{U}_*) and (\mathbf{U}_*, U_r) that are respectively either a S and a CD, or a PT and a possibly null CD. As a consequence $\Delta\hat{\Upsilon}_n \leq 0 = \Delta\text{TV}_v = \Delta\text{TV}_w = \Delta\check{\Upsilon}_n$, therefore $\Delta\sharp \leq 0$ and $\Delta\mathcal{T}_n \leq 0$.

CD-RS₀ (U_ℓ, U_m) is a CD and (U_m, U_r) is a RS. In this case $v_\ell = v_m < v_r$, $\mathbf{w}_m = \mathbf{w}_r$, $\mathbf{w}_* = \mathbf{w}_\ell$, $f(U_\ell) < f(\mathbf{U}_*)$, $f(U_m) < f(U_r)$, $\max\{f(U_m), f(\mathbf{U}_*)\} \leq q$ and $U_\ell, U_m, \mathbf{U}_*, U_r \in \Omega_c$. $\mathcal{CRS}_R^n[U_\ell, U_r]$ has two waves (U_ℓ, \mathbf{U}_*) and (\mathbf{U}_*, U_r) that are a RS and a CD, respectively. As a consequence

$$\begin{aligned} \Delta\text{TV}_v &= 0, & \Delta\hat{\Upsilon}_n &\leq 0, \\ \Delta\text{TV}_w &= 0, & \Delta\check{\Upsilon}_n &\leq 0, \end{aligned}$$

therefore $\Delta\sharp = 0$ and $\Delta\mathcal{T}_n \leq 0$.

CD-NS₀ (U_ℓ, U_m) is a CD and (U_m, U_r) is a NS. In this case $\mathbf{v}_q^- \leq v_\ell = v_m < v_r \leq \mathbf{v}_q^+$, $\mathbf{w}^- \leq \mathbf{w}_\ell \leq \mathbf{w}_r < \mathbf{w}_m$, $f(U_\ell) < f(\mathbf{U}_*) \leq q = f(U_m) = f(U_r)$ and $U_\ell, U_m, \mathbf{U}_*, U_r \in \Omega_c$. $\mathcal{CRS}_R^n[U_\ell, U_r]$ has a fan of RSs ranging from U_ℓ to \mathbf{U}_* and a possibly null CD (\mathbf{U}_*, U_r) . As a consequence $\Delta\text{TV}_w = -2(\mathbf{w}_m - \mathbf{w}_r) < 0 = \Delta\text{TV}_v = \Delta\hat{\Upsilon}_n = \Delta\check{\Upsilon}_n$, therefore $\Delta\sharp \in [-1, 2^n - 1]$ and $\Delta\mathcal{T}_n < 0$.

CD-PT₀ (U_ℓ, U_m) is a CD and (U_m, U_r) is a PT. In this case $v_\ell = v_m = \mathbf{v}_{\max} > v_r = v_*$, $\mathbf{w}_m < \mathbf{w}^- \leq \mathbf{w}_r$, \mathbf{w}_* belongs to the closed interval between \mathbf{w}_ℓ and \mathbf{w}_r , $\min\{f(U_\ell), f(\mathbf{U}_*)\} \leq q$, $\max\{f(U_m), f(U_r)\} \leq q$, $U_\ell \in \Omega_f$, $U_m \in \Omega_f^-$ and $\mathbf{U}_*, U_r \in \Omega_c$. $\mathcal{CRS}_R^n[U_\ell, U_r]$ has at most two waves (U_ℓ, \mathbf{U}_*) and (\mathbf{U}_*, U_r) that are either a PT or a S and a possibly null CD, respectively. As a consequence

$$\begin{aligned} \Delta\text{TV}_v &= 0, & \Delta\hat{\Upsilon}_n &\leq 0, \\ \Delta\text{TV}_w &= |\mathbf{w}_\ell - \mathbf{w}_r| - (|\mathbf{w}_\ell - \mathbf{w}_m| + |\mathbf{w}_m - \mathbf{w}_r|) \leq 0, & \Delta\check{\Upsilon}_n &= 0, \end{aligned}$$

therefore $\Delta\sharp \in \{-1, 0\}$ and $\Delta\mathcal{T}_n \leq 0$.

S-S₀ (U_ℓ, U_m) and (U_m, U_r) are Ss. In this case $v_\ell > v_m > v_r$, $\mathbf{w}_\ell = \mathbf{w}_m = \mathbf{w}_r \geq \mathbf{w}^-$, $f(U_r) < f(U_\ell) \leq q$ and $U_\ell, U_m, U_r \in \Omega_c$. $\mathcal{CRS}_R^n[U_\ell, U_r]$ has one wave (U_ℓ, U_r) , which is a S. As a consequence $0 = \Delta\text{TV}_v = \Delta\text{TV}_w = \Delta\hat{\Upsilon}_n = \Delta\check{\Upsilon}_n$, therefore $\Delta\sharp = -1$ and $\Delta\mathcal{T}_n = 0$.

S-RS₀ (U_ℓ, U_m) is a S and (U_m, U_r) is a RS. In this case $v_\ell > v_r > v_m$, $\mathbf{w}_\ell = \mathbf{w}_m =$

$\mathbf{w}_r \geq \mathbf{w}^-$, $f(U_r) < f(U_\ell) \leq q$ and $U_\ell, U_m, U_r \in \Omega_c$. $\mathcal{CRS}_R^n[U_\ell, U_r]$ has one wave (U_ℓ, U_r) , which is a S. As a consequence

$$\begin{aligned} \Delta \text{TV}_v &= -2(v_r - v_m) < 0, & \Delta \hat{\Upsilon}_n &= 0, \\ \Delta \text{TV}_w &= 0, & \Delta \check{\Upsilon}_n &\leq 0, \end{aligned}$$

therefore $\Delta \sharp = -1$ and $\Delta \mathcal{T}_n < 0$.

RS-S₀ (U_ℓ, U_m) is a RS and (U_m, U_r) is a S. In this case $v_m > v_\ell > v_r$, $\mathbf{w}_\ell = \mathbf{w}_m = \mathbf{w}_r \geq \mathbf{w}^-$, $f(U_r) < f(U_\ell) \leq q$ and $U_\ell, U_m, U_r \in \Omega_c$. $\mathcal{CRS}_R^n[U_\ell, U_r]$ has one wave (U_ℓ, U_r) , which is a S. As a consequence

$$\begin{aligned} \Delta \text{TV}_v &= -2(v_m - v_\ell) < 0, & \Delta \hat{\Upsilon}_n &= 0, \\ \Delta \text{TV}_w &= 0, & \Delta \check{\Upsilon}_n &\leq 0, \end{aligned}$$

therefore $\Delta \sharp = -1$ and $\Delta \mathcal{T}_n < 0$.

NS-S₀ (U_ℓ, U_m) is a NS and (U_m, U_r) is a S. In this case $v_m > v_\ell \geq v_r = v_*$, $\mathbf{w}_* = \mathbf{w}_\ell > \mathbf{w}_m = \mathbf{w}_r \geq \mathbf{w}^-$, $f(U_\ell) = f(U_m) = q > f(U_r)$ and $U_\ell, U_m, U_r \in \Omega_c$. $\mathcal{CRS}_R^n[U_\ell, U_r]$ has at most two waves (U_ℓ, \mathbf{U}_*) and (\mathbf{U}_*, U_r) that are a possibly null S and CD, respectively. As a consequence $\Delta \text{TV}_v = -2(v_m - v_\ell) < 0 = \Delta \text{TV}_w = \Delta \hat{\Upsilon}_n = \Delta \check{\Upsilon}_n$, therefore $\Delta \sharp \in \{-1, 0\}$ and $\Delta \mathcal{T}_n < 0$.

NS-PT₀ (U_ℓ, U_m) is a NS and (U_m, U_r) is a PT. In this case $v_m = \mathbf{v}_{\max} > v_\ell \geq v_r = v_*$, $\mathbf{w}_\ell = \mathbf{w}_* \geq \mathbf{w}_r = \mathbf{w}^- > \mathbf{w}_m$, $f^- > f(U_\ell) = f(U_m) = q > f(U_r)$, $f(\mathbf{U}_*) \leq q$, $U_\ell, U_r \in \Omega_c$ and $U_m \in \Omega_f^-$. $\mathcal{CRS}_R^n[U_\ell, U_r]$ has at most two waves (U_ℓ, \mathbf{U}_*) and (\mathbf{U}_*, U_r) that are a possibly null S and a possibly null CD (but not both null), respectively. As a consequence

$$\begin{aligned} \Delta \text{TV}_v &= -2(\mathbf{v}_{\max} - v_\ell) < 0, & \Delta \hat{\Upsilon}_n &= 0, \\ \Delta \text{TV}_w &= -2(\mathbf{w}^- - \mathbf{w}_m) < 0, & \Delta \check{\Upsilon}_n &= 0, \end{aligned}$$

therefore $\Delta \sharp \in \{-1, 0\}$ and $\Delta \mathcal{T}_n < 0$.

PT-S₀ (U_ℓ, U_m) is a PT and (U_m, U_r) is a S. In this case $v_\ell = \mathbf{v}_{\max} > v_m > v_r$, $\mathbf{w}_\ell < \mathbf{w}^- \leq \mathbf{w}_m = \mathbf{w}_r$, $f(U_r) < f(U_m) \leq \max\{f(U_\ell), f(U_m)\} \leq q$, $U_\ell \in \Omega_f^-$ and $U_m, U_r \in \Omega_c^-$. $\mathcal{CRS}_R^n[U_\ell, U_r]$ has one wave (U_ℓ, U_r) , which is a PT. As a

consequence $0 = \Delta TV_v = \Delta TV_w = \Delta \hat{Y}_n = \Delta \check{Y}_n$, therefore $\Delta \sharp = -1$ and $\Delta \mathcal{T}_n = 0$.

PT-RS₀ (U_ℓ, U_m) is a PT and (U_m, U_r) is a RS. In this case $v_\ell = v_{\max} \geq v_r > v_m$, $w_\ell < w^- \leq w_m = w_r$, $U_\ell \in \Omega_f^-$ and $U_m, U_r \in \Omega_c$. $\mathcal{CRS}_R^n[U_\ell, U_r]$ has one wave (U_ℓ, U_r) , which is either a PT or a CD. As a consequence

$$\begin{aligned} \Delta TV_v &= -2(v_r - v_m) < 0, & \Delta \hat{Y}_n &= 0, \\ \Delta TV_w &= 0, & \Delta \check{Y}_n &\leq 0, \end{aligned}$$

therefore $\Delta \sharp = -1$ and $\Delta \mathcal{T}_n < 0$.

PT-NS₀ (U_ℓ, U_m) is a PT and (U_m, U_r) is a NS. In this case $v_\ell = v_{\max} \geq v_r > v_m$, $w_\ell < w^- \leq w_r < w_m$, $f(U_\ell) < f(U_m) = f(U_r) = q$, $U_\ell \in \Omega_f^-$ and $U_m, U_r \in \Omega_c$. $\mathcal{CRS}_R^n[U_\ell, U_r]$ has one wave (U_ℓ, U_r) , which is either a CD or a PT. As a consequence

$$\begin{aligned} \Delta TV_v &= -2(v_r - v_m) < 0, & \Delta \hat{Y}_n &= 0, \\ \Delta TV_w &= -2(w_m - w_r) < 0, & \Delta \check{Y}_n &= 0, \end{aligned}$$

therefore $\Delta \sharp = -1$ and $\Delta \mathcal{T}_n < 0$.

- Assume that two waves (U_ℓ, U_m) and (U_m, U_r) interact at $x = 0$ and $(U_\ell, U_r) \in \mathcal{D}_2$.

If $q \in [f^-, f^+)$, then one of the following cases occurs:

CD-S_q⁺ (U_ℓ, U_m) is a CD and (U_m, U_r) is a S. In this case $\hat{v}_r \geq v_\ell = v_m > v_r = \check{v}_r > \hat{v}_\ell$, $w_\ell = \hat{w}_\ell > \check{w}_r > w_m = w_r$, $w_\ell > \hat{w}_r$, $f(U_\ell) > f(\mathbf{U}_*) > q \geq f(U_m) > f(U_r)$ and $U_\ell, U_m, U_r \in \Omega_c$. $\mathcal{CRS}_R^n[U_\ell, U_r]$ has three waves (U_ℓ, \hat{U}_ℓ) , $(\hat{U}_\ell, \check{U}_r)$ and (\check{U}_r, U_r) , which are a S, a NS and a CD, respectively. As a consequence

$$\begin{aligned} \Delta TV_v &= 2(v_r - \hat{v}_\ell) > 0, & \Delta \hat{Y}_n &= -(\hat{v}_m - \hat{v}_\ell) - (w_\ell - \hat{w}_m) < 0, \\ \Delta TV_w &= 0, & \Delta \check{Y}_n &= 0, \end{aligned}$$

therefore $\Delta \sharp = 1$ and $\Delta \mathcal{T}_n = -2(\hat{v}_r - v_r) - 2(w_\ell - \hat{w}_r) < 0$.

CD-RS_q⁺ (U_ℓ, U_m) is a CD and (U_m, U_r) is a RS. In this case $\hat{v}_\ell \leq v_\ell = v_m = \check{v}_m < v_r = \check{v}_r$, $\hat{v}_\ell < \hat{v}_m$, $\mathbf{w}_\ell = \hat{\mathbf{w}}_\ell > \hat{\mathbf{w}}_m \geq \mathbf{w}_m = \mathbf{w}_r$, $\check{\mathbf{w}}_r < \check{\mathbf{w}}_m$, $f(U_m) < f(U_r) \leq f(U_\ell) < f(\mathbf{U}_*)$, $f(U_m) \leq q < f(\mathbf{U}_*)$ and $U_\ell, U_m, U_r \in \Omega_c$. $\mathcal{CRS}_R^n[U_\ell, U_r]$ has at most three waves (U_ℓ, \hat{U}_ℓ), ($\hat{U}_\ell, \check{U}_r$) and (\check{U}_r, U_r), which are a possibly null S, a NS and a possibly null CD, respectively. As a consequence

$$\begin{aligned}\Delta TV_v &= 2(v_\ell - \hat{v}_\ell) \geq 0, \\ \Delta TV_w &= \begin{cases} 2(\mathbf{w}_r - \check{\mathbf{w}}_r) & \text{if } f(U_m) = q \\ 0 & \text{if } f(U_m) < q \end{cases} \geq 0, \\ \Delta \hat{Y}_n &= -(\hat{v}_m - \hat{v}_\ell) - (\hat{\mathbf{w}}_\ell - \hat{\mathbf{w}}_m) < -(\hat{v}_m - \hat{v}_\ell) < 0, \\ \Delta \check{Y}_n &= -(v_r - v_m) - (\check{\mathbf{w}}_m - \check{\mathbf{w}}_r) < -(\check{\mathbf{w}}_m - \check{\mathbf{w}}_r) < 0,\end{aligned}$$

and therefore

$$\Delta \# \in \{-1, 0, 1\}, \quad \Delta \mathcal{T}_n < -2(\hat{v}_m - v_\ell) + \begin{cases} 0 & \text{if } f(U_m) = q \\ -2(\check{\mathbf{w}}_m - \check{\mathbf{w}}_r) & \text{if } f(U_m) < q \end{cases} \leq 0.$$

CD-NS_q⁺ (U_ℓ, U_m) is a CD and (U_m, U_r) is a NS. In this case $v_\ell = v_m < v_r$, $\mathbf{w}_r < \min\{\mathbf{w}_\ell, \mathbf{w}_m\}$, $\mathbf{w}_\ell \neq \mathbf{w}_m$, $f(U_m) = f(U_r) = q \neq f(U_\ell)$ and $U_\ell, U_m, U_r \in \Omega_c$.

If $f(U_\ell) < q$, then $\mathcal{CRS}_R^n[U_\ell, U_r]$ has a fan of RSs from U_ℓ to \hat{U}_ℓ and a NS (\hat{U}_ℓ, U_r); as a consequence $\Delta TV_w = -2(\mathbf{w}_m - \mathbf{w}_\ell) < 0 = \Delta TV_v = \Delta \hat{Y}_n = \Delta \check{Y}_n$, therefore $\Delta \# \in [0, 2^n - 2]$ and $\Delta \mathcal{T}_n = -2(\mathbf{w}_m - \mathbf{w}_\ell) < 0$.

If $f(U_\ell) > q$, then $\hat{v}_\ell < v_\ell = v_m = \hat{v}_m$, $\hat{\mathbf{w}}_\ell = \mathbf{w}_\ell > \mathbf{w}_m = \hat{\mathbf{w}}_m$, $\mathcal{CRS}_R^n[U_\ell, U_r]$ has a two waves (U_ℓ, \hat{U}_ℓ) and (\hat{U}_ℓ, U_r), that are a S and a NS, respectively; as a consequence

$$\begin{aligned}\Delta TV_v &= 2(v_\ell - \hat{v}_\ell) > 0, & \Delta \hat{Y}_n &= -(v_\ell - \hat{v}_\ell) - (\mathbf{w}_\ell - \mathbf{w}_m) < 0, \\ \Delta TV_w &= 0, & \Delta \check{Y}_n &= 0,\end{aligned}$$

therefore $\Delta \# = 0$ and $\Delta \mathcal{T}_n = -2(\mathbf{w}_\ell - \mathbf{w}_m) < 0$.

CD-PT_q⁺ (U_ℓ, U_m) is a CD and (U_m, U_r) is a PT. In this case $\mathbf{w}_m < \mathbf{w}^- \leq \mathbf{w}_q = \hat{\mathbf{w}}_m < \mathbf{w}_\ell$, $v_\ell = v_m = \hat{v}_m = \mathbf{v}_{\max} > v_r = \check{v}_r > \hat{v}_\ell$, $\mathbf{w}_m < \mathbf{w}^- \leq \mathbf{w}_r < \check{\mathbf{w}}_r < \mathbf{w}_\ell = \hat{\mathbf{w}}_\ell$, $f(U_\ell) > f(\mathbf{U}_*) > q \geq \max\{f(U_m), f(U_r)\}$, $U_\ell \in \Omega_f^+$, $U_m \in \Omega_f^-$ and $U_r \in \Omega_c$.

$\mathcal{CRS}_R^n[U_\ell, U_r]$ has three waves (U_ℓ, \hat{U}_ℓ) , $(\hat{U}_\ell, \check{U}_r)$ and (\check{U}_r, U_r) that are a S, a NS and a CD, respectively. As a consequence

$$\begin{aligned}\Delta TV_v &= 2(v_r - \hat{v}_\ell) > 0, & \Delta \hat{Y}_n &= -(v_{\max} - \hat{v}_\ell) - (\mathbf{w}_\ell - \mathbf{w}_q) < 0, \\ \Delta TV_w &= -2(\mathbf{w}_r - \mathbf{w}_m) < 0, & \Delta \check{Y}_n &= 0,\end{aligned}$$

therefore $\Delta \sharp = 1$ and $\Delta \mathcal{T}_n < -2(v_{\max} - v_r) - 2(\mathbf{w}_\ell - \mathbf{w}_q) < 0$.

NS-S_q⁺ (U_ℓ, U_m) is a NS and (U_m, U_r) is a S. In this case $v_m > v_r = \check{v}_r > v_\ell$, $\mathbf{w}_\ell > \check{\mathbf{w}}_r > \mathbf{w}_m = \mathbf{w}_r \geq \mathbf{w}_q \geq \mathbf{w}^-$, $f(\mathbf{u}_*) > q = f(U_\ell) = f(U_m) > f(U_r)$ and $U_\ell, U_m, U_r \in \Omega_c$. $\mathcal{CRS}_R^n[U_\ell, U_r]$ has two waves (U_ℓ, \check{U}_r) and (\check{U}_r, U_r) that are a NS and a CD, respectively. As a consequence $\Delta TV_v = -2(v_m - v_r) < 0 = \Delta TV_w = \Delta \hat{Y}_n = \Delta \check{Y}_n$, therefore $\Delta \sharp = 0$ and $\Delta \mathcal{T}_n = -2(v_m - v_r) < 0$.

NS-RS_q⁺ (U_ℓ, U_m) is a NS and (U_m, U_r) is a RS. In this case $v_\ell < v_m = \check{v}_m < v_r = \check{v}_r$, $\mathbf{w}_\ell > \mathbf{w}_m = \check{\mathbf{w}}_m = \mathbf{w}_r > \check{\mathbf{w}}_r$, $f(\mathbf{u}_*) > f(U_r) > q = f(U_\ell) = f(U_m)$ and $U_\ell, U_m, U_r \in \Omega_c$. $\mathcal{CRS}_R^n[U_\ell, U_r]$ has two waves (U_ℓ, \check{U}_r) and (\check{U}_r, U_r) that are a NS and a CD, respectively. As a consequence

$$\begin{aligned}\Delta TV_v &= 0, & \Delta \hat{Y}_n &= 0, \\ \Delta TV_w &= 2(\mathbf{w}_r - \check{\mathbf{w}}_r) > 0, & \Delta \check{Y}_n &= -(v_r - v_m) - (\mathbf{w}_r - \check{\mathbf{w}}_r) < 0,\end{aligned}$$

therefore $\Delta \sharp = 0$ and $\Delta \mathcal{T}_n = -2(v_r - v_m) < 0$.

If $q \in [0, f^-)$, then one of the following cases occurs:

CD-S_q⁻ (U_ℓ, U_m) is a CD and (U_m, U_r) is a S. In this case $\hat{v}_m \geq v_\ell = v_m > v_r = \check{v}_r > \hat{v}_\ell$, $\mathbf{w}_\ell = \hat{\mathbf{w}}_\ell > \check{\mathbf{w}}_r > \mathbf{w}_m = \hat{\mathbf{w}}_m = \mathbf{w}_r \geq \mathbf{w}^-$, $f(U_\ell) > f(\mathbf{u}_*) > q \geq f(U_m) > f(U_r)$ and $U_\ell, U_m, U_r \in \Omega_c$. $\mathcal{CRS}_R^n[U_\ell, U_r]$ has three waves (U_ℓ, \hat{U}_ℓ) , $(\hat{U}_\ell, \check{U}_r)$ and (\check{U}_r, U_r) , which are a S, a NS and a CD, respectively. As a consequence

$$\begin{aligned}\Delta TV_v &= 2(v_r - \hat{v}_\ell) > 0, & \Delta \hat{Y}_n &= -(\hat{v}_m - \hat{v}_\ell) - (\mathbf{w}_\ell - \mathbf{w}_m) < 0, \\ \Delta TV_w &= 0, & \Delta \check{Y}_n &= 0,\end{aligned}$$

therefore $\Delta \sharp = 1$ and $\Delta \mathcal{T}_n = -2(\hat{v}_m - v_r) - 2(\mathbf{w}_\ell - \mathbf{w}_m) < 0$.

CD- \mathbf{RS}_q^- (U_ℓ, U_m) is a CD and (U_m, U_r) is a RS. In this case $\hat{v}_\ell \leq v_\ell = v_m \leq \hat{v}_m$, $v_m = \check{v}_m < v_r \leq \check{v}_r$, $\mathbf{w}_\ell = \hat{\mathbf{w}}_\ell \geq \check{\mathbf{w}}_m \geq \mathbf{w}_m = \mathbf{w}_r \geq \mathbf{w}^-$, $\mathbf{w}_\ell > \mathbf{w}_m$, $f(U_m) < f(U_r) \leq f(U_\ell) < f(\mathbf{U}_*)$, $f(U_m) \leq q < f(\mathbf{U}_*)$ and $U_\ell, U_m, U_r \in \Omega_c$. $\mathcal{CRS}_R^n[U_\ell, U_r]$ has at most three waves (U_ℓ, \hat{U}_ℓ), ($\hat{U}_\ell, \check{U}_r$) and (\check{U}_r, U_r), which are a possibly null S, a NS and a possibly null CD or PT, respectively. As a consequence

$$\begin{aligned}\Delta\text{TV}_v &= 2(v_\ell - \hat{v}_\ell) + 2(\check{v}_r - v_r) \geq 0, \\ \Delta\text{TV}_w &= \begin{cases} 2(\mathbf{w}_r - \check{\mathbf{w}}_r) & \text{if } f(U_m) = q \\ 0 & \text{if } f(U_m) < q \end{cases} \geq 0, \\ \Delta\hat{\Upsilon}_n &= -(\hat{v}_m - \hat{v}_\ell) - (\mathbf{w}_\ell - \mathbf{w}_m) < 0, \\ \Delta\check{\Upsilon}_n &= -(\check{v}_r - v_m) - \begin{cases} (\mathbf{w}_r - \check{\mathbf{w}}_r) & \text{if } f(U_m) = q \\ (\check{\mathbf{w}}_m - \check{\mathbf{w}}_r) & \text{if } f(U_m) < q \end{cases} < 0,\end{aligned}$$

and therefore

$$\begin{aligned}\Delta\sharp \in \{-1, 0, 1\}, \quad \Delta\mathcal{T}_n &= -2(\hat{v}_m - v_\ell) - 2(v_r - v_m) - 2(\mathbf{w}_\ell - \mathbf{w}_m) \\ &\quad - \begin{cases} 0 & \text{if } f(U_m) = q \\ 2(\check{\mathbf{w}}_m - \check{\mathbf{w}}_r) & \text{if } f(U_m) < q \end{cases} < 0.\end{aligned}$$

CD- \mathbf{NS}_q^- (U_ℓ, U_m) is a CD and (U_m, U_r) is a NS. In this case $v_\ell = v_m = \hat{v}_m < v_r$, $\mathbf{w}_r < \min\{\mathbf{w}_\ell, \mathbf{w}_m\}$, $\mathbf{w}_\ell = \hat{\mathbf{w}}_\ell$, $\mathbf{w}_m = \hat{\mathbf{w}}_m$, $f(U_m) = f(U_r) = q \neq f(U_\ell)$ and $U_\ell, U_m \in \Omega_c$.

If $f(U_\ell) < q$, then $v_r > \hat{v}_\ell > v_\ell = v_m$, $\mathbf{w}_r < \mathbf{w}_\ell < \mathbf{w}_m$ and $\mathcal{CRS}_R^n[U_\ell, U_r]$ has a fan of RSs from U_ℓ to \hat{U}_ℓ and a NS (\hat{U}_ℓ, U_r); as a consequence $\Delta\text{TV}_w = -2(\mathbf{w}_m - \mathbf{w}_\ell) < 0 = \Delta\text{TV}_v = \Delta\hat{\Upsilon}_n = \Delta\check{\Upsilon}_n$, therefore $\Delta\sharp \in [0, 2^n - 2]$ and $\Delta\mathcal{T}_n = -2(\mathbf{w}_m - \mathbf{w}_\ell) < 0$.

If $f(U_\ell) > q$, then $v_r > v_\ell = v_m = \hat{v}_m > \hat{v}_\ell$, $\mathbf{w}_\ell > \mathbf{w}_m > \mathbf{w}_r$ and $\mathcal{CRS}_R^n[U_\ell, U_r]$ has a two waves (U_ℓ, \hat{U}_ℓ) and (\hat{U}_ℓ, U_r), that are a S and a NS, respectively; as a consequence

$$\begin{aligned}\Delta\text{TV}_v &= 2(v_\ell - \hat{v}_\ell) > 0, & \Delta\hat{\Upsilon}_n &= -(v_\ell - \hat{v}_\ell) - (\mathbf{w}_\ell - \mathbf{w}_m) < 0, \\ \Delta\text{TV}_w &= 0, & \Delta\check{\Upsilon}_n &= 0,\end{aligned}$$

therefore $\Delta\sharp = 0$ and $\Delta\mathcal{T}_n = -2(\mathbf{w}_\ell - \mathbf{w}_m) < 0$.

CD-PT $_{\mathbf{q}}^-$ (U_ℓ, U_m) is a CD and (U_m, U_r) is a PT. In this case $v_\ell = v_m = \hat{v}_m = \mathbf{v}_{\max} > v_r = \check{v}_r > \hat{v}_\ell$, $\mathbf{w}_\ell = \hat{\mathbf{w}}_\ell > \check{\mathbf{w}}_r \geq \mathbf{w}_r \geq \mathbf{w}^- > \mathbf{w}_q = \hat{\mathbf{w}}_m \geq \mathbf{w}_m$, $f(U_\ell) > f(\mathbf{U}_*) > q \geq \max\{f(U_m), f(U_r)\}$, $U_\ell \in \Omega_f^+$, $U_m \in \Omega_f^-$ and $U_r \in \Omega_c$. $\mathcal{CRS}_R^n[U_\ell, U_r]$ has at most three waves (U_ℓ, \hat{U}_ℓ), ($\hat{U}_\ell, \check{U}_r$) and (\check{U}_r, U_r) that are a S, a NS and a possibly null CD, respectively. As a consequence

$$\begin{aligned} \Delta\text{TV}_v &= 2(v_r - \hat{v}_\ell) > 0, & \Delta\hat{\mathcal{Y}}_n &= -(v_m - \hat{v}_\ell) - (\mathbf{w}_\ell - \mathbf{w}_q) < 0, \\ \Delta\text{TV}_w &= -2(\mathbf{w}_r - \mathbf{w}_m) < 0, & \Delta\check{\mathcal{Y}}_n &= 0, \end{aligned}$$

therefore $\Delta\sharp \in \{0, 1\}$ and $\Delta\mathcal{T}_n = -2(v_m - v_r) - 2(\mathbf{w}_r - \mathbf{w}_m) - 2(\mathbf{w}_\ell - \mathbf{w}_q) < 0$.

NS-S $_{\mathbf{q}}^-$ (U_ℓ, U_m) is a NS and (U_m, U_r) is a S. In this case $v_m > v_r = \check{v}_r > v_\ell$, $\mathbf{w}_\ell > \check{\mathbf{w}}_r > \mathbf{w}_m = \mathbf{w}_r \geq \mathbf{w}^-$, $f(U_\ell) = f(U_m) = q > f(U_r)$ and $U_\ell, U_m, U_r \in \Omega_c$. $\mathcal{CRS}_R^n[U_\ell, U_r]$ has two waves (U_ℓ, \check{U}_r) and (\check{U}_r, U_r) that are a NS and a CD, respectively. As a consequence $\Delta\text{TV}_v = -2(v_m - v_r) < 0 = \Delta\text{TV}_w = \Delta\hat{\mathcal{Y}}_n = \Delta\check{\mathcal{Y}}_n$, therefore $\Delta\sharp = 0$ and $\Delta\mathcal{T}_n = -2(v_m - v_r) < 0$.

NS-RS $_{\mathbf{q}}^-$ (U_ℓ, U_m) is a NS and (U_m, U_r) is a RS. In this case $v_\ell < v_m = \check{v}_m < v_r \leq \check{v}_r$, $\mathbf{w}_\ell > \mathbf{w}_m = \check{\mathbf{w}}_m = \mathbf{w}_r > \check{\mathbf{w}}_r$, $f(U_r) > q = f(U_\ell) = f(U_m)$ and $U_\ell, U_m, U_r \in \Omega_c$. $\mathcal{CRS}_R^n[U_\ell, U_r]$ has two waves (U_ℓ, \check{U}_r) and (\check{U}_r, U_r) that are a NS and either a PT or a CD, respectively. As a consequence

$$\begin{aligned} \Delta\text{TV}_v &= 2(\check{v}_r - v_r) \geq 0, & \Delta\hat{\mathcal{Y}}_n &= 0, \\ \Delta\text{TV}_w &= 2(\mathbf{w}_r - \check{\mathbf{w}}_r) > 0, & \Delta\check{\mathcal{Y}}_n &= -(\check{v}_r - v_m) - (\mathbf{w}_r - \check{\mathbf{w}}_r) < 0, \end{aligned}$$

therefore $\Delta\sharp = 0$ and $\Delta\mathcal{T}_n = -2(v_r - v_m) < 0$. Notice that $\check{v}_r > v_r$ if and only if $\mathbf{w}_m = \mathbf{w}_r = \mathbf{w}^-$ and $\check{v}_r = \mathbf{v}_{\max} > v_r > v_m = \mathbf{v}_q^+$.

NS-PT $_{\mathbf{q}}^-$ (U_ℓ, U_m) is a NS and (U_m, U_r) is a PT. In this case $v_m = \mathbf{v}_{\max} > v_r = \check{v}_r > v_\ell$, $\mathbf{w}_\ell > \check{\mathbf{w}}_r > \mathbf{w}_r = \mathbf{w}^- > \mathbf{w}_m$, $f(\mathbf{U}_*) > f(U_\ell) = f(U_m) = q > f(U_r)$, $U_\ell, U_r \in \Omega_c$ and $U_m \in \Omega_f^-$. $\mathcal{CRS}_R^n[U_\ell, U_r]$ has two waves (U_ℓ, \check{U}_r) and (\check{U}_r, U_r) that are a NS and a CD, respectively. As a consequence

$$\begin{aligned} \Delta\text{TV}_v &= -2(\mathbf{v}_{\max} - v_r) < 0, & \Delta\hat{\mathcal{Y}}_n &= 0, \\ \Delta\text{TV}_w &= -2(\mathbf{w}^- - \mathbf{w}_m) < 0, & \Delta\check{\mathcal{Y}}_n &= 0, \end{aligned}$$

therefore $\Delta\sharp = 0$ and $\Delta\mathcal{T}_n = -2(v_{\max} - v_r) - 2(w^- - w_m) < 0$.

This concludes the proof.

A.6 Proof of Proposition 5.8

We underline that for any interaction $\Delta\sharp \leq 2^n - 1$, see Table A.1.

From what we already show in the proof of Proposition 5.7, see Table A.1, we deduce that

$$t \mapsto 2^n \frac{\mathcal{T}_n(t)}{\varepsilon_n} + \sharp(t)$$

strictly decreases after any interaction, except the following cases.

A CD (U_ℓ, U_m) interacts with (U_m, U_r) and one of the following conditions is satisfied:

- (U_m, U_r) is a S and $w_\ell = w^- - 1$;
 - (U_m, U_r) is a S and $w^- - 1 < w_\ell \leq w^- = w_r$;
 - (U_m, U_r) is a RS;
 - (U_m, U_r) is a PT and $w_\ell > w^-$.
- (A.1)

For this reason it remains to bound the number of only the above type of interactions. We observe that the number of waves of U_n do not change after interactions as in (A.1). This implies that the number of waves is uniformly bounded. We also observe that any interaction as in (A.1) has exactly one incoming CD and exactly one outgoing CD. Since no wave can reach any CD from the left (and then possibly have with it an interaction as in (A.1)), we have that as long as a CD remains a CD (possible further interactions involving it have to be taken into account), it can interact only once with another wave W (or with waves generated by *further* interactions involving W), moreover in this case W is slower than such CD and is not another CD. Since furthermore we already know that the number of waves is uniformly bounded, there can be only finitely many interactions involving CDs. It is therefore now clear that also the number of the interactions described in (A.1) is bounded.

Technical proofs of Subsection 4.3.1

In this section we collect the proofs concerning the non-conservative constrained ARZ model.

B.1 Proof of Lemma 4.1

It is enough to show that the function $h_q(v) \doteq v + p(q/v)$ is Lipschitz and convex in the interval $I = [\hat{v}(w_N), v^b(w_N)] \subset (0, +\infty)$. For any $v \in I$ we have

$$h'_q(v) = 1 - \frac{q}{v^2} p' \left(\frac{q}{v} \right) \quad \text{and} \quad h''_q(v) = \frac{q}{v^3} \left(2p' \left(\frac{q}{v} \right) + \frac{q}{v} p'' \left(\frac{q}{v} \right) \right).$$

By (2.12) we have $p'(\rho) > 0$ and $2p'(\rho) + \rho p''(\rho) > 0$. As a result $h''_q(v) > 0$, so that

$$h'_q(v) \in \left[1 - \frac{q}{\hat{v}(w_N)^2} p' \left(\frac{q}{\hat{v}(w_N)} \right), 1 - \frac{q}{v^b(w_N)^2} p' \left(\frac{q}{v^b(w_N)} \right) \right],$$

and therefore h_q is Lipschitz. Furthermore the inverse of h_q restricted to intervals $[\hat{v}(w_N), \hat{v}(\omega_1^0)]$ and $[v^b(\omega_1^0), v^b(w_N)]$ are Lipschitz. Notice that $\hat{v}(\omega_1^0) = \tilde{v}(q) = v^b(\omega_1^0)$.

B.2 Proof of Lemma 4.2

We denote by CD a contact discontinuity, R a rarefaction shock, S a shock and NS a non-classical shock. For completeness, we compute below

$$\begin{aligned}\Delta_v &\doteq \text{TV}(v(t_i^+)) - \text{TV}(v(t_i^-)), & \Delta_w &\doteq \text{TV}(w(t_i^+)) - \text{TV}(w(t_i^-)), \\ \Delta_{\hat{v}} &\doteq \text{TV}(\hat{v}(t_i^+); \mathbb{R}_-) - \text{TV}(\hat{v}(t_i^-); \mathbb{R}_-), \\ \Delta_{v^b} &\doteq \text{TV}(v^b(t_i^+); \mathbb{R}_-) - \text{TV}(v^b(t_i^-); \mathbb{R}_-), \\ \Delta_w^- &\doteq \text{TV}(w(t_i^+); \mathbb{R}_-) - \text{TV}(w(t_i^-); \mathbb{R}_-), \\ \Delta\gamma &\doteq \gamma(t_i^+) - \gamma(t_i^-), & \Delta\Gamma &\doteq \Gamma(t_i^+) + \Gamma(t_i^-), & \Delta\sharp &\doteq \sharp J(t_i^+) - \sharp J(t_i^-),\end{aligned}$$

and

$$\Delta_\eta \doteq \sum_{x \in J(t_i^+)} \eta(U(t_i^+, x^-), U(t_i^+, x^+)) - \sum_{x \in J(t_i^-)} \eta(U(t_i^-, x^-), U(t_i^-, x^+)).$$

A Assume now that at time $t_i > 0$ exactly one interaction between two waves (U_ℓ, U_m) and (U_m, U_r) occurs at $x = 0$. For notational simplicity let $f_\ell = f(U_\ell)$, $\hat{v}_\ell = \hat{v}(w_\ell)$, $v_\ell^b = v^b(w_\ell)$, $\tilde{U} = \tilde{U}(U_\ell, U_r) \doteq (w_\ell, v_r)$ and so on. We distinguish the following cases:

A1 Assume that (U_ℓ, U_m) is a S and (U_m, U_r) an NS. Clearly $w_\ell = w_m \geq \dot{w}$, $v_m < \min\{v_\ell, v_r\}$ and $f_\ell < f_m = f_r = q$. As a consequence $(U_\ell, U_r) \in \Omega_1$, see Figure B.1.

A1.a If $v_r > v_\ell$, then $\Delta\sharp \geq 0$ because $\mathcal{RS}_{\text{ARZ}}^{c,2}[U_\ell, U_r]$ has a fan of Rs (U_ℓ, \tilde{U}) and a CD (\tilde{U}, U_r) , see Figure B.1. Obviously

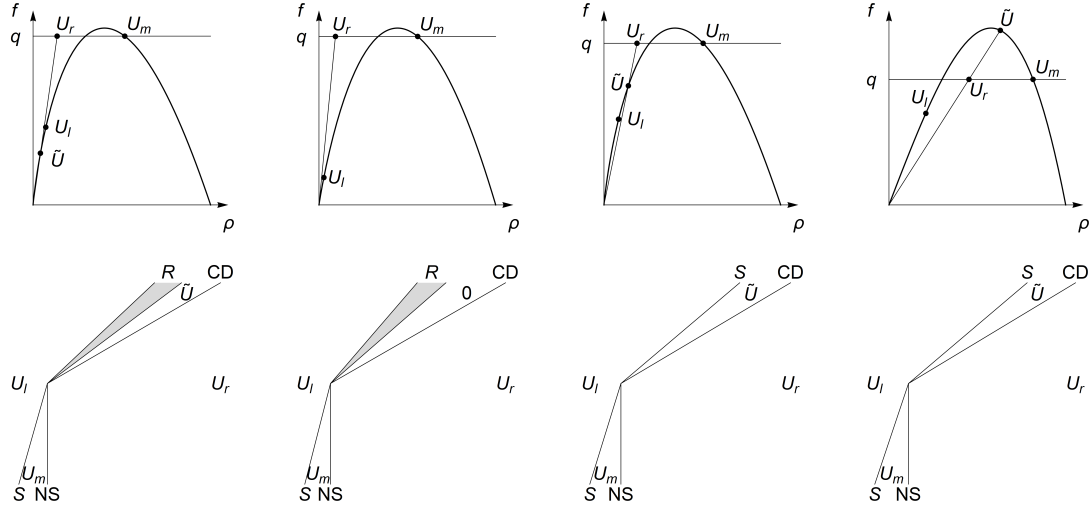
$$\Delta_w^- = 0, \quad \Delta_{\hat{v}}^- = 0, \quad \Delta_{v^b}^- = 0.$$

Since $v_m \leq \dot{v} < v_\ell < \tilde{v} = v_r$, $\dot{w} \leq \tilde{w} = w_\ell = w_m \leq w_r$ and $v_r > v_\ell^b = v_m^b$, we have

$$\Delta_v = -2(v_\ell - v_m) < 0, \quad \Delta\gamma = -(v_m^b - v_m) < 0, \quad \Delta_w = 0, \quad \Delta_\eta = 0.$$

In conclusion we have $\Delta\Gamma = -2(v_\ell - v_m^b) \leq -2\varepsilon$.

A1.b If $v_r \leq v_\ell$, then $\Delta\sharp \leq 0$ because $\mathcal{RS}_{\text{ARZ}}^{c,2}[U_\ell, U_r]$ has a possibly null S (U_ℓ, \tilde{U})

Figure B.1: Case **A1**.

and a possibly null CD (\tilde{U}, U_r) (but not both null), see Figure B.1. Obviously

$$0 = \Delta_w^- = \Delta_{\hat{v}}^- = \Delta_{v^b}^- = \Delta_\eta.$$

Since $v_m < \tilde{v} = v_r < v_\ell$, $\dot{w} \leq \tilde{w} = w_\ell = w_m$, $\dot{w} \leq w_r$ and $v_\ell^b = v_m^b$, we have

$$\Delta_v = -2(v_r - v_m) < 0, \quad \Delta_w = 0, \quad \Delta\gamma = -(\min\{v_m^b, v_r\} - v_m) < 0.$$

In conclusion we have

$$\Delta\Gamma = -2(v_r - \min\{v_m^b, v_r\}) \leq 0.$$

A2 Assume that (U_ℓ, U_m) is a CD and (U_m, U_r) an NS. Clearly $v_\ell = v_m = \hat{v}_m < v_r$, $\dot{w} \leq \min\{w_m, w_r\}$ and $f_m = f_r = q$.

A2.a If $(U_\ell, U_r) \in \Omega_1$, then $\Delta_\# \geq -1$ because $\mathcal{RS}_{\text{ARZ}}^{c,2}[U_\ell, U_r]$ has a fan of Rs (U_ℓ, \tilde{U}) and a possibly null CD (\tilde{U}, U_r) , see Figure B.2. Since $\tilde{v} = v_r > v_\ell = v_m$, $\check{w}_\ell = w_m$ and $\check{w}(v_r) = w_r$ we have

$$\Delta_v = 0, \quad \Delta_\eta = \begin{cases} \check{w}_\ell - \check{w}(\tilde{v}) & \text{if } \tilde{v} \leq \dot{v} \\ \check{w}_\ell - \dot{w} & \text{if } \tilde{v} > \dot{v} \end{cases} = \begin{cases} w_m - w_r & \text{if } v_r \leq \dot{v}, \\ w_m - \dot{w} & \text{if } v_r > \dot{v}. \end{cases}$$

Since $\tilde{w} = w_\ell < w_m$, $w_\ell \leq w_r$ and $\dot{w} \leq \min\{w_m, w_r\}$ we have that

$$\Delta_w = (w_r - w_m) - |w_r - w_m| \leq 0, \quad \Delta_w^- = -(w_m - w_\ell) < 0.$$

Since $w_\ell < w_m$ and $f_m = q$, we have that $v_m^b \geq v_\ell^b \geq \dot{v} \geq \hat{v}_\ell \geq \hat{v}_m = v_m$ we have

$$\begin{aligned} \Delta_{\hat{v}}^- &= -(\hat{v}_\ell - v_m) \leq 0, & \Delta_{v^b}^- &= -(v_m^b - v_\ell^b) \leq 0, \\ \Delta_\gamma &= -(\min\{v_m^b, v_r\} - v_m) \leq 0. \end{aligned}$$

In conclusion we have that if $v_r \in (v_m, \dot{v}]$ then $\hat{v}_\ell \geq v_r$, $w_\ell \leq w_r < w_m$ and

$$\Delta\Gamma \leq -w_m - 2w_r + 3w_\ell - 2(\hat{v}_\ell - \min\{v_m^b, v_r\}) - 2(v_m^b - v_\ell^b) \leq -3\varepsilon,$$

while if $v_r > \dot{v}$ then $w_\ell \leq \dot{w}$, $w_\ell < w_m$, $\hat{v}_\ell = \dot{v} = v_\ell^b$ and

$$\Delta\Gamma \leq -w_m - 2\dot{w} + 3w_\ell - 2(v_m^b - \min\{v_m^b, v_r\}) \leq -\varepsilon.$$

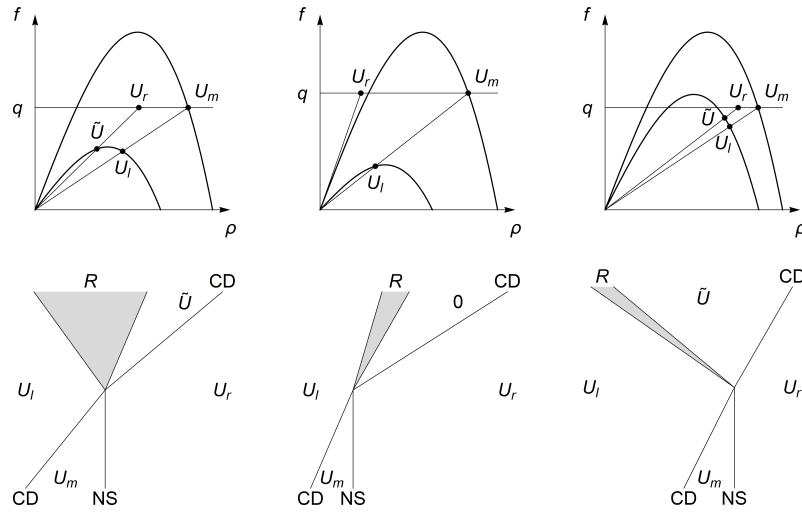


Figure B.2: Case **A2.a**.

A2.b If $(U_\ell, U_r) \in \Omega_2$ and $\dot{w} < w_\ell < w_m$, then $\Delta\sharp \geq 0$ because $\mathcal{RS}_{\text{ARZ}}^{c,2}[U_\ell, U_r]$ has a fan of Rs (U_ℓ, \hat{U}_ℓ) and a NS (\hat{U}_ℓ, U_r) , see Figure B.3, left. Since $v_r > \hat{v}_\ell > v_\ell = v_m$

and $\check{w}(\hat{v}_\ell) = \hat{w}_\ell = w_\ell < \check{w}_\ell = w_m$, we have

$$\Delta_v = 0, \quad \Delta_\eta = (w_m - w_\ell) > 0.$$

Since $w_\ell = \hat{w}_\ell < w_m$ we have that

$$\Delta_w = |w_r - w_\ell| - ((w_m - w_\ell) + |w_r - w_m|) \leq 0, \quad \Delta_w^- = -(w_m - w_\ell) < 0.$$

Since $\dot{w} < w_\ell < w_m$ and $f_m = q$, we have that $v_m^b > v_\ell^b > \hat{v}_\ell > v_\ell = v_m = \hat{v}_m$ we have

$$\begin{aligned} \Delta_{\hat{v}}^- &= -(\hat{v}_\ell - v_\ell) < 0, & \Delta_{v^b}^- &= -(v_m^b - v_\ell^b) < 0, \\ \Delta\gamma &= -(\hat{v}_\ell - v_\ell) - (\min\{v_m^b, v_r\} - \min\{v_\ell^b, v_r\}) < 0. \end{aligned}$$

In conclusion we have that $\Delta\sharp \geq 0$ and

$$\begin{aligned} \Delta\Gamma &\leq 3\Delta_w^- + 2(\Delta_\eta + \Delta_{\hat{v}}^- + \Delta_{v^b}^- - \Delta\gamma) \\ &\leq -(w_m - w_\ell) - 2(v_m^b - v_\ell^b) + 2(\min\{v_m^b, v_r\} - \min\{v_\ell^b, v_r\}) \\ &\leq -(w_m - w_\ell) \leq -\varepsilon. \end{aligned}$$

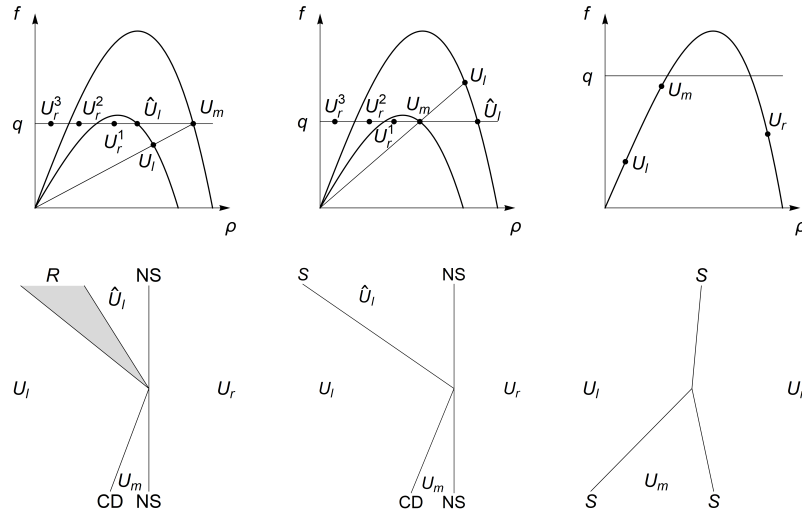


Figure B.3: Cases **A2.b**, **A2.c** and **A3**.

A2.c If $(U_\ell, U_r) \in \Omega_2$ and $\dot{w} < w_m < w_\ell$, then $\Delta\sharp = 0$ because $\mathcal{RS}_{\text{ARZ}}^{c,2}[U_\ell, U_r]$ has

a **S** (U_ℓ, \hat{U}_ℓ) and a **NS** (\hat{U}_ℓ, U_r) , see Figure B.3, right. Since $v_r > v_m = v_\ell > \hat{v}_\ell$ and no **R** is involved, we have

$$\Delta_v = 2(v_\ell - \hat{v}_\ell) > 0, \quad \Delta_\eta = 0.$$

Since $w_m < w_\ell = \hat{w}_\ell$ we have that

$$\Delta_w = |w_r - w_\ell| - ((w_\ell - w_m) + |w_r - w_m|) \leq 0, \quad \Delta_w^- = -(w_\ell - w_m) < 0.$$

Since $\dot{w} < w_m < w_\ell$ and $f_m = q$, we have that $v_\ell^b > v_m^b > v_m = \hat{v}_m = v_\ell > \hat{v}_\ell$ we have

$$\begin{aligned} \Delta_{\hat{v}}^- &= -(v_\ell - \hat{v}_\ell) < 0, & \Delta_{v^b}^- &= -(v_\ell^b - v_m^b) < 0, \\ \Delta\gamma &= (v_\ell - \hat{v}_\ell) + (\min\{v_\ell^b, v_r\} - \min\{v_m^b, v_r\}) \geq 0. \end{aligned}$$

In conclusion we have that $\Delta\sharp = 0$ and $\Delta\Gamma < \Delta_v + 2\Delta_{\hat{v}}^- = 0$.

A3 Assume that (U_ℓ, U_m) and (U_m, U_r) are two shocks. Clearly $v_r < v_m < v_\ell$, $w_\ell = w_m = w_r$ and $\max\{f_\ell, f_m, f_r\} \leq q$. Hence, the solution consists of a shock (U_ℓ, U_r) , see Figure B.3. In this case we have

$$0 = \Delta_v = \Delta_w = \Delta_{\hat{v}}^- = \Delta_{v^b}^- = \Delta\gamma = \Delta_w^- = \Delta_\eta = \Delta\Gamma.$$

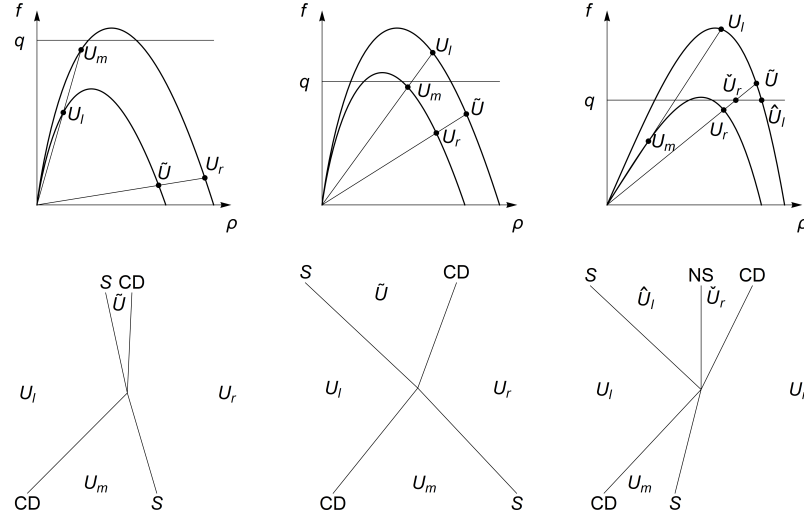
A4 Assume that (U_ℓ, U_m) is a **CD** and (U_m, U_r) is a **S**. Clearly $w_m = w_r$, $v_\ell = v_m > v_r = \tilde{v}$ and $\max\{f_m, f_r\} \leq q$.

A4.a If $(U_\ell, U_r) \in \Omega_1$, i.e. $\min\{f_\ell, \tilde{f}\} \leq q$, then $\Delta\sharp = 0$ because $\mathcal{RS}_{\text{ARZ}}^{c,2}[U_\ell, U_r]$ has a **S** (U_ℓ, \tilde{U}) and a **CD** (\tilde{U}, U_r) , see Figure B.4. Since $v_\ell = v_m > v_r = \tilde{v}$, $w_\ell = \tilde{w}$, $w_m = w_r$ and neither **R** or **NS** are involved, we have

$$\begin{aligned} 0 = \Delta_v = \Delta_\eta = \Delta_w = \Delta\gamma, & \quad \Delta_w^- = -|w_\ell - w_r| < 0, \\ \Delta_{\hat{v}}^- = -|\hat{v}_\ell - \hat{v}_r| < 0, & \quad \Delta_{v^b}^- = -|v_\ell^b - v_r^b| < 0. \end{aligned}$$

In conclusion we have that $\Delta\sharp = 0$ and $\Delta\Gamma < 0$.

A4.b If $(U_\ell, U_r) \in \Omega_2$, namely $\min\{f_\ell, \tilde{f}\} > q$, then $w_\ell = \tilde{w} > w_m = w_r$, $v_r > \hat{v}_\ell$ and $\Delta\sharp \geq 0$ because $\mathcal{RS}_{\text{ARZ}}^{c,2}[U_\ell, U_r]$ has a **S** (U_ℓ, \hat{U}_ℓ) , a **NS** $(\hat{U}_\ell, \check{U}_r)$ and a possibly

Figure B.4: Cases **A4.a** and **A4.b**.

null CD (\check{U}_r, U_r) , see Figure B.4. Since $w_m = w_r < \check{w}_r < w_\ell = \tilde{w}$, $\hat{v}_\ell < \tilde{v} = v_r = \check{v}_r < v_\ell = v_m < v_\ell^b$ and no R is involved, we have $\hat{v}_\ell < \hat{v}_r \leq v_r^b < v_\ell^b$ and

$$\begin{aligned} \Delta_v &= 2(v_r - \hat{v}_\ell) > 0, & \Delta_{\hat{v}}^- &= -(\hat{v}_r - \hat{v}_\ell) < 0, & \Delta_{v^b}^- &= -(v_\ell^b - v_r^b) < 0, \\ \Delta_w &= 0, & \Delta_w^- &= -(w_\ell - w_m) < 0, & \Delta\gamma &= (v_r - \hat{v}_\ell) > 0, \\ \Delta_\eta &= 0. \end{aligned}$$

In conclusion we have that $\Delta\sharp \geq 0$ and $\Delta\Gamma < \Delta_v + 2(\Delta_{\hat{v}}^- - \Delta\gamma) = -2(\hat{v}_r - \hat{v}_\ell) \leq -2\varepsilon$.

A5 Assume that (U_ℓ, U_m) is a NS and (U_m, U_r) is a S. Clearly $w_m = w_r$, $v_m > \max\{v_\ell, v_r\}$ and $f_r < f_m = q = f_\ell$.

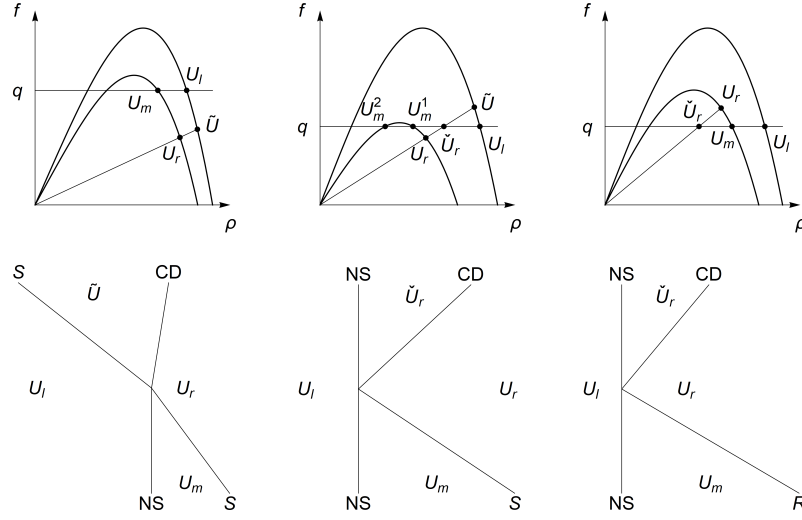
A5.a If $(U_\ell, U_r) \in \Omega_1$, then $v_r < v_\ell$, $\max\{f_r, \tilde{f}\} < f_\ell = q = f_m$. Moreover $\Delta\sharp \leq 0$ because $\mathcal{RS}_{\text{ARZ}}^{c,2}[U_\ell, U_r]$ has a S (U_ℓ, \tilde{U}) and a possibly null CD (\tilde{U}, U_r) , see Figure B.5. Clearly

$$0 = \Delta_{\hat{v}}^- = \Delta_{v^b}^- = \Delta_w^- = \Delta_\eta.$$

Since $v_r = \tilde{v} < v_\ell < v_m$, $v_\ell \leq v_\ell^b$, $w_\ell = \tilde{w}$ and $w_m = w_r$, we have

$$\Delta_v = -2(v_m - v_\ell) < 0, \quad \Delta\gamma = -[\min\{v_\ell^b, v_m\} - v_\ell] \leq 0, \quad \Delta_w = 0.$$

In conclusion we have that $\Delta\sharp \leq 0$ and $\Delta\Gamma = -2[v_m - \min\{v_\ell^b, v_m\}] \leq 0$.

Figure B.5: Cases **A5.a**, **A5.b** and **A6**.

A5.b If $(U_\ell, U_r) \in \Omega_2$, then $v_\ell < v_r$, $f_r < f_\ell = q = f_m < \tilde{f}$. Moreover $\Delta\sharp = 0$ because $\mathcal{RS}_{\text{ARZ}}^{c,2}[U_\ell, U_r]$ has a NS (U_ℓ, \check{U}_r) and a CD (\check{U}_r, U_r) , see Figure B.5. Clearly

$$0 = \Delta_{\check{v}}^- = \Delta_{v^b}^- = \Delta_w^- = \Delta_\eta.$$

Since $v_\ell < v_r = \check{v}_r < v_m < v_\ell^b$ and $w_m = w_r < \check{w}_r < w_\ell$, we have

$$\Delta_v = -2(v_m - v_r) < 0, \quad \Delta_w = 0, \quad \Delta\gamma = -(v_m - v_r) < 0.$$

In conclusion we have that $\Delta\sharp = 0$ and $\Delta\Gamma = 0$.

A6 Assume that (U_ℓ, U_m) is a NS and (U_m, U_r) a R. Clearly $w_m = w_r < w_\ell$, $v_m \leq v_r - \varepsilon$ and $q = f_\ell = f_m < f_r$. Moreover $\Delta\sharp = 0$ because $\mathcal{RS}_{\text{ARZ}}^{c,2}[U_\ell, U_r]$ has a NS (U_ℓ, \check{U}_r) and a CD (\check{U}_r, U_r) , see Figure B.5. Clearly

$$0 = \Delta_{\check{v}}^- = \Delta_{v^b}^- = \Delta_w^-.$$

Since $v_\ell^b > \check{v}_r = v_r > v_m > v_\ell$ and $w_\ell > w_m = \check{w}_m = w_r > \check{w}_r$, we have

$$\Delta_v = 0, \quad \Delta_w = 2(w_r - \check{w}_r) > 0, \quad \Delta\gamma = (v_r - v_m) > 0, \quad \Delta_\eta = -(w_r - \check{w}_r) < 0.$$

In conclusion we have that $\Delta\sharp = 0$ and $\Delta\Gamma = -2(v_r - v_m) < -2\varepsilon$.

A7 Assume that (U_ℓ, U_m) is a R and (U_m, U_r) a S. Clearly $w_\ell = w_m = w_r$ and $v_\ell \geq v_m - \varepsilon$. It is easy to check that $(U_\ell, U_r) \in \Omega_1$. Thus $\mathcal{RS}_{\text{ARZ}}^{c,2}[U_\ell, U_r]$ is a S (U_ℓ, U_r) and $\Delta_\# = -1$, see Figure B.6. Clearly

$$0 = \Delta_w = \Delta_{\hat{v}}^- = \Delta_{v^b}^- = \Delta_w^- = \Delta\gamma, \quad \Delta_\eta \leq 0.$$

Since $v_m > v_\ell > v_r$ we have

$$\Delta_v = -2(v_m - v_\ell) < 0.$$

In conclusion we have that $\Delta_\# = -1$ and $\Delta\Gamma < 0$.

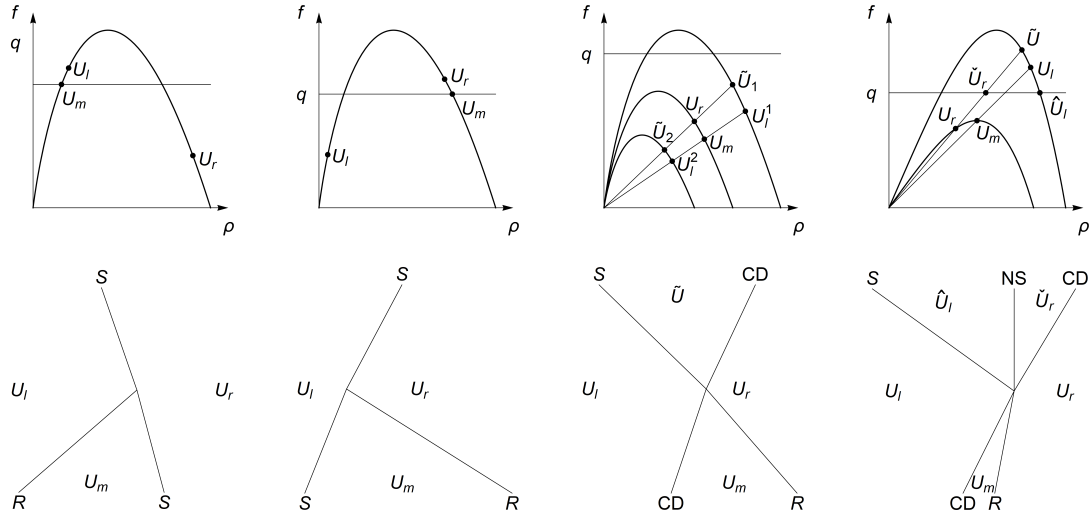


Figure B.6: Cases **A7**, **A8.a** and **A8.b**.

A8 Assume that (U_ℓ, U_m) is a CD and (U_m, U_r) is a R. Clearly $v_\ell = v_m < v_r$, $w_m = w_r$ and $\min\{f_m, f_r\} \leq q$.

A8.a If $(U_\ell, U_r) \in \Omega_1$, namely $\max\{f_\ell, \tilde{f}\} \leq q$, then $\mathcal{RS}_{\text{ARZ}}^{c,2}[U_\ell, U_r]$ has a single R (U_ℓ, \tilde{U}) and a CD (\tilde{U}, U_r) , see Figure B.6. Clearly

$$\Delta_{\hat{v}}^- = \begin{cases} -|\hat{v}_\ell - \hat{v}_m| & \text{if } v_\ell > 0 \\ 0 & \text{if } v_\ell = 0 \end{cases} \leq 0, \quad \Delta_{v^b}^- = \begin{cases} -|v_\ell^b - v_m^b| & \text{if } v_\ell > 0 \\ 0 & \text{if } v_\ell = 0 \end{cases} \leq 0,$$

$$\Delta_w^- = \begin{cases} -|w_\ell - w_m| & \text{if } v_\ell > 0 \\ 0 & \text{if } v_\ell = 0 \end{cases} \leq 0, \quad \Delta\gamma = 0.$$

Since $v_\ell = v_m < v_r = \tilde{v}$, $\tilde{w} = w_\ell$ and $w_m = w_r$, we have

$$\Delta_v = 0, \quad \Delta_w = 0, \quad \Delta_\eta = 0.$$

In conclusion we have that $\Delta\sharp = 0$ and $\Delta\Gamma \leq 0$.

A8.b If $(U_\ell, U_r) \in \Omega_2$, i.e. $\max\{f_\ell, \tilde{f}\} > q$, then $\Delta\sharp \geq -1$ because $\mathcal{RS}_{\text{ARZ}}^{c,2}[U_\ell, U_r]$ has a possibly null **S** (U_ℓ, \hat{U}_ℓ) , a **NS** $(\hat{U}_\ell, \check{U}_r)$ and a possibly null **CD** (\check{U}_r, U_r) , see Figure B.6. Since $\check{w}_r \geq w_r - \varepsilon$, $w_m = w_r < w_\ell = \hat{w}_\ell$, $\hat{v}_\ell \leq v_\ell = v_m < \check{v}_r = v_r = \tilde{v} \leq v_\ell^b$, $\hat{v}_\ell < \hat{v}_m = \hat{v}_r$ and $v_\ell^b > v_m^b = v_r^b$, we have

$$\begin{aligned} \Delta_v &= 2(v_\ell - \hat{v}_\ell) \geq 0, & \Delta_w &= \begin{cases} 2(w_r - \check{w}_r) & \text{if } f_m = q < f_r \\ 0 & \text{otherwise} \end{cases} \geq 0, \\ \Delta_{\hat{v}}^- &= -(\hat{v}_r - \hat{v}_\ell) < 0, & \Delta_w^- &= -(w_\ell - w_r) < 0, \\ \Delta_{v^b}^- &= -(v_\ell^b - v_r^b) < 0, & \Delta_\eta &= \begin{cases} -(\check{w}_m - \check{w}_r) & \text{if } \hat{v}(w_{\max}) \leq v_m < v_r \leq \hat{v} \\ 0 & \text{otherwise} \end{cases} \leq 0, \\ \Delta\gamma &= (v_r - \hat{v}_\ell) > 0. \end{aligned}$$

In conclusion we have that $\Delta\sharp \geq -1$ and

$$\begin{aligned} \Delta\Gamma &< \Delta_v - 2\Delta\gamma + \Delta_w + 2\Delta_\eta \\ &= -2(v_r - v_\ell) + \begin{cases} 2(w_r - \check{w}_m) = 0 & \text{if } f_m = q < f_r \\ 0 & \text{otherwise} \end{cases} \leq -2\varepsilon. \end{aligned}$$

A9 Assume that (U_ℓ, U_m) is a **S** and (U_m, U_r) is a **R**. Clearly $v_m < v_r < v_\ell$ and $w_\ell = w_m = w_r$. By observing that $f(\mathcal{RS}_{\text{ARZ}}[U_\ell, U_r])(0^\pm) = \min\{f_\ell, f_r\} \leq q$, we have that $(U_\ell, U_r) \in \Omega_1$. Hence $\mathcal{RS}_{\text{ARZ}}^{c,2}[U_\ell, U_r] \equiv \mathcal{RS}_{\text{ARZ}}[U_\ell, U_r]$ has a **S** (U_ℓ, U_r) and $\Delta\sharp = -1$, see Figure B.7. As a consequence $\Delta_\eta \leq 0$, $\Delta\gamma = 0$ because no **NS** is involved, $\Delta_w = \Delta_w^- = \Delta_{\hat{v}}^- = \Delta_{v^b}^- = 0$ because no **CD** is involved. Since $v_m < v_m + \varepsilon \leq v_r < v_\ell$ we have $\Delta_v = -2(v_r - v_m) < 0$. In conclusion $\Delta\sharp = -1$ and $\Delta\Gamma < 0$.

B Assume now that at time $t_i > 0$ exactly one wave (U_ℓ, U_r) reaches $x = 0$. We distinguish the following cases:

B1 Assume (U_ℓ, U_r) is a **CD**. Clearly $v_\ell = v_r$ and $f_r \leq q$.

B1.a If $(U_\ell, U_r) \in \Omega_1$, namely $f_\ell \leq q$, then $\Delta\sharp = 0$ because $\mathcal{RS}_{\text{ARZ}}^{c,2}[U_\ell, U_r]$ has a

CD (U_ℓ, U_r) , see Figure B.7, left. Clearly $0 = \Delta_v = \Delta_w = \Delta\gamma = \Delta_\eta$ and

$$\Delta_w^- = -|w_\ell - w_r| \leq -\varepsilon, \quad \Delta_{\hat{v}}^- = -|\hat{v}_\ell - \hat{v}_r| \leq -\varepsilon, \quad \Delta_{v^b}^- = -|v_\ell^b - v_r^b| \leq -\varepsilon,$$

therefore $\Delta\Gamma = 3\Delta_w^- + 2(\Delta_{\hat{v}}^- + \Delta_{v^b}^-) \leq -7\varepsilon \leq 0$.

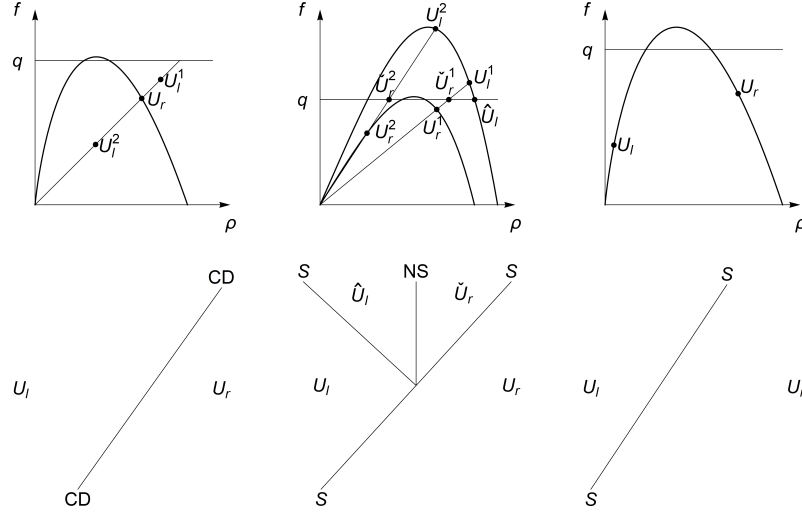


Figure B.7: Cases **A9**, **B1.a**, **B1.b** and **B2**.

B1.b If $(U_\ell, U_r) \in \Omega_2$, namely $f_\ell > q$, then $\Delta\sharp > 0$ because $\mathcal{RS}_{\text{ARZ}}^{c,2}[U_\ell, U_r]$ has a shock (U_ℓ, \hat{U}_ℓ) , a NS $(\hat{U}_\ell, \check{U}_r)$ and a possibly null CD (\check{U}_r, U_r) , see Figure B.7, center. Since $v_\ell = v_r = \check{v}_r > \hat{v}_\ell$ and no R is involved, we have

$$\Delta_v = 2(v_\ell - \hat{v}_\ell) > 0, \quad \Delta_\eta = 0.$$

Since $w_r \leq \check{w}_r < w_\ell = \hat{w}_\ell$ we have that

$$\Delta_w = 0, \quad \Delta_w^- = -(w_\ell - w_r) < 0.$$

Since $w_r < w_\ell$, we have that $v_\ell^b > v_r^b > \hat{v}_r > \hat{v}_\ell$, $\check{v}_r = v_r = v_\ell < v_\ell^b$ and

$$\Delta_{\hat{v}}^- = -(\hat{v}_r - \hat{v}_\ell) < 0, \quad \Delta_{v^b}^- = -(v_\ell^b - v_r^b) < 0, \quad \Delta\gamma = v_\ell - \hat{v}_\ell > 0.$$

In conclusion we have that $\Delta\sharp > 0$ and

$$\Delta\Gamma = \Delta_v + 2(\Delta_{\hat{v}}^- + \Delta_{v^b}^- - \Delta\gamma) + 3\Delta_w^- = -2(v_\ell^b - v_r^b) - 2(\hat{v}_r - \hat{v}_\ell) - 3(w_\ell - w_r) \leq -7\varepsilon.$$

B2 Assume that (U_ℓ, U_r) is a **S**. Clearly $w_\ell = w_r$ and $\max\{f_\ell, f_r\} \leq q$. Hence, $\Delta\sharp = 0$ because $\mathcal{RS}_{\text{ARZ}}^{c,2}[U_\ell, U_r]$ has a **S** (U_ℓ, U_r) , see Figure B.7, right. In this case we have

$$\Delta\sharp = 0 = \Delta_v = \Delta_w = \Delta_{\hat{v}}^- = \Delta_{v^b}^- = \Delta\gamma = \Delta_w^- = \Delta_{\eta 23} = \Delta\Gamma.$$

B3 Assume that (U_ℓ, U_r) is a **R**. Clearly $w_\ell = w_r$ and $v_\ell \leq v_r - \varepsilon$.

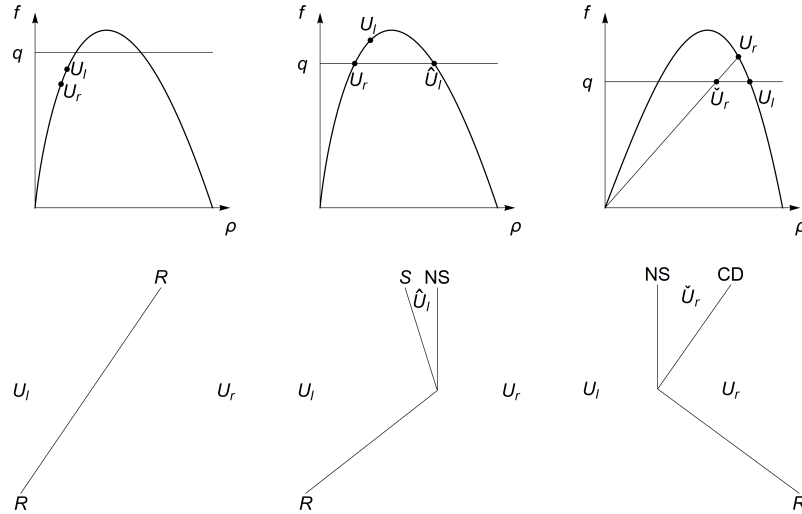


Figure B.8: Cases **B3.a**, **B3.b** and **B3.c**.

B3.a If $(U_\ell, U_r) \in \Omega_1$, namely $\max\{f_\ell, f_r\} \leq q$, then $\mathcal{RS}_{\text{ARZ}}^{c,2}[U_\ell, U_r]$ has a single **R** (U_ℓ, U_r) , see Figure B.8, center. In this case we have

$$\Delta\sharp = 0 = \Delta_v = \Delta_w = \Delta_{\hat{v}}^- = \Delta_{v^b}^- = \Delta\gamma = \Delta_w^- = \Delta_\eta = \Delta\Gamma.$$

B3.b If $(U_\ell, U_r) \in \Omega_2$ and $f_r = q < f_\ell$, then $\Delta\sharp = 1$ because $\mathcal{RS}_{\text{ARZ}}^{c,2}[U_\ell, U_r]$ has a **S** (U_ℓ, \hat{U}_ℓ) and a **NS** (\hat{U}_ℓ, U_r) , see Figure B.8, right. Since $w_\ell = \hat{w}_\ell = w_r$ and $\hat{v}_\ell < \hat{v} < v_\ell < v_r = v_\ell^b$, we have

$$\Delta_v = 2(v_\ell - \hat{v}_\ell) > 0, \quad 0 = \Delta_w = \Delta_{\hat{v}}^- = \Delta_{v^b}^- = \Delta_w^- = \Delta_\eta, \quad \Delta\gamma = (v_r - \hat{v}_\ell) > 0.$$

In conclusion we have $\Delta\sharp = 1$ and $\Delta\Gamma = -2(v_r - v_\ell) \leq -2\varepsilon$.

B3.c If $(U_\ell, U_r) \in \Omega_2$ and $f_\ell = q < f_r$, then $\Delta\sharp = 1$ because $\mathcal{RS}_{\text{ARZ}}^{c,2}[U_\ell, U_r]$ has a NS (U_ℓ, \check{U}_r) and a CD (\check{U}_r, U_r) , see Figure B.6. Since $\check{w}_r < w_r = w_\ell = \check{w}_\ell$ and $v_\ell < \check{v}_r = v_r < v_\ell^b$, we have

$$\begin{aligned} 0 = \Delta_v = \Delta_{\check{v}}^- = \Delta_{v^b}^- = \Delta_w^-, & \quad \Delta_\eta = -(w_\ell - \check{w}_r) < 0, \\ \Delta\gamma = (v_r - v_\ell) > 0, & \quad \Delta_w = 2(w_r - \check{w}_r) = -2\Delta_\eta > 0. \end{aligned}$$

In conclusion we have $\Delta\sharp = 1$ and $\Delta\Gamma = -2(v_r - v_\ell) \leq -2\varepsilon$.

C At last, assume that at time $t_i > 0$ exactly one interaction between two waves occurs at $x \neq 0$. In this case $\Delta_v \leq 0$, the number of the waves does not increase, $\Delta\sharp \leq 0$, the size of the jumps in the w -coordinate does not change, hence $0 = \Delta_w = \Delta_w^- = \Delta_{\check{v}}^- = \Delta_{v^b}^-$, no R is created, hence $\Delta_\eta \leq 0$, and clearly no NSs are involved, hence $\Delta\gamma$. As a consequence $\Delta\sharp \leq 0$ and $\Delta\Gamma \leq 0$.

Bibliography

- [1] B. Andreianov and C. Cancès. On interface transmission conditions for conservation laws with discontinuous flux of general shape. *Journal of Hyperbolic Differential Equations*, 12(02):343–384, 2015.
- [2] B. Andreianov, C. Donadello, U. Razafison, and M. D. Rosini. Qualitative behaviour and numerical approximation of solutions to conservation laws with non-local point constraints on the flux and modeling of crowd dynamics at the bottlenecks. *ESAIM: M2AN*, 50(5):1269–1287, 2016.
- [3] B. Andreianov, C. Donadello, and M. D. Rosini. Crowd dynamics and conservation laws with nonlocal constraints and capacity drop. *Mathematical Models and Methods in Applied Sciences*, 24(13):2685–2722, 2014.
- [4] B. Andreianov, C. Donadello, and M. D. Rosini. A second-order model for vehicular traffics with local point constraints on the flow. *Mathematical Models and Methods in Applied Sciences*, 26(04):751–802, 2016.
- [5] B. Andreianov, P. Goatin, and N. Seguin. Finite volume schemes for locally constrained conservation laws. *Numerische Mathematik*, 115(4):609–645, 2010.
- [6] B. Andreianov, K. H. Karlsen, and N. H. Risebro. A theory of l_1 -dissipative solvers for scalar conservation laws with discontinuous flux. *Archive for rational mechanics and analysis*, 201(1):27–86, 2011.
- [7] A. Aw and M. Rascle. Resurrection of “Second Order” Models of Traffic Flow. *SIAM Journal on Applied Mathematics*, 60(3):pp. 916–938, 2000.
- [8] P. Bagnerini, R. M. Colombo, and A. Corli. On the role of source terms in continuum traffic flow models. *Math. Comput. Modelling*, 44(9-10):917–930, 2006.

- [9] N. Bellomo and C. Dogbe. On the modeling of traffic and crowds: A survey of models, speculations, and perspectives. *SIAM review*, 53(3):409–463, 2011.
- [10] M. Benyahia, C. Donadello, **N. Dymski**, and M. D. Rosini. An existence result for a constrained two-phase transition model with metastable phase for vehicular traffic. *NoDEA Nonlinear Differential Equations Appl.*, 25(5):Art. 48, 42, 2018.
- [11] M. Benyahia and M. D. Rosini. Entropy solutions for a traffic model with phase transitions. *Nonlinear Analysis: Theory, Methods & Applications*, 141:167 – 190, 2016.
- [12] M. Benyahia and M. D. Rosini. A macroscopic traffic model with phase transitions and local point constraints on the flow. *arXiv:1605.08191*, 2016.
- [13] S. Benzoni-Gavage and R. Colombo. An n -populations model for traffic flow. *European Journal of Applied Mathematics*, 14(05):587–612, 2003.
- [14] S. Blandin, P. Goatin, B. Piccoli, A. Bayen, and D. Work. A general phase transition model for traffic flow on networks. *Procedia - Social and Behavioral Sciences*, 54:302 – 311, 2012. Proceedings of EWGT2012 - 15th Meeting of the EURO Working Group on Transportation, September 2012, Paris.
- [15] S. Blandin, D. Work, P. Goatin, B. Piccoli, and A. Bayen. A general phase transition model for vehicular traffic. *SIAM J. Appl. Math.*, 71(1):107–127, 2011.
- [16] R. Borsche, R. M. Colombo, and M. Garavello. On the coupling of systems of hyperbolic conservation laws with ordinary differential equations. *Nonlinearity*, 23(11):2749–2770, 2010.
- [17] D. Braess, A. Nagurney, and T. Wakolbinger. On a paradox of traffic planning. *Transportation Science*, 39(4):446–450, 2005.
- [18] A. Bressan. *Hyperbolic systems of conservation laws*, volume 20 of *Oxford Lecture Series in Mathematics and its Applications*. Oxford University Press, Oxford, 2000.
- [19] D. J. BUCKLEY. A semi-poisson model of traffic flow. *Transportation Science*, 2(2):107–133, 1968.
- [20] C. Cancès and N. Seguin. Error Estimate for Godunov Approximation of Locally Constrained Conservation Laws. *SIAM Journal on Numerical Analysis*, 50(6):3036–3060, 2012.

- [21] C. Chalons, P. Goatin, and N. Seguin. General constrained conservation laws. Application to pedestrian flow modeling. *Netw. Heterog. Media*, 8(2):433–463, 2013.
- [22] R. E. Chandler, R. Herman, and E. W. Montroll. Traffic dynamics: Studies in car following. *Operations Research*, 6(2):165–184, 1958.
- [23] G. Coclite, M. Garavello, and B. Piccoli. Traffic flow on a road network. *SIAM J. Math. Anal.*, 36(6):1862–1886 (electronic), 2005.
- [24] R. Colombo, A. Corli, and M. Rosini. Non local balance laws in traffic models and crystal growth. *ZAMM Z. Angew. Math. Mech.*, 87(6):449–461, 2007.
- [25] R. Colombo, P. Goatin, and M. Rosini. Conservation laws with unilateral constraints in traffic modeling. In L. Mussone and U. Crisalli, editors, *Transport Management and Land-Use Effects in Presence of Unusual Demand*, Atti del convegno SIDT 2009, June 2009.
- [26] R. Colombo, P. Goatin, and M. Rosini. On the management of traffic queues. *Preprint*, 2009.
- [27] R. Colombo and M. Rosini. Existence of nonclassical solutions in a Pedestrian flow model. *Nonlinear Analysis: Real World Applications*, 10(5):2716 – 2728, 2009.
- [28] R. M. Colombo. Hyperbolic phase transitions in traffic flow. *SIAM J. Appl. Math.*, 63(2):708–721 (electronic), 2002.
- [29] R. M. Colombo and P. Goatin. A well posed conservation law with a variable unilateral constraint. *Journal of Differential Equations*, 234(2):654 – 675, 2007.
- [30] R. M. Colombo and M. D. Rosini. Pedestrian flows and non-classical shocks. *Math. Methods Appl. Sci.*, 28(13):1553–1567, 2005.
- [31] C. Dafermos. *Hyperbolic conservation laws in continuum physics*, volume 325 of *Grundlehren der Mathematischen Wissenschaften*. Springer-Verlag, Berlin, second edition, 2005.
- [32] C. Daganzo. Requiem for high-order fluid approximations of traffic flow. *Trans. Res.*, 29B(4):277–287, August 1995.
- [33] C. F. Daganzo. The cell transmission model: A dynamic representation of highway traffic consistent with the hydrodynamic theory. *Transportation Research Part B: Methodological*, 28(4):269–287, 1994.

- [34] E. Dal Santo, M. D. Rosini, and **N. Dymski**. The riemann problem for a general phase transition model on networks. In C. Klingenberg and M. Westdickenberg, editors, *Theory, Numerics and Applications of Hyperbolic Problems I*, pages 445–457, Cham, 2018. Springer International Publishing.
- [35] E. Dal Santo, M. D. Rosini, **N. Dymski**, and M. Benyahia. General phase transition models for vehicular traffic with point constraints on the flow. *Mathematical Methods in the Applied Sciences*, pages 1–19, 2017.
- [36] C. D’apice, R. Manzo, and B. Piccoli. Packet flow on telecommunication networks. *SIAM J. Math. Anal.*, 38(3):717–740, 2006.
- [37] M. L. Delle Monache and P. Goatin. A front tracking method for a strongly coupled PDE-ODE system with moving density constraints in traffic flow. *Discrete Contin. Dyn. Syst. Ser. S*, 7(3):435–447, 2014.
- [38] M. L. Delle Monache and P. Goatin. Scalar conservation laws with moving constraints arising in traffic flow modeling: an existence result. *J. Differential Equations*, 257(11):4015–4029, 2014.
- [39] M. L. Delle Monache and P. Goatin. A numerical scheme for moving bottlenecks in traffic flow. *Bull. Braz. Math. Soc. (N.S.)*, 47(2):605–617, 2016. Joint work with C. Chalons.
- [40] M. L. Delle Monache, P. Goatin, and B. Piccoli. Priority-based Riemann solver for traffic flow on networks. *Commun. Math. Sci.*, 16(1):185–211, 2018.
- [41] J. Drake, J. Schofer, A. May, and A. May. *A statistical analysis of speed density hypotheses*. Report (Expressway Surveillance Project (Ill.)). Expressway Surveillance Project, 1965.
- [42] **N. Dymski**, P. Goatin, and M. D. Rosini. Existence of **BV** solutions for a non-conservative constrained Aw-Rascle-Zhang model for vehicular traffic. *J. Math. Anal. Appl.*, 467(1):45–66, 2018.
- [43] **N. Dymski**, P. Goatin, and M. D. Rosini. Modeling moving bottlenecks on road networks. preprint, Jan. 2019.
- [44] R. E. Ferreira and C. I. Kondo. Glimm method and wave-front tracking for the Aw-Rascle traffic flow model. *Far East J. Math. Sci. (FJMS)*, 43(2):203–223, 2010.
- [45] M. Flynn, A. Kasimov, J. Nave, R. Rosales, and B. Seibold. Self-sustained nonlinear waves in traffic flow. *Phys. Rev. E*, 79:056113, May 2009.

- [46] M. Garavello and P. Goatin. The Aw-Rascle traffic model with locally constrained flow. *Journal of Mathematical Analysis and Applications*, 378(2):634–648, 2011.
- [47] M. Garavello, K. Han, and B. Piccoli. *Models for vehicular traffic on networks*, volume 9 of *AIMS Series on Applied Mathematics*. American Institute of Mathematical Sciences (AIMS), Springfield, MO, 2016.
- [48] M. Garavello and B. Piccoli. *Traffic flow on networks*, volume 1 of *AIMS Series on Applied Mathematics*. American Institute of Mathematical Sciences (AIMS), Springfield, MO, 2006. Conservation laws models.
- [49] M. Garavello and B. Piccoli. Coupling of Lighthill-Whitham-Richards and phase transition models. *J. Hyperbolic Differ. Equ.*, 10(3):577–636, 2013.
- [50] M. Garavello and S. Villa. The Cauchy problem for the Aw–Rascle–Zhang traffic model with locally constrained flow. *Journal of Hyperbolic Differential Equations*, 14(03):393–414, 2017.
- [51] D. C. Gazis, R. Herman, and R. W. Rothery. Nonlinear follow-the-leader models of traffic flow. *Operations Research*, 9(4):545–567, 1961.
- [52] F. Giorgi. Prise en compte des transports en commun de surface dans la modélisation macroscopique de l’écoulement du trafic. *Institut National des Sciences Appliquées de Lyon*, 2002.
- [53] P. Goatin. The Aw-Rascle vehicular traffic flow model with phase transitions. *Mathematical and computer modelling*, 44(3):287–303, 2006.
- [54] B. Greenshields. A study of traffic capacity. *Highway Research Board*, pages 14:448–477, 1934.
- [55] B. Greenshields. A study of traffic capacity. *Proceedings of the Highway Research Board*, 14:448–477, 1935.
- [56] D. Helbing. Traffic and related self-driven many-particle systems, *Reviews of modern physics*, 2001.
- [57] D. Helbing and M. Schreckenberg. Cellular automata simulating experimental properties of traffic flow. *Physical review E*, 59(3):R2505, 1999.
- [58] M. Herty and A. Klar. Modeling, simulation, and optimization of traffic flow networks. *SIAM J. Sci. Comput.*, 25(3):1066–1087, 2003.
- [59] H. Holden and N. Risebro. *Front tracking for hyperbolic conservation laws*, volume 152 of *Applied Mathematical Sciences*. Springer-Verlag, New York, 2002.

- [60] F. Kessels. *Traffic flow modelling*. EURO Advanced Tutorials on Operational Research. Springer, Cham, 2019. Introduction to traffic flow theory through a genealogy of models.
- [61] W. Knödel. *Graphentheoretische Methoden und ihre Anwendungen*. Econometrics and operations research. Springer, 1969.
- [62] S. N. Kruzhkov. First order quasilinear equations with several independent variables. *Mat. Sb. (N.S.)*, 81 (123):228–255, 1970.
- [63] R. Kühne, R. Mahnke, I. Lubashevsky, and J. Kaupužs. Probabilistic description of traffic breakdowns. *Phys. Rev. E*, 65:066125, Jun 2002.
- [64] C. Lattanzio, A. Maurizi, and B. Piccoli. Moving bottlenecks in car traffic flow: a PDE-ODE coupled model. *SIAM J. Math. Anal.*, 43(1):50–67, 2011.
- [65] N. Laurent-Brouty, C. Guillaume, and P. Goatin. A coupled pde-ode model for bounded acceleration in macroscopic traffic flow models. *IFAC-PapersOnLine*, 51:37–42, 01 2018.
- [66] P. Lax. Hyperbolic Systems of Conservation Laws II. In P. Sarnak and A. Majda, editors, *Selected Papers Volume I*, pages 233–262. Springer New York, 2005.
- [67] L. Li and X. M. Chen. Vehicle headway modeling and its inferences in macroscopic/microscopic traffic flow theory: A survey. *Transportation Research Part C: Emerging Technologies*, 76:170 – 188, 2017.
- [68] M. Lighthill and G. Whitham. On kinematic waves. II. A theory of traffic flow on long crowded roads. In *Royal Society of London. Series A, Mathematical and Physical Sciences*, volume 229, pages 317–345, 1955.
- [69] G. Liu, A. Lyrintzis, and P. Michalopoulos. Improved High-Order Model for Freeway Traffic Flow. *Transportation Research Record*, 1644(1):37–46, 1998.
- [70] T. P. Liu. The Riemann problem for general systems of conservation laws. *J. Differential Equations*, 18:218–234, 1975.
- [71] A. May and H. E. Keller. Non-integer car-following models. *Highway Research Record*, 199(1):19–32, 1967.
- [72] R. Mohan and G. Ramadurai. State-of-the art of macroscopic traffic flow modelling. *International Journal of Advances in Engineering Sciences and Applied Mathematics*, 5(2-3):158–176, 2013.
- [73] K. Nagel and M. Schreckenberg. A cellular automaton model for freeway traffic. *Journal de Physique I*, 2(12):2221–2229, dec 1992.

- [74] G. F. Newell. A simplified car-following theory: a lower order model. *Transportation Research Part B: Methodological*, 36(3):195–205, March 2002.
- [75] M. Papageorgiou. Some remarks on macroscopic traffic flow modelling. *Transportation Research Part A: Policy and Practice*, 32(5):323–329, 1998.
- [76] S. Pavari-Fontana. On Boltzmann-like treatments for traffic flow: A critical review of the basic model and an alternative proposal for dilute traffic analysis. *Transportation Research*, 9(4):225 – 235, 1975.
- [77] H. Payne. Models of freeway traffic and control. *Math. Models Publ. Sys. Simul. Council Proc.*, 1(28):51–61, 1971.
- [78] B. Piccoli and A. Tosin. Vehicular traffic: A review of continuum mathematical models. In R. A. Meyers, editor, *Mathematics of Complexity and Dynamical Systems*, pages 1748–1770. Springer New York, 2011.
- [79] L. A. Pipes. An operational analysis of traffic dynamics. *Journal of Applied Physics*, 24(3):274–281, 1953.
- [80] I. Prigogine and F. C. Andrews. A boltzmann-like approach for traffic flow. *Operations Research*, 8(6):789–797, 1960.
- [81] P. I. Richards. Shock waves on the highway. *Operations Research*, 4(1):pp. 42–51, 1956.
- [82] M. D. Rosini. *Macroscopic models for vehicular flows and crowd dynamics: theory and applications*. Understanding Complex Systems. Springer, Heidelberg, 2013. Classical and non-classical advanced mathematics for real life applications.
- [83] S. Smulders. Control of freeway traffic flow by variable speed signs. *Transportation Research Part B: Methodological*, 24(2):111–132, 1990.
- [84] F. van Wageningen-Kessels, H. van Lint, K. Vuik, and S. Hoogendoorn. Genealogy of traffic flow models. *EURO Journal on Transportation and Logistics*, pages 1–29, 2014.
- [85] H. Zhang. A non-equilibrium traffic model devoid of gas-like behavior. *Transportation Research Part B: Methodological*, 36(3):275–290, 2002.